



LUND UNIVERSITY

Mucosal interactions during Trichuris infections

Sorobetea, Daniel

2017

Document Version:

Publisher's PDF, also known as Version of record

[Link to publication](#)

Citation for published version (APA):

Sorobetea, D. (2017). *Mucosal interactions during Trichuris infections*. [Doctoral Thesis (compilation), Department of Experimental Medical Science]. Lund University: Faculty of Medicine.

Total number of authors:

1

General rights

Unless other specific re-use rights are stated the following general rights apply:

Copyright and moral rights for the publications made accessible in the public portal are retained by the authors and/or other copyright owners and it is a condition of accessing publications that users recognise and abide by the legal requirements associated with these rights.

- Users may download and print one copy of any publication from the public portal for the purpose of private study or research.
- You may not further distribute the material or use it for any profit-making activity or commercial gain
- You may freely distribute the URL identifying the publication in the public portal

Read more about Creative commons licenses: <https://creativecommons.org/licenses/>

Take down policy

If you believe that this document breaches copyright please contact us providing details, and we will remove access to the work immediately and investigate your claim.

LUND UNIVERSITY

PO Box 117
221 00 Lund
+46 46-222 00 00

Mucosal interactions during *Trichuris* infections

Daniel Sorobetea

Section for Immunology
Lund University, Faculty of Medicine



LUND
UNIVERSITY

Doctoral dissertation

With the approval of the Faculty of Medicine, Lund University,
this thesis will be defended on March 31st, 2017 at 13.00
in Belfragesalen, BMC D15, Sölvegatan 19, Lund, Sweden

Faculty opponent

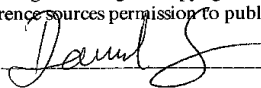
Professor David Vöhringer
Friedrich-Alexander-University Erlangen-Nürnberg
Erlangen, Germany

Organization LUND UNIVERSITY Section for Immunology Department of Experimental Medical Science Faculty of Medicine Lund, Sweden	Document name DOCTORAL DISSERTATION	
	Date of issue 31/3-2017	
	Sponsoring organization	
Author(s) Daniel Sorobetea		
Title and subtitle Mucosal interactions during <i>Trichuris</i> infections		
Abstract <p><i>The intestinal immune system is of fundamental importance to human health as it must be able to eradicate pathogens, while remaining tolerant to harmless dietary antigens and the countless microorganisms that make up the gut microbiota. A collapse in this balance might result in various immune-associated disorders, such as inflammatory bowel disease and food allergies. Interestingly, as our exposure to intestinal parasites has diminished, the incidence of these disorders has steadily risen. Humans have harbored parasitic worms throughout history, and their continued survival is thought to depend upon their ability to modulate the immune system of their host. Thus, the lack of worm infections, particularly early in life, might contribute to the rising incidence of inflammatory disorders.</i></p> <p><i>The aim of this thesis was to characterize the influence of intestinal parasite infection on the mucosal environment using the murine large-intestinal nematode <i>Trichuris muris</i>, a close relative to the human parasite <i>Trichuris trichiura</i>. In the first paper, we found that acute <i>T. muris</i> infection resulted in the accumulation of mucosal mast cells in the intestinal epithelium, which persisted several months beyond expulsion and had a notable impact on epithelial homeostasis, but without affecting the intestinal microbiota. By contrast, in the second paper, we demonstrated that chronic infection led to decreased bacterial diversity and an increase in the relative abundance of Lactobacilli, as well as a skewed balance between inflammatory and regulatory T cells in favor of inflammatory cells. In the third paper, we investigated how secreted antigens from <i>T. muris</i> are recognized by the innate immune system and found that worm-derived molecules were capable of licensing macrophages for the activation of a non-conventional inflammasome. Lastly, we extended our studies into the mesentery to assess the role of eosinophils in adipose tissue and surprisingly discovered that eosinophils contribute to regulation of vascular function.</i></p> <p><i>In conclusion, our results suggest that <i>T. muris</i> has a considerable influence on both the mucosal immune system and the commensal microbiota, with potential consequences on the development of immune-associated disorders, although further studies are required to determine the extent to which these findings apply to humans.</i></p>		
Key words: <i>Trichuris muris</i> , intestinal parasite infection, mucosal mast cell, microbiota, inflammasome, eosinophil, adipose tissue		
Classification system and/or index terms (if any):		
Supplementary bibliographical information:		Language English
ISSN and key title: 1652-8220		ISBN 978-91-7619-430-0
Recipient's notes	Number of pages	Price Priceless
	Security classification	

Distribution by (name and address)

I, the undersigned, being the copyright owner of the abstract of the above-mentioned dissertation, hereby grant to all reference sources permission to publish and disseminate the abstract of the above-mentioned dissertation.

Signature



Date

14/2-2017

Mucosal interactions during *Trichuris* infections

Daniel Sorobetea

Section for Immunology
Lund University, Faculty of Medicine



LUND
UNIVERSITY

The front cover features a cross section of a murine large intestine infected with the whipworm *Trichuris muris* (~10x magnification). The thinner anterior ends of the worms can be seen embedded within the epithelium whereas the posterior ends are free in the lumen.

The back cover features a cross section of the posterior end of a female worm (~40x magnification). Unembryonated parasite eggs can be seen within the oviduct.

Both sections were stained with Hematoxylin (dark purple) and Eosin (pink) to visualize cellular components.

Paper 1 was reproduced with permission from Wiley-VCH Verlag GmbH & co. KGaA.

© Daniel Sorobetea

ISSN 1652-8220

ISBN 978-91-7619-430-0

Lund University, Faculty of Medicine

Doctoral Dissertation Series 2017:50

Printed by Exakta Printing AB, Malmö, Sweden

*To my mother and father,
for their unwavering support,
literally from day one.*

Preface

Approximately five thousand years ago, on a late afternoon in early spring, a middle-aged man was hiking in the Alps, in a region called Ötztal, between what is now Austria and Italy. He was clad in thick leather, as the weather was still very chilly at high altitudes. Among other things, he carried a copper axe, flint and tinder, some medicinal herbs, and he had packed provisions consisting of dried ibex meat, wheat bread, sloan berries and flax seeds. However, unbeknownst to him, he also carried an infectious parasite in his large intestine; the whipworm *Trichuris trichiura*. In any case, the man had worse things to worry about, as he would die later that day from a violent encounter with a stranger. The man I've described is of course the Tyrolean iceman, colloquially known as Ötzi, who was discovered mummified in ice in 1991.

Ötzi is interesting in many ways, and the analyses of his remarkably well-preserved remains have given us great insight into our past as a species, not the least of which is that we have been hosting parasites throughout our evolutionary history. So, why do I bring this up? Well, parasites can usually survive for many years within their hosts, as they are often capable of manipulating the immune system in their favor to avoid being killed. However, we are in a unique transition in human history. After evolving alongside our worms for countless millennia, we have finally managed to rid ourselves of these unwelcome guests with the advent of water sanitation and proper waste disposal, thus preventing their spread. Furthermore, in rare cases of infection we are quick to treat it with anti-helminthic drugs. The result though, is that allergies, diabetes, inflammatory bowel disease and many other immune-associated disorders are more common than ever before. Perhaps we need these parasites just like they need us, as without their influence on our bodies the immune system is missing a key signal, which tells it that everything is all right.

During my brief time at the section for immunology I've studied how the body interacts with parasites, to better understand the fundamental workings of our immune system, in the hopes that someday we will be able to get all the benefits they provide without having to carry an actual infection. Having the cake, and eating it too, if you will. Our group has studied how chronic infections affect the composition of intestinal bacteria, we've assessed what happens to the immune system after an infection is cleared, and slowly begun to elucidate how immune cells recognize and respond to the presence of parasitic worms. It's been a joy working with these disgusting little creatures, and I hope that you find some pleasure in reading what we discovered.

*Daniel Sorobetea
Lund, February 2017*

Table of contents

Popularized summary in Swedish	11
Thesis summary	13
<u>Background</u>	
Introduction	17
The intestinal milieu	18
The intestinal barrier	18
The microbiota	19
The mucosal immune system	21
Homeostasis	21
Inflammation	22
Host-parasite interactions	25
Parasite biology	25
<i>T. muris</i>	25
Parasite immunology	28
Detection	29
Transmission	29
Induction	32
Execution	33
Resolution	35
Consequences	36
<u>Synopses</u>	
Paper 1	41
Paper 2	44
Paper 3	47
Paper 4	49
Concluding remarks	53
Acknowledgements	55
References	57
Abbreviations	77

Popularized summary in Swedish

Tarmens immunförsvar är oundgängligt för vår hälsa då det måste kunna bekämpa farliga mikroorganismer utan att skada den egna kroppsvävnaden eller de nyttiga bakterierna i tarmkanalen. När denna balans rubbas ökar risken för att utveckla diverse immunrelaterade sjukdomar, så som allergier eller diabetes. Vi står därför inför ett problem. Samtidigt som omgivningen i vår del av världen har blivit allt renare, och vi har lyckats göra oss av med parasitmaskar, så drabbas allt fler människor av inflammatoriska sjukdomar, vilket skulle kunna tyda på att immunförsvaret saknar en viktig signal eller kanske inte får rätt träning under dess utveckling tidigt i livet. Maskinfektioner har således föreslagits som möjlig terapi för att behandla vissa typer av inflammatoriska sjukdomar.

Syftet med denna avhandling har varit att undersöka hur parasitmaskar påverkar miljön i tarmen, både under och efter infektion, i hopp om att kunskapen kan komma att bidra till utvecklingen av botemedel för de ovan nämnda sjukdomarna. Min forskning har kretsat kring tarmparasiten *Trichuris muris* som infekterar möss och är nära besläktad med mänsklig piskmask. I avhandlingens första studie upptäckte vi att *T. muris*-infektion ledde till en stor ansamling av mastceller i tarmen, som stannade kvar i vävnaden långt efter att maskarna stötts ut och mössen blivit friska igen. Mastceller är tätt förknippade med allergiska reaktioner, vilket skulle kunna tyda på att maskinfektionen ökar risken för att utveckla matallergi eller andra inflammatoriska tarmsjukdomar. I den andra studien analyserade vi huruvida kronisk infektion med *T. muris* påverkar sammansättningen av tarmens godartade bakterier, och vilka eventuella konsekvenser detta har på kroppens immunförsvar. Vi upptäckte att tarmens bakterier ändrades drastiskt inom loppet av ett par veckor efter infektion. Bland annat så fann vi att ett antal bakteriefamiljer hade ökat i antal, speciellt *Lactobacilli*, som tros vara viktiga för att bibehålla en frisk tarm. Däremot så minskade andra bakterier avsevärt i antal, så pass att den totala mångfalden av bakterier påverkades negativt, något som sker även i patienter med inflammatoriska tarmsjukdomar. Dessutom kunde vi visa att balansen mellan inflammatoriska och dämpande immunceller skiftat till förmån för de inflammatoriska cellerna. I den tredje studien ville vi gå på djupet kring hur immunförsvaret känner av närvaron av parasiter, och upptäckte att molekyler som utsöndras av *T. muris* under infektion kan aktivera immunceller till att producera inflammationsdrivande proteiner. Slutligen så studerade vi funktionen av eosinofiler som befinner sig i den fettväv som omgärdar tarmen. Eosinofiler associeras vanligtvis med maskinfektioner, men till vår överraskning så fann vi att de har en roll i att reglera funktionen hos blodkärl, och att de på så sätt har inverkan på kroppens blodtryck, även under normalförhållande.

Det är i nuläget oklart hur våra resultat relaterar till människor, och mer forskning behövs för att i detalj förstå de långsiktiga konsekvenser som parasitinfektioner har på vår hälsa. Min förhoppning är att våra studier har hjälpt oss en bit på vägen.

Thesis summary

The intestinal immune system is of fundamental importance to human health as it must be able to eradicate pathogens, while remaining tolerant to harmless dietary antigens and the countless microorganisms that make up the gut microbiota. A collapse in this balance might result in various immune-associated disorders, such as inflammatory bowel disease and food allergies. Interestingly, as our exposure to intestinal parasites has diminished, the incidence of these disorders has steadily risen. Humans have harbored parasitic worms throughout history, and their continued survival is thought to depend upon their ability to modulate the immune system of their host. Thus, the lack of worm infections, particularly early in life, might contribute to the rising incidence of inflammatory disorders.

The aim of this thesis was to characterize the influence of intestinal parasite infection on the mucosal environment using the murine large-intestinal nematode *Trichuris muris*, a close relative to the human parasite *Trichuris trichiura*. In the first paper, we found that acute *T. muris* infection resulted in the accumulation of mucosal mast cells in the intestinal epithelium, which persisted several months beyond expulsion and had a notable impact on epithelial homeostasis, but without affecting the intestinal microbiota. By contrast, in the second paper, we demonstrated that chronic infection led to decreased bacterial diversity and an increase in the relative abundance of *Lactobacilli*, as well as a skewed balance between inflammatory and regulatory T cells in favor of inflammatory cells. In the third paper, we investigated how secreted antigens from *T. muris* are recognized by the innate immune system and found that worm-derived molecules were capable of licensing macrophages for the activation of a non-conventional inflammasome. Lastly, we extended our studies into the mesentery to assess the role of eosinophils in adipose tissue and surprisingly discovered that eosinophils contribute to regulation of vascular function.

In conclusion, our results suggest that *T. muris* has a considerable influence on both the mucosal immune system and the commensal microbiota, with potential consequences on the development of immune-associated disorders, although further studies are required to determine the extent to which these findings apply to humans.

Background

Introduction

From the moment we are born, our bodies are constantly exposed to microorganisms. Most of these creatures do us little or no harm, but a significant portion like nothing better than to devour our blood and feast on our flesh. Nature is rife with parasitism, and it has been estimated that one fifth of the world population is hosting one or more species of parasite¹. Although the majority of these organisms reside in our intestines, symptoms vary significantly depending on the species, ranging from abdominal pain and mild anemia to stunted development, cognitive disability and, in rare cases, death. As with many other pathogens, parasitic worm infections are most common among children in developing countries where hygienic conditions are poor. The tragedy is that most parasites are easily avoided by access to clean water, which is evident in the industrialized parts of the world. Efforts to treat infected individuals with anti-helminthic drugs are thus rendered useless, since people are prone to reinfection due to continued exposure to infective eggs and larvae in their immediate environment.

With that being said, there are reasons to believe that some parasites could incur benefits as well. Epidemiological data indicate that over the past decades, as certain countries have experienced high rates of economic development, both the prevalence and incidence of immunological disorders has risen steadily²⁻⁴, while the occurrence of parasite infections has decreased dramatically. This inverse correlation has given rise to the hygiene hypothesis, which as the name implies proposes that excessive cleanliness might alter the balance of the immune system, in part due to the lack of parasite exposure, thus resulting in aberrant reactions to harmless environmental molecules like enzymes from cat saliva, plant pollen and peanuts, or to the body's own cells and proteins, as in the case of type 1 diabetes, rheumatoid arthritis and multiple sclerosis. Given that our species evolved in close contact with a diverse array of pathogens, this explanation is certainly plausible. Furthermore, the literature on the topic is extensive and has gained more credence in recent years^{5,6}, so much so that some have considered using worm infections as treatment for the disorders mentioned above⁷. Regardless, it is clear that parasites have had, and will continue to have, a significant impact on our species in the foreseeable future.

During my studies, I have explored the interaction between intestinal parasites and the mucosal immune system using the nematode *Trichuris muris*, a natural model of murine infection. In the following chapters I will attempt to summarize the current state of the field, as well as contextualize our own findings within this topic.

The intestinal milieu

It goes without saying that the intestinal tract is responsible for digestion and uptake of nutrients. However, its massive surface area also provides a convenient route of entry for potential pathogens and must therefore be continuously guarded by the mucosal immune system, which is burdened with the difficult task of mounting protective immunity toward invading pathogens, while simultaneously remaining tolerant toward harmless environmental stimuli, food-derived molecules and commensal microbes. This balancing act is highly intricate, and if perturbed might result in food allergies, inflammatory bowel disease and other immune-associated disorders, although the precise causes of these conditions are unknown. While the function of the mucosal immune system is relatively well characterized, it is only in recent years that we have begun to unravel the complex nature of the myriad of microbial species that populate the intestinal lumen. Our understanding of this microenvironment thus remains fairly limited and will likely be revised in coming years as technologies improve and our abilities to process large amounts of data become more sophisticated. Nevertheless, the intestinal environment clearly has a profound influence on both health and disease.

The intestinal barrier

Before discussing mucosal immunity, it is important that we familiarize ourselves with the structure, organization and function of the intestinal barrier⁸. The gastrointestinal tract encompasses the stomach, as well as the small and large intestines. Food is digested mainly in the stomach and is subsequently passed on to the small intestine, which is the main site of nutrient absorption. This uptake is facilitated by the countless folds of the epithelium known as villi and microvilli, which dramatically increase the total surface area available for nutrient absorption. By contrast, the large-intestinal epithelium is devoid of villi, instead being important for reabsorption of water. Both barriers are composed of a single layer of epithelial cells lined with mucus on the luminal side. In addition to these structural barriers, vast numbers of immune cells reside in the epithelium and the underlying lamina propria, to guard against the multitude of commensal microorganisms that make up the microbiota, as well as potential pathogens. Given this close interaction, the intestinal barrier is also interspersed with secondary lymphoid organs, such as Peyer's patches and isolated lymphoid follicles, and is richly supplied with lymphatic vessels that drain into mesenteric lymph nodes where adaptive immune responses are initiated. The lymph nodes, in turn, are coated in adipose tissue, which contains immune cells that have been implicated in both metabolic and immune regulation. Collectively, these organs and tissues are responsible for generating both protective immunity and oral tolerance.

The intestinal epithelium is composed of at least five distinct cell types, including absorptive enterocytes, enteroendocrine cells, tuft cells, Paneth cells, goblet

cells, as well as the pluripotent stem cells that generate them⁹. Unsurprisingly, enterocytes make up the vast majority of epithelial cells given their role in nutrient uptake. Similarly, enteroendocrine cells are responsible for hormonal regulation of various digestive functions, thus forming a link between the gastrointestinal tract and the pancreas. Tuft cells appear to have a unique function in regulating immunity to parasites, as will be discussed in the next chapter. Paneth and goblet cells, on the other hand, are heavily implicated in maintaining the physical barrier by release of anti-microbial peptides and mucus, respectively. Paneth cells are most abundant in the small-intestinal epithelium, but unlike other epithelial cells do not shift outward as the stem cells proliferate, instead residing in the crypts where they release defensins, lysozyme, RegIIIγ and other bactericidal molecules that maintain a sterile niche to protect the epithelial stem cells. By contrast, goblet cells increase along the intestinal tract and are most abundant in the large intestine where they secrete numerous glycoproteins, most importantly mucins, which form a gel-like matrix that coats the luminal side of the epithelium, thereby forming a barrier toward invading microbes¹⁰. This is particularly evident in the large intestine where the bacterial load is the highest and the mucus layer is the thickest. Indeed, whereas the small intestine is covered by a single mucus layer, the large-intestinal mucus is composed of two distinct layers, with commensal bacteria residing in the outer layer, but rarely penetrating the dense network of the inner layer under normal circumstances¹⁰, although some pathogens have evolved specific strategies to breach the barrier. Furthermore, a certain degree of interaction between the epithelium and microbiota is of critical importance for immune development and oral tolerance^{11–16}. The importance of mucus is further emphasized by the fact that defects in mucin production enables entry of commensal microbes into the mucosa¹⁰ and predisposes to inflammatory bowel disease and cancer^{17,18}. Together, these cells and molecules effectively maintain a physical barrier between the outside world and us.

The microbiota

The adult human gastrointestinal tract is colonized by approximately 10^{14} microorganisms, collectively referred to as the intestinal microbiota. Composed mainly of bacteria, the microbiota outnumbers our own cells by at least two-fold, and has a substantial impact on both health and disease. Given that most luminal bacteria are anaerobic and difficult to culture, the complexity of the intestinal microbiota was not fully recognized until modern genetic sequencing became widely available. Since then however, we have come to appreciate the intricate nature of intestinal microbes and slowly begun to elucidate their profound influence on important physiological and developmental processes in the body, including nutrient digestion and metabolic regulation^{19–22}, bone²³, blood vessel^{24,25} and immune development^{26–29}, as well as out-competing pathogens^{30,31}, maintaining tissue homeostasis^{11,32} and influencing brain function^{33–37}.

While the precise number is unclear, there are somewhere between four hundred³⁸ and one thousand³⁹ different bacterial species present in the intestinal tract. However, most of these belong to only two phyla, namely *Firmicutes* and *Bacteroidetes*^{38,39}, with minor contributions from *Actinobacteria* and *Proteobacteria*, which instead are abundant on the skin⁴⁰, likely due to differences in oxygen and moisture content. Thus, each tissue can be viewed as a unique habitat with its own physical characteristics and niches. Microbial diversity is therefore equally important for providing stability in the intestinal tract as in any ecological habitat. The composition of the microbiota is nevertheless not rigid, but fluctuates over time, and is under the influence of several factors, including host genetics and immunity, as well as diet and other environmental factors. Indeed, humans are presumed to be sterile prior to birth, but are rapidly colonized by bacteria from the mother's vagina⁴¹. The microbiota thus becomes established in the neonatal period and evolves over the course of several years. This process is genetically regulated and partly determined by the mucosal immune system⁴²⁻⁴⁵, as illustrated by the fact that family members have similar microbiota, with monozygotic twins being the most alike⁴⁶. However, host factors are insufficient to fully explain the variability between people, which is more pronounced than within any given individual^{38,40,46}, despite that most people have a core set of species in common^{39,46}. Diet, in particular, appears to have an important role in shaping the microbiota⁴⁷⁻⁴⁹. For instance, children in rural Africa have a different microbial composition than children in Europe, characterized by lower abundance of *Firmicutes*, as well as the presence of certain phyla that are absent in European children, largely due to the plant-rich diet in rural communities⁴⁸. Our commensal microbes thus digest complex plant-derived carbohydrates for which we lack the enzymatic machinery²¹ and are susceptible to changes in diet as specialized communities expand and contract in response to their preferred energy source⁵⁰. As a result, the microbiota also has a strong impact on obesity^{46,51-54}, which is associated with increases in *Firmicutes*^{47,51,55}. This inherent plasticity in the composition of commensal microbes has likely been advantageous throughout human evolution. Thus, whereas obesity has become a major health issue in modern times, the efficient uptake and utilization of lipids and polysaccharides might have been a selective advantage in nutrient-scarce environments. In situations where food is limited, growth of bacterial communities that are able to maximize energy harvest for the host might increase the likelihood of survival. This is further illustrated by the observation that cold temperatures, which are associated with periods of food scarcity, have a significant impact on the abundance of certain microbial groups that promote nutrient uptake and expenditure⁵⁶, notably *Firmicutes*, which mirrors the microbiota during obesity^{47,51,55}. Similar changes can be seen in pregnant women, notably in the third trimester, where demand for caloric intake is highest⁵⁷. Unfortunately, this plasticity comes at a price. Given their important role in immune development, dysregulated microbial communities are thought to have a substantial impact on the development of several immune-associated disorders, notably type 1 diabetes^{58,59} and inflammatory bowel disease. Indeed, patients with

inflammatory bowel disease have altered bacterial communities⁶⁰⁻⁶², which are less diverse⁶¹, despite having higher bacterial loads than healthy controls^{63,64}, although it is unclear whether this shift is a direct cause or simply a consequence of disease. Nevertheless, these findings have prompted therapeutic use of various bacteria, notably *Lactobacilli*⁶⁵, and in some cases complete fecal transplants from healthy individuals, to ameliorate disease. However, it remains to be determined whether certain microbial populations can be manipulated to effectively prevent or cure these disorders.

The mucosal immune system

Unlike most other peripheral tissues, the intestine is continuously exposed to foreign material; some of it harmful, but most of it innocuous. It is perhaps not surprising then that many of the cell types in the intestinal tract are suppressive in nature, leading to a collective state of immunological tolerance in the steady state mucosa. However, when faced with an invasive microbe, the mucosal immune system must rapidly initiate inflammation and eliminate the pathogen. The intestinal mucosa is thus composed of a highly diverse set of cell types, some of which are vital for the maintenance of homeostasis by acting as tissue sentinels, whereas others are recruited or expanded upon inflammation.

Homeostasis

The maintenance of tissue homeostasis is largely dependent on resident antigen-presenting cells and regulatory helper T cells, which are most abundant in the large intestine (likely reflecting the high microbial load), with contributions from various innate cells including ILCs and eosinophils. Hence, in contrast to inflammatory monocytes, and most other tissue-resident macrophages, which respond to microbial stimuli with the production of inflammatory cytokines, intestinal macrophages are generally suppressive⁶⁶⁻⁶⁸ and act mainly to limit inflammation, partly via recognition of the cytokine IL-10^{69,70}. Likewise, dendritic cells are necessary for the uptake of both luminal and tissue-derived antigens⁷¹⁻⁷⁷, migration to mesenteric lymph nodes and the subsequent induction of regulatory T cells^{73,78-80}, which suppress immune responses at mucosal surfaces^{81,82} predominantly via production of IL-10⁸³⁻⁸⁵. In addition, ILCs have been implicated in regulating barrier function^{86,87}, maintaining secondary lymphoid organs^{88,89} and facilitating IgA secretion^{89,90}, largely in response to the microbiota^{91,92}, thus being strongly implicated in the maintenance of intestinal homeostasis. Eosinophils, which make up only a fraction of circulating leukocytes, are relatively abundant in the intestinal tract⁹³ and have traditionally been associated with combating parasites. However, recent findings instead suggest that intestinal eosinophils are also important for promoting tissue homeostasis, through the maintenance of both regulatory T cells^{94,95} and IgA-secreting plasma cells^{94,96}, as will be discussed in greater detail in the subsequent chapter. Moreover, eosinophils accumulate in mesenteric lymph nodes upon parasite infection⁹⁷ and are also present in adipose tissue⁹⁸, where they have been implicated in the maintenance

of alternatively activated macrophages and glucose homeostasis, highlighting their potential role in both metabolic and immune regulation.

Inflammation

As a consequence of these mechanisms, the mucosal immune system is able to effectively maintain intestinal homeostasis and oral tolerance. However, from time to time, a pathogen is able to breach the barrier and infect the tissue, resulting in inflammation, which serves to contain the spread of invading microbes, recruit additional immune effector cells, and initiate the adaptive immune response to generate long-term memory. The first step of the inflammatory cascade is pathogen recognition, which relies on a broad group of cytosolic and membrane-bound receptors that recognize evolutionarily conserved microbial structures, as well as endogenous stress molecules. These include the TLRs, NLRs, CLRs and RLRs, which are expressed by both hematopoietic cells, mainly of the innate immune system, as well as by non-hematopoietic cells, notably intestinal epithelial cells. Once triggered, these receptors initiate intracellular signaling cascades that lead to the production of inflammatory cytokines and mediators. Perhaps the most prominent example is TLR4, which is ubiquitously expressed and signals in response to LPS, a major component of the Gram-negative bacterial cell membrane, as well as certain damage-associated molecules⁹⁹. With the help of several accessory proteins, TLR4 transmits its signal through the adaptor proteins MyD88 and TRIF, resulting in the phosphorylation of a series of kinases and scaffolding proteins, culminating in the activation of NF- κ B and IRF3, respectively^{100,101}. These transcription factors, in turn, translocate to the nucleus and promote increased migratory or phagocytic capacity of dendritic cells and macrophages, respectively, as well as expression of several inflammatory genes, such as TNF and IL-6, which enable the recruitment of effector cells, including neutrophils and monocytes, as well as adaptive immune cells. Consequently, neutralizing antibodies against TNF (infliximab) are, along with corticosteroids, the predominant treatment for patients with inflammatory bowel disease.

Another important feature of the inflammatory response is the formation of large cytosolic protein complexes called inflammasomes¹⁰², which serve to activate and release the highly potent cytokines IL-1 β and IL-18. Unlike most other cytokines, IL-1 β and IL-18 are translated as inactive pro-forms upon NF- κ B and AP-1 activation, and must be cleaved prior to being released. This process occurs predominantly in dendritic cells, macrophages, neutrophils and epithelial cells, and is mainly accomplished by the enzyme caspase-1¹⁰³. Several distinct inflammasomes have been identified based on the pattern-recognition receptors that govern their activation. For instance, Naip5, which activates the Nlrc4 inflammasome^{104,105} in response to flagellin^{106–109}, is highly expressed in the large intestine¹¹⁰ and is important for protection against *Salmonella* infection¹¹¹. Likewise, Aim2, which is activated upon binding of cytosolic double-stranded DNA, is required for protection

against certain intracellular bacteria, such as *Francisella tularensis*^{112,113}. However, the most studied inflammasome contains the sensor Nlrp3, which unlike the other inflammasomes mentioned is activated in response to a broad spectrum of both endogenous^{114–118} and pathogen-derived^{118–120} molecules. Given the diverse nature of these triggers, it is unlikely that they are all sensed directly by the Nlrp3 protein itself, but rather that several different physiological mechanisms converge on a signal that enables Nlrp3 to bind the adaptor protein Asc, which can recruit caspase-1 and form the inflammasome. A number of mechanisms have been proposed to explain this phenomenon, most of which pertain to inherent signs of stress, such as organelle dysfunction, membrane destabilization and ion imbalance. These include cathepsin release from ruptured lysosomes¹²¹, decreased concentration of cytosolic potassium^{122–124} and accumulation of damaged mitochondria due to impaired autophagy^{125,126}, as well as leakage of mitochondrial DNA^{127,128}, ROS^{127,129} and cardiolipin¹³⁰ into the cytosol. By contrast, mitochondrial apoptosis itself does not seem to affect inflammasome activation¹³¹, indicating that dying mitochondria or defective organelles are not inherently inflammatory if recycled under controlled conditions. The exact contribution of each pathway *in vivo* is largely unexplored and likely depends on the nature of the trigger and cell type in question. However, what is clear is that not all pathways are required at any given time; for instance, Nlrp3 activation can occur independently of potassium efflux^{132,133} or mitochondrial ROS production¹³⁰, highlighting the complex and context-dependent nature of inflammasome activation. Another possible explanation for the wide range of Nlrp3-inducing stimuli is the convergence of post-translational modifications of inflammasome components. Indeed, Nlrp3 activation is a rapid process that does not require *de novo* transcription, instead relying on deubiquitination of Nlrp3, as well as Asc ubiquitination and phosphorylation^{134,135}, lending credence to this hypothesis. Furthermore, intestinal macrophages, which are largely unresponsive to Nlrp3 stimuli, appear to be so due to continuous ubiquitination and degradation of Nlrp3 mRNA¹³⁶. Similarly, IL-1 β is also regulated at the post-translational level by ubiquitination via the protein A20, which suppresses inflammasome activation¹³⁷, illustrating the importance of post-transcriptional and post-translational processes in the regulation of inflammasome activation.

A feature often associated with inflammasome activation is a controlled form of lytic cell death called pyroptosis. While inflammasome activation and subsequent IL-1 β release have been tightly associated with pyroptosis, it has become increasingly evident that these are separate events that do not necessarily occur in unison, or depend upon the same factors^{132,138}. Caspase-1, which was presumed to be essential for both IL-1 β maturation and the induction of pyroptosis, does not appear to be critical for either, depending on the circumstance. Instead, other caspases can provide these functions in a redundant fashion. Caspase-8, which is mainly associated with apoptosis, has several additional inflammasome-related functions, including indirect regulation of Nlrp3 and IL-1 β mRNA via effects on NF- κ B

activation^{131,139–143}, direct cleavage of both IL-1 β ^{138,144–148} and caspase-1¹⁴⁹, as well as scaffolding properties¹⁵⁰ and formation of a Rip kinase-dependent type of cell death termed necroptosis^{146,148,150,151} in both the presence or absence of caspase-1, and in some cases without NLR-involvement^{145,146}. Similarly, a non-canonical inflammasome dependent on caspase-11 has been shown to be involved in the pyroptotic response to cytosolic LPS^{152–154}, further complicating the process.

Once the inflammasome complex has been assembled, pro-IL-1 β and pro-IL-18 are proteolytically cleaved into their mature forms, which are released into the extracellular space by an unknown mechanism. Interestingly, the functions of these cytokines in the intestinal environment appear to be somewhat opposing, with IL-1 β mainly promoting inflammation^{155–157}, whereas IL-18 appears to be involved in more anti-inflammatory processes, notably epithelial repair^{158–161}, as well as promoting type 1 immunity¹⁶² and being strongly associated with inflammatory bowel disease^{163,164}. Due to these conflicting functions, the role of inflammasomes in intestinal homeostasis and inflammation is still largely unclear^{156,159,165–167} and the precise role for each inflammasome, as well as possible redundancy between them, remains to be determined.

In summary, the intestinal immune system plays a central role in the generation of both protective immunity to invading pathogens, as well as tolerance to commensal microbes and harmless environmental and dietary antigens. This delicate balance is regulated by both the immune system and the microbiota, and is crucial for human health. Now that the basic mechanisms that govern this process have been established, we can turn our attention to the interaction between intestinal parasites and the host, which is the main focus of this thesis.

Host-parasite interactions

Parasite biology

In contrast to various parasites, most pathogens are too small to be seen with the unaided eye, and so for a long time were completely unknown. In fact, prior to the discovery of microscopic life forms by Antonie van Leeuwenhoek, it was assumed that most diseases were caused by parasitic worms, many of which belong to the nematode family. Indeed, nematodes are so abundant that it led the notable nematologist Nathan Augustus Cobb to proclaim that:

...“if all the matter in the universe except the nematodes were swept away, our world would still be dimly recognizable, and if, as disembodied spirits, we could then investigate it, we should find its mountains, hills, vales, rivers, lakes, and oceans represented by a film of nematodes. The location of towns would be decipherable, since for every massing of human beings there would be a corresponding massing of certain nematodes. Trees would still stand in ghostly rows representing our streets and highways. The location of the various plants and animals would still be decipherable, and, had we sufficient knowledge, in many cases even their species could be determined by an examination of their erstwhile nematode parasites.”¹⁶⁸

Roundworms, hookworms, pinworms, whipworms and filarial worms all belong to the nematode family, and are further grouped into the ecdysozoan superfamily due to their ability to undergo ecdysis, or molting. Nematodes need to molt several times in their lifespan in order to grow and mature, as they are covered in an exoskeleton known as a cuticle, primarily composed of collagen and chitin. The cuticle not only affords protection, but also is critical to maintain body pressure, and functions both as an absorptive and excretory organ. Life cycles vary substantially between different parasitic nematode species. However, most reproduce sexually, whereby eggs are shed, which after a period of embryonation become infective. Furthermore, each species is fairly specific to its host, suggesting a long coevolution between parasite and host. Given that nematodes are found in every biotope and can parasitize both animals (including humans) and plants, they are of tremendous scientific, medical and economical importance; so much so that one of the major model organisms in biology, *Caenorhabditis elegans*, is a roundworm. My work has focused on the parasitic whipworm *T. muris*, a close relative of the important human pathogen *Trichuris trichiura*.

T. muris

Research conducted with *T. muris* dates back over sixty years¹⁶⁹. Many of the core findings are common to other extracellular parasites and have thus provided substantial insight into the interaction between nematodes and the immune system.

As with other *Trichuris* species, *T. muris* infection begins with ingestion of infective eggs by the host, with larvae hatching mainly in the cecum of the large intestine within a few hours of infection^{169,170}. Hatching is sensitive to temperature, pH and the presence of both commensal and pathogenic bacteria, including *Escherichia coli*, *Lactobacillus reuteri*, *Pseudomonas aeruginosa* and *Staphylococcus aureus*^{171,172}, which in some cases appears to involve direct contact between eggs and bacterial fimbriae^{171,173}, although this might vary between *T. muris* strains¹⁷⁴ and species of *Trichuris*¹⁷². Larvae subsequently penetrate the mucus and burrow into the epithelium (without breaching the basal lamina) where they remain embedded throughout their lifespan. *Trichuris* worms are presumed to accomplish this feat by releasing a mixture of molecules termed E/S antigens, which aid in degrading mucins¹⁷⁵ and extracellular matrix proteins¹⁷⁶, as well as weakening epithelial membrane integrity^{177,178}. Worms reach patency and mate approximately five weeks later (unless expelled by the host), then females release eggs into the lumen that are shed with the feces, which after a period of embryonation become infective and can complete the life cycle.

The outcome of *T. muris* infection is determined by several factors, which converge to render mice resistant or susceptible. The first is genetic diversity among worms, which is made evident by the observation that different strains have varying infectivity^{179,180}. For instance, most studies (including ours) have employed a strain initially derived from wild mice in Scotland¹⁶⁹, whereas a more recent strain was obtained in Portugal, which is less efficiently expelled^{179,180}. The second determining factor is genetic diversity among hosts, which is reflected by varying susceptibility between different mouse strains¹⁸¹, as well as humans^{182,183}, with similar patterns observed for other parasites¹⁸⁴⁻¹⁸⁷. The underlying cause for these discrepancies has been attributed to the MHC alleles¹⁸⁸⁻¹⁹⁰, which strongly implies that resistance and susceptibility is governed by adaptive immunity. Thus, while BALB/c mice (H-2d) are inherently resistant, expelling within two to three weeks after infection, AKR mice (H-2k) are fully susceptible and do not expel at all. The third factor is the sex of the host, as males tend to be more susceptible than females within some mouse strains¹⁹¹. These differences are also under genetic control, and are largely due to inherent variation in cytokine production¹⁹², which will be discussed in more detail further on. The fourth and final factor is egg dose, where interestingly, high infection doses promote worm expulsion whereas infection with low doses results in chronicity¹⁹³. Thus, C57BL/6 mice (H-2b), which lie in-between BALB/c and AKR mice in the spectrum of resistance and susceptibility, are generally not capable of expelling less than 40 worms, but efficiently clear over 400. This dose-response phenomenon is not unique to *T. muris*, as infection with the intracellular protozoan *Leishmania* is expelled at high but not low doses¹⁹⁴, also being associated with infection-induced adaptive immune responses, similar to *T. muris* infections. The fact that low-dose infections with *T. muris* result in chronicity, whereas high doses are efficiently cleared, might seem counterintuitive but speaks to the coevolution of parasites and their

hosts¹⁹⁵. High-dose parasite infections are probably rare in the wild^{196,197}, and mice are rather more prone to be exposed to several low doses, amounting to higher doses over time. This phenomenon can also be observed under experimental conditions, where several consecutive low-dose infections give rise to a high-dose infection, which is not as efficiently expelled as a single high dose¹⁹⁸. The reason why one high dose does not elicit more of the same inefficient response is unclear, but might be due to a particular threshold being crossed, perhaps of tissue damage caused by increasing numbers of worms. Consistently, engagement of the tissue-repair arm of the immune system is, as we shall see, tightly associated with the response required to successfully combat parasites. Together, these four factors form the basis of resistance and susceptibility by shaping the innate and adaptive immune response into one of three types, which ultimately dictates the outcome of infection. Resistant mice are consequently characterized by the induction of type 2 immunity, with expulsion primarily driven by IL-13^{187,199–201}, which will be discussed at length in the subsequent section. The importance of the immune system can be further illustrated by the fact that genetically susceptible mice that have been infected with a low dose of *T. muris* eggs, which under normal circumstances would amount to chronicity, are able to clear the infection if there is appropriate immune intervention. Accordingly, if recombinant cytokines or neutralizing antibodies that promote protective immunity are administered, mice can be rendered resistant (and *vice versa*), a pattern which holds true for several parasites^{191,202–208}. In other words, what ultimately determines whether the host will expel the parasite or be chronically infected is the immune system.

Immunity toward *T. muris* is generated during the first few weeks after infection, before worms reach patency, given that parasite-specific cytokine responses can be detected within this period, and that expulsion can occur during the earlier larval stages in some mouse strains⁹⁷. Moreover, cortisone treatment can prevent worm clearance in normally resistant mice if administered early after infection^{209,210}, clearly implicating the immune system. Indeed, T cells play a critical role in protection, as is evident from athymic mice^{211,212}. Furthermore, immunity is mediated by helper T cells rather than cytotoxic T cells, as shown by the neutralization of CD4⁺ but not CD8⁺ cells²¹³, and by adoptive transfer of CD4⁺ T cells from a previously infected resistant strain, which confers protection in normally susceptible lymphopenic mice²¹⁴. By contrast, the role of B cells in the immune response to *T. muris* is somewhat complicated. Adoptive transfer of B cells alone from previously infected mice is insufficient to confer resistance²¹⁵. However, mice that lack mature B cells appear to have less efficient expulsion²¹⁶, and transfer of IgA²¹⁷ or IgG²¹⁸ antibodies from resistant mice confers partial resistance, most likely due to their neutralizing effect on secreted parasite antigens, or by trapping larvae, which is mirrored by other parasite models^{219–221}. These findings suggest that B cells might play a role in promoting the generation and/or polarization of the T cell response, either by antigen-presentation or cytokine secretion. Whether or not antibodies generated

by long-lived plasma cells or memory cells can be protective upon secondary *T. muris* challenge has yet to be determined.

Clearly, the expulsion of parasitic worms is a complicated event involving more than just one cell type, and likely dependent on several distinct mechanisms. I therefore want to discuss the intricate process from infection to expulsion in more detail.

Parasite immunology

Extracellular parasite infections are fundamentally different from other pathogen encounters. While the average bacterium is around two micrometers in length, multicellular organisms like *T. muris* can be upwards of two centimeters in length when fully mature, and although the mental image is amusing, a macrophage cannot degrade, let alone phagocytose, a parasite several hundred times its own size. Thus, it is not surprising that the fundamental physiological and immunological mechanisms required to deal with these infections are completely different from those involved in response to bacterial, fungal or viral infections. This inherent difference between groups of pathogens has given rise to the idea that immunity can be categorized into several arms; each highly specialized for particular types of microorganisms, and able to counteract one another. Type 1 immunity for instance, which is characterized by the production of IFN- γ , is critical for combating small intracellular pathogens like viruses and bacteria, but is essentially useless against large multicellular organisms such as parasitic worms²⁰⁴. Similarly, extracellular bacteria and fungi elicit a related form of immunity, characterized by the production of IL-17, which for simplicity will be referred to as type 3 immunity. The inefficiency of these types of immunity against parasitic infections is not due to proportion, where if anything, the stronger the response the less likely the host will be to expel any worms. Moreover, an improper immune response is not only ineffective, but can also be dangerous by causing chronic inflammation and increased tissue destruction^{222,223}. Instead, a wholly different set of mechanisms is required for expulsion of parasitic worms, which has been termed type 2 immunity.

The type 2 response entails several biological processes that serve to disrupt the parasite niche, and revolve around strengthening the physical barrier and promoting tissue-repair. These mechanisms are highly coordinated and involve many different cell types and molecules, which have been implicated at various stages in the generation and execution of this response. Indeed, immunity to gastrointestinal parasites can be categorized into five distinct steps: detection, transmission, induction, execution and resolution. Each step is critical and involves unique cell types and effector molecules, which are essential for protective immunity. In this chapter, I will attempt to summarize our current understanding of the inflammatory cascade elicited upon parasite infection. Several model organisms besides *T. muris* have been frequently used and will be included in the discussion where possible to highlight general trends or unique exceptions in the field.

Detection

Although the early events after *T. muris* infection are poorly understood, epithelial cells are clearly the first cells to come in contact with *T. muris* larvae once the mucus barrier has been breached. However, whether or not infected epithelial cells remain alive and are capable of recognizing and responding to parasite-derived antigens is unknown. Alternatively, uninfected epithelial cells adjacent to infected cells might sense the ongoing infection and respond. Regardless, mice in which NF- κ B signaling is abrogated specifically in epithelial cells are incapable of mediating worm expulsion²²⁴, strongly indicating that there is need for epithelial activation. Recent evidence from several other models of nematode infection, including *Heligmosomoides polygyrus*, *Nippostrongylus brasiliensis* and *Trichinella spiralis*, indicate that specialized chemosensory cells called tuft cells are critical for providing the early signals that drive type 2 immunity^{225–227}. However, it is unclear whether the worms are sensed directly by tuft cells or indirectly via signals from other epithelial cell subsets prior to activation. Also, it should be noted that in contrast to *T. muris*, the parasites mentioned all infect the small intestine at some point in their life cycle, and so it remains to be determined whether tuft cells are involved in large-intestinal immunity to parasite infection as well. Nevertheless, mice that lack tuft cells do not expel *N. brasiliensis*²²⁵ thus implicating tuft cells in the generation of protective immunity.

What epithelial cells are actually recognizing is still largely unknown. In the case of *T. muris*, it is clear that IgA²¹⁷ and IgG1²¹⁸ antibodies, both of which can confer protection, bind to proteins within the E/S antigens. However, these antigens are not necessarily recognized by epithelial cells, but rather by dendritic cells or macrophages²²⁸, and thus might not serve as the initial trigger of type 2 immunity. Interestingly, chitin induces strong type 2 immunity in the lungs of mice infected with *N. brasiliensis*²²⁹. In line with these data, acidic chitinase, which is expressed in both intestinal and pulmonary epithelial cells and macrophages^{230–232}, and serves to break down chitin, is required for optimal protection against both *N. brasiliensis* and *H. polygyrus*²³³. However, chitin alone is an insufficient explanation for the induction of type 2 immunity, as it is also a major component of the fungal cell wall, which normally induces type 3 immunity^{234,235}. Given that multicellular parasites tend to cause more tissue destruction than other pathogens (due to their sheer size and invasiveness) it is perhaps more likely that type 2 immunity results from combined recognition of both endogenous damage-associated alarmins and worm-derived molecules that become available for uptake after molting, including chitin, as well as parasite-derived antigens that are continuously secreted throughout infection.

Transmission

Once a parasite has been detected by the epithelium, the signal must be transmitted to cells of the innate immune system so that an appropriate inflammatory cascade can be initiated, along with the induction of adaptive immunity. The main epithelial-

derived cytokines implicated in the early generation of type 2 immunity are IL-25^{225–227,236,237}, IL-33^{238–240} and TSLP^{224,241,242}, which strongly synergize and prompt the release of IL-4, IL-5, IL-9 and IL-13 from various innate immune cells, notably ILC2s, which appear to play a prominent role early after infection^{225–227,236,243–247}. While ILC2s share many characteristics with Th2 cells, for instance the requirement of GATA-3 expression during their differentiation^{248–252}, they are primarily activated by cytokines rather than antigen, in contrast to T cells. Epithelium-derived IL-25 and IL-33, in particular, are important for driving IL-5 and IL-13 production from ILCs, the latter of which induces a number of responses, including goblet and tuft cell expansion, thus resulting in a strong positive feedback loop with increased production of IL-25 by epithelial cells^{225–227,240,243–246}. Indeed, mice lacking IL-25 have less efficient worm expulsion, *T. muris* included^{236,237,253,254}. Furthermore, exogenous administration of IL-25 fails to restore expulsion in IL-13-deficient mice^{236,253}, whereas the reverse is true^{225,227}, illustrating that IL-25 acts upstream of IL-13 rather than directly on expulsion. Strikingly, exogenous administration of IL-25 in the early stages of *N. brasiliensis* infection results in worm expulsion in both wild-type and lymphopenic mice, strongly suggesting that at high enough concentrations, IL-25-mediated ILC2 activation can overcome T and B cell deficiency, which normally is associated with chronicity²³⁶. Also, it should be noted that while epithelial tuft cells appear to be the main producers of IL-25 in mice^{225,227}, human eosinophils and basophils are capable of secreting this cytokine as well²⁵⁵. Nevertheless, mice that lack the IL-25-regulating protein Act1 specifically in epithelial cells cannot expel *N. brasiliensis*²⁵⁶, further emphasizing the importance of epithelial-derived IL-25 in mediating type 2 immunity.

Whereas IL-25 is predominantly tuft cell-derived, IL-33 is expressed by several epithelial cell subsets²²⁷, as well as some dendritic cells²⁵⁷, and functions in a slightly different way. It belongs to the IL-1 family of cytokines and is thus translated in a pro-form that can be further processed. However, in contrast to IL-1 β and IL-18, IL-33 is biologically active prior to cleavage and localizes to the nucleus where it binds chromatin, although its precise function is unclear²⁵⁸, but appears to be inactivated rather than activated upon cleavage by caspase-1²⁵⁹, thus preventing its function as an epithelial-derived alarmin under normal conditions. By contrast, once IL-33 is released in the setting of tissue damage, it can be further activated by granulocyte-derived proteases to exert its function^{260,261}. Much like IL-25, it is important for driving IL-13-production by ILC2s during infection^{240,244}, and can also be recognized by other cell types, including granulocytes^{262,263}, dendritic cells²⁶⁴, as well as activated helper T cells²⁶⁵. Furthermore, while exogenous administration of IL-33 at early time points after *T. muris* infection promotes worm clearance, injection at later stages of infection does not induce expulsion²³⁸, suggesting that there is an early window of opportunity in which it exerts its effects. In addition, neither IL-25 nor IL-33 alone is sufficient to drive expansion or activation of ILCs²⁴⁴, indicating that there is a concerted activity between the two cytokines.

Another function of IL-33 is to induce the expression of TSLP in the epithelium²³⁸. The data on TSLP are sparse, but unlike IL-25 and IL-33, which are critical for the expulsion of multiple parasites, TSLP appears to be involved only during *T. muris*, but not *N. brasiliensis* or *H. polygyrus* infections^{224,241,242}, which is understandable given that TSLP is mainly expressed in the large intestine²⁴². TSLP can be directly recognized by dendritic cells²⁶⁶, as well as basophils²⁶⁷, again suggesting that epithelial-derived cytokines can bypass ILCs. Indeed, although the main target of IL-25, IL-33 and TSLP appear to be ILC2s, it should be noted that both murine and human memory T cells are strongly activated by IL-25^{255,265}, IL-33^{265,268,269} and TSLP^{265,270}, without the need for T cell-receptor engagement^{269,271}, unlike their naive counterparts, thus being able to respond antigen non-specifically. Hence it remains to be determined whether ILCs are truly critical for anti-parasitic immunity in previously challenged hosts.

In contrast to epithelial-derived cytokines and alarmins, the hematopoietic-derived type 2 cytokines are likely involved during both early and late stages of infection, but while there is considerable functional redundancy between IL-4, IL-5, IL-9 and IL-13, they have unique characteristics in driving the type 2 response. IL-13 is by all accounts the most pivotal, being required, at least in the skin and lungs, for the recruitment of dendritic cells, which subsequently drive adaptive immunity^{272,273}. IL-13 is also critical for inducing many of the expulsion mechanisms in the intestine, which will be discussed further on. This redundancy is revealed by the fact that even in the absence of IL-4, IL-13 can compensate in some cases. For instance, while IL-4 deficiency strongly affects the expulsion of *T. spiralis* in C57BL/6 mice, BALB/c mice are not affected by the lack of this cytokine, whereas IL-13 deficiency is equally debilitating in both strains¹⁸⁷. Similarly, IL-4-deficient female mice are still resistant to *T. muris* infection, in contrast to their male counterparts, mostly due to a stronger propensity for IL-13 production¹⁹¹. Furthermore, with the exception of in the skin²⁷⁴, IL-4 appears to be dispensable for *N. brasiliensis* expulsion^{200,250}. The redundancy between IL-4 and IL-13 likely stems from their shared usage of the IL-4R α subunit^{275–277}, although interestingly, IL-4R α deficiency in T cells has no impact on worm expulsion during either *T. spiralis*²⁷⁸, *H. polygyrus*²⁷⁹ or *N. brasiliensis*^{200,201} infections, in contrast to total IL-4R α ablation^{187,279–281}. Instead, IL-4 might need to be produced by T cells, rather than being recognized, as it is mostly secreted by follicular helper T cells to promote IgG1 class switching of B cells²⁵⁰. Nonetheless, IL-4 production by ILC2s has recently been critically linked to *H. polygyrus* expulsion, and interestingly was dependent on leukotriene D4²⁸². However, leukotriene D4 did not induce IL-13 or IL-5 expression, which as mentioned is mainly promoted by IL-25 and IL-33, illustrating a compartmentalized activation mechanism. IL-4 is also produced by basophils^{250,283,284}, which is also more likely to be important for humoral immunity.

IL-5 has a complicated and context-dependent role in type 2 immunity. As with IL-13, it is secreted mainly by ILCs, but functions predominantly as an eosinophil

recruitment and growth factor^{285,286}. There is little data, however, to suggest that deficiency in either IL-5 or eosinophils has an effect on parasite expulsion, despite that eosinophil-derived mediators can skew dendritic cells to promote type 2 immunity^{287,288}. Thus, eosinophils do not appear to be critical for the generation of Th2 immunity or clearance of *T. muris*⁹⁷, and blocking IL-5 does not affect *H. polygyrus* expulsion despite significantly decreasing eosinophil numbers²⁰². However, mice that overexpress IL-5 have massive eosinophilia and are less susceptible to *N. brasiliensis*²⁸⁹. By contrast, eosinophil-deficient mice are unimpaired in their ability to expel *N. brasiliensis*²⁹⁰, illustrating that IL-5 has additional unknown functions beyond those associated with eosinophils.

As with the role of IL-5 in promoting eosinophil responses, IL-9 acts mainly as a maturation factor for mucosal mast cells^{291–293}, and is largely T cell-derived^{294–296}, although it can be secreted by ILC2s²⁹⁷, as well as by mast cells themselves^{298,299}, which in turn promote enhanced secretion of IL-25, IL-33 and TSLP from epithelial cells³⁰⁰. As a result, *T. muris* and *H. polygyrus* expulsion are impaired in mast cell-deficient mice^{300,301}, as well as upon administration of neutralizing IL-9 antibodies^{302,303}. Furthermore, mast cells might contribute to worm expulsion through the release of various proteases, which serve to loosen tight junctions between epithelial cells, thus aiding in the shedding of embedded worms, notably during *T. spiralis* infection^{304–306}. However, mast cells appear to be dispensable for the expulsion of *N. brasiliensis* infection^{307–309}, illustrating the context-specific nature of mast cell responses.

Clearly, there is substantial complexity and functional redundancy within the innate immune system given that the same type of response is elicited in various tissues upon different stimuli, such as parasites and allergens. However, the precise sequential mechanisms that govern type 2 immunity remain to be elucidated.

Induction

Once the innate immune system has been alerted to the presence of an infectious parasite, it must propagate the signal further and engage the adaptive immune system; a task mainly accomplished by dendritic cells. During *T. muris* infection, dendritic cells accumulate in the intestinal mucosa, preferentially in resistant mouse strains, where they localize in vicinity of the epithelium^{310,311}. Intestinal dendritic cells can be divided into three distinct subsets based on the sole or combined expression of CD11b and CD103, all of which are capable of migrating to intestinal-draining mesenteric lymph nodes upon activation, as well as priming naive T cells. Our unpublished data (courtesy of Mimoza Demiri) indicate that IRF4-dependent CD11b⁺ dendritic cells are crucial for expulsion of acute *T. muris* infection. Consistently, migratory IRF4-dependent dendritic cells in both the skin and the lungs are required for the generation of Th2 responses to infection with the parasitic trematode *Schistosoma mansoni*^{312,313} and *N. brasiliensis*^{314,315}, as well as to allergic

challenge in the lungs^{264,312,313,316} and the skin³¹⁷. Conversely, IRF8-dependent CD103⁺ dendritic cells are important for the generation of type 1 helper^{318,319} and cytotoxic⁷⁷ T cell responses, thus promoting *T. muris*³¹⁹ and *H. polygyrus*³²⁰ chronicity. Together, these data illustrate that a specialized subset of dendritic cells is responsible for the induction of Th2 responses in various tissues. However, the precise mechanisms behind this compartmentalization are not clear, but might involve cell-intrinsic signals that actively suppress the generation of type 1 immunity, and vice versa. One such example is the phosphatase SHIP-1, which if specifically deleted from dendritic cells results in impaired *T. muris* expulsion via enhanced production of IL-12³²¹. Similarly, the notch ligand jagged appears to be important for dendritic cells to prime effective Th2 responses *in vitro*³²², as is the expression of CD40 in response to *S. mansoni* egg-derived antigens³²³. Furthermore, different dendritic cell subsets likely have divergent expression of certain cytokine and pattern-recognition receptors, and might thus be inherently more or less prone to respond to specific pathogens and cytokines^{324–327}. These types of signals, in combination with cell-extrinsic signals, including those from ILCs²⁷³, could determine which type of dendritic cell that gets activated upon parasite infection. Furthermore, the nature of the initial stimulus is likely to have an impact on the resulting response. For instance, dendritic cells in the skin of mice that are exposed to *N. brasiliensis* infection or the contact sensitizer dibutyl phthalate, both of which induce type 2 immunity, acquire completely distinct transcriptional profiles, revealing a novel role for type 1 interferons during *N. brasiliensis* infection³²⁸, and highlighting the complicated nature of pathogen recognition by the innate immune system.

Interestingly, some studies suggest that both basophils^{329–331} and ILCs^{332,333} can express MHC-II and directly prime Th2 responses, including toward *T. muris*³²⁹, without the need for dendritic cells. However, neither of these cell types typically migrate to draining lymph nodes upon infection, and given that Th2 immunity is abolished in mice where dendritic cells have been depleted^{334,335}, it is perhaps more likely that basophils and ILCs contribute to local tissue immunity by promoting dendritic cell activation, or by further enhancing the cytokine response of mature T cells that have migrated to the infected tissue²⁶⁵. Furthermore, the common strategies hitherto employed to deplete ILCs are not as specific as previously thought, and mice deficient in activated ILC2s are equally capable of expelling *N. brasiliensis* from the intestine of lymphopenic mice that have been reconstituted with naive CD4⁺ T cells, regardless of whether or not the ILCs expressed MHC-II²⁶⁵, indicating that naive T cells can be primed in the absence of ILCs. Moreover, dendritic cells are responsive not only to ILC-derived cytokines, but also to epithelium-derived cytokines, including TSLP²⁶⁶ and IL-33²⁶⁴, thus possibly bypassing the innate immune system completely.

Execution

Once adaptive immunity has been induced in the local lymph nodes, activated

T cells must home back to the site of infection where expulsion can take place. *T. muris* expulsion depends on a combination of physiological mechanisms that include enhanced mucus secretion by goblet cells, release of neutralizing proteins by granulocytes and epithelial cells, as well as epithelial hyper-proliferation and intestinal peristalsis via increased smooth-muscle contractility. The first, and perhaps most important, mechanism is increased production of mucins, which trap worms and impede motility, thus preventing further burrowing into the epithelium. Mice lacking mucin 2, the major component of the mucus layer, are rendered susceptible and cannot expel *T. muris*³³⁶, illustrating the importance of this barrier. Nonetheless, *T. muris* larvae are still able to penetrate the mucus layer of normal mice upon hatching, indicating that they have evolved strategies to circumvent this obstacle. Indeed, one of the main E/S components is a serine protease with the capacity to degrade mucin 2¹⁷⁵. The type 2 immune response however, acts not only to increase goblet cell proliferation and mucus production, but also by switching to secretion of mucin 5ac, which is resistant to degradation by the E/S antigens¹⁷⁵. In addition, the host can produce serine-protease inhibitors that prevent further loss of mucin 2¹⁷⁵. Consistent with these data, mucin 5ac is only up-regulated in resistant mouse strains³³⁶ and mucin 5ac-deficient mice have impaired expulsion of *T. muris*, *N. brasiliensis* and *T. spiralis*³³⁷. Increased mucus production and the mucin switch are largely driven by IL-13³³⁷, IL-4³³⁸ and IL-22³³⁹, all of which render mice susceptible when ablated genetically. The principle of physical obstruction provided by mucus layers can also be extended to other mucosal sites like the lungs where the lectin surfactant protein-D, which acts as a lubricant, is needed for optimal protection against *N. brasiliensis*³⁴⁰.

The second, and often overlooked, expulsion mechanism is the release of various compounds by activated granulocytes and epithelial cells, most of which are toxic to parasites. The relative contribution of each molecule is highly context-dependent. For instance, although eosinophils release a plethora of toxic compounds, which are potent in killing worms *in vitro*^{341,342}, eosinophils appear to be dispensable during most worm infections, as was mentioned. However, eosinophil-deficient mice appear to have a thinner mucus layer⁹⁶, which might impact on their susceptibility to infection rather than on subsequent expulsion given the protective nature of mucus. Goblet cells, by contrast, secrete several molecules besides mucins that could contribute to defense against parasites³⁴³⁻³⁴⁵. The RELMs, in particular, appear to prevent worms from feeding by effectively coating their cuticle, thus hampering growth, as well as blocking motility and attachment to the host epithelium^{343,345}. For instance, RELM β expression is highly increased in the intestinal epithelium during several parasite infections³⁴³, likely induced by ILC-derived type 2 cytokines³⁴⁵, and might be required for efficient expulsion of *N. brasiliensis*, although the data are conflicting^{345,346}. By contrast, there seems to be no role for RELM β in the expulsion of *H. polygyrus* or *T. muris*^{344,345}. RELM α , on the other hand, is mainly expressed in the pulmonary epithelium and might be important for *N. brasiliensis* expulsion³⁴⁶. RELM α

is further implicated in the functioning of alternatively activated macrophages, which although not critical during *T. muris* infection³⁴⁷, have been implicated in the expulsion of *H. polygyrus*³⁴⁸ and *N. brasiliensis*³⁴⁹, highlighting its role in type 2 immune responses.

After being trapped in mucus and coated by various toxic proteins and neutralizing antibodies, worms are expelled by a combination of increased epithelial proliferation and intestinal peristalsis. Given that the epithelium has a rapid turnover, worms need to continuously burrow in order to remain within their niche. Accordingly, epithelial hyper-proliferation serves to shift the epithelium outward from the crypts, whereas peristalsis could aid in shedding the infected cells. Increased epithelial turnover seems to occur mainly in resistant mouse strains, largely driven by IL-13³⁵⁰. However, IFN- γ also induces crypt hyperplasia in susceptible strains, but is insufficient in driving expulsion³⁵¹, likely due to the absence of appropriate mucus secretion, and perhaps because of increased apoptosis of epithelial cells³⁵², which might impede the outward epithelial movement or just extend crypt length without affecting turnover. Intestinal peristalsis is mediated by contraction of smooth muscle cells, and is induced by both IL-9³⁰³, as well as IL-4 and IL-13^{253,279,349}, and seems to be controlled mainly by T cells. While highly correlative, it appears to play a role during *T. muris* infection³⁰³ but is dispensable for *N. brasiliensis*²⁷⁹ and *T. spiralis*³⁰³ infection. Together however, these mechanisms effectively expel the invading parasite.

Both innate and adaptive immune cells secrete many of the cytokines implicated in the execution of type 2 immunity. Which is the more important source is not entirely clear, and likely depends on both the parasite in question and precise timing after infection. Whereas the role for Th2 cells in parasite expulsion is paramount, some data suggest that T cell-derived IL-4 and IL-13 are dispensable for parasite expulsion, at least in the case of *N. brasiliensis* infection^{247,353}, and can likely be provided by ILCs. However, given that T cells represent a much larger pool of effector cells in most infectious contexts, the two populations probably amplify each other in a concerted effort to expel the invading parasite.

Resolution

Once a parasite has been expelled, the affected tissue must be repaired. This process is partly orchestrated by type 2 cytokines and involves several cell types, including eosinophils and alternatively activated macrophages. Thus, despite being redundant for *T. muris* expulsion⁹⁷, eosinophils might be important for wound healing and tissue regeneration in which they have been implicated in non-mucosal tissues^{354–356}. Similarly, whereas macrophages are mostly unresponsive to pathogen stimulation, as was discussed in the previous chapter, type 2 cytokines give rise to alternatively activated macrophages, which might be involved in the expulsion of certain parasites^{281,348}. Furthermore, resident macrophages in the intestinal mucosa are also likely to play an important role in tissue repair, as has been shown in various

settings of inflammation^{357–362}. Thus, eosinophil or macrophage depletion might not necessarily have any visible impact on worm expulsion, but rather on tissue healing after clearance. Eosinophils have also been shown to promote the survival of long-lived plasma cells in the bone marrow³⁶³, as well as the generation of IgA-secreting plasma cells in the gastrointestinal tract^{94,96} (at least in the small intestine³⁶⁴) via the production of IL-1 β , suggesting that they might impact on secondary challenge infections where antibodies presumably play a larger role. Indeed, both IL-5 and eosinophil-deficient mice have increased *N. brasiliensis* larvae after secondary infection²⁹⁰, with similar results during secondary *T. spiralis* infection³⁶⁵. Furthermore, eosinophils negatively regulate Th17 cells³⁶⁶, and promote the expansion of regulatory T cells in the steady state^{94,95}, which might impact on overall inflammation, illustrating their complex contribution to tissue homeostasis.

Consequences

Whereas most research on host-parasite interactions has focused on the underlying factors that govern resistance and susceptibility, the long-term consequences of both acute and chronic worm infections are still largely unknown. Given the inverse correlation between parasite exposure and the occurrence of immune-associated disorders, it is quite surprising that so little attention has been devoted to this subject, particularly in the case of *Trichuris* infections that have been in clinical trial for the treatment of various inflammatory disorders^{367,368}. Chronically infected mice do not display any overt symptoms of disease, but are by no means unaffected considering that persistent *T. muris* infections are lethal in the absence of IL-10²²², indicating that there is ongoing inflammation beyond the spontaneous inflammation inherent to IL-10-deficient mice. Indeed, chronic *T. muris* infection results in the accumulation of IFN- γ ⁺ T cells in the bone marrow³⁶⁹, and does not appear to protect against the development of colitis^{370,371}, but rather exacerbates disease (our own unpublished data). Furthermore, depending on the strain, chronically infected mice gain less weight than their uninfected counterparts³⁷², and in some cases even acquire colitis-like symptoms, thus losing weight²²³, mirroring the malnutrition and wasting of some infected humans. By contrast, lung pathology appears to be decreased in response to papain challenge³⁷³, illustrating that worm-induced protection against inflammatory disorders is highly context-specific. Data on the long-term effects of acute *T. muris* infection are even sparser. Alternatively activated macrophages seem to increase in number after expulsion³⁷⁴, likely being involved in tissue repair. However, other potential long-lasting consequences of acute *T. muris* infection remain largely unexplored.

In summary, parasitic nematodes are found in essentially every biotope, and have played an important role in the evolution of the intestinal immune system. Their presence leads to the induction of the type 2 response, which involves a vast array of cell types and molecules that work in concert to promote protective immunity to a wide range of extracellular parasites at mucosal surfaces. While some worm

infections might be beneficial to human health, the long-term consequences of chronic or acute infections remain poorly understood.

Synopses

Paper 1

Acute infection with the intestinal nematode *Trichuris muris* has long-term consequences on mucosal mast cell homeostasis and barrier integrity

Daniel Sorobetea, Jacob Bak Holm, Henrietta Henningsson, Karsten Kristiansen and Marcus Svensson-Frej

European Journal of Immunology, 47, 257-268 (2017)

Background

Whereas host-parasite interactions are frequently studied during the course of infection, the long-term consequences of acute parasite infections beyond expulsion have been largely overlooked. *Trichuris* infections, in particular, are of substantial importance given their proposed use for the treatment of inflammatory disorders. The aim of this study was therefore to characterize the long-term consequences of acute *T. muris* infection on intestinal homeostasis, with a particular emphasis on innate immunity.

Results

- Mucosal mast cells accumulated in the large-intestinal epithelium upon acute *T. muris* infection, and persisted for several months after worm expulsion.
- Accumulation was due to a combination of increased output from mast cell progenitors in the lamina propria and prolonged mast cell survival in the epithelium, largely driven by the type 2 immune response.
- Epithelial mast cells acquired a unique phenotype as compared to their lamina propria counterparts, notably expressing Siglec-F, a lectin previously associated mainly with eosinophils.
- High levels of the mucosal mast cell-derived chymase MCPt-1 could be detected both locally in the tissue, as well as systemically in the circulation, indicating that the cells were activated.
- The integrity of the intestinal barrier was compromised, which was reversed by mast cell depletion.

Discussion

During recovery from an acute infection or inflammatory process, inflammation is resolved and the affected tissues are presumed to return to their previous steady state. Our data strongly indicate that this is not always the case however; rather, a new steady state can be formed after pathogen clearance, with drastically altered proportions of effector cells in the intestinal mucosa. Accordingly, after acute *T. muris* infection, we observed a large increase in mucosal mast cell numbers in the large-intestinal epithelium. These cells appeared to be activated, as judged by their

granular appearance and the high levels of mast cell-derived MCPt-1 being released upon *ex vivo* culture, despite the lack of parasite-derived antigens present or any overt signs of inflammation. While type 2 immunity appeared to be of importance, the driving factor behind the accumulation and activation of epithelial mast cells remains unclear, although TGF β might be involved given its documented role in promoting the induction of CD103 and IgE-independent MCPt-1 expression in mucosal mast cells^{375,376}. Regardless, the intestinal epithelium was more permeable after infection, indicating that tissue homeostasis had been affected long-term as a result of acute *T. muris* infection. Moreover, while the prolonged accumulation of mucosal mast cells was specific to the site of infection, MCPt-1 could also be detected in the circulation, suggesting that acute *T. muris* infection might have long-lasting systemic effects as well, which might influence the outcome of subsequent immune challenge in other peripheral tissues, perhaps in settings of allergy. Indeed, while mast cells and their secreted products are implicated in type 2 immunity to certain parasites, they are also tightly associated with hypersensitivity reactions^{293,299} and are still the main therapeutic target in the form of anti-histamines.

It is difficult to reconcile our findings with the hygiene hypothesis, which as mentioned suggests that parasite exposure might prevent the development of immune-associated disorders. However, the possible protective nature of parasite infection might depend on the precise timing of infection, and the pathogen itself might be of crucial importance in this scenario. Whereas the E/S products from some other parasites have been shown to induce regulatory T cells^{377–379} and suppress inflammation^{380–383}, no such protein has yet been characterized within *T. muris*-derived antigens. Furthermore, out of the various parasite models in use, only *T. muris* infects the large intestine specifically. Due to the higher bacterial load, a disturbed barrier at this site might enable bacterial translocation into the tissue and thus counteract the possible anti-inflammatory effects of the worm itself. It thus remains to be determined whether the long-term consequences of *T. muris* infection are protective against or predispose to experimental food allergy.

Another interesting observation following acute *T. muris* infection is that we did not detect any striking effects on adaptive immune cells, but rather on mast cells. It is well established that acute infections generate long-lasting memory mediated by T and B cells. Our findings that acute *T. muris* infection has long-term consequences specifically on mucosal mast cells is therefore somewhat surprising and suggests that immunological memory in some form or another might apply to innate cells as well. Indeed, some recent studies have shown that monocytes and macrophages acquire epigenetic changes upon pathogen stimuli, which are long-lasting and result in enhanced responsiveness to subsequent infectious challenge^{384,385}, indicating that the concept of immunological memory might need to be revised. Given that the mucosal mast cells observed in the epithelium were essentially absent prior to *T. muris* infection, innate memory (if any) likely resides within the progenitors found in

the lamina propria, as they seemed to be the main source of mature epithelial mast cells.

In conclusion, our results suggest that acute *T. muris* infection has a profound long-term effect on tissue homeostasis and might influence the response to subsequent immune challenge.

Paper 2

Chronic *Trichuris muris* Infection Decreases Diversity of the Intestinal Microbiota and Concomitantly Increases the Abundance of *Lactobacilli*

Jacob Bak Holm, Daniel Sorobetea, Pia Kiillerich, Yulixais Ramayo-Caldas, Jordi Estellé, Tao Ma, Lise Madsen, Karsten Kristiansen and Marcus Svensson-Frej

PLOS ONE, 10, e0125495

Background

Parasitic nematodes come in close contact with the intestinal microbiota of the host upon infection, thus allowing for possible interaction. However, whereas infection-induced changes to microbial populations have been demonstrated in pigs and humans, the effect of *Trichuris* parasites on the intestinal microbiota is unclear, due to conflicting data^{386–389}. We therefore sought to assess the influence of chronic *T. muris* infection on the intestinal microbiota of mice, under controlled conditions, to gain a better understanding of its downstream consequences, which is of importance given the substantial impact of bacterial communities on intestinal homeostasis, the inverse correlation between parasite exposure and immune-associated disorders, as well as the potential use of nematode infections for therapeutic purposes.

Results

- Chronic *T. muris* infection resulted in a drastically altered intestinal microbiota composition, which became apparent after approximately three weeks of infection.
- Bacterial diversity was decreased as a consequence of infection, both within individual mice and the group as a whole.
- Several bacterial families were affected, with a notable increase in the relative abundance of *Lactobacilli*.
- Chronic infection was associated with a shift in the ratio between inflammatory and regulatory T cells in favor of inflammatory cells.

Discussion

In the present study, we found that chronic *T. muris* infection had strong effects on the intestinal microbiota, resulting in decreased bacterial diversity and increased relative abundance of *Lactobacilli*. These data illustrate that chronic parasite infections do not occur in isolation, but might have profound impact on host physiology, perhaps in positive ways, via indirect effects on commensal microbes. As such, worm infections have been inversely correlated with immune-associated disorders, including inflammatory bowel disease. A noteworthy case study reported how a man with ulcerative colitis self-medicated with *T. trichiura* eggs and went into remission for a lengthy period of time⁷. His symptoms returned after a couple

of years and a colonoscopy found that the parasites had largely disappeared, presumably due to their limited lifespan. He then proceeded to take another dose of eggs and went into remission again. While this was an isolated study involving only one person, it illustrates that worm therapy might be a possible alternative under controlled conditions. However, clinical trials with *Trichuris* eggs have been performed using *Trichuris suis* eggs (the porcine-equivalent), the fear being that a patent human parasite might cause too much tissue damage in severe cases of disease. *T. suis* is not well adapted to the human intestinal tract and only transiently infects the epithelium before being shed, thus leading patients to have to undergo repeated and costly egg treatments. Furthermore, the rationale for using *Trichuris* eggs was that they infect the large intestine, which is the primary site of inflammation in patients with ulcerative colitis. However, the clinical trials conducted have been for Crohn's disease⁶⁵, which although able to afflict any part of the gastrointestinal tract, affects mainly the terminal ileum, and so the infection is not situated at the site of inflammation. Thus, the overall evidence does not currently support the idea of a protective role for this particular parasite⁶⁵. Furthermore, no *Trichuris*-derived antigen has yet been shown to induce regulatory T cells, which presumably is one major contributing factor underlying the hygiene hypothesis. Accordingly, in our model we saw a shift in the balance between inflammatory and regulatory T cells, in favor of IFN- γ ⁺ T cells. Thus, despite the increase in *Lactobacilli*, which are thought to have dampening effects on some types of inflammation, this is likely not enough to offset the overall inflammatory response. Moreover, parallel studies from another group suggest that these changes in microbial communities reverted upon administration of anti-helminthic drugs³⁷², indicating that infection-induced microbial alterations are transient. We, in turn, have shown that acute infection does not result in any changes to the microbiota; thus, patients with ulcerative colitis would have to carry persistent parasite infections to remain healthy.

What also speaks against the therapeutic use of *Trichuris* parasites is their effects on microbial diversity. Decreased bacterial diversity has been associated with several immune-associated disorders, including inflammatory bowel disease, indicating that chronic *T. muris* infection in fact might impact negatively on the outcome of disease due to its negative effects on microbial diversity. Accordingly, our unpublished data suggest that *T. muris* infection exacerbates disease in a chronic model of colitis, and many of the features of chronic *T. muris* infection resemble the inflammatory environment of ulcerative colitis³⁷⁰, such as high levels of IFN- γ , thus questioning whether this particular parasite is protective against the disease development. There is no inherent reason why all human parasites must have some protective quality, but instead might depend on how well adapted the parasite is to the host. After all, parasites are still pathogens and come with disease symptoms, some quite dangerous, and thus what ultimately matters is perhaps the balance between harm and good, where some parasites tip the scale in favor of immune modulation and suppression of inflammation, whereas others cause excessive tissue damage.

In conclusion, further studies are required to determine whether *Trichuris* parasites, in particular, are capable of modulating the immune system and protecting against inflammatory diseases.

Paper 3

Secreted antigens from the parasite *Trichuris muris* facilitate inflammasome activation by modulating Toll-like receptor signaling

Daniel Sorobetea, Dóra Hancz, Henrietta Henningsson, Christine Valfridsson, Marcus Svensson-Frej and Jenny J. Persson

Manuscript

Background

While the role of inflammasomes *per se* during parasite infection is unclear, some studies have assessed the contribution of the inflammasome-associated cytokines IL-1 β and IL-18. Thus, IL-1 β seems to promote protective immunity toward *T. muris* infection³⁹⁰, whereas it inhibits *H. polygyrus* expulsion³⁹¹. By contrast, IL-18 appears to be detrimental during both *T. muris*²⁰⁸ and *T. spiralis*³⁹² infection, suggesting a complex and context-dependent role of inflammasome-derived cytokines during worm infections. Moreover, the cellular source of these cytokines *in vivo*, and which inflammasomes that are involved, have not been addressed. By contrast, some studies have investigated the potential of parasite-derived antigens to activate the inflammasome *in vitro*. For instance, *S. mansoni* and *H. polygyrus*-derived products have been shown to induce IL-1 β secretion by antigen-presenting cells^{391,393,394}, via a Nlrp3-dependent mechanism. *T. muris*-derived E/S antigens are known to stimulate production of inflammatory cytokines by macrophages²²⁸, however the potential involvement of the inflammasome in this process has been largely overlooked. We therefore sought to investigate the mechanisms by which macrophages recognize *T. muris*-derived antigens and its consequences on inflammasome activation.

Results

- E/S antigens were capable of priming bone marrow-derived macrophages for canonical Nlrp3 inflammasome activation in a TLR4-dependent manner.
- E/S antigens licensed macrophages for Nlrp3 inflammasome activation via subsequent TLR ligation, which was mediated by a protein within the E/S mixture.
- TLR-induced Nlrp3 inflammasome activation was slower than conventional activation, did not involve pyroptosis and was caspase-8 dependent.

Discussion

In this preliminary study, we have demonstrated that *T. muris*-derived E/S antigens can license bone marrow-derived macrophages to induce Nlrp3 inflammasome activation upon TLR ligation, a process that normally does not occur. Bone marrow-derived macrophages are a useful tool to study inflammasome activation, but are not equivalent to tissue-resident macrophages in the lamina propria of the large

intestine, which do not induce inflammation upon TLR ligation, as mentioned previously. Instead, our data are more likely to apply to inflammatory monocytes rather than tissue-resident macrophages. Inflammatory monocytes exit the bone marrow in a CCR2-dependent manner, due to its interaction with CCL2. Accordingly, CCL2 is up-regulated upon *T. muris* infection and mice deficient in CCL2 do not expel a normally acute infection³⁹⁵, illustrating that inflammatory monocytes might be of importance in the generation of protective immunity. Indeed, human monocytes respond to LPS stimulation with a very similar form of Nlrp3 activation¹³². Whether TLR-induced inflammasome activation upon E/S antigen-stimulation occurs *in vivo* remains to be determined. Furthermore, epithelial-associated inflammasome activation is also likely to be involved in the response to *T. muris* infection, due to the important role of epithelial cells in the generation of protective immunity, which was discussed earlier, thus adding another layer of complexity to the contribution of inflammasomes. Regardless, given our results showing that *T. muris* infection can alter the permeability of the epithelial barrier, it is plausible that bacteria can translocate into the lamina propria, thus providing the TLR ligands capable of inducing inflammasome activation after E/S antigen recognition also to immune cells situated in the lamina propria.

The precise mechanism through which E/S antigens mediate their effects is currently under investigation. We are thus in the process of characterizing and comparing intracellular signaling between macrophages primed with either LPS or E/S products in an attempt to dissect the potential pathway involved in the licensing effect mediated by E/S antigens. Moreover, we recently discovered endogenous proteins capable of facilitating the same kind of TLR-induced Nlrp3 activation as the E/S antigens. Thus, whereas E/S products are a mix of many different proteins, it appears that a single ligand is sufficient, which could narrow down the potential receptors involved.

In conclusion, E/S antigens license macrophages to release IL-1 β upon TLR ligation, and further experiments are needed to determine the precise mechanism.

Paper 4

Eosinophils are key regulators of perivascular adipose tissue and vascular functionality

Sarah Withers, Ruth Forman, Selene Meza-Perez, Daniel Sorobetea, Kasia Sitnik, Thomas Hopwood, Catherine B. Lawrence, William W. Agace, Kathryn J. Else, Anthony M. Heagerty, Marcus Svensson-Frej and Sheena M. Cruickshank

Scientific Reports (2017; in press)

Background

Most peripheral vessels, including mesenteric arteries, are insulated in a sheath of perivascular adipose tissue that supports the vessel and plays an important role in modulating its contractile function, thus indirectly contributing to regulation of blood pressure³⁹⁶. This perivascular adipose tissue is also populated by various immune cells under homeostatic conditions, notably eosinophils⁹⁸, which are recruited into the tissue by ILC2-derived IL-5²⁸⁵ and, in turn, control differentiation and maintenance of alternatively activate macrophages that have an important role in regulating glucose homeostasis⁹⁸. Interestingly, adipose tissue eosinophils are significantly fewer during obesity⁹⁸. However, the potential involvement of eosinophils in directly regulating adipocytes has been largely ignored. We thus sought to study the possible role of adipose tissue eosinophils in regulating perivascular adipose tissue function during homeostasis.

Results

- Perivascular adipose tissue exerts an anti-contractile effect on mesenteric arteries.
- The anti-contractile effect is lost in eosinophil-deficient mice, as well as in obese mice, which have a reduction in adipose tissue eosinophils, thus implicating eosinophils in the regulation of vascular function.
- Eosinophil reconstitution *in vitro* and *in vivo* can restore the anti-contractile effect, largely via indirect effects on adiponectin and nitric oxide production in the adipose tissue.
- Eosinophil-mediated effects are rapidly induced upon norepinephrine stimulation and involve the release of catecholamines, which exert their effects on β 3-adreno receptors.

Discussion

In this study, we were able to show for the first time that eosinophils play a non-redundant role in promoting the function of mesenteric arteries via the release of catecholamines. These data hence expand the growing literature on the versatility of eosinophil function, in regulation of immune and non-immune processes.

As previously discussed, eosinophils have a number of homeostatic functions in several organs, and so we hypothesized that they likely served a homeostatic role in adipose tissue as well. Indeed, eosinophils appeared to have considerable effect on vascular function via indirect effects on adipocytes, with downstream consequences on mean arterial blood pressure, which was lost during obesity. This finding strengthens the idea that obesity has an inherent inflammatory component and might have important implications for the treatment of various obesity-associated diseases, such as type 2 diabetes.

In conclusion, adipose tissue eosinophils have an important role in the regulation of perivascular adipose tissue, with possible implications on blood pressure function.

Concluding remarks

Mucosal immunology has come to the forefront of biomedical research in recent years, and rightly so. The complex interactions between the immune system, our commensal microorganisms and the various pathogens that afflict us are of fundamental importance for our well-being. However, whereas the microbiota has received significant attention, parasite immunity was until recently a largely neglected part of immunology. Indeed, the World Health Organization refers to these pathogens as neglected tropical diseases, as they have all but been eradicated in the industrialized world. However, parasitic worm infections are an integral part of the mucosal milieu and an important part of our evolutionary history. Given the rise in immune-associated disorders around the world, it is important that we do not forget these creatures, or the influence they have on our bodies and the immune system in particular, whether direct or indirect.

My studies suggest that the intestinal parasite *T. muris* has a substantial impact on the intestinal environment, upon both acute and chronic infections. Chronic infection, in particular, which is supposed to mimic patent infection in humans, had drastic effects on the intestinal microbiota, as well as on the adaptive immune system. By contrast, acute infection did not affect the composition of commensal bacteria, but rather had long-term consequences on innate immunity, highlighting that even a temporary infection might influence the response to subsequent immune challenge. However, whereas the hygiene hypothesis would indicate that parasite exposure could protect against the development of immune-associated disorders, our preliminary data suggest the opposite. Thus, the hygiene hypothesis might be context-specific and depend on a number of factors, including parasite species and dose, timing and length of exposure, previous infections, composition of commensal microbes, and so on. It is important to take all these factors into account, especially given the proposed use for parasites as treatment for some of the diseases attributed to the lack of parasite exposure.

As one might expect, our results have generated more questions than they have answered. For instance, why does the host mount different immune responses to varying doses of the same pathogen? To what extent are parasites able to directly manipulate the immune system, and what are the effects on responses to concurrent infections or inflammatory disorders? What are the long-term consequences of chronic or acute infections? How does early parasite exposure affect the development of the immune system? What is the contribution of the microbiota in regulating immune responses to extracellular parasites? One can only hope that, unlike the parasites, these important questions will not be neglected.

Acknowledgements

It takes a village, as the saying goes, and so I want to express my gratitude to those who've helped me along this journey, and made my time at the section an unforgettable experience. Thank you:

Mimoza Demiri, my main comrade in the *T. muris* struggle, for being a constant pillar of support and putting up with me in the same office for so long.

Selene Meza-Perez, my exiled postdoc, for teaching me the tricks of the trade and always encouraging me to try new experiments (without asking Marcus). Your outgoing and cheerful nature made Sweden less bleak for a moment.

Holger Weishaupt, for being the wonderfully weird you, which hopefully distracted everyone from my own weirdness. Needless to say, you left too early and my cover was blown.

Madelene Dahlgren, for immediately thrusting me into the social life of the section and making me feel at home, as well as being a great badminton partner.

William Agace, for welcoming me into your group meetings with open arms, which have been absolutely formative (the meetings, not your arms).

Thorsten Joeris, for teaching me the most valuable lesson in science, which is to "increase the frustration threshold", and for the countless times we burst out laughing, whether or not it was appropriate.

Aymeric Rivollier, for your inspiring work ethic, nice personality and willingness to help if needed, no matter how busy you were. I also consider myself lucky to be your friend (more for what happened off-camera than on, but still).

Adnan Dersonic, the former queen of D14, for showing me a whole new level of organization, which I didn't think was possible. Your professional demeanor on the seminar stage is only surpassed by your craziness on the dance floor.

Fredric Carlsson, and the girls next door, for letting me be your Danny boy.

Ruth Forman, Sarah Withers, Sheena Cruickshank and Kathryn Else, across the North Sea, for all the fun Skype meetings where we kept telling ourselves that we would be done soon.

Jacob Bak Holm and Karsten Kristiansen, across the Öresund, for broadening my interests and somehow making feces seem exciting.

Dóra Hancz, Henrietta Henningson, Christine Valfridsson and Jenny Persson, across the hall, for making me realize that molecular biology isn't torture. I still have no idea how inflammsamoses work, but hey, at least I tried.

Finally, I wish to thank my supervisor Marcus Svensson-Frej. I came to you with long hair and an unkempt beard, looking like a hippie and looking for a job. You took me in without hesitation and were fully committed, supportive and enthusiastic from day one. You gave me the freedom to pursue my own ideas and incredibly enough let me keep trying when most of them failed. Perhaps more importantly though, you've been a kind and understanding person; always willing to spare some time, patiently listen to my ramblings or just share a laugh. My hair is shorter now, and the beard is trimmed, so clearly everything worked out in the end.

References

1. Pullan, R. L., Smith, J. L., Jasrasaria, R. & Brooker, S. J. Global numbers of infection and disease burden of soil transmitted helminth infections in 2010. *Parasit. Vectors* 7, 37 (2014).
2. Asher, M. I. et al. Worldwide time trends in the prevalence of symptoms of asthma, allergic rhinoconjunctivitis, and eczema in childhood: ISAAC Phases One and Three repeat multicountry cross-sectional surveys. *Lancet* 368, 733–743 (2006).
3. Molodecky, N. A. et al. Increasing Incidence and Prevalence of the Inflammatory Bowel Diseases With Time, Based on Systematic Review. *Gastroenterology* 142, 46–54 (2012).
4. Zhou, B. et al. Worldwide trends in diabetes since 1980: A pooled analysis of 751 population-based studies with 4.4 million participants. *Lancet* 387, 1513–1530 (2016).
5. Kondrashova, A., Seiskari, T., Ilonen, J., Knip, M. & Hyöty, H. The ‘Hygiene hypothesis’ and the sharp gradient in the incidence of autoimmune and allergic diseases between Russian Karelia and Finland. *Acta. Pathol. Microbiol. Immunol. Scand.* 121, 478–493 (2013).
6. Ramanan, D. et al. Helminth infection promotes colonization resistance via type 2 immunity. *Science* 352, 608–612 (2016).
7. Broadhurst, M. J. et al. IL-22⁺ CD4⁺ T Cells Are Associated with Therapeutic *Trichuris trichiura* Infection in an Ulcerative Colitis Patient. *Sci. Transl. Med.* 2, 60ra88 (2010).
8. Mowat, A. M. & Agace, W. W. Regional specialization within the intestinal immune system. *Nat. Rev. Immunol.* 14, 667–685 (2014).
9. Peterson, L. W. & Artis, D. Intestinal epithelial cells: regulators of barrier function and immune homeostasis. *Nat. Rev. Immunol.* 14, 141–153 (2014).
10. Johansson, M. E. V et al. The inner of the two Muc2 mucin-dependent mucus layers in colon is devoid of bacteria. *Proc. Natl. Acad. Sci. U. S. A.* 105, 15064–15069 (2008).
11. Rakoff-Nahoum, S., Paglino, J., Eslami-Varzaneh, F., Edberg, S. & Medzhitov, R. Recognition of Commensal Microflora by Toll-Like Receptors Is Required for Intestinal Homeostasis. *Cell* 118, 229–241 (2004).
12. Lotz, M. et al. Postnatal acquisition of endotoxin tolerance in intestinal epithelial cells. *J. Exp. Med.* 203, 973–984 (2006).
13. Cario, E., Gerken, G. & Podolsky, D. K. Toll-Like Receptor 2 Controls Mucosal Inflammation by Regulating Epithelial Barrier Function. *Gastroenterology* 132, 1359–1374 (2007).
14. Nenci, A. et al. Epithelial NEMO links innate immunity to chronic intestinal inflammation. *Nature* 446, 557–561 (2007).
15. Brandl, K. et al. MyD88 signaling in nonhematopoietic cells protects mice against induced colitis by regulating specific EGF receptor ligands. *Proc. Natl. Acad. Sci. U. S. A.* 107, 19967–19972 (2010).
16. Vereecke, L. et al. Enterocyte-specific A20 deficiency sensitizes to tumor necrosis factor-induced toxicity and experimental colitis. *J. Exp. Med.* 207, 1513–1523 (2010).
17. Velcich, A. et al. Colorectal Cancer in Mice Genetically Deficient in the Mucin Muc2. *Science* 295, 1726–1729 (2002).
18. Van der Sluis, M. et al. Muc2-Deficient Mice Spontaneously Develop Colitis, Indicating That Muc2 Is Critical for Colonic Protection. *Gastroenterology* 131, 117–129 (2006).
19. Hooper, L. V et al. Molecular Analysis of Commensal Host-Microbial Relationships in the Intestine. *Science* 291, 881–884 (2001).
20. Bäckhed, F. et al. The gut microbiota as an environmental factor that regulates fat storage. *Proc. Natl. Acad. Sci. U. S. A.* 101, 15718–15723 (2004).
21. Gill, S. R. et al. Metagenomic Analysis of the Human Distal Gut Microbiome. *Science* 312, 1355–1359 (2006).
22. Bäckhed, F., Manchester, J. K., Semenkovich, C. F. & Gordon, J. I. Mechanisms underlying the resistance to diet-induced obesity in germ-free mice. *Proc. Natl. Acad. Sci. U. S. A.* 104, 979–984 (2007).
23. Sjögren, K. et al. The Gut Microbiota Regulates Bone Mass in Mice. *J. Bone Miner. Res.* 27, 1357–

- 1367 (2012).
24. Stappenbeck, T. S., Hooper, L. V & Gordon, J. I. Developmental regulation of intestinal angiogenesis by indigenous microbes via Paneth cells. *Proc. Natl. Acad. Sci. U. S. A.* 99, 15451–15455 (2002).
 25. Reinhardt, C. et al. Tissue factor and PAR1 promote microbiota-induced intestinal vascular remodelling. *Nature* 483, 627–631 (2012).
 26. Mazmanian, S. K., Cui, H. L., Tzianabos, A. O. & Kasper, D. L. An Immunomodulatory Molecule of Symbiotic Bacteria Directs Maturation of the Host Immune System. *Cell* 122, 107–118 (2005).
 27. Ivanov, I. I. et al. Induction of Intestinal Th17 Cells by Segmented Filamentous Bacteria. *Cell* 139, 485–498 (2009).
 28. Atarashi, K. et al. Treg induction by a rationally selected mixture of *Clostridia* strains from the human microbiota. *Nature* 500, 232–236 (2013).
 29. Furusawa, Y. et al. Commensal microbe-derived butyrate induces the differentiation of colonic regulatory T cells. *Nature* 504, 446–450 (2013).
 30. Kamada, N. et al. Regulated Virulence Controls the Ability of a Pathogen to Compete with the Gut Microbiota. *Science* 336, 1325–1329 (2012).
 31. Reeves, A. E., Koenigsnecht, M. J., Bergin, I. L. & Young, V. B. Suppression of *Clostridium difficile* in the Gastrointestinal Tracts of Germfree Mice Inoculated with a Murine Isolate from the Family *Lachnospiraceae*. *Infect. Immun.* 80, 3786–3794 (2012).
 32. Maslowski, K. M. et al. Regulation of inflammatory responses by gut microbiota and chemoattractant receptor GPR43. *Nature* 461, 1282–1286 (2009).
 33. Sudo, N. et al. Postnatal microbial colonization programs the hypothalamic-pituitary-adrenal system for stress response in mice. *J. Physiol.* 558, 263–275 (2004).
 34. Li, W., Dowd, S. E., Scurlock, B., Acosta-Martinez, V. & Lyte, M. Memory and learning behavior in mice is temporally associated with diet-induced alterations in gut bacteria. *Physiol. Behav.* 96, 557–567 (2009).
 35. Gareau, M. G. et al. Bacterial infection causes stress-induced memory dysfunction in mice. *Gut* 60, 307–317 (2011).
 36. Heijtz, R. D. et al. Normal gut microbiota modulates brain development and behavior. *Proc. Natl. Acad. Sci. U. S. A.* 108, 3047–3052 (2011).
 37. Neufeld, K. M., Kang, N., Bienenstock, J. & Foster, J. A. Reduced anxiety-like behavior and central neurochemical change in germ-free mice. *Neurogastroenterol. Motil.* 23, 255–e119 (2011).
 38. Eckburg, P. B. et al. Diversity of the Human Intestinal Microbial Flora. *Science* 308, 1635–1638 (2005).
 39. Qin, J. et al. A human gut microbial gene catalogue established by metagenomic sequencing. *Nature* 464, 59–65 (2010).
 40. Grice, E. A. et al. Topographical and Temporal Diversity of the Human Skin Microbiome. *Science* 324, 1190–1192 (2009).
 41. Mändar, R. & Mikelsaar, M. Transmission of Mother's Microflora to the Newborn at Birth. *Biol. Neonate* 69, 30–35 (1996).
 42. Hooper, L. V, Stappenbeck, T. S., Hong, C. V & Gordon, J. I. Angiogenins: a new class of microbicidal proteins involved in innate immunity. *Nat. Immunol.* 4, 269–273 (2003).
 43. Brandl, K. et al. Vancomycin-resistant enterococci exploit antibiotic-induced innate immune deficits. *Nature* 455, 804–807 (2008).
 44. Kinnebrew, M. A. et al. Interleukin 23 Production by Intestinal CD103⁺CD11b⁺ Dendritic Cells in Response to Bacterial Flagellin Enhances Mucosal Innate Immune Defense. *Immunity* 36, 276–287 (2012).
 45. Larsson, E. et al. Analysis of gut microbial regulation of host gene expression along the length of the gut and regulation of gut microbial ecology through MyD88. *Gut* 61, 1124–1131 (2012).
 46. Turnbaugh, P. J. et al. A core gut microbiome in obese and lean twins. *Nature* 457, 480–484 (2009).
 47. Ley, R. E., Turnbaugh, P. J., Klein, S. & Gordon, J. I. Human gut microbes associated with obesity. *Nature* 444, 1022–1023 (2006).
 48. De Filippo, C. et al. Impact of diet in shaping gut microbiota revealed by a comparative study in

- children from Europe and rural Africa. *Proc. Natl. Acad. Sci. U. S. A.* 107, 14691–14696 (2010).
49. Sonnenburg, E. D. et al. Specificity of Polysaccharide Use in Intestinal Bacteroides Species Determines Diet-Induced Microbiota Alterations. *Cell* 141, 1241–1252 (2010).
 50. Wu, G. D. et al. Linking Long-Term Dietary Patterns with Gut Microbial Enterotypes. *Science* 334, 105–109 (2011).
 51. Turnbaugh, P. J. et al. An obesity-associated gut microbiome with increased capacity for energy harvest. *Nature* 444, 1027–1031 (2006).
 52. Samuel, B. S. et al. Effects of the gut microbiota on host adiposity are modulated by the short-chain fatty-acid binding G protein-coupled receptor, Gpr41. *Proc. Natl. Acad. Sci. U. S. A.* 105, 16767–16772 (2008).
 53. Kameyama, K. & Itoh, K. Intestinal Colonization by a *Lachnospiraceae* Bacterium Contributes to the Development of Diabetes in Obese Mice. *Microbes Environ.* 29, 427–430 (2014).
 54. Suárez-Zamorano, N. et al. Microbiota depletion promotes browning of white adipose tissue and reduces obesity. *Nat. Med.* 21, 1497–1501 (2015).
 55. Ley, R. E. et al. Obesity alters gut microbial ecology. *Proc. Natl. Acad. Sci. U. S. A.* 102, 11070–11075 (2005).
 56. Chevalier, C. et al. Gut Microbiota Orchestrates Energy Homeostasis during Cold. *Cell* 163, 1360–1374 (2015).
 57. Koren, O. et al. Host Remodeling of the Gut Microbiome and Metabolic Changes during Pregnancy. *Cell* 150, 470–480 (2012).
 58. Yurkovetskiy, L. et al. Gender Bias in Autoimmunity Is Influenced by Microbiota. *Immunity* 39, 400–412 (2013).
 59. Burrows, M. P., Volchkov, P., Kobayashi, K. S. & Chervonsky, A. V. Microbiota regulates type 1 diabetes through Toll-like receptors. *Proc. Natl. Acad. Sci. U. S. A.* 112, 9973–9977 (2015).
 60. Frank, D. N. et al. Molecular-phylogenetic characterization of microbial community imbalances in human inflammatory bowel diseases. *Proc. Natl. Acad. Sci. U. S. A.* 104, 13780–13785 (2007).
 61. Dicksved, J. et al. Molecular analysis of the gut microbiota of identical twins with Crohn's disease. *ISME J.* 2, 716–727 (2008).
 62. Willing, B. P. et al. A Pyrosequencing Study in Twins Shows that Gastrointestinal Microbial Profiles Vary With Inflammatory Bowel Disease Phenotypes. *Gastroenterology* 139, 1844–1854 (2010).
 63. Kleessen, B., Kroesen, A. J., Buhr, H. J. & Blaut, M. Mucosal and Invading Bacteria in Patients with Inflammatory Bowel Disease Compared with Controls. *Scand. J. Gastroenterol.* 37, 1034–1041 (2002).
 64. Swidsinski, A. et al. Mucosal Flora in Inflammatory Bowel Disease. *Gastroenterology* 122, 44–54 (2002).
 65. Butterworth, A. D., Thomas, A. G. & Akobeng, A. K. Probiotics for induction of remission in Crohn's disease. *Cochrane Database Syst. Rev.* CD006634 (2008).
 66. Smythies, L. E. et al. Human intestinal macrophages display profound inflammatory anergy despite avid phagocytic and bacteriocidal activity. *J. Clin. Invest.* 115, 66–75 (2005).
 67. Rivollier, A., He, J., Kole, A., Valatas, V. & Kelsall, B. L. Inflammation switches the differentiation program of Ly6C^{hi} monocytes from antiinflammatory macrophages to inflammatory dendritic cells in the colon. *J. Exp. Med.* 209, 139–155 (2012).
 68. Bain, C. C. et al. Resident and pro-inflammatory macrophages in the colon represent alternative context-dependent fates of the same Ly6C^{hi} monocyte precursors. *Mucosal Immunol.* 6, 498–510 (2013).
 69. Shouval, D. S. et al. Interleukin-10 Receptor Signaling in Innate Immune Cells Regulates Mucosal Immune Tolerance and Anti-Inflammatory Macrophage Function. *Immunity* 40, 706–719 (2014).
 70. Zigmond, E. et al. Macrophage-Restricted Interleukin-10 Receptor Deficiency, but Not IL-10 Deficiency, Causes Severe Spontaneous Colitis. *Immunity* 40, 720–733 (2014).
 71. Huang, F.-P. et al. A Discrete Subpopulation of Dendritic Cells Transports Apoptotic Intestinal Epithelial Cells to T Cell Areas of Mesenteric Lymph Nodes. *J. Exp. Med.* 191, 435–443 (2000).

72. Jang, M. H. et al. CCR7 Is Critically Important for Migration of Dendritic Cells in Intestinal Lamina Propria to Mesenteric Lymph Nodes. *J. Immunol.* 176, 803–810 (2006).
73. Worbs, T. et al. Oral tolerance originates in the intestinal immune system and relies on antigen carriage by dendritic cells. *J. Exp. Med.* 203, 519–527 (2006).
74. Bogunovic, M. et al. Origin of the Lamina Propria Dendritic Cell Network. *Immunity* 31, 513–525 (2009).
75. Cerovic, V. et al. Intestinal CD103⁺ dendritic cells migrate in lymph and prime effector T cells. *Mucosal Immunol.* 6, 104–113 (2013).
76. Diehl, G. E. et al. Microbiota restricts trafficking of bacteria to mesenteric lymph nodes by CX3CR1^{hi} cells. *Nature* 494, 116–120 (2013).
77. Cerovic, V. et al. Lymph-borne CD8 α ⁺ dendritic cells are uniquely able to cross-prime CD8⁺ T cells with antigen acquired from intestinal epithelial cells. *Mucosal Immunol.* 8, 38–48 (2015).
78. Hadis, U. et al. Intestinal Tolerance Requires Gut Homing and Expansion of FoxP3⁺ Regulatory T Cells in the Lamina Propria. *Immunity* 34, 237–246 (2011).
79. Esterházy, D. et al. Classical dendritic cells are required for dietary antigen-mediated induction of peripheral Treg cells and tolerance. *Nat. Immunol.* 17, 545–555 (2016).
80. Loschko, J. et al. Absence of MHC class II on cDCs results in microbial-dependent intestinal inflammation. *J. Exp. Med.* 213, 517–534 (2016).
81. Powrie, F., Leach, M. W., Mauze, S., Caddle, L. B. & Coffman, R. L. Phenotypically distinct subsets of CD4⁺ T cells induce or protect from chronic intestinal inflammation in C. B-17 scid mice. *Int. Immunol.* 5, 1461–1471 (1993).
82. Powrie, F., Correa-Oliveira, R., Mauze, S. & Coffman, R. L. Regulatory Interactions between CD45RB^{high} and CD45RB^{low} CD4⁺ T Cells Are Important for the Balance between Protective and Pathogenic Cell-mediated Immunity. *J. Exp. Med.* 179, 589–600 (1994).
83. Asseman, C., Mauze, S., Leach, M. W., Coffman, R. L. & Powrie, F. An Essential Role for Interleukin 10 in the Function of Regulatory T Cells That Inhibit Intestinal Inflammation. *J. Exp. Med.* 190, 995–1003 (1999).
84. Annacker, O. et al. CD25⁺ CD4⁺ T Cells Regulate the Expansion of Peripheral CD4 T Cells Through the Production of IL-10. *J. Immunol.* 166, 3008–3018 (2001).
85. Rubtsov, Y. P. et al. Regulatory T Cell-Derived Interleukin-10 Limits Inflammation at Environmental Interfaces. *Immunity* 28, 546–558 (2008).
86. Sonnenberg, G. F. et al. Innate Lymphoid Cells Promote Anatomical Containment of Lymphoid-Resident Commensal Bacteria. *Science* 336, 1321–1325 (2012).
87. Qiu, J. et al. Group 3 Innate Lymphoid Cells Inhibit T-Cell-Mediated Intestinal Inflammation through Aryl Hydrocarbon Receptor Signaling and Regulation of Microflora. *Immunity* 39, 386–399 (2013).
88. Scandella, E. et al. Restoration of lymphoid organ integrity through the interaction of lymphoid tissue-inducer cells with stroma of the T cell zone. *Nat. Immunol.* 9, 667–675 (2008).
89. Tsuji, M. et al. Requirement for Lymphoid Tissue-Inducer Cells in Isolated Follicle Formation and T Cell-Independent Immunoglobulin A Generation in the Gut. *Immunity* 29, 261–271 (2008).
90. Kruglov, A. A. et al. Nonredundant Function of Soluble LT α 3 Produced by Innate Lymphoid Cells in Intestinal Homeostasis. *Science* 342, 1243–1246 (2013).
91. Bouskra, D. et al. Lymphoid tissue genesis induced by commensals through NOD1 regulates intestinal homeostasis. *Nature* 456, 507–510 (2008).
92. Qiu, J. et al. The Aryl Hydrocarbon Receptor Regulates Gut Immunity through Modulation of Innate Lymphoid Cells. *Immunity* 36, 92–104 (2012).
93. Carlens, J. et al. Common γ -Chain-Dependent Signals Confer Selective Survival of Eosinophils in the Murine Small Intestine. *J. Immunol.* 183, 5600–5607 (2009).
94. Chu, V. T. et al. Eosinophils Promote Generation and Maintenance of Immunoglobulin-A-Expressing Plasma Cells and Contribute to Gut Immune Homeostasis. *Immunity* 40, 582–593 (2014).
95. Chen, H.-H. et al. Eosinophils from Murine Lamina Propria Induce Differentiation of Naïve T Cells into Regulatory T Cells via TGF- β 1 and Retinoic Acid. *PLoS One* 10, e0142881 (2015).

96. Jung, Y. et al. IL-1 β in eosinophil-mediated small intestinal homeostasis and IgA production. *Mucosal Immunol.* 8, 930–942 (2015).
97. Svensson, M. et al. Accumulation of eosinophils in intestine-draining mesenteric lymph nodes occurs after *Trichuris muris* infection. *Parasite Immunol.* 33, 1–11 (2011).
98. Wu, D. et al. Eosinophils Sustain Adipose Alternatively Activated Macrophages Associated with Glucose Homeostasis. *Science* 332, 243–247 (2011).
99. Riva, M. et al. Induction of nuclear factor- κ B responses by the S100A9 protein is Toll-like receptor-4-dependent. *Immunology* 137, 172–182 (2012).
100. Cheng, Z., Taylor, B., Ourthiague, D. R. & Hoffmann, A. Distinct single-cell signaling characteristics are conferred by the MyD88 and TRIF pathways during TLR4 activation. *Sci. Signal.* 8, 1–12 (2015).
101. Ryu, J.-K. et al. Reconstruction of LPS Transfer Cascade Reveals Structural Determinants within LBP, CD14, and TLR4-MD2 for Efficient LPS Recognition and Transfer. *Immunity* 46, 1–13 (2017).
102. Martinon, F., Burns, K. & Tschopp, J. The Inflammasome: A Molecular Platform Triggering Activation of Inflammatory Caspases and Processing of proIL- β . *Mol. Cell* 10, 417–426 (2002).
103. Li, P. et al. Mice Deficient in IL-1 β -Converting Enzyme Are Defective in Production of Mature IL-1 β and Resistant to Endotoxic Shock. *Cell* 80, 401–411 (1995).
104. Kofoed, E. M. & Vance, R. E. Innate immune recognition of bacterial ligands by NALPs determines inflammasome specificity. *Nature* 477, 592–595 (2011).
105. Zhao, Y. et al. The NLRC4 inflammasome receptors for bacterial flagellin and type III secretion apparatus. *Nature* 477, 596–600 (2011).
106. Ren, T., Zamboni, D. S., Roy, C. R., Dietrich, W. F. & Vance, R. E. Flagellin-Deficient *Legionella* mutants Evade Caspase-1- and Naip5-Mediated Macrophage Immunity. *PLoS Pathog.* 2, e18 (2006).
107. Molofsky, A. B. et al. Cytosolic recognition of flagellin by mouse macrophages restricts *Legionella pneumophila* infection. *J. Exp. Med.* 203, 1093–1104 (2006).
108. Lightfield, K. L. et al. Critical function for Naip5 in inflammasome activation by a conserved carboxy-terminal domain of flagellin. *Nat. Immunol.* 9, 1171–1178 (2008).
109. Rauch, I. et al. NALP proteins are required for cytosolic detection of specific bacterial ligands *in vivo*. *J. Exp. Med.* 213, 657–665 (2016).
110. Allam, R. et al. Epithelial NALPs protect against colonic tumorigenesis. *J. Exp. Med.* 212, 369–383 (2015).
111. Franchi, L. et al. NLRC4-driven production of IL-1 β discriminates between pathogenic and commensal bacteria and promotes host intestinal defense. *Nat. Immunol.* 13, 449–456 (2012).
112. Fernandes-Alnemri, T. et al. The AIM2 inflammasome is critical for innate immunity to *Francisella tularensis*. *Nat. Immunol.* 11, 385–393 (2010).
113. Rathinam, V. A. K. et al. The AIM2 inflammasome is essential for host defense against cytosolic bacteria and DNA viruses. *Nat. Immunol.* 11, 395–402 (2010).
114. Martinon, F., Pétrilli, V., Mayor, A., Tardivel, A. & Tschopp, J. Gout-associated uric acid crystals activate the NALP3 inflammasome. *Nature* 440, 237–241 (2006).
115. Li, H., Nookala, S. & Re, F. Aluminum Hydroxide Adjuvants Activate Caspase-1 and Induce IL-1 β and IL-18 Release. *J. Immunol.* 178, 5271–5276 (2007).
116. Eisenbarth, S. C., Colegio, O. R., O'Connor, W., Sutterwala, F. S. & Flavell, R. A. Crucial role for the Nalp3 inflammasome in the immunostimulatory properties of aluminium adjuvants. *Nature* 453, 1122–1126 (2008).
117. Hornung, V. et al. Silica crystals and aluminum salts activate the NALP3 inflammasome through phagosomal destabilization. *Nat. Immunol.* 9, 847–856 (2008).
118. Mariathasan, S. et al. Cryopyrin activates the inflammasome in response to toxins and ATP. *Nature* 440, 228–232 (2006).
119. Broz, P. et al. Redundant roles for inflammasome receptors NLRP3 and NLRC4 in host defense against *Salmonella*. *J. Exp. Med.* 207, 1745–1755 (2010).
120. Wang, X. et al. RNA viruses promote activation of the NLRP3 inflammasome through a RIP1-RIP3-DRP1 signaling pathway. *Nat. Immunol.* 15, 1126–1133 (2014).

121. Orłowski, G. M. et al. Multiple Cathepsins Promote Pro-IL-1 β Synthesis and NLRP3-Mediated IL-1 β Activation. *J. Immunol.* 195, 1685–1697 (2015).
122. Pétrilli, V. et al. Activation of the NALP3 inflammasome is triggered by low intracellular potassium concentration. *Cell Death Differ.* 14, 1583–1589 (2007).
123. Muñoz-Planillo, R. et al. K⁺ Efflux Is the Common Trigger of NLRP3 Inflammasome Activation by Bacterial Toxins and Particulate Matter. *Immunity* 38, 1142–1153 (2013).
124. Katsnelson, M. A., Rucker, L. G., Russo, H. M. & DuByak, G. R. K⁺ Efflux Agonists Induce NLRP3 Inflammasome Activation Independently of Ca²⁺ Signaling. *J. Immunol.* 194, 3937–3952 (2015).
125. Park, S. et al. Defective mitochondrial fission augments NLRP3 inflammasome activation. *Sci. Rep.* 5, 15489 (2015).
126. Zhong, Z. et al. NF- κ B Restricts Inflammasome Activation via Elimination of Damaged Mitochondria. *Cell* 164, 896–910 (2016).
127. Nakahira, K. et al. Autophagy proteins regulate innate immune responses by inhibiting the release of mitochondrial DNA mediated by the NALP3 inflammasome. *Nat. Immunol.* 8, 222–230 (2011).
128. Shimada, K. et al. Oxidized Mitochondrial DNA Activates the NLRP3 Inflammasome during Apoptosis. *Immunity* 36, 401–414 (2012).
129. Zhou, R., Yazdi, A. S., Menu, P. & Tschopp, J. A role for mitochondria in NLRP3 inflammasome activation. *Nature* 469, 221–225 (2011).
130. Iyer, S. S. et al. Mitochondrial Cardiolipin Is Required for Nlrp3 Inflammasome Activation. *Immunity* 39, 311–323 (2013).
131. Allam, R. et al. Mitochondrial apoptosis is dispensable for NLRP3 inflammasome activation but non-apoptotic caspase-8 is required for inflammasome priming. *EMBO Rep.* 15, 982–990 (2014).
132. Gaidt, M. M. et al. Human Monocytes Engage an Alternative Inflammasome Pathway. *Immunity* 44, 833–846 (2016).
133. Groß, C. J. et al. K⁺ Efflux-Independent NLRP3 Inflammasome Activation by Small Molecules Targeting Mitochondria. *Immunity* 45, 761–773 (2016).
134. Juliana, C. et al. Non-transcriptional Priming and Deubiquitination Regulate NLRP3 Inflammasome Activation. *J. Biol. Chem.* 287, 36617–36622 (2012).
135. Hara, H. et al. Phosphorylation of the adaptor ASC acts as a molecular switch that controls the formation of speck-like aggregates and inflammasome activity. *Nat. Immunol.* 14, 1247–1255 (2013).
136. Filardy, A. A., He, J., Bennink, J., Yewdell, J. & Kelsall, B. L. Posttranscriptional control of NLRP3 inflammasome activation in colonic macrophages. *Mucosal Immunol.* 9, 850–858 (2016).
137. Duong, B. H. et al. A20 Restricts Ubiquitination of Pro-Interleukin-1 β Protein Complexes and Suppresses NLRP3 Inflammasome Activity. *Immunity* 42, 55–67 (2015).
138. Conos, S. A., Lawlor, K. E., Vaux, D. L., Vince, J. E. & Lindqvist, L. M. Cell death is not essential for caspase-1-mediated interleukin-1 β activation and secretion. *Cell Death Differ.* 23, 1827–1838 (2016).
139. Chaudhary, P. M. et al. Activation of the NF- κ B pathway by caspase 8 and its homologs. *Oncogene* 19, 4451–4460 (2000).
140. Hu, W.-H., Johnson, H. & Shu, H.-B. Activation of NF- κ B by FADD, Casper, and caspase-8. *J. Biol. Chem.* 275, 10838–10844 (2000).
141. Su, H. et al. Requirement for Caspase-8 in NF- κ B Activation by Antigen Receptor. *Science* 307, 1465–1468 (2005).
142. Man, S. M. et al. Salmonella Infection Induces Recruitment of Caspase-8 to the Inflammasome to Modulate IL-1 β Production. *J. Immunol.* 191, 5239–5246 (2013).
143. Gurung, P. et al. FADD and Caspase-8 Mediate Priming and Activation of the Canonical and Noncanonical Nlrp3 Inflammasomes. *J. Immunol.* 192, 1835–1846 (2014).
144. Mœlfaït, J. et al. Stimulation of Toll-like receptor 3 and 4 induces interleukin-1 β maturation by caspase-8. *J. Exp. Med.* 205, 1967–1973 (2008).
145. Gringhuis, S. I. et al. Dectin-1 is an extracellular pathogen sensor for the induction and processing of IL-1 β via a noncanonical caspase-8 inflammasome. *Nat. Immunol.* 13, 246–254 (2012).
146. Vince, J. E. et al. Inhibitor of Apoptosis Proteins Limit RIP3 Kinase-Dependent Interleukin-1

- Activation. *Immunity* 36, 215–227 (2012).
147. Shenderov, K. et al. Endoplasmic Reticulum Stress Licenses Macrophages To Produce Mature IL-1 β in Response to TLR4 Stimulation through a Caspase-8- and TRIF-dependent pathway. *J. Immunol.* 192, 2029–2033 (2014).
 148. Antonopoulos, C. et al. Caspase-8 as an Effector and Regulator of NLRP3 Inflammasome Signaling. *J. Biol. Chem.* 290, 20167–20184 (2015).
 149. Philip, N. H. et al. Caspase-8 mediates caspase-1 processing and innate immune defense in response to bacterial blockade of NF- κ B and MAPK signaling. *Proc. Natl. Acad. Sci. U. S. A.* 111, 7385–7390 (2014).
 150. Kang, S. et al. Caspase-8 scaffolding function and MLKL regulate NLRP3 inflammasome activation downstream of TLR3. *Nat. Commun.* 6, 7515 (2015).
 151. Weng, D. et al. Caspase-8 and RIP kinases regulate bacteria-induced innate immune responses and cell death. *Proc. Natl. Acad. Sci. U. S. A.* 111, 7391–7396 (2014).
 152. Kayagaki, N. et al. Non-canonical inflammasome activation targets caspase-11. *Nature* 479, 117–121 (2011).
 153. Hagar, J. A., Powell, D. A., Achoui, Y., Ernst, R. K. & Miao, E. A. Cytoplasmic LPS Activates Caspase-11: Implications in TLR4-Independent Endotoxic Shock. *Science* 341, 1250–1253 (2013).
 154. Shi, J. et al. Inflammatory caspases are innate immune receptors for intracellular LPS. *Nature* 514, 187–192 (2014).
 155. Coccia, M. et al. IL-1 β mediates chronic intestinal inflammation by promoting the accumulation of IL-17A secreting innate lymphoid cells and CD4⁺ Th17 cells. *J. Exp. Med.* 209, 1595–1609 (2012).
 156. Zhang, J., Fu, S., Sun, S., Li, Z. & Guo, B. Inflammasome activation has an important role in the development of spontaneous colitis. *Mucosal Immunol.* 7, 1139–1150 (2014).
 157. Shouval, D. S. et al. Interleukin 1 β Mediates Intestinal Inflammation in Mice and Patients With Interleukin 10 Receptor Deficiency. *Gastroenterology* 151, 1100–1104 (2016).
 158. Takagi, H. et al. Contrasting Action of IL-12 and IL-18 in the Development of Dextran Sodium Sulphate Colitis in Mice. *Scand. J. Gastroenterol.* 38, 837–844 (2003).
 159. Dupaul-Chicoine, J. et al. Control of Intestinal Homeostasis, Colitis, and Colitis-Associated Colorectal Cancer by the Inflammatory Caspases. *Immunity* 32, 367–378 (2010).
 160. Salcedo, R. et al. MyD88-mediated signaling prevents development of adenocarcinomas of the colon: role of interleukin 18. *J. Exp. Med.* 207, 1625–1636 (2010).
 161. Hu, S. et al. The DNA Sensor AIM2 Maintains Intestinal Homeostasis via Regulation of Epithelial Antimicrobial Host Defense. *Cell Rep.* 13, 1922–1936 (2015).
 162. Kohno, K. et al. IFN- γ -Inducing Factor (IGIF) Is a Costimulatory Factor on the Activation of Th1 but not Th2 Cells and Exerts its Effect Independently of IL-12. *J. Immunol.* 158, 1541–1550 (1997).
 163. Monteleone, G. et al. Bioactive IL-18 Expression is Up-Regulated in Crohn's Disease. *J. Immunol.* 163, 143–147 (1999).
 164. Pizarro, T. T. et al. IL-18, a Novel Immunoregulatory Cytokine, is Up-Regulated in Crohn's Disease: Expression and Localization in Intestinal Mucosal Cells. *J. Immunol.* 162, 6829–6835 (1999).
 165. Allen, I. C. et al. The NLRP3 inflammasome functions as a negative regulator of tumorigenesis during colitis-associated cancer. *J. Exp. Med.* 207, 1045–1056 (2010).
 166. Zaki, M. H. et al. The NLRP3 Inflammasome Protects against Loss of Epithelial Integrity and Mortality during Experimental Colitis. *Immunity* 32, 379–391 (2010).
 167. Elinav, E. et al. NLRP6 Inflammasome Regulates Colonic Microbial Ecology and Risk for Colitis. *Cell* 145, 745–757 (2011).
 168. Yearbook of the United States Department of Agriculture, 472 (1914).
 169. Fahmy, M. A. M. An investigation on the life cycle of *Trichuris muris*. *Parasitology* 44, 50–57 (1954).
 170. Panesar, T. S. & Croll, N. A. The location of parasites within their hosts: site selection by *Trichuris muris* in the laboratory mouse. *Int. J. Parasitol.* 10, 261–273 (1980).
 171. Hayes, K. S. et al. Exploitation of the Intestinal Microflora by the Parasitic Nematode *Trichuris muris*. *Science* 328, 1391–1394 (2010).

172. Vejzagić, N. et al. Bacteria-induced egg hatching differs for *Trichuris muris* and *Trichuris suis*. *Parasit. Vectors* 8, 371 (2015).
173. Koyama, K. Bacteria-induced hatching of *Trichuris muris* eggs occurs without direct contact between eggs and bacteria. *Parasitol. Res.* 115, 437–440 (2016).
174. Koyama, K. Evidence for bacteria-independent hatching of *Trichuris muris* eggs. *Parasitol. Res.* 112, 1537–1542 (2013).
175. Hasnain, S. Z., McGuckin, M. A., Grecnis, R. K. & Thornton, D. J. Serine Protease(s) Secreted by the Nematode *Trichuris muris* Degrade the Mucus Barrier. *PLoS Negl. Trop. Dis.* 6, e1856 (2012).
176. Drake, L. J., Bianco, A. E., Bundy, D. A. P. & Ashall, F. Characterization of peptidases of adult *Trichuris muris*. *Parasitology* 109, 623–630 (1994).
177. Drake, L. J. et al. The major secreted product of the whipworm *Trichuris*, is a pore-forming protein. *Proc. R. Soc. London B* 257, 255–261 (1994).
178. Hiemstra, I. H. et al. Excreted/secreted *Trichuris suis* products reduce barrier function and suppress inflammatory cytokine production of intestinal epithelial cells. *Mol. Immunol.* 60, 1–7 (2014).
179. Bellaby, T., Robinson, K., Wakelin, D. & Behnke, J. M. Isolates of *Trichuris muris* vary in their ability to elicit protective immune responses to infection in mice. *Parasitology* 111, 353–357 (1995).
180. Koyama, K. & Ito, Y. Comparative studies on immune responses to infection in susceptible B10. BR mice infected with different strains of the murine nematode parasite *Trichuris muris*. *Parasite Immunol.* 18, 257–263 (1996).
181. Wakelin, D. Genetic control of immune responses to parasites: immunity to *Trichuris muris* in inbred and random-bred strains of mice. *Parasitology* 71, 51–60 (1975).
182. Williams-Blangero, S. et al. Genetic Component to Susceptibility to *Trichuris trichiura*: Evidence from Two Asian Populations. *Genet. Epidemiol.* 22, 254–264 (2002).
183. Williams-Blangero, S. et al. Two Quantitative Trait Loci Influence Whipworm (*Trichuris trichiura*) Infection in a Nepalese Population. *J. Infect. Dis.* 197, 1198–1203 (2008).
184. Wahid, F. N., Robinson, M. & Behnke, J. M. Immunological relationships during primary infection with *Heligmosomoides polygyrus* (*Nematospiroides dubius*): expulsion of adult worms from fast responder syngeneic and hybrid strains of mice. *Parasitology* 98, 459–469 (1989).
185. Peisong, G. et al. An asthma-associated genetic variant of STAT6 predicts low burden of ascaris worm infestation. *Genes Immun.* 5, 58–62 (2004).
186. Kouriba, B. et al. Analysis of the 5q31-q33 Locus Shows an Association between IL13-1055C/T IL-13-591A/G Polymorphisms and *Schistosoma haematobium* Infections. *J. Immunol.* 174, 6274–6281 (2005).
187. Scales, H. E., Ierna, M. X. & Lawrence, C. E. The role of IL-4, IL-13 and IL-4R α in the development of protective and pathological responses to *Trichinella spiralis*. *Parasite Immunol.* 29, 81–91 (2007).
188. Else, K. J. & Wakelin, D. The effects of H-2 and non-H-2 genes on the expulsion of the nematode *Trichuris muris* from inbred and congenic mice. *Parasitology* 96, 543–550 (1988).
189. Else, K. J., Wakelin, D. & Roach, T. I. A. Host predisposition to trichuriasis: the mouse - *T. muris* model. *Parasitology* 98, 275–282 (1989).
190. Else, K. J., Wakelin, D., Wassom, D. L. & Hauda, K. M. The influence of genes mapping within the major histocompatibility complex on resistance to *Trichuris muris* infections in mice. *Parasitology* 101, 61–67 (1990).
191. Bancroft, A. J., Artis, D., Donaldson, D. D., Sypek, J. P. & Grecnis, R. K. Gastrointestinal nematode expulsion in IL-4 knockout mice is IL-13 dependent. *Eur. J. Immunol.* 30, 2083–2091 (2000).
192. Hayes, K. S., Hager, R. & Grecnis, R. K. Sex-dependent genetic effects on immune responses to a parasitic nematode. *BMC Genomics* 15, 193 (2014).
193. Bancroft, A. J., Else, K. J. & Grecnis, R. K. Low-level infection with *Trichuris muris* significantly affects the polarization of the CD4 response. *Eur. J. Immunol.* 24, 3113–3118 (1994).
194. Dorea, R. C. C., Alexander, J. & Gallagher, G. New Zealand black mice are immunologically resistant to high-dose, but not low-dose *Leishmania mexicana* infection. *Clin. Exp. Immunol.* 85, 231–235 (1991).

195. Woolhouse, M. E. J., Webster, J. P., Domingo, E., Charlesworth, B. & Levin, B. R. Biological and biomedical implications of the co-evolution of pathogens and their hosts. *Nat. Genet.* 32, 569–577 (2002).
196. Behnke, J. M. & Wakelin, D. The survival of *Trichuris muris* in wild populations of its natural hosts. *Parasitology* 67, 157–164 (1973).
197. Gregory, R. D. On the interpretation of host-parasite ecology: Heligmosomoides polygyrus (Nematoda) in wild wood mouse (*Apodemus sylvaticus*) populations. *J. Zool. London* 226, 109–121 (1992).
198. Bancroft, A. J., Else, K. J., Humphreys, N. E. & Grecnis, R. K. The effect of challenge and trickle *Trichuris muris* infections on the polarisation of the immune response. *Int. J. Parasitol.* 31, 1627–1637 (2001).
199. Bancroft, A. J., McKenzie, A. N. J. & Grecnis, R. K. A Critical Role for IL-13 in Resistance to Intestinal Nematode Infection. *J. Immunol.* 160, 3453–3461 (1998).
200. McKenzie, G. J., Bancroft, A. J., Grecnis, R. K. & McKenzie, A. N. J. A distinct role for interleukin-13 in Th2-cell-mediated immune responses. *Curr. Biol.* 8, 339–342 (1998).
201. Urban Jr, J. F. et al. IL-13, IL-4 α , and Stat6 Are Required for the Expulsion of the Gastrointestinal Nematode Parasite *Nippostrongylus brasiliensis*. *Immunity* 8, 255–264 (1998).
202. Urban Jr, J. F., Katona, I. M., Paul, W. E. & Finkelman, F. D. Interleukin 4 is important in protective immunity to a gastrointestinal nematode infection in mice. *Proc. Natl. Acad. Sci. U. S. A.* 88, 5513–5517 (1991).
203. Urban Jr, J. F. et al. IFN Inhibits Inflammatory Responses and Protective Immunity in Mice Infected with the Nematode Parasite, *Nippostrongylus brasiliensis*. *J. Immunol.* 151, 7086–7094 (1993).
204. Else, K. J., Finkelman, F. D., Maliszewski, C. R. & Grecnis, R. K. Cytokine-mediated Regulation of Chronic Intestinal Helminth Infection. *J. Exp. Med.* 179, 347–351 (1994).
205. Finkelman, F. D. et al. Effects of Interleukin 12 on Immune Responses and Host Protection in Mice Infected with Intestinal Nematode Parasites. *J. Exp. Med.* 179, 1563–1572 (1994).
206. Urban Jr, J. F., Maliszewski, C. R., Madden, K. B., Katona, I. M. & Finkelman, F. D. IL-4 Treatment Can Cure Established Gastrointestinal Nematode Infections in Immunocompetent and Immunodeficient Mice. *J. Immunol.* 154, 4675–4684 (1995).
207. Bancroft, A. J., Else, K. J., Sypek, J. P. & Grecnis, R. K. Interleukin-12 promotes a chronic intestinal nematode infection. *Eur. J. Immunol.* 27, 866–870 (1997).
208. Helmbj, H., Takeda, K., Akira, S. & Grecnis, R. K. Interleukin (IL)-18 Promotes the Development of Chronic Gastrointestinal Helminth Infection by Downregulating IL-13. *J. Exp. Med.* 194, 355–364 (2001).
209. Campbell, W. C. & Collette, J. V. Effect of cortisone upon infection with *Trichuris muris* in albino mice. *J. Parasitol.* 48, 933–934 (1962).
210. Wakelin, D. Acquired immunity to *Trichuris muris* in the albino laboratory mouse. *Parasitology* 57, 515–524 (1967).
211. Wakelin, D. & Selby, G. R. Thymus-dependency of the immune response of mice to a primary infection with the nematode *Trichuris muris*. *Int. J. Parasitol.* 4, 657–661 (1974).
212. Ito, Y. The absence of resistance in congenitally athymic nude mice toward infection with the intestinal nematode, *Trichuris muris*: resistance restored by lymphoid cell transfer. *Int. J. Parasitol.* 21, 65–69 (1991).
213. Koyama, K., Tamauchi, H. & Ito, Y. The role of CD4⁺ and CD8⁺ T cells in protective immunity to the murine nematode parasite *Trichuris muris*. *Parasite Immunol.* 17, 161–165 (1995).
214. Else, K. J. & Grecnis, R. K. Antibody-Independent Effector Mechanisms in Resistance to the Intestinal Nematode Parasite *Trichuris muris*. *Infect. Immun.* 64, 2950–2954 (1996).
215. Lee, T. D. G., Wakelin, D. & Grecnis, R. K. Cellular mechanisms of immunity to the nematode *Trichuris muris*. *Int. J. Parasitol.* 13, 349–353 (1983).
216. Blackwell, N. M. & Else, K. J. B cells and Antibodies Are Required for Resistance to the Parasitic Gastrointestinal Nematode *Trichuris muris*. *Infect. Immun.* 69, 3860–3868 (2001).

217. Roach, T. I. A., Else, K. J., Wakelin, D., McLaren, D. J. & Grecis, R. K. *Trichuris muris*: antigen recognition and transfer of immunity in mice by IgA monoclonal antibodies. *Parasite Immunol.* 13, 1–12 (1991).
218. Else, K. J., Wakelin, D., Wassom, D. L. & Hauda, K. M. MHC-restricted antibody responses to *Trichuris muris* excretory/secretory (E/S) antigen. *Parasite Immunol.* 12, 509–527 (1990).
219. Ramalho-Pinto, F. J., De Rossi, R. & Smithers, S. R. Murine *schistosomiasis mansoni*: anti-schistosomula antibodies and the IgG subclasses involved in the complement- and eosinophil-mediated killing of schistosomula *in vitro*. *Parasite Immunol.* 1, 295–308 (1979).
220. Pritchard, D. I., Williams, D. J. L., Behnke, J. M. & Lee, T. D. G. The role of IgG1 hypergammaglobulinaemia in immunity to the gastrointestinal nematode *Nematospiroides dubius*. The immunochemical purification, antigen-specificity and *in vivo* anti-parasite effect of IgG1 from immune serum. *Immunology* 49, 353–365 (1983).
221. Hewitson, J. P. et al. Concerted Activity of IgG1 Antibodies and IL-4/IL-25-Dependent Effector Cells Trap Helminth Larvae in the Tissues following Vaccination with Defined Secreted Antigens, Providing Sterile Immunity to Challenge Infection. *PLoS Pathog.* 11, e1004676 (2015).
222. Schopf, L. R., Hoffmann, K. F., Cheever, A. W., Urban Jr, J. F. & Wynn, T. A. IL-10 Is Critical for Host Resistance and Survival During Gastrointestinal Helminth Infection. *J. Immunol.* 168, 2383–2392 (2002).
223. Levison, S. E. et al. Colonic Transcriptional Profiling in Resistance and Susceptibility to Trichuriasis: Phenotyping a Chronic Colitis and Lessons for Iatrogenic Helminthiasis. *Inflamm. Bowel Dis.* 16, 2065–2079 (2010).
224. Zaph, C. et al. Epithelial-cell-intrinsic IKK-beta expression regulates intestinal immune homeostasis. *Nature* 446, 552–556 (2007).
225. Gerbe, F. et al. Intestinal epithelial tuft cells initiate type 2 mucosal immunity to helminth parasites. *Nature* 529, 226–230 (2016).
226. Howitt, M. R. et al. Tuft cells, taste-chemosensory cells, orchestrate parasite type 2 immunity in the gut. *Science* 351, 1329–1333 (2016).
227. von Moltke, J., Ji, M., Liang, H.-E. & Locksley, R. M. Tuft-cell-derived IL-25 regulates an intestinal ILC2-epithelial response circuit. *Nature* 529, 221–225 (2016).
228. DeSchoolmeester, M. L., Martinez-Pomares, L., Gordon, S. & Else, K. J. The mannose receptor binds *Trichuris muris* excretory/secretory proteins but is not essential for protective immunity. *Immunology* 126, 246–255 (2009).
229. Van Dyken, S. J. et al. Chitin Activates Parallel Immune Modules that Direct Distinct Inflammatory Responses via Innate Lymphoid Type 2 and $\gamma\delta$ T cells. *Immunity* 40, 414–424 (2014).
230. Zhu, Z. et al. Acidic Mammalian Chitinase in Asthmatic Th2 Inflammation and IL-13 Pathway Activation. *Science* 304, 1678–1682 (2004).
231. Nair, M. G. et al. Chitinase and Fizz family members are a generalized feature of nematode infection with selective upregulation of Ym1 and Fizz1 by antigen-presenting cells. *Infect. Immun.* 73, 385–394 (2005).
232. Reese, T. A. et al. Chitin induces accumulation in tissue of innate immune cells associated with allergy. *Nature* 447, 92–96 (2007).
233. Vannella, K. M. et al. Acidic chitinase primes the protective immune response to gastrointestinal nematodes. *Nat. Immunol.* 17, 538–544 (2016).
234. Conti, H. R. et al. Th17 cells and IL-17 receptor signaling are essential for mucosal host defense against oral candidiasis. *J. Exp. Med.* 206, 299–311 (2009).
235. Gladiator, A., Wangler, N., Trautwein-Weidner, K. & LeibundGut-Landmann, S. IL-17-Secreting Innate Lymphoid Cells Are Essential for Host Defense against Fungal Infection. *J. Immunol.* 190, 521–525 (2013).
236. Fallon, P. G. et al. Identification of an interleukin (IL)-25-dependent cell population that provides IL-4, IL-5, and IL-13 at the onset of helminth expulsion. *J. Exp. Med.* 203, 1105–1116 (2006).
237. Owyang, A. M. et al. Interleukin 25 regulates type 2 cytokine-dependent immunity and limits chronic

- inflammation in the gastrointestinal tract. *J. Exp. Med.* 203, 843–849 (2006).
238. Humphreys, N. E., Xu, D., Hepworth, M. R., Liew, F. Y. & Grencis, R. K. IL-33, a Potent Inducer of Adaptive Immunity to Intestinal Nematodes. *J. Immunol.* 180, 2443–2449 (2008).
 239. Wills-Karp, M. et al. Trefoil factor 2 rapidly induces interleukin 33 to promote type 2 immunity during allergic asthma and hookworm infection. *J. Exp. Med.* 209, 607–622 (2012).
 240. Hung, L.-Y. et al. IL-33 drives biphasic IL-13 production for noncanonical Type 2 immunity against hookworms. *Proc. Natl. Acad. Sci. U. S. A.* 110, 282–287 (2013).
 241. Massacand, J. C. et al. Helminth products bypass the need for TSLP in Th2 immune responses by directly modulating dendritic cell function. *Proc. Natl. Acad. Sci. U. S. A.* 106, 13968–13973 (2009).
 242. Taylor, B. C. et al. TSLP regulates intestinal immunity and inflammation in mouse models of helminth infection and colitis. *J. Exp. Med.* 206, 655–667 (2009).
 243. Moro, K. et al. Innate production of TH2 cytokines by adipose tissue-associated c-Kit⁺Sca-1⁺ lymphoid cells. *Nature* 463, 540–544 (2010).
 244. Neill, D. R. et al. Nuocytes represent a new innate effector leukocyte that mediates type-2 immunity. *Nature* 464, 1367–1370 (2010).
 245. Price, A. E. et al. Systemically dispersed innate IL-13-expressing cells in type 2 immunity. *Proc. Natl. Acad. Sci. U. S. A.* 107, 11489–11494 (2010).
 246. Saenz, S. A. et al. IL25 elicits a multipotent progenitor cell population that promotes TH2 cytokine responses. *Nature* 464, 1362–1366 (2010).
 247. Oeser, K., Schwartz, C. & Voehringer, D. Conditional IL-4/IL-13-deficient mice reveal a critical role of innate immune cells for protective immunity against gastrointestinal helminths. *Mucosal Immunol.* 8, 672–682 (2015).
 248. Zhang, D.-H., Cohn, L., Ray, P., Bottomly, K. & Ray, A. Transcription Factor GATA-3 Is Differentially Expressed in Murine Th1 and Th2 Cells and Controls Th2-specific Expression of the Interleukin-5 gene. *J. Biol. Chem.* 272, 21597–21603 (1997).
 249. Zheng, W. & Flavell, R. A. The Transcription Factor GATA-3 Is Necessary and Sufficient for Th2 Cytokine Gene Expression in CD4 T Cells. *Cell* 89, 587–596 (1997).
 250. Liang, H.-E. et al. Divergent expression patterns of IL-4 and IL-13 define unique functions in allergic immunity. *Nat. Immunol.* 13, 58–66 (2011).
 251. Hoyler, T. et al. The Transcription Factor GATA-3 Controls Cell Fate and Maintenance of Type 2 Innate Lymphoid Cells. *Immunity* 37, 634–648 (2012).
 252. Mjösberg, J. et al. The Transcription Factor GATA3 Is Essential for the Function of Human Type 2 Innate Lymphoid Cells. *Immunity* 37, 649–659 (2012).
 253. Zhao, A. et al. Critical Role of IL-25 in Nematode Infection-Induced Alterations in Intestinal Function. *J. Immunol.* 185, 6921–6929 (2010).
 254. Mearns, H. et al. IL-25 exhibits disparate roles during Th2-cell differentiation versus effector function. *Eur. J. Immunol.* 44, 1976–1980 (2014).
 255. Wang, Y.-H. et al. IL-25 augments type 2 immune responses by enhancing the expansion and functions of TSLP-DC-activated Th2 memory cells. *J. Exp. Med.* 204, 1837–1847 (2007).
 256. Kang, Z. et al. Epithelial Cell-Specific Act1 Adaptor Mediates Interleukin-25-Dependent Helminth Expulsion through Expansion of Lin⁻c-Kit⁺ Innate Cell Population. *Immunity* 36, 821–833 (2012).
 257. Tjota, M. Y. et al. IL-33-dependent induction of allergic lung inflammation by FcγRIII signaling. *J. Clin. Invest.* 123, 2287–2297 (2013).
 258. Carriere, V. et al. IL-33, the IL-1-like cytokine ligand for ST2 receptor, is a chromatin-associated nuclear factor *in vivo*. *Proc. Natl. Acad. Sci. U. S. A.* 104, 282–287 (2007).
 259. Cayrol, C. & Girard, J.-P. The IL-1-like cytokine IL-33 is inactivated after maturation by caspase-1. *Proc. Natl. Acad. Sci. U. S. A.* 106, 9021–9026 (2009).
 260. Lefrançois, E. et al. IL-33 is processed into mature bioactive forms by neutrophil elastase and cathepsin G. *Proc. Natl. Acad. Sci. U. S. A.* 109, 1673–1678 (2012).
 261. Lefrançois, E. et al. Central domain of IL-33 is cleaved by mast cell proteases for potent activation of group-2 innate lymphoid cells. *Proc. Natl. Acad. Sci. U. S. A.* 111, 15502–15507 (2014).

262. Moulin, D. et al. Interleukin (IL)-33 induces the release of pro-inflammatory mediators by mast cells. *Cytokine* 40, 216–225 (2007).
263. Cherry, W. B., Yoon, J., Bartemes, K. R., Iijima, K. & Kita, H. A novel IL-1 family cytokine, IL-33, potently activates human eosinophils. *J. Allergy Clin. Immunol.* 121, 1484–1490 (2008).
264. Plantinga, M. et al. Conventional and Monocyte-Derived CD11b⁺ Dendritic Cells Initiate and Maintain T Helper 2 Cell-Mediated Immunity to House Dust Mite Allergen. *Immunity* 38, 322–335 (2013).
265. Van Dyken, S. J. et al. A tissue checkpoint regulates type 2 immunity. *Nat. Immunol.* 17, 1381–1387 (2016).
266. Soumelis, V. et al. Human epithelial cells trigger dendritic cell-mediated allergic inflammation by producing TSLP. *Nat. Immunol.* 3, 673–680 (2002).
267. Siracusa, M. C. et al. TSLP promotes interleukin-3-independent basophil haematopoiesis and type 2 inflammation. *Nature* 477, 229–233 (2011).
268. Endo, Y. et al. The Interleukin-33-p38 Kinase Axis Confers Memory T Helper 2 Cell Pathogenicity in the Airway. *Immunity* 42, 294–308 (2015).
269. Guo, L. et al. Innate immunological function of TH2 cells *in vivo*. *Nat. Immunol.* 16, 1051–1059 (2015).
270. Wang, Q., Du, J., Zhu, J., Yang, X. & Zhou, B. Thymic stromal lymphopoietin signaling in CD4⁺ T cells is required for TH2 memory. *J. Allergy Clin. Immunol.* 135, 781–791 (2015).
271. Holmkvist, P. et al. A major population of mucosal memory CD4⁺ T cells, coexpressing IL-18R α and DR3, display innate lymphocyte functionality. *Mucosal Immunol.* 8, 545–558 (2015).
272. Halim, T. Y. F. et al. Group 2 Innate Lymphoid Cells Are Critical for the Initiation of Adaptive T Helper 2 Cell-Mediated Allergic Lung Inflammation. *Immunity* 40, 425–435 (2014).
273. Halim, T. Y. F. et al. Group 2 innate lymphoid cells license dendritic cells to potentiate memory TH2 cell responses. *Nat. Immunol.* 17, 57–64 (2016).
274. Obata-Ninomiya, K. et al. The skin is an important bulwark of acquired immunity against intestinal helminths. *J. Exp. Med.* 210, 2583–2595 (2013).
275. Lin, J.-X. et al. The Role of Shared Receptor Motifs and Common Stat Proteins in the Generation of Cytokine Pleiotropy and Redundancy by IL-2, IL-4, IL-7, IL-13, and IL-15. *Immunity* 2, 331–339 (1995).
276. Smerz-Bertling, C. & Duschl, A. Both Interleukin 4 and Interleukin 13 Induce Tyrosine Phosphorylation of the 140-kDa Subunit of the Interleukin 4 Receptor. *J. Biol. Chem.* 270, 966–970 (1995).
277. Zurawski, S. M. et al. The Primary Binding Subunit of the Human Interleukin-4 Receptor Is Also a Component of the Interleukin-13 Receptor. *The Journal of Biological Chemistry* 270, 13869–13878 (1995).
278. Michels, C. E. et al. Neither interleukin-4 receptor α expression on CD4⁺ T cells, or macrophages and neutrophils is required for protective immunity to *Trichinella spiralis*. *Immunology* 128, e385–394 (2009).
279. Schmidt, S. et al. *Nippostrongylus*-Induced Intestinal Hypercontractility Requires IL-4 Receptor Alpha-Responsiveness by T Cells in Mice. *PLoS One* 7, e52211 (2012).
280. Barner, M., Mohrs, M., Brombacher, F. & Kopf, M. Differences between IL-4R α -deficient and IL-4-deficient mice reveal a role for IL-13 in the regulation of Th2 responses. *Curr. Biol.* 8, 669–672 (1998).
281. Filbey, K. J. et al. Innate and adaptive type 2 immune cell responses in genetically controlled resistance to intestinal helminth infection. *Immunol. Cell Biol.* 92, 436–448 (2014).
282. Pelly, V. S. et al. IL-4-producing ILC2s are required for the differentiation of TH2 cells following *Heligmosomoides polygyrus* infection. *Mucosal Immunol.* 9, 1407–1417 (2016).
283. Min, B. et al. Basophils Produce IL-4 and Accumulate in Tissues after Infection with a Th2-inducing Parasite. *J. Exp. Med.* 200, 507–517 (2004).
284. Motomura, Y. et al. Basophil-Derived Interleukin-4 Controls the Function of Natural Helper Cells, a Member of ILC2s, in Lung Inflammation. *Immunity* 40, 758–771 (2014).
285. Molofsky, A. B. et al. Innate lymphoid type 2 cells sustain visceral adipose tissue eosinophils and alternatively activated macrophages. *J. Exp. Med.* 210, 535–549 (2013).
286. Nussbaum, J. C. et al. Type 2 innate lymphoid cells control eosinophil homeostasis. *Nature* 502,

- 245–248 (2013).
287. Yang, D. et al. Eosinophil-derived neurotoxin acts as an alarmin to activate the TLR2-MyD88 signal pathway in dendritic cells and enhances Th2 immune responses. *J. Exp. Med.* 205, 79–90 (2008).
288. Chu, D. K. et al. Indigenous enteric eosinophils control DCs to initiate a primary Th2 immune response *in vivo*. *J. Exp. Med.* 211, 1657–1672 (2014).
289. Dent, L. A. et al. Interleukin-5 Transgenic Mice Show Enhanced Resistance to Primary Infections with *Nippostrongylus brasiliensis* but Not Primary Infections with *Toxocara canis*. *Infect. Immun.* 67, 989–993 (1999).
290. Knott, M. L. et al. Impaired resistance in early secondary *Nippostrongylus brasiliensis* infections in mice with defective eosinophilopoiesis. *Int. J. Parasitol.* 37, 1367–1378 (2007).
291. Faulkner, H., Humphreys, N. E., Renauld, J.-C., Van Snick, J. & Grecis, R. K. Interleukin-9 is involved in host protective immunity to intestinal nematode infection. *Eur. J. Immunol.* 27, 2536–2540 (1997).
292. Matsuzawa, S. et al. IL-9 Enhances the Growth of Human Mast Cell Progenitors Under Stimulation with Stem Cell Factor. *J. Immunol.* 170, 3461–3467 (2003).
293. Forbes, E. E. et al. IL-9- and mast cell-mediated intestinal permeability predisposes to oral antigen hypersensitivity. *J. Exp. Med.* 205, 897–913 (2008).
294. Ruitenber, E. J. & Elgersma, A. Absence of intestinal mast cell response in congenitally athymic mice during *Trichinella spiralis* infection. *Nature* 264, 258–260 (1976).
295. Irani, A.-M. A. et al. Deficiency of the tryptase-positive, chymase-negative mast cell type in gastrointestinal mucosa of patients with defective T lymphocyte function. *J. Immunol.* 138, 4381–4386 (1987).
296. Licona-Limón, P. et al. Th9 Cells Drive Host Immunity against Gastrointestinal Worm Infection. *Immunity* 39, 744–757 (2013).
297. Wilhelm, C. et al. An IL-9 fate reporter demonstrates the induction of an innate IL-9 response in lung inflammation. *Nat. Immunol.* 12, 1071–1077 (2011).
298. Hültner, L. et al. In Activated Mast Cells, IL-1 Up-Regulates the Production of Several Th2-Related Cytokines Including IL-9. *J. Immunol.* 164, 5556–5563 (2000).
299. Chen, C.-Y. et al. Induction of Interleukin-9-Producing Mucosal Mast Cells Promotes Susceptibility to IgE-Mediated Experimental Food Allergy. *Immunity* 43, 788–802 (2015).
300. Hepworth, M. R. et al. Mast cells orchestrate type 2 immunity to helminths through regulation of tissue-derived cytokines. *Proc. Natl. Acad. Sci. U. S. A.* 109, 6644–6649 (2012).
301. Koyama, K. & Ito, Y. Mucosal mast cell responses are not required for protection against infection with the murine nematode parasite *Trichuris muris*. *Parasite Immunol.* 22, 21–28 (2000).
302. Richard, M., Grecis, R. K., Humphreys, N. E., Renauld, J.-C. & Van Snick, J. Anti-IL-9 vaccination prevents worm expulsion and blood eosinophilia in *Trichuris muris*-infected mice. *Proc. Natl. Acad. Sci. U. S. A.* 97, 767–772 (2000).
303. Khan, W. I. et al. Modulation of Intestinal Muscle Contraction by Interleukin-9 (IL-9) or IL-9 Neutralization: Correlation with Worm Expulsion in Murine Nematode Infections. *Infect. Immun.* 71, 2430–2438 (2003).
304. Knight, P. A., Wright, S. H., Lawrence, C. E., Paterson, Y. Y. W. & Miller, H. R. P. Delayed Expulsion of the Nematode *Trichinella spiralis* in Mice Lacking the Mucosal Mast Cell-specific Granule Chymase, Mouse Mast Cell Protease-1. *J. Exp. Med.* 192, 1849–1856 (2000).
305. McDermott, J. R. et al. Mast cells disrupt epithelial barrier function during enteric nematode infection. *Proc. Natl. Acad. Sci. U. S. A.* 100, 7761–7766 (2003).
306. Lawrence, C. E., Paterson, Y. Y. W., Wright, S. H., Knight, P. A. & Miller, H. R. P. Mouse Mast Cell Protease-1 Is Required for the Enteropathy Induced by Gastrointestinal Helminth Infection in the Mouse. *Gastroenterology* 127, 155–165 (2004).
307. Crowle, P. K. & Reed, N. D. Rejection of the Intestinal Parasite *Nippostrongylus brasiliensis* by Mast Cell-Deficient *W/W^v* Anemic Mice. *Infect. Immun.* 33, 54–58 (1981).
308. Crowle, P. K. Mucosal mast cell reconstitution and *Nippostrongylus brasiliensis* rejection by *W/W^v* mice. *J. Parasitol.* 69, 66–69 (1983).

309. Townsend, M. J. et al. IL-9-Deficient Mice Establish Fundamental Roles for IL-9 in Pulmonary Mastocytosis and Goblet Cell Hyperplasia but Not T Cell Development. *Immunity* 13, 573–583 (2000).
310. Cruickshank, S. M. et al. Rapid dendritic cell mobilization to the large intestinal epithelium is associated with resistance to *Trichuris muris* infection. *J. Immunol.* 182, 3055–3062 (2009).
311. Bowcutt, R. et al. A role for the pattern recognition receptor Nod2 in promoting recruitment of CD103⁺ dendritic cells to the colon in response to *Trichuris muris* infection. *Mucosal Immunol.* 7, 1094–1105 (2014).
312. Cook, P. C. et al. A dominant role for the methyl-CpG-binding protein Mbd2 in controlling Th2 induction by dendritic cells. *Nat. Commun.* 6, 6920 (2015).
313. Tussiwand, R. et al. Klf4 Expression in Conventional Dendritic Cells Is Required for T Helper 2 Cell Responses. *Immunity* 42, 916–928 (2015).
314. Gao, Y. et al. Control of T Helper 2 Responses by Transcription Factor IRF4-Dependent Dendritic Cells. *Immunity* 39, 722–732 (2013).
315. Kumamoto, Y. et al. CD301b⁺ Dermal Dendritic Cells Drive T Helper 2 Cell-Mediated Immunity. *Immunity* 39, 733–743 (2013).
316. Williams, J. W. et al. Transcription factor IRF4 drives dendritic cells to promote Th2 differentiation. *Nat. Commun.* 4, 2990 (2013).
317. Murakami, R. et al. A Unique Dermal Dendritic Cell Subset That Skews the Immune Response toward Th2. *PLoS One* 8, e73270 (2013).
318. Martínez-López, M., Iborra, S., Conde-Garrosa, R. & Sancho, D. Batf3-dependent CD103⁺ dendritic cells are major producers of IL-12 that drive local Th1 immunity against *Leishmania major* infection in mice. *Eur. J. Immunol.* 45, 119–129 (2015).
319. Luda, K. M. et al. IRF8 Transcription-Factor-Dependent Classical Dendritic Cells Are Essential for Intestinal T Cell Homeostasis. *Immunity* 44, 860–874 (2016).
320. Everts, B. et al. Migratory CD103⁺ dendritic cells suppress helminth-driven type 2 immunity through constitutive expression of IL-12. *J. Exp. Med.* 213, 35–51 (2015).
321. Gold, M. J., Antignano, F., Hughes, M. R., Zaph, C. & McNagny, K. M. Dendritic-cell expression of Ship1 regulates Th2 immunity to helminth infection in mice. *Eur. J. Immunol.* 46, 122–130 (2016).
322. Amsen, D. et al. Instruction of Distinct CD4 T Helper Cell Fates by Different Notch Ligands on Antigen-Presenting Cells. *Cell* 117, 515–526 (2004).
323. MacDonald, A. S., Straw, A. D., Dalton, N. M. & Pearce, E. J. Th2 Response Induction by Dendritic Cells: A Role for CD40. *J. Immunol.* 168, 537–540 (2002).
324. Yrlid, U. et al. A distinct subset of intestinal dendritic cells responds selectively to oral TLR7/8 stimulation. *Eur. J. Immunol.* 36, 2639–2648 (2006).
325. Fujimoto, K. et al. A New Subset of CD103⁺CD8 α ⁺ Dendritic Cells in the Small Intestine Expresses TLR3, TLR7, and TLR9 and Induces Th1 Response and CTL Activity. *J. Immunol.* 186, 6287–6295 (2011).
326. Watchmaker, P. B. et al. Comparative transcriptional and functional profiling defines conserved programs of intestinal DC differentiation in humans and mice. *Nat. Immunol.* 15, 98–108 (2014).
327. Liu, H. et al. TLR5 mediates CD172 α ⁺ intestinal lamina propria dendritic cell induction of Th17 cells. *Sci. Rep.* 6, 22040 (2016).
328. Connor, L. M. et al. Th2 responses are primed by skin dendritic cells with distinct transcriptional profiles. *J. Exp. Med.* 214, 125–142 (2017).
329. Perrigoue, J. G. et al. MHC class II-dependent basophil-CD4⁺ T cell interactions promote TH2 cytokine-dependent immunity. *Nat. Immunol.* 10, 697–705 (2009).
330. Sokol, C. L. et al. Basophils function as antigen-presenting cells for an allergen-induced T helper type 2 response. *Nat. Immunol.* 10, 713–720 (2009).
331. Yoshimoto, T. et al. Basophils contribute to Th2-IgE responses *in vivo* via IL-4 production and presentation of peptide-MHC class II complexes to CD4⁺ T cells. *Nat. Immunol.* 10, 706–712 (2009).
332. Mirchandani, A. S. et al. Type 2 Innate Lymphoid Cells Drive CD4⁺ Th2 Cell Responses. *J. Immunol.*

- 192, 2442–2448 (2014).
333. Oliphant, C. J. et al. MHCII-Mediated Dialog Between Group 2 Innate Lymphoid Cells and CD4⁺ T Cells Potentiates Type 2 Immunity and Promotes Parasitic Helminth Expulsion. *Immunity* 41, 283–295 (2014).
334. Phythian-Adams, A. T. et al. CD11c depletion severely disrupts Th2 induction and development *in vivo*. *J. Exp. Med.* 207, 2089–2096 (2010).
335. Lundie, R. J. et al. A central role for hepatic conventional dendritic cells in supporting Th2 responses during helminth infection. *Immunol. Cell Biol.* 94, 400–410 (2016).
336. Hasnain, S. Z. et al. Mucin Gene Deficiency in Mice Impairs Host Resistance to an Enteric Parasitic Infection. *Gastroenterology* 138, 1763–1771 (2010).
337. Hasnain, S. Z. et al. Muc5ac: a critical component mediating the rejection of enteric nematodes. *J. Exp. Med.* 208, 893–900 (2011).
338. Dabbagh, K. et al. IL-4 Induces Mucin Gene Expression and Goblet Cell Metaplasia *In Vitro* and *In Vivo*. *J. Immunol.* 162, 6233–6237 (1999).
339. Turner, J. E., Stockinger, B. & Helmsby, H. IL-22 Mediates Goblet Cell Hyperplasia and Worm Expulsion in Intestinal Helminth Infection. *PLoS Pathog.* 9, e1003698 (2013).
340. Thawer, S. et al. Surfactant Protein-D Is Essential for Immunity to Helminth Infection. *PLoS Pathog.* 12, e1005461 (2016).
341. Glauert, A. M., Butterworth, A. E., Sturrock, R. F. & Houba, V. The mechanism of antibody-dependent, eosinophil-mediated damage to schistosomula of *Schistosoma mansoni in vitro*: a study by phase-contrast and electron microscopy. *J. Cell Sci.* 34, 173–192 (1978).
342. Hamann, K. J. et al. *In vitro* killing of microfilariae of *Brugia pahangi* and *Brugia malayi* by eosinophil granule proteins. *J. Immunol.* 144, 3166–3173 (1990).
343. Artis, D. et al. RELM β /FIZZ2 is a goblet cell-specific immune-effector molecule in the gastrointestinal tract. *Proc. Natl. Acad. Sci. U. S. A.* 101, 13596–13600 (2004).
344. Nair, M. G. et al. Goblet Cell-Derived Resistin-Like Molecule β Augments CD4⁺ T Cell Production of IFN- γ and Infection-Induced Intestinal Inflammation. *J. Immunol.* 181, 4709–4715 (2008).
345. Herbert, D. R. et al. Intestinal epithelial cell secretion of RELM- β protects against gastrointestinal worm infection. *J. Exp. Med.* 206, 2947–2957 (2009).
346. Chen, G., Wang, S. H., Jang, J. C., Odgaard, J. I. & Nair, M. G. Comparison of RELM α and RELM β Single- and Double-Gene-Deficient Mice Reveals that RELM α Expression Dictates Inflammation and Worm Expulsion in Hookworm Infection. *Infect. Immun.* 84, 1100–1111 (2016).
347. Bowcutt, R. et al. Arginase-1-expressing macrophages are dispensable for resistance to infection with the gastrointestinal helminth *Trichuris muris*. *Parasite Immunol.* 33, 411–420 (2011).
348. Anthony, R. M. et al. Memory TH2 cells induce alternatively activated macrophages to mediate protection against nematode parasites. *Nat. Med.* 12, 955–960 (2006).
349. Zhao, A. et al. Th2 Cytokine-Induced Alterations in Intestinal Smooth Muscle Function Depend on Alternatively Activated Macrophages. *Gastroenterology* 135, 217–225 (2008).
350. Cliffe, L. J. et al. Accelerated Intestinal Epithelial Cell Turnover: A New Mechanism of Parasite Expulsion. *Science* 308, 1463–1465 (2005).
351. Artis, D., Potten, C. S., Else, K. J., Finkelman, F. D. & Grencis, R. K. *Trichuris muris*: Host Intestinal Epithelial Cell Hyperproliferation during Chronic Infection Is Regulated by Interferon- γ . *Exp. Parasitol.* 92, 144–153 (1999).
352. Cliffe, L. J., Potten, C. S., Booth, C. E. & Grencis, R. K. An Increase in Epithelial Cell Apoptosis Is Associated with Chronic Intestinal Nematode Infection. *Infect. Immun.* 75, 1556–1564 (2007).
353. Voehringer, D., Reese, T. A., Huang, X., Shinkai, K. & Locksley, R. M. Type 2 immunity is controlled by IL-4/IL-13 expression in hematopoietic non-eosinophil cells of the innate immune system. *J. Exp. Med.* 203, 1435–1446 (2006).
354. Yamada, T. et al. Eosinophils promote resolution of acute peritonitis by producing proresolving mediators in mice. *FASEB J.* 25, 561–568 (2011).
355. Goh, Y. P. S. et al. Eosinophils secrete IL-4 to facilitate liver regeneration. *Proc. Natl. Acad. Sci. U. S. A.*

- A. 110, 9914–9919 (2013).
356. Heredia, J. E. et al. Type 2 Innate Signals Stimulate Fibro/Adipogenic Progenitors to Facilitate Muscle Regeneration. *Cell* 153, 376–388 (2013).
 357. Qualls, J. E., Kaplan, A. M., van Rooijen, N. & Cohen, D. A. Suppression of experimental colitis by intestinal mononuclear phagocytes. *J. Leukoc. Biol.* 80, 802–815 (2006).
 358. Herbert, D. R. et al. Arginase I Suppresses IL-12/IL-23p40-Driven Intestinal Inflammation during Acute Schistosomiasis. *J. Immunol.* 184, 6438–6446 (2010).
 359. Chen, F. et al. An essential role for Th2-type responses in limiting tissue damage during experimental helminth infection. *Nat. Med.* 18, 260–266 (2012).
 360. Malvin, N. P., Seno, H. & Stappenbeck, T. S. Colonic epithelial response to injury requires Myd88 signaling in myeloid cells. *Mucosal Immunol.* 5, 194–206 (2012).
 361. Esser-von Bieren, J. et al. Immune Antibodies and Helminth Products Drive CXCR2-Dependent Macrophage-Myofibroblast Crosstalk to Promote Intestinal Repair. *PLoS Pathog.* 11, e1004778 (2015).
 362. Cosin-Roger, J. et al. The activation of Wnt signaling by a STAT6-dependent macrophage phenotype promotes mucosal repair in murine IBD. *Mucosal Immunol.* 9, 986–998 (2015).
 363. Chu, V. T. et al. Eosinophils are required for the maintenance of plasma cells in the bone marrow. *Nat. Immunol.* 12, 151–159 (2011).
 364. Forman, R. et al. Eosinophils may play regionally disparate roles in influencing IgA⁺ plasma cell numbers during large and small intestinal inflammation. *BMC Immunol.* 17, 12 (2016).
 365. Huang, L. et al. Eosinophils Mediate Protective Immunity against Secondary Nematode Infection. *J. Immunol.* 194, 283–290 (2015).
 366. Sugawara, R. et al. Small intestinal eosinophils regulate Th17 cells by producing IL-1 receptor antagonist. *J. Exp. Med.* 213, 555–567 (2016).
 367. Croft, A. M., Bager, P. & Kumar, S. Helminth therapy (worms) for allergic rhinitis. *Cochrane Database Syst. Rev.* CD009238 (2012).
 368. Garg, S. K., Croft, A. M. & Bager, P. Helminth therapy (worms) for induction of remission in inflammatory bowel disease. *Cochrane Database Syst. Rev.* CD009400 (2014).
 369. Chenery, A. L. et al. Chronic *Trichuris muris* infection alters hematopoiesis and causes IFN- γ -expressing T-cell accumulation in the mouse bone marrow. *Eur. J. Immunol.* 46, 2587–2596 (2016).
 370. Levison, S. E. et al. Genetic analysis of the *Trichuris muris*-induced model of colitis reveals QTL overlap and a novel gene cluster for establishing colonic inflammation. *BMC Genomics* 14, 127 (2013).
 371. Bhardwaj, E. K., Else, K. J., Rogan, M. T. & Warhurst, G. Increased susceptibility to *Trichuris muris* infection and exacerbation of colitis in Mdr1a^{-/-} mice. *World J. Gastroenterol.* 20, 1797–1806 (2014).
 372. Houlden, A. et al. Chronic *Trichuris muris* Infection in C57BL/6 Mice Causes Significant Changes in Host Microbiota and Metabolome: Effects Reversed by Pathogen Clearance. *PLoS One* 10, e0125945 (2015).
 373. Chenery, A. L. et al. Low-Dose Intestinal *Trichuris muris* Infection Alters the Lung Immune Microenvironment and Can Suppress Allergic Airway Inflammation. *Infect. Immun.* 84, 491–501 (2015).
 374. Little, M. C., Hurst, R. J. M. & Else, K. J. Dynamic Changes in Macrophage Activation and Proliferation during the Development and Resolution of Intestinal Inflammation. *J. Immunol.* 193, 4684–4695 (2014).
 375. Miller, H. R. P., Wright, S. H., Knight, P. A. & Thornton, E. M. A Novel Function for Transforming Growth Factor- β 1: Upregulation of the Expression and the IgE-Independent Extracellular Release of a Mucosal Mast Cell Granule-Specific β -Chymase, Mouse Mast Cell Protease-1. *Blood* 93, 3473–3486 (1999).
 376. Wright, S. H. et al. Transforming growth factor- β 1 mediates coexpression of the integrin subunit α E and the chymase mouse mast cell protease-1 during the early differentiation of bone marrow-derived mucosal mast cell homologues. *Clin. Exp. Allergy* 31, 315–324 (2002).

377. McSorley, J. H., Harcus, Y. M., Murray, J., Taylor, M. D. & Maizels, R. M. Expansion of Foxp3⁺ Regulatory T Cells in Mice Infected with the Filarial Parasite *Brugia malayi*. *J. Immunol.* 181, 6456–6466 (2008).
378. Grainger, J. R. et al. Helminth secretions induce *de novo* T cell Foxp3 expression and regulatory function through the TGF- β pathway. *J. Exp. Med.* 207, 2331–2341 (2010).
379. Kang, S. A. et al. Parasitic Nematode-Induced CD4⁺Foxp3⁺T Cells Can Ameliorate Allergic Airway Inflammation. *PLoS Negl. Trop. Dis.* 8, e3410 (2014).
380. Elliott, D. E. et al. *Heligmosomoides polygyrus* inhibits established colitis in IL-10-deficient mice. *Eur. J. Immunol.* 34, 2690–2698 (2004).
381. Smith, P. et al. Infection with a Helminth Parasite Prevents Experimental Colitis via a Macrophage-Mediated Mechanism. *J. Immunol.* 178, 4557–4566 (2007).
382. Ferreira, I. et al. Hookworm Excretory/Secretory Products Induce Interleukin-4 (IL-4)⁺ IL-10⁺ CD4⁺ T Cell Responses and Suppress Pathology in a Mouse Model of Colitis. *Infect. Immun.* 81, 2104–2111 (2013).
383. Ottow, M. K. et al. The helminth *Trichuris suis* suppresses TLR4-induced inflammatory responses in human macrophages. *Genes Immun.* 15, 477–486 (2014).
384. Quintin, J. et al. *Candida albicans* Infection Affords Protection against Reinfection via Functional Reprogramming of Monocytes. *Cell Host Microbe* 12, 223–232 (2012).
385. Yoshida, K. et al. The transcription factor ATF7 mediates lipopolysaccharide-induced epigenetic changes in macrophages involved in innate immunological memory. *Nat. Immunol.* 16, 1034–1043 (2015).
386. Li, R. W. et al. Alterations in the Porcine Colon Microbiota Induced by the Gastrointestinal Nematode *Trichuris suis*. *Infect. Immun.* 80, 2150–2157 (2012).
387. Wu, S. et al. Worm Burden-Dependent Disruption of the Porcine Colon Microbiota by *Trichuris suis* Infection. *PLoS One* 7, e35470 (2012).
388. Cooper, P. et al. Patent Human Infections with the Whipworm, *Trichuris trichiura*, Are Not Associated with Alterations in the Faecal Microbiota. *PLoS One* 8, e76573 (2013).
389. Lee, S. C. et al. Helminth Colonization Is Associated with Increased Diversity of the Gut Microbiota. *PLoS Negl. Trop. Dis.* 8, e2880 (2014).
390. Helmbly, H. & Grecis, R. K. Interleukin-1 plays a major role in the development of Th2-mediated immunity. *Eur. J. Immunol.* 34, 3674–3681 (2004).
391. Zaiss, M. M. et al. IL-1 β Suppresses Innate IL-25 and IL-33 Production and Maintains Helminth Chronicity. *PLoS Pathog.* 9, e1003531 (2013).
392. Helmbly, H. & Grecis, R. K. IL-18 Regulates Intestinal Mastocytosis and Th2 Cytokine Production Independently of IFN- γ During *Trichinella spiralis* Infection. *J. Immunol.* 169, 2553–2560 (2002).
393. Ritter, M. et al. *Schistosoma mansoni* triggers Dectin-2, which activates the Nlrp3 inflammasome and alters adaptive immune responses. *Proc. Natl. Acad. Sci. U. S. A.* 107, 20459–20464 (2010).
394. Ferguson, B. J. et al. The *Schistosoma mansoni* T2 ribonuclease omega-1 modulates inflammasome-dependent IL-1 β secretion in macrophages. *Int. J. Parasitol.* 45, 809–813 (2015).
395. DeSchoolmeester, M. L., Little, M. C., Rollins, B. J. & Else, K. J. Absence of CC Chemokine Ligand 2 Results in an Altered Th1/Th2 Cytokine Balance and Failure to Expel *Trichuris muris* Infection. *J. Immunol.* 170, 4693–4700 (2003).
396. Verlohren, S. et al. Visceral Periadventitial Adipose Tissue Regulates Arterial Tone of Mesenteric Arteries. *Hypertension* 44, 271–276 (2004).

Abbreviations

Aim	Absent in melanoma
AP-1	Activator protein 1
Asc	Apoptosis-associated speck-like protein containing a card
Caspase	Cysteine aspartic protease
CCL	Chemokine (C-C motif) ligand
CCR	C-C chemokine receptor type 2
CD	Cluster of differentiation
CLR	C-type lectin receptor
E/S	Excretory/Secretory
GATA	Transcription factor GATA
IFN	Interferon
Ig	Immunoglobulin
IL	Interleukin
ILC	Innate lymphoid cell
IRF	Interferon regulatory factor
LPS	Lipopolysaccharide
MCPt	Mast cell-protease
MHC	Major histocompatibility complex
MyD88	Myeloid differentiation primary response gene 88
Naip	Baculoviral IAP repeat-containing protein
NF- κ B	Nuclear factor κ -light-chain-enhancer of activated B cells
Nlr	Nod-like receptor
Nlrc	NLR family CARD domain-containing protein
Nlrp	NACHT, LRR and PYD domains-containing protein
RegIII γ	Regenerating islet-derived protein 3 gamma
RELM	Resistin-like molecule
Rip	Receptor-interacting protein
RLR	RIG-I-like receptor
ROS	Reactive oxygen species
SHIP	SH2-containing inositol 5'-phosphatase
TGF	Transforming growth factor
Th	Helper T cell
TLR	Toll-like receptor
TNF	Tumor necrosis factor
TRIF	TIR-domain-containing adaptor-inducing interferon
TSLP	Thymic stromal lymphopoietin

Paper 1

Research Article

Acute infection with the intestinal parasite *Trichuris muris* has long-term consequences on mucosal mast cell homeostasis and epithelial integrity

Daniel Sorobetea¹, Jacob Bak Holm², Henrietta Henningsson¹,
Karsten Kristiansen² and Marcus Svensson-Frej¹

¹ Immunology Section, Department of Experimental Medical Sciences, Medical Faculty, Lund University, Lund, Sweden

² Laboratory of Genomics and Molecular Biomedicine, Department of Biology, University of Copenhagen, Copenhagen, Denmark

A hallmark of parasite infection is the accumulation of innate immune cells, notably granulocytes and mast cells, at the site of infection. While this is typically viewed as a transient response, with the tissue returning to steady state once the infection is cleared, we found that mast cells accumulated in the large-intestinal epithelium following infection with the nematode *Trichuris muris* and persisted at this site for several months after worm expulsion. Mast cell accumulation in the epithelium was associated with the induction of type-2 immunity and appeared to be driven by increased maturation of local progenitors in the intestinal lamina propria. Furthermore, we also detected increased local and systemic levels of the mucosal mast cell protease MCPT-1, which correlated highly with the persistent epithelial mast cell population. Finally, the mast cells appeared to have striking consequences on epithelial barrier integrity, by regulation of gut permeability long after worm expulsion. These findings highlight the importance of mast cells not only in the early phases of infection but also at later stages, which has functional implications on the mucosal tissue.

Keywords: Acute parasite infection · Large-intestinal epithelium · MCPT-1 · Mucosal mast cell · *Trichuris muris*



Additional supporting information may be found in the online version of this article at the publisher's web-site

Introduction

The intestinal epithelium acts as a barrier to invading pathogens, thus being important for host defense and maintenance of homeostasis. Critical for this process is the intestinal immune system, which populates both the lamina propria and the epithelium.

Reciprocal interaction between immune cells and the epithelium is of paramount importance as improperly regulated immune responses can result in inflammatory bowel disease (IBD), food allergies, and other immune-associated disorders [1–3]. Innate immune cells, including granulocytes and mast cells, are crucial components of this defense as they are often the first to respond to epithelial breach; however, the possible role for granulocytes in maintaining barrier integrity at later stages of immune responses remains unclear.

Correspondence: Dr. Marcus Svensson-Frej
e-mail: marcus.svensson_frej@med.lu.se

The murine-specific parasitic nematode *Trichuris muris* has been an invaluable tool to study intestinal immunity for nearly 50 years [4]. Once eggs are ingested, *Trichuris*-larvae hatch and burrow into the large-intestinal epithelium without penetrating the basal lamina, and remain in this niche unless expelled. Acute infections with *T. muris* are characterized by an early innate inflammatory response, accompanied by the induction of adaptive Th2 immunity and subsequent worm clearance [4]. After expulsion, the host immune system undergoes a complex and coordinated homeostatic event whereby inflammation is resolved and the infected tissue returns to steady state; a process characterized by immune contraction, clearance of apoptotic cells, and tissue repair. However, little attention has been focused to this latter part of the immune response to *T. muris*.

Utilizing *T. muris*, we have investigated the long-term consequences of acute intestinal nematode infection on innate immunity, specifically granulocytes and mast cells. Mast cells, which are present only at very low numbers in the large intestine at steady state, accumulated in high numbers after infection, notably in the epithelium, and persisted for several months after worm expulsion. The epithelial mast cells displayed a unique surface phenotype and were relatively long-lived, being maintained by maturation of local progenitors. Furthermore, mast cell-derived proteases were detected both locally and systemically long after pathogen clearance, indicative of the mast cells being activated. Finally, accumulation of epithelial mast cells appeared to have striking consequences on barrier integrity by regulation of gut permeability well after worm expulsion. These findings highlight the importance of granulocytes not only in the early phases of infection but also at later stages, with functional implications on the mucosal tissue.

Results

Accumulation of granular cells in the large-intestinal epithelium upon acute *T. muris* infection

Granulocytes and mast cells are rapidly recruited to sites of inflammation, notably during parasite infections. We infected C57BL/6 mice with a high dose of *T. muris* eggs and monitored the accumulation of granular cells in the intestinal mucosa over time. As expected, infection with *T. muris* brought about an increase of granular cells in the large intestine, particularly the epithelium (Fig. 1A), the majority of which expressed Siglec-F, a lectin most commonly associated with eosinophils. Upon further assessment of the epithelial granulocytes, two distinct Siglec-F⁺ populations became apparent; one high in both Siglec-F and the integrin CD11b (resembling true eosinophils), and the other intermediate in Siglec-F and negative for CD11b (Fig. 1B). Conversely, the Siglec-F^{int} population expressed high levels of the epithelium-associated integrin CD103, whereas all Siglec-F^{hi} cells lacked CD103 (Fig. 1B). Neither population displayed phenotypic characteristics pertaining to T cells, B cells, monocytes, macrophages,

dendritic cells, natural killer cells, or neutrophils (Supporting Information Fig. 1A).

High-dose infection with *T. muris* elicits strong type-2 immunity in genetically resistant mouse strains, resulting in worm expulsion between days 14 and 21 postinfection (Supporting Information Fig. 1B). We therefore performed a series of experiments to address the recruitment kinetics of the two granular cell populations and noted that they followed distinct patterns of accumulation (Fig. 1C). While there was only a modest change in total cell numbers of the large-intestinal lamina propria and epithelium (Supporting Information Fig. 1C), the Siglec-F^{hi} cells increased markedly in the epithelium during infection and peaked at the time of worm expulsion, followed by a slow decline as inflammation abated (Fig. 1C). On the other hand, the Siglec-F^{int} cells accumulated toward the end of infection, peaked after worm expulsion had occurred and remained at a stable level for at least 2 more months (Fig. 1C). In the small-intestinal epithelium, by contrast, there was no accumulation of Siglec-F^{hi} cells postinfection, whereas the Siglec-F^{int} population increased dramatically during infection, but disappeared rapidly after worm clearance (Supporting Information Fig. 1D). We did not observe any remaining worms at these late time points, and as expected did not detect parasite-specific IgG2c serum antibodies that are associated with chronic infections (Supporting Information Fig. 1E). Taken together, the phenotypic and kinetic analyses indicated that the two Siglec-F⁺ populations might represent unique cell types, and perhaps serve different functions.

To conclusively rule out that both populations were eosinophils we infected eosinophil-deficient Δ dblGATA-1 mice [5], and monitored the accumulation of Siglec-F⁺ cells in the large-intestinal epithelium. While we failed to detect any Siglec-F^{hi} cells in the large intestine of Δ dblGATA-1 mice (confirming their eosinophilic identity), the Siglec-F^{int} population accumulated with equal efficiency in Δ dblGATA-1 as in littermate control mice (Fig. 1D). Furthermore, we found that the Siglec-F^{int} population expressed c-kit (CD117), the receptor for stem cell factor, indicating that they might be of mast cell origin (Fig. 1D). Consistent with this hypothesis, Siglec-F^{int} CD117⁺ cells also expressed the high-affinity IgE receptor (Fc ϵ R1 α), and interleukin-33 receptor (IL-33R α) (Fig. 1E), both of which are commonly found on mast cells [6]. To confirm that the Siglec-F^{int} population consisted of mast cells, we isolated CD45⁺ Siglec-F^{int} CD103⁺ CD117⁺ Fc ϵ R1 α ⁺ cells from the large-intestinal epithelium at day 49 postinfection and performed PCR analysis for mast cell protease-1 (*mcpt1*) and *mcpt5* (specific to mucosal and connective-tissue mast cells, respectively [7, 8]), as well as eosinophil peroxidase (*epx*). As expected, sorted cells expressed *mcpt1*, but had no detectable *mcpt5* or *epx* mRNA, confirming that these cells were de facto mucosal mast cells (Fig. 1F). Finally, to verify their epithelial localization, we stained paraffin-embedded biopsies from the cecal-colonic junction with toluidine blue. There was a distinct accumulation of toluidine-stained cells in the large intestine of infected mice, many of which were in close proximity to, or in direct contact with, the epithelial layer, corroborating the flow-cytometry data (Supporting Information Fig. 1F). Taken together, these data demonstrate that a population

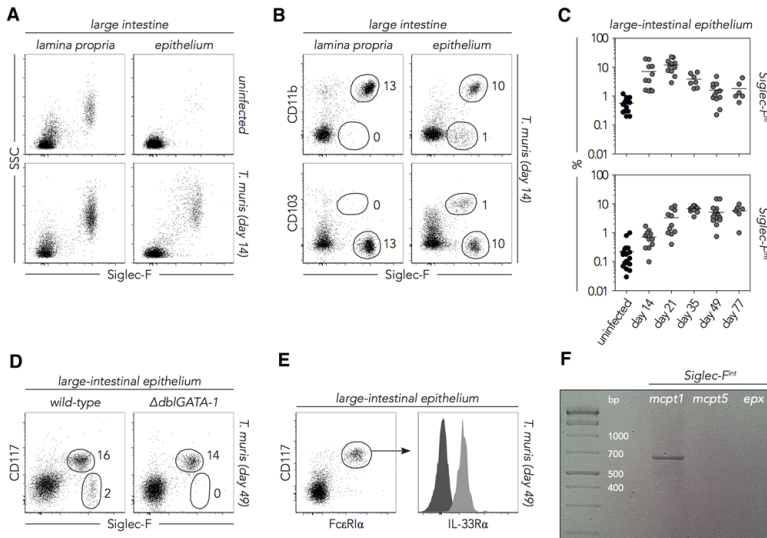


Figure 1. Accumulation of granular cells in the large-intestinal epithelium after acute *T. muris* infection. C57BL/6 mice were infected with a high dose of *T. muris* eggs and monitored over time for accumulation of granular cells in the large intestine. (A–C) Flow-cytometry analysis of hematopoietic cells and quantification of granular cell populations in the large-intestinal lamina propria and epithelium of (A) uninfected and (A and B) *T. muris*-infected mice at day 14 postinfection. Data are from a single experiment representative of three experiments with three individual mice/experiment. (C) Quantification of Siglec-F^{hi} (top) and Siglec-F^{int} (bottom) cells in the large-intestinal epithelium after infection. Lines depict the mean frequency of cells, with each symbol representing individual mice ($n = 6–19$, from three to seven individual experiments with three to five mice/time point). (D–E) Flow-cytometry analysis of hematopoietic cells in the large-intestinal epithelium of *T. muris*-infected (D) $\Delta dbfGATA-1$ and (D–E) C57BL/6 mice at day 49 postinfection. Dark gray = isotype control. Data are from a single experiment representative of one (D) and three (E) experiments with three to five mice/experiment. (F) Gene-expression analysis of *mcpt1*, *mcpt5*, and *epx* in sorted viable CD45⁺ Siglec-F^{int} CD103⁺ CD117⁺ FcεRIα⁺ cells from the large-intestinal epithelium of *T. muris*-infected mice at day 49 postinfection. Data are from a single experiment with three pooled mice.

of mucosal mast cells appeared in the large-intestinal epithelium of *T. muris*-infected mice, displaying an unexpected phenotype and accumulation at later stages of infection.

Type-2 inflammation-associated accumulation of epithelial mast cells

We next sought to determine whether the accumulation of epithelial mast cells was a direct response to the presence of *T. muris* worms, or rather driven by the type-2 response associated with acute *T. muris* infection. To this end, mice were infected with a low dose of *T. muris* eggs, which in C57BL/6 mice results in a chronic infection characterized by a strong type-1 response [4]. Interestingly, there was no specific accumulation of epithelial mast cells in mice infected with a low dose of *T. muris* eggs at day 35 postinfection (Fig. 2A), a time point corresponding to the peak of mast cell accumulation during high-dose infection (Fig. 1C), despite a robust increase in both eosinophils and neutrophils (Supporting Information Fig. 2A). This suggested that the accumulation of mast cells during high-dose infections likely was an indirect consequence of the strong type-2 response induced upon infection rather than being directly worm-driven.

We [9], and others [10], have shown that chronic *T. muris* infection causes a shift in microbial communities of the large intestine. However, it remains unknown whether acute *T. muris* infection can have long-lasting effects on the intestinal microbiota that persist after worm expulsion. Since the composition of the microbiota can have a significant impact on immune cells in the gastrointestinal tract [11], it was plausible that the long-term accumulation of mast cells in the intestinal epithelium was a consequence of altered bacterial populations. We therefore performed 16S ribosomal gene-based sequencing on the fecal microbiota and analyzed the composition of microbial communities over time. As reported [9], chronic infection with *T. muris* led to massive alterations in bacterial families of the large intestine, notably *Lactobacillaceae* (Fig. 2B). By contrast, although minor changes occurred upon acute *T. muris* infection around the time of worm expulsion, these were quickly restored to normal, whereas the microbiota of chronically infected mice continued to diverge (Fig. 2B and Supporting Information Fig. 2B). It is therefore unlikely that the persistence of epithelial mast cells is due indirectly to any long-lasting effects of the nematode on the microbiota.

As it appeared that the driving force behind the accumulation of mucosal mast cells was the type-2 response, we next set up ex vivo cultures of intestinal cells with *T. muris*-derived

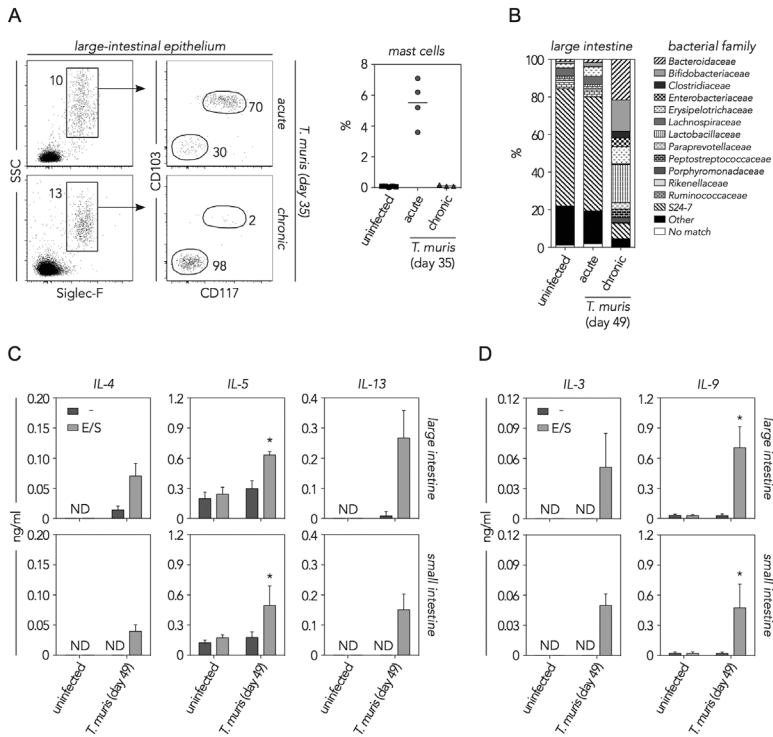


Figure 2. Epithelial mast cell accumulation occurs under type-2 inflammation. (A and B) C57BL/6 mice were infected with a high (acute) or low (chronic) dose of *T. muris* eggs and monitored for accumulation of granular cells in the large intestine and changes in microbiota composition. (A) Identification (left) and quantification (right) of mast cells in the large-intestinal epithelium at day 35 after acute (top) or chronic (bottom) infection. Data are representative of >3 (acute) and one (chronic) experiment with three to five mice/experiment. (B) Bar graph depicting the relative abundance of bacterial families in the colonic microbiota of uninfected and *T. muris*-infected mice at day 49 postinfection ($n = 5-10$), with indicated keys. "Other" = families that were identified at higher taxonomical level, but not at family level. "No match" = unidentified in database. Data represent mean relative abundance from a single experiment with 30 mice/experiment. (C and D) Cytokines (measured by CBA) from the supernatants of ex vivo-cultured cells (48 h) isolated from the large (top) and small-intestinal (bottom) lamina propria of uninfected and high-dose-infected mice at day 49 postinfection, in the presence or absence of *T. muris*-derived E/S antigens. (C) IL-4, IL-5, and IL-13, and (D) IL-3 and IL-9 ($n = 4$). ND: not detected. Bars represent mean + SD of 4-5 biological replicates and are from a single experiment representative of two experiments. Data were analyzed with Mann-Whitney *U*-test comparing E/S-stimulated cells from infected mice with uninfected mice as control. * $p < 0.05$.

excretory/secretory (E/S) antigens and measured the secretion of a panel of cytokines associated with type-2 responses, as well as with mast cell maturation. While uninfected mice displayed little to no type-2 cytokines, previously infected mice showed enhanced levels of antigen-specific IL-4, IL-5, and IL-13 in both the large and small intestine at day 49 postinfection (Fig. 2C), albeit expectedly with higher levels in the large intestine. The levels of general inflammatory cytokines such as IL-6 and TNF- α were not substantially altered in the large intestine at this time point (Supporting Information Fig. 2C). In addition, there was a clear induction of IL-3 and IL-9 (Fig. 2D), both of which have been implicated during mast cell maturation [12, 13]. In summary, accumulation of epithelial mast cells is unrelated to infection-induced changes to the intestinal microbiota, but appears to be driven by type-2 inflammation.

Epithelial mast cells are sustained by increased maturation of lamina propria progenitors

Given that mast cells were detected in the large-intestinal epithelium for at least 2 months after worm expulsion we next wanted to assess whether the cells had accumulated early after infection and persisted long term, or were continuously recruited and replaced as the response to infection progressed. To this end, we fed mice with the thymidine analog 5-bromo-2'-deoxyuridine (BrdU) via the drinking water between days 17 and 24 after high-dose infection (thus overlapping with worm expulsion) to allow for BrdU incorporation in dividing cells, and tracked its decay over time (Fig. 3A). Approximately half of the epithelial mast cells were labeled with BrdU after 1 week of administration (Fig. 3B). The BrdU-labeled mast cells remained positive for several weeks after

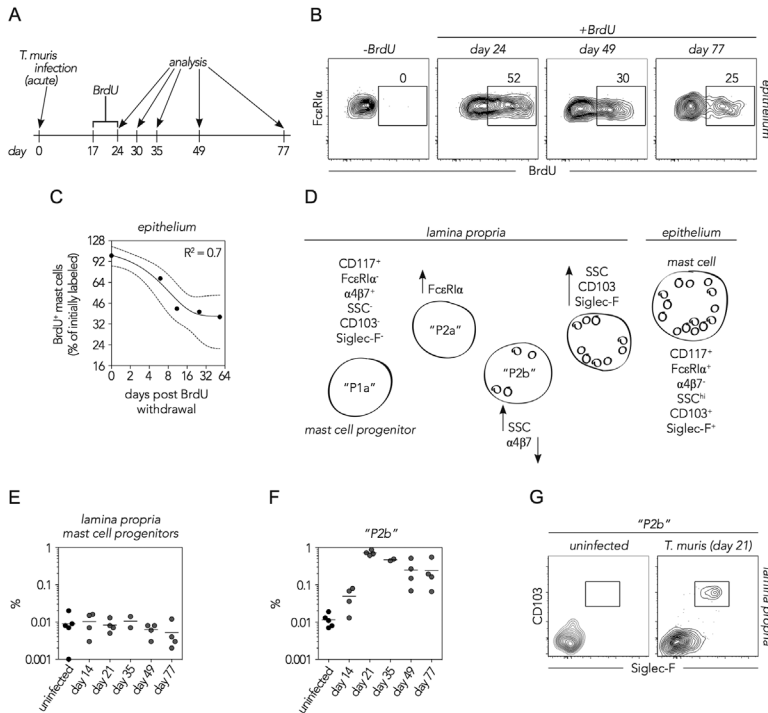


Figure 3. Maturation of local mast cell progenitors maintains the epithelial mast cell pool. (A–C) BrdU-incorporation assay evaluating the lifespan of mast cells in the large-intestinal epithelium following infection with a high dose of *T. muris* eggs. (A) Schematic depiction of the experimental setup; mice were infected with *T. muris*, given BrdU via the drinking water between days 17 and 24 postinfection, and sacrificed at various time points after BrdU administration to assess BrdU decay. (B) Representative flow-cytometry plots of BrdU⁺ mast cells compared to control. (C) Logarithmic graph depicting BrdU-decay in epithelial mast cells, with each dot representing the mean frequency of BrdU⁺ cells (*n* = 3–6). Nonlinear regression (black line) with 95% confidence-interval bands (dotted lines) was calculated using a one-phase decay equation. Data are pooled from two individual lamina experiments with ten mice/experiment. (D–G) Identification and quantification of mast cell progenitors and mast cells in the large-intestinal lamina propria of mice infected with a high dose of *T. muris* eggs. (D) Schematic overview of mast cell maturation in the intestinal mucosa. (E) Kinetics depicting the frequency of mast cell progenitors (P1a gate in Supporting Information Fig. 3A) at day 21 postinfection. (F) Identification and quantification of $\alpha 4\beta 7^-$ CD117⁺ Fc ϵ RI α^+ mast cells (P2b gate in Supporting Information Fig. 3A) at day 21 postinfection. (G) Representative flow-cytometry plots of $\alpha 4\beta 7^-$ mast cells at day 21 postinfection. Data are from a single experiment with four to five mice/time point.

BrdU administration, with only a slow decline in the frequency of labeled cells over time (Fig. 3B). Nonlinear-regression analysis indicated that the BrdU-labeled epithelial mast cells disappeared rapidly immediately after BrdU withdrawal, but had a highly prolonged survival at later stages in the kinetic (Fig. 3C). Considering that the number of epithelial mast cells was stable for several months after pathogen clearance (Fig. 1C) this suggests that although relatively long-lived, the epithelial mast cells were to some extent also being continuously replaced by newly recruited cells.

Unlike classical granulocytes, which circulate as mature effector cells, mast cells leave the bone marrow as agranular progenitors and mature in peripheral tissues in response to local factors, predominantly at mucosal sites and the skin. While connective-tissue mast cells are mostly self-maintained, the maturation of

mucosal mast cells is largely dependent on T-cell-derived IL-9 [14, 15], which also plays an important role in the protective response to some parasites, including *T. muris* [16]. We hypothesized that the accumulation of epithelial mast cells was a consequence of increased bone marrow output, recruitment, and/or differentiation of local progenitors driven by the type-2 response, notably IL-9 (Fig. 2D). As mentioned previously, the epithelial mast cells were uniform in their phenotype prompting us to more closely investigate mast cells and their progenitors in the lamina propria. Consistent with previous reports [6, 17–20], we could detect a small population of agranular lineage⁻ CD117⁺ Fc ϵ RI α^- $\alpha 4\beta 7^+$ IL-33R α^+ Fc γ RIII/II⁺ mast cell progenitors (population “P1a”) in the large-intestinal lamina propria of both uninfected and *T. muris*-infected mice, none of which expressed Siglec-F or CD103 (Supporting Information Fig. 3A). Upon entry into

the intestinal mucosa, mast cell progenitors undergo a series of maturation steps (Fig. 3D) by first upregulating FcεRIα and downregulating α4β7 that is crucial for their entry into the intestinal tissue [21, 22]. There was no accumulation of mast cell progenitors in the lamina propria of infected mice postinfection (Fig. 3E). Similarly, no increase could be detected in either the bone marrow or spleen, but rather a decrease (Supporting Information Fig. 3B). By contrast, in infected mice, a vast majority of the intestinal progenitors had given rise to partially granular FcεRIα⁺ α4β7⁻ mast cells (population “P2b” in Supporting Information Fig. 3A), peaking in number at day 21 postinfection (Fig. 3F), i.e. prior to the accumulation of mast cells in the epithelium (Fig. 1C). Similar to epithelial mast cells, lamina propria mast cells remained elevated in number after worm clearance (Fig. 3F). Consistent with the possibility that lamina propria mast cells can be further activated during infection, a proportion of the cells (P2b) became Siglec-F⁺ CD103⁺ (Fig. 3G), resembling the phenotype of epithelial mast cells. This suggests that instead of an accumulation of circulating progenitors, local mast cell progenitors were giving rise to more mature cells after infection leading to the observed increase in epithelial mast cells.

Altered epithelial permeability after acute *T. muris* infection

Mast cells have been implicated in the generation of type-2 responses against several parasites [23], including *T. muris* [24]. However, as the bulk of epithelial mast cells accumulated after expulsion, we hypothesized that they might serve additional functions, possibly regulating epithelial barrier function given their localization. Consistent with such a possibility, mast cell-derived proteases (notably including MCPT-1) have been shown to regulate epithelial permeability [25]. As mucosal mast cells are characterized by the specific production of MCPT-1, we measured the levels of MCPT-1 locally in the large intestine, distally in the small intestine, as well as systemically in the serum. Although absent in uninfected mice, serum concentrations of MCPT-1 increased dramatically during infection and remained elevated throughout the experimental kinetic (Fig. 4A). We did not detect any substantial MCPT-1 secretion by cells isolated from the small intestine (Supporting Information Fig. 4A), nor by cells from the large-intestinal lamina propria at day 49 postinfection (Fig. 4B). By contrast, high levels of MCPT-1 were secreted by cells isolated from the large-intestinal epithelium (Fig. 4B), correlating with the mature granular phenotype of epithelial mast cells (Fig. 1A and Supporting Information Fig. 4B). The serum levels of MCPT-1 correlated strongly with the frequency of mast cells in the large-intestinal epithelium regardless of time point postinfection, as determined by Spearman-correlation analysis (Fig. 4C). Furthermore, as there was no prolonged accumulation of mast cells at other mucosal sites, such as the small intestine (Supporting Information Fig. 1C) or lungs (data not shown), it is likely that the elevated serum levels of MCPT-1 at later stages in the kinetic derive from large-intestinal

mast cells, although we cannot exclude a possible contribution from mast cells at other peripheral tissues.

To address the role of mast cells on intestinal permeability postinfection we gave repeated intraperitoneal injections of either depleting anti-CD117 [16, 26], or isotype-control antibodies, and measured the uptake of FITC-dextran administered by oral gavage at day 49 postinfection (Fig. 4D). Interestingly, previously infected mice had higher serum levels of FITC-dextran than their uninfected counterparts (Fig. 4E), consistent with increased intestinal permeability in response to prior infection. Strikingly, despite only a partial reduction of large-intestinal mast cells (Supporting Information Fig. 4C), this effect was reversed in mice treated with anti-CD117 (Fig. 4E). Importantly, the increased permeability after infection correlated with increased serum levels of MCPT-1, which were also reduced following mast cell depletion (Fig. 4F). Taken together, these results suggest that mast cells accumulating in the large intestine in response to *T. muris* infection may have functional implications on intestinal barrier integrity, and that this effect appears to persist long after the infection has been cleared.

Discussion

Here, we demonstrate that acute *T. muris* infection leads to the accumulation of a long-lived mast cell population in the large-intestinal epithelium. This accumulation was associated with induction of a type-2 response, and correlated with increased levels of the mucosal mast cell-specific protease MCPT-1 in the serum and locally in the intestine, as well as increased epithelial permeability, suggesting that prior infection may have long-lasting consequences on the local environment as well as influence on subsequent responses.

Mast cells have previously been shown to localize to epithelial surfaces in several models of intestinal inflammation [7, 26]. For example, infection with the small-intestinal nematode *T. richinella spiralis* induces a robust accumulation of mast cells in the jejunal epithelium during active infection [7]. Similarly, mice that transgenically overexpress IL-9, systemically [16, 26] or restricted to the intestinal epithelium (iFABPP-IL-9Tg mice) [27], have increased numbers of mast cells in the small-intestinal epithelium. In contrast to our findings in the large-intestinal epithelium during *T. muris* infection however, *T. spiralis*-infection fails to cause epithelial mastocytosis beyond expulsion of the parasite [7]. The reasons for this disparity could be several, and could be linked to the different nature of the small and large intestine, or relate to differences between infection models. Although one may suspect regional differences in microbiota composition to be involved, our data suggest that changes to microbial communities most likely play little part in the accumulation of epithelial mast cells. Instead, our results indicate that induction of type-2 immunity is crucial in driving epithelial mast cell accumulation. Thus, we failed to detect epithelial mast cells following type-1-dominated low-dose *T. muris* infection. By contrast, high-dose infection with *T. muris* resulted in mast cell accumulation associated with high levels of type-2 cytokines in the large-intestinal lamina propria.

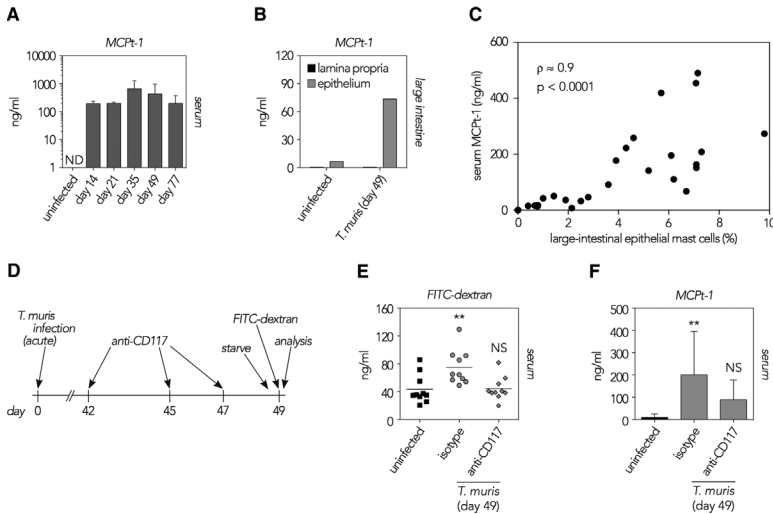


Figure 4. Altered epithelial permeability after *T. muris* infection. (A–C) C57BL/6 mice were infected with a high dose of *T. muris* eggs and monitored over time for mast cell proteases in the large intestine and serum. (A) Serum concentrations of MCPt-1 (measured by ELISA) at various time points after *T. muris* infection. Bars represent the mean \pm SD concentration of MCPt-1 ($n = 4–8$), from two individual experiments with 15 mice/experiment. (B) Cells were isolated from the large-intestinal lamina propria and epithelium of uninfected and *T. muris*-infected mice at day 49 postinfection and cultured ex vivo, followed by analysis of MCPt-1 in the culture supernatants. Each bar represents the concentration of MCPt-1 in pooled cell suspensions from four to five mice. Data are from one representative experiment of two performed. (C) Scatter plot depicting the correlation (Spearman’s ρ) between the frequency of mast cells in the large-intestinal epithelium and serum levels of MCPt-1. Dots represent individual mice (from two experiments with 15 mice/experiment). (D–F) Mast cell depletion affects epithelial barrier permeability. (D) Schematic depiction of the experimental setup; mice were infected with *T. muris* and administered anti-CD117 or isotype-control antibodies intraperitoneally at three time points postinfection, after which mice were starved overnight, given FITC-dextran orally in the morning and sacrificed 4 h later for analysis of FITC-dextran uptake. (E) Serum concentrations of FITC-dextran (measured by spectrophotometry). Dots represent individual mice, with the line depicting the mean concentration. Sera from untreated mice were used as blank controls for FITC-dextran measurements. Data are pooled from two individual experiments with 15 mice/experiment and analyzed with one-way ANOVA and Tukey’s posttest for multiple comparison. ** $p < 0.01$, NS: not significant. (F) Serum concentration of MCPt-1 (mean \pm SD, $n = 10$). Data are pooled from two individual experiments with 15 mice/experiment and analyzed with one-way ANOVA and Tukey’s posttest for multiple comparison. ** $p < 0.01$, NS: not significant.

The earliest mast cell progenitors in the lamina propria have been described as agranular CD117⁺ FcεRIα[−] α4β7⁺ IL-33Rα⁺ FcγRIII/II⁺ cells [6, 17–20]. Under the influence of local factors, these cells upregulate FcεRIα while downregulating α4β7 [6]. Our results suggest that a proportion of these cells can go through additional maturation steps in response to infection, characterized by induction of Siglec-F and CD103, translocation to the intestinal epithelium and acquisition of a more granular appearance (summarized in Fig. 3D). Interestingly, while we detected dramatically increased numbers of epithelial mast cells, there was no accumulation of mast cell progenitors in the lamina propria. These data are consistent with those observed in IFABPp-IL-9Tg mice, where intestinal mastocytosis occurred despite unchanged numbers of mast cell progenitors [27], and suggest that accumulation relies on increased maturation and/or survival rather than recruitment of progenitors. While the factors that promote induction of epithelial mast cells remain to be identified, it is interesting to note that TGF-β has been implicated in regulation of several aspects of mast cell biology, including expression of CD103 and MCPt-1 [28, 29]. CD103 (the integrin αE) pairs with β7, together forming the ligand

for E-cadherin that is expressed by intestinal epithelial cells, and might therefore facilitate the interaction between mast cells and the epithelium. Thus, we hypothesize that TGF-β could be one of the important factors that promote transition of lamina propria mast cells into their epithelial counterpart.

The observation that epithelial mast cells are uniformly positive for Siglec-F is to our knowledge the first report on expression of this receptor by mast cells. Thus, expression of Siglec-F has been documented on murine eosinophils, and now on mast cells, similar to its human ortholog Siglec-8 [30]. In addition, Siglec-F expression has also been described on alveolar macrophages [31], intestinal epithelial tuft cells [32], as well as on a subpopulation of CD11b⁺ CD103⁺ dendritic cells in the small intestine (our unpublished observation).

While our BrdU experiments indicated that the epithelial mast cells had a relatively short lifespan immediately after expulsion, BrdU⁺ cells displayed a much longer half-life at later stages after infection. A possible explanation for this pattern may be the timing of BrdU administration, which took place during the peak inflammatory response and overlapping with worm expulsion

(complete at day 21 postinfection). Hence, mast cells labeled at the early stages of BrdU administration, prior to worm expulsion, will likely have encountered parasite-derived antigens, cellular debris from damaged epithelial cells, and a more inflamed tissue in general. In contrast, mast cells that developed and were labeled after parasite expulsion might have been exposed to a less inflamed environment, which could reflect on their lifespan.

Mast cells have been implicated in regulation of epithelial barrier function [25, 27, 33], at least in part via release of MCPt-1 [25]. Therefore, given the sustained presence of mast cells in the epithelium, as well as the high levels of MCPt-1 in the serum, we assessed epithelial permeability by measuring uptake of FITC-dextran in the serum upon oral administration in mice injected with anti-CD117 antibodies. Similar to our observations in mice following chronic *T. muris* infection (unpublished observation), previously infected mice had more permeable intestines. Interestingly, despite only partial mast cell depletion following antibody treatment, we observed a robust reduction in permeability following anti-CD117 injections, consistent with a role for mast cells in regulating epithelial barrier integrity. While the underlying mechanism remains to be established it may be related to regulation of the tight-junction protein occludin, which has been identified as a target of mast cell-derived proteases [25], or via activation of protease-activated receptor-2 by mast cell-derived tryptases, which have been demonstrated to regulate tight-junction integrity [34].

The consequences of increased epithelial permeability associated with long-term epithelial mastocytosis remain to be investigated. Increased leakiness at epithelial surfaces, particularly in the gastrointestinal tract, is linked to higher risk of developing IBD [35] and food allergies [36]. Indeed, although infection with some parasites has proven beneficial in treating various murine models of IBD [37, 38], the data on *T. muris* (including our unpublished data) seem to suggest the opposite [39]. Furthermore, whether the long-term effects observed have any bearing on the risk of developing food allergies remains to be determined. Interestingly, several reports strongly link overexpression of IL-9, intestinal mastocytosis and increased epithelial permeability to a predisposition to oral-antigen hypersensitivity [22, 27], and vice versa in IL-9-deficient mice [40], suggesting that mice that have undergone acute *T. muris* infection could be more prone to develop food allergy. Finally, our preliminary data suggest that acute *T. muris* infection might also have systemic consequences. Thus, we observed effects on both the number and phenotype of granulocytes in the lungs, as well as on the local cytokine environment (data not shown). In addition, if the observed epithelial leakiness is indeed due to circulating MCPt-1, one might expect to see similar effects on the lung epithelium, which could have consequences on the outcome of allergic challenge also at this site.

In summary, acute *T. muris* infection results in accumulation of a population of long-lived mucosal mast cells in the large-intestinal epithelium. Epithelial mastocytosis appears to be associated with type-2 responses, and have long-lasting consequences

on the intestinal environment, including regulation of epithelial barrier permeability.

Materials and methods

Mice

C57BL/6 mice were obtained from ENVIGO (An Venray, the Netherlands). Δ dblGATA-1 mice were bred in the BMC barrier facility, Lund University, and were a kind gift from Professors Alison Humbles (MedImmune, LLC, Gaithersburg, USA) and Avery August (Cornell University, Ithaca, USA). Experiments were conducted with age-matched male/female mice (6–8 weeks old), in strict accordance with animal welfare laws determined by Swedish authorities (Swedish Board of Agriculture, Act 1988:534). The protocol was approved by Malmö/Lund Ethical Board for Animal Research, Lund/Malmö, Sweden (permit: M14-16), and all efforts were made to minimize animal suffering.

Trichuris muris

Trichuris muris (strain E) was maintained as previously described [41]. Mice were infected with a high (350–400) or low (20) dose of eggs in sterile-filtered (0.2 μ m) tap water by oral gavage to obtain acute or chronic infection, respectively. To assess the worm burden of infected mice, large intestines were excised and frozen at -20°C . Intestines were opened longitudinally upon analysis, and scraped free of worms that were counted under a reverse phase-contrast microscope.

Parasite-derived antigens

Mice of a susceptible strain were infected with approximately 150 *T. muris* eggs and killed 6 weeks later. Large intestines were excised, opened longitudinally, and rinsed thrice with sterile Dulbecco's phosphate-buffered saline (DPBS; Thermo-Fisher Scientific) supplemented with 500 U/mL penicillin + 500 μ g/mL streptomycin (Thermo-Fisher Scientific). Adult worms were pulled out with forceps, placed in sterile RPMI 1640 (Thermo-Fisher Scientific) supplemented with antibiotics as described above and incubated at 37°C for 20 min, followed by a 24-h incubation in fresh medium. The medium was collected the following day and centrifuged at $500 \times g$ for 10 min to pellet the eggs. E/S antigens were concentrated in a series of 10–30 min centrifugation steps in centriprep-centrifugal columns with 10 000 NMWL (Merck-Millipore) at $2000 \times g$, and dialyzed to DPBS in a series of centrifugation steps in Amicon Ultracel-3K Centrifugal Filters with 3000 NMWL (Merck-Millipore) at $14\,000 \times g$. The resulting protein concentration was measured by Bradford's assay (280 nm) on a SPECTROstar Nano plate reader (BMG Labtech). The antigens were frozen at -80°C .

Tissue preparation and cell isolation

Spleens were mashed in DPBS and passed through 70 μm cell strainers (Thermo-Fisher Scientific). Femurs were flushed through with DPBS to obtain the bone marrow, which was homogenized and filtered through 70 μm cell strainers. Intestines were stripped of adipose tissue, opened longitudinally and washed thoroughly in DPBS to remove the feces. To isolate immune cells from the large- and small-intestinal epithelium, intestines were cut into approximately 1 cm pieces, and incubated thrice in epithelial-dissociation buffer consisting of Hank's balanced salt solution (Thermo-Fisher Scientific) supplemented with 15 mM N-2-hydroxyethylpiperazine-N'-2-ethanesulfonic acid (HEPES; Thermo-Fisher Scientific), 2% fetal bovine serum (FBS; Sigma-Aldrich), 5 mM ethylenediaminetetraacetic acid (Merck-Millipore), 100 U/mL penicillin + 100 $\mu\text{g}/\text{mL}$ streptomycin, 50 $\mu\text{g}/\text{mL}$ gentamicin (Thermo-Fisher Scientific), and 1.25 $\mu\text{g}/\text{mL}$ Fungizone (Thermo-Fisher Scientific) for 15 min at 37°C, on continuous shaking. The loosened epithelium was subjected to density-gradient centrifugation using Percoll (GE Healthcare). Briefly, cells were suspended in 40% Percoll and centrifuged over a 70% Percoll layer for 20 min, 600 \times g without brake at room temperature. Cells collected between the 40/70 phases were washed with DPBS. To isolate cells from the lamina propria remaining tissue pieces were enzymatically digested in R10 buffer consisting of RPMI 1640 supplemented with 10 mM HEPES, 10% FBS, 2 mM L-glutamine (Thermo-Fisher Scientific), 1 mM sodium pyruvate (Thermo-Fisher Scientific), 100 U/mL penicillin + 100 $\mu\text{g}/\text{mL}$ streptomycin, 50 $\mu\text{g}/\text{mL}$ gentamicin, and 1.25 $\mu\text{g}/\text{mL}$ Fungizone, along with 0.3 Wünsch units/mL liberase TM (Roche), 30 $\mu\text{g}/\text{mL}$ DNase I (Roche), and 5 mM CaCl_2 for 45 min at 37°C with magnetic stirring. The resulting cell suspensions were filtered through 100 μm cell strainers (Fisher Scientific), and subjected to density-gradient centrifugation as described above. Lung cells were obtained by first perfusing the mice with DPBS; lungs were subsequently excised, minced into small pieces, and digested in R10 buffer for 45 min at 37°C, on continuous shaking. The resulting cell suspension was filtered through a 70 μm cell strainer, and subjected to density-gradient centrifugation as described above. Cells were enumerated using a KX-21N automated hematology analyzer (Sysmex).

Flow cytometry

Cells were fluorescently labeled for 30 min on ice with the following antibodies and reagents: AF700-conjugated mouse (SJL) anti-mouse CD45.2 (clone 104; BioLegend), APC-eF780-conjugated rat anti-mouse CD11b (M1/70; eBioscience), APC-conjugated Armenian hamster anti-mouse Fc ϵ R1 α (MAR1; BioLegend), PerCP-eF710-conjugated rat anti-mouse CD117 (2B8; eBioscience), PE-CF594-conjugated rat anti-mouse α 4 β 7 (DATK32; BD Biosciences), PE-conjugated rat anti-mouse SiglecF (E50-2440; BD Biosciences), FITC-conjugated rat anti-mouse Ly-6G (1A8; BD Biosciences), BV786-conjugated rat anti-mouse

CD103 (M290; BD Biosciences), BV711-conjugated rat anti-mouse Fc γ RIII/II (93; BioLegend), BV650-conjugated rat anti-mouse I-A/I-E (M5/114.15.2; BD Biosciences), BV605-conjugated rat anti-mouse CD3 (17A2; BD Biosciences), rat anti-mouse CD19 (1D3; BD Biosciences), and mouse (CH3xBALB/c) anti-mouse NK1.1 (PK136; BD Biosciences), BV421-conjugated rat anti-mouse IL-33R α (DIH9; BioLegend) along with Aqua-Live/Dead (Thermo-Fisher Scientific) according to manufacturer's instructions. Cells were analyzed on an LSR II flow cytometer (BD Biosciences), and data analyzed with FlowJo software v9.7 (Tree Star Inc.).

Ex vivo-cell stimulations and protein analyses

For cytokine secretion analyses, cells were suspended in R10 buffer, seeded at 2.5×10^6 cells/mL in TC-MicroWell 96U-Nunclon plates (Thermo-Fisher Scientific), and incubated with 25 $\mu\text{g}/\text{mL}$ E/S antigens for 48 h at 37°C, 5% CO_2 . Cell-free supernatants were collected and frozen at -20°C for subsequent analyses. Cytokines were measured with cytometric bead array (BD Biosciences) according to manufacturer's instructions with the following modification: the amount of capture beads, detection reagents, and sample volumes was scaled down fivefold. Data was collected on an Accuri (BD Biosciences) and analyzed with FCAP array v3.0 (SoftFlow Inc.). For MCPT-1 secretion analyses, cells were suspended in R10 buffer, seeded at 10^6 cells/mL in TC-MicroWell 96U-Nunclon plates (Thermo-Fisher Scientific), and incubated for 30 min at 37°C, 5% CO_2 . MCPT-1 was measured using a commercial ELISA kit (eBioscience) according to manufacturer's instructions with the following modification: standard and sample volumes were reduced to 50 $\mu\text{L}/\text{well}$. E/S-specific antibodies were measured by a standard ELISA with biotin-conjugated anti-mouse IgG2c antibodies (RMG2a-62; BioLegend), and HRP-conjugated streptavidin (BioLegend).

Mast cell depletion

Anti-CD117 antibodies were generated from a hybridoma (clone; ACK2); a kind gift from Professor Kathryn Else (University of Manchester, Manchester, UK). Once confluent, hybridomas were cultured in growth medium containing 2% FBS to minimize nonspecific immunoglobulins. IgG antibodies were purified on a protein-A/G column and dialyzed to DPBS by consecutive centrifugation and washing steps using Amicon Ultracel-3K Centrifugal Filters (Merck-Millipore). The concentration was determined by Bradford's assay (280 nm absorbance) with 1.4 extinction coefficient for IgG. Rat IgG2b isotype control was purchased from BioXcell. Antibodies were injected intraperitoneally on days 42, 45, and 47 postinfection (0.5 mg/mouse for the first injection, and 0.25 mg for subsequent time points).

BrdU-incorporation assay

Mice were given 0.8 mg/mL BrdU (Sigma-Aldrich) via the drinking water between days 17 and 24. Cells were isolated at varying time points after BrdU removal, and BrdU-incorporation measured by staining with FITC-conjugated anti-BrdU antibodies from a commercially available kit (BD Biosciences), according to manufacturer's instructions. Data were collected on an LSR II flow cytometer.

Assessment of intestinal permeability by FITC-dextran feeding

Mice were starved overnight, fed the following morning with 0.4 mg/g body weight FITC-dextran (4 kDa; Sigma-Aldrich) dissolved in water, and sacrificed 4 h later. Blood was collected into Microtainer-SST tubes (BD Biosciences) and centrifuged at 12 000 × g for 5 min to obtain serum. FITC-dextran measurements were performed using 488 ± 12 nm excitation and 525 ± 12 nm emission on a Varioskan LUX Multimode-Microplate Reader (Thermo-Fisher Scientific).

Mast cell isolation and validation

Cells were isolated as described from the large-intestinal epithelium of three mice on day 49 postinfection. Approximately 10⁴ mast cells were sorted to high purity on a FACSAria II (BD Biosciences) based on surface expression of CD45, CD117, FcεRIα, Siglec-F, and CD103, with dead cells excluded by propidium iodide staining. Sorted cells were centrifuged, suspended in 100 μL lysis buffer (Absolutely RNA Microprep Kit; Agilent Technologies), and frozen at –80°C for RNA isolation. RNA was isolated using Absolutely RNA Microprep Kit according to manufacturer's instructions (including optional DNase treatment). cDNA synthesis was performed with SuperScript III First-Strand Synthesis System (Thermo-Fisher Scientific) according to manufacturer's instructions (using random hexamers). The cDNA was amplified with SsoFast EvaGreen Supermix (Bio-Rad Laboratories) using the following primers (purchased from Eurofins Genomics): *epx* (forward:5'-CCTTTTGACAACCTGCATGA-3', reverse:5'-CCCAGATGTCATGTGTGCG-3'), *mcp1* (forward:5'-GCTGGAGCTGAGGAGATT-3', reverse:5'-GGTGAAGACTGCAGGGG-3'), and *mcp5* (forward:5'-GAACTACCTGTCGGCCTGCAG-3', reverse:5'-AGAACCTTCTGGAAGCTCAGG-3').

Microbiota analyses and bioinformatics

Fresh fecal samples were collected and immediately frozen in liquid nitrogen. DNA extraction (NucleoSpin Soil; Macherey-Nagel) and PCR-based library formation and sequencing were performed as described [9]. Raw sequencing data were processed using QIIME including de novo-OTU picking, chimera-checking, and

taxonomical assignment using the Greengenes database v13.8 [42]. Subsequent analyses were performed in R using the packages Vegan [43] and PhyloSeq [44]. Data were filtered for low-abundance OTUs by removal of OTUs present in <three of the samples, or with a relative abundance across all samples of ≤0.005% resulting in 33 991 ± 12 378 (mean ± SD) reads/sample.

Histology

Biopsies (approximately 0.5 cm in size) from the cecal-colonic junction were collected in Carnoy's solution (60% ethanol, 30% chloroform, 10% acetic acid) and stored at room temperature until further processed. Tissue pieces were embedded in paraffin by standard histological techniques and cut into 5 μm sections using a Leica microtome. Sections were stained with toluidine blue and mounted in standard fashion. Slides were scanned and analyzed with Aperio ImageScope (Leica Biosystems).

Statistical analyses

All statistical analyses were performed using Prism v5.0 (GraphPad software).

Acknowledgments: We would like to express our gratitude to Professor William Agace for constructive comments on the manuscript, and Maja Toft Løvbakke for technical assistance. This work was supported by grants from the Åke Wiberg, OE&Edla Johansson and Clas Groschinsky Foundations (M.S.-F.), and the Royal Physiological Society (D.S.). D.S., J.B.H., H.H., and M.S.-F. performed the experiments and analyzed the data. D.S. and M.S.-F. conceived the project, with guidance from J.B.H. and K.K. on the microbiota analysis. D.S. and M.S.-F., with input from J.B.H. and K.K., wrote the manuscript.

Conflict of interest: The authors declare no commercial or financial conflict of interest.

References

- 1 Maloy, K. J. and Powrie, F., Intestinal homeostasis and its breakdown in inflammatory bowel disease. *Nature* 2011. 474: 298–306.
- 2 Miner-Williams, W. M. and Moughan, P. J., Intestinal barrier dysfunction: implications for chronic inflammatory conditions of the bowel. *Nutr. Rev.* 2016. 29: 40–59.
- 3 Perrier, C. and Corthésy, B., Gut permeability and food allergies. *Clin. Exp. Allergy* 2011. 41: 20–28.

- 4 Cliffe, L. J. and Grenicis, R. K., The *Trichuris muris* system: a paradigm of resistance and susceptibility to intestinal nematode infection. *Adv. Parasitol.* 2004. 57: 255–307.
- 5 Yu, C., Cantor, A. B., Yang, H., Browne, C., Wells, R. A., Fujiwara, Y. and Orkin, S. H., Targeted deletion of a high-affinity GATA-binding site in the GATA-1 promoter leads to selective loss of the eosinophil lineage in vivo. *J. Exp. Med.* 2002. 195: 1387–1395.
- 6 Arinobu, Y., Iwasaki, H., Gurish, M. F., Mizuno, S., Shigematsu, H., Ozawa, H., Tenen, D. G. et al., Developmental checkpoints of the basophil/mast cell lineages in adult murine hematopoiesis. *Proc. Natl. Acad. Sci. USA* 2005. 102: 18105–18110.
- 7 Friend, D. S., Ghildyal, N., Austen, L. K. F., Gurish, M. F., Matsumoto, R. and Stevens, R. L., Mast cells that reside at different locations in the jejunum of mice infected with *Trichinella spiralis* exhibit sequential changes in their granule ultrastructure and chymase phenotype. *J. Cell Biol.* 1996. 135: 279–290.
- 8 Scudamore, C. L., McMillan, L., Thornton, E. M., Wright, S. H., Newlands, G. F. and Miller, H. R., Mast cell heterogeneity in the gastrointestinal tract: variable expression of mouse mast cell protease-1 (mMCP-1) in intraepithelial mucosal mast cells in nematode-infected and normal BALB/c mice. *Am. J. Pathol.* 1997. 150: 1661–1672.
- 9 Holm, J. B., Sorobetea, D., Kiilerich, P., Ramayo-Caldas, Y., Estellé, J., Ma, T., Madsen, L. et al., Chronic *Trichuris muris* infection decreases diversity of the intestinal microbiota and concomitantly increases the abundance of lactobacilli. *PLoS One* 2015. 10: e0125495.
- 10 Houlden, A., Hayes, K. S., Bancroft, A. J., Worthington, J. J., Wang, P., Grenicis, R. K. and Roberts, I. S., Chronic *Trichuris muris* infection in C57BL/6 mice causes significant changes in host microbiota and metabolome: effects reversed by pathogen clearance. *PLoS One* 2015. 10: e0125945.
- 11 Hooper, L. V., Littman, D. R., Macpherson, A. J. and Program, M. P., Interactions between the microbiota and the immune system. *Science* 2012. 336: 1268–1273.
- 12 Razin, E., Ihle, J. N., Seldin, D., Katz, R., Paul, I. I., Hein, A. N. N., Caulfield, J. P. et al., Interleukin 3: a differentiation and growth factor for the mouse mast cell that contains chondroitin sulfate E. *J. Immunol.* 1984. 132: 1479–1485.
- 13 Matsuzawa, S., Sakashita, K., Kinoshita, T., Ito, S., Yamashita, T. and Koike, K., IL-9 enhances the growth of human mast cell progenitors under stimulation with stem cell factor. *J. Immunol.* 2003. 170: 3461–3467.
- 14 Ruitenber, E. J. and Elgersma, A., Absence of intestinal mast cell response in congenitally athymic mice during *Trichinella spiralis* infection. *Nature* 1976. 264: 258–260.
- 15 Licona-Limón, P., Henao-Mejia, J., Temann, A. U., Gagliani, N., Licona-Limón, I., Ishigame, H., Hao, L. et al., Th9 cells drive host immunity against gastrointestinal worm infection. *Immunity* 2013. 39: 744–757.
- 16 Faulkner, H., Humphreys, N., Renaud, J. C., Van Snick, J. and Grenicis, R., Interleukin-9 is involved in host protective immunity to intestinal nematode infection. *Eur. J. Immunol.* 1997. 27: 2536–2540.
- 17 Jamur, M. and Grodzki, A., Identification and characterization of undifferentiated mast cells in mouse bone marrow. *Blood* 2005. 105: 4282–4289.
- 18 Chen, C.-C., Grimbaldston, M. A., Tsai, M., Weissman, I. L. and Galli, S. J., Identification of mast cell progenitors in adult mice. *Proc. Natl. Acad. Sci. USA* 2005. 102: 11408–11413.
- 19 Dahlin, J. S., Heyman, B. and Hallgren, J., Committed mast cell progenitors in mouse blood differ in maturity between Th1 and Th2 strains. *Allergy Eur. J. Allergy Clin. Immunol.* 2013. 68: 1333–1337.
- 20 Bankova, L. G., Dwyer, D. F., Liu, A. Y., Austen, K. F. and Gurish, M. F., Maturation of mast cell progenitors to mucosal mast cells during allergic pulmonary inflammation in mice. *Mucosal Immunol.* 2014. 8: 1–11.
- 21 Gurish, M. F., Tao, H., Abonia, J. P., Arya, A., Friend, D. S., Parker, C. M. and Austen, K. F., Intestinal mast cell progenitors require CD49beta7 (alpha4beta7 integrin) for tissue-specific homing. *J. Exp. Med.* 2001. 194: 1243–1252.
- 22 Chen, C. Y., Lee, J. B., Liu, B., Ohta, S., Wang, P. Y., Kartashov, A. V., Mugge, L. et al., Induction of interleukin-9-producing mucosal mast cells promotes susceptibility to IgE-mediated experimental food allergy. *Immunity* 2015. 43: 788–802.
- 23 Lawrence, C. E., Paterson, Y. Y. W., Wright, S. H., Knight, P. A. and Miller, H. R. P., Mouse mast cell protease-1 is required for the enteropathy induced by gastrointestinal helminth infection in the mouse. *Gastroenterology* 2004. 127: 155–165.
- 24 Hepworth, M., Danilowicz-Luebert, E., Rausch, S., Metz, M., Klotz, C., Maurer, M. and Hartmann, S., Mast cells orchestrate type 2 immunity to helminths through regulation of tissue-derived cytokines. *Proc. Natl. Acad. Sci. USA* 2012. 109: 6644–6649.
- 25 McDermott, J. R., Bartram, R. E., Knight, P. A., Miller, H. R. P., Garrod, D. R. and Grenicis, R. K., Mast cells disrupt epithelial barrier function during enteric nematode infection. *Proc. Natl. Acad. Sci. USA* 2003. 100: 7761–7766.
- 26 Godfraind, C., Louahed, J., Faulkner, H., Vink, A., Warnier, G., Grenicis, R. and Renaud, J. C., Intraepithelial infiltration by mast cells with both connective tissue-type and mucosal-type characteristics in gut, trachea, and kidneys of IL-9 transgenic mice. *J. Immunol.* 1998. 160: 3989–3996.
- 27 Forbes, E. E., Groschwitz, K., Abonia, J. P., Brandt, E. B., Cohen, E., Blanchard, C., Ahrens, R. et al., IL-9- and mast cell-mediated intestinal permeability predisposes to oral antigen hypersensitivity. *J. Exp. Med.* 2008. 205: 897–913.
- 28 Miller, H. R., Wright, S. H., Knight, P. A. and Thornton, E. M., A novel function for transforming growth factor-beta1: upregulation of the expression and the IgE-independent extracellular release of a mucosal mast cell granule-specific beta-chymase, mouse mast cell protease-1. *Blood* 1999. 93: 3473–3486.
- 29 Wright, S. H., Brown, J., Knight, P. A., Thornton, E. M., Kilshaw, P. J. and Miller, H. R. P., Transforming growth factor-beta1 mediates coexpression of the integrin subunit alphaE and the chymase mouse mast cell protease-1 during the early differentiation of bone marrow-derived mucosal mast cell homologues. *Clin. Exp. Allergy* 2002. 32: 315–324.
- 30 Bochner, B. S., Siglec-8 on human eosinophils and mast cells, and Siglec-F on murine eosinophils, are functionally related inhibitory receptors. *Clin. Exp. Allergy* 2009. 39: 317–324.
- 31 Feng, Y. and Mao, H., Expression and preliminary functional analysis of Siglec-F on mouse macrophages. *J. Zhejiang Univ.* 2012. 13: 386–394.
- 32 Gerbe, F., Sidot, E., Smyth, D. J., Ohmoto, M., Matsumoto, I., Dardalhon, V., Cesses, P. et al., Intestinal epithelial tuft cells initiate type 2 mucosal immunity to helminth parasites. *Nature* 2016. 529: 226–230.
- 33 Scudamore, C. L., Thornton, E. M., McMillan, L., Newlands, G. F. and Miller, H. R., Release of the mucosal mast cell granule chymase, rat mast cell protease-II, during anaphylaxis is associated with the rapid development of paracellular permeability to macromolecules in rat jejunum. *J. Exp. Med.* 1995. 182: 1871–1881.
- 34 Jacob, C., Yang, P. C., Darmoul, D., Amadesi, S., Saito, T., Cottrell, G. S., Coelho, A. M. et al., Mast cell tryptase controls paracellular permeability of the intestine: role of protease-activated receptor 2 and beta-arrestins. *J. Biol. Chem.* 2005. 280: 31936–31948.
- 35 Landy, J., Ronde, E., English, N., Clark, S. K., Hart, A. L., Knight, S. C., Ciclitira, P. J. et al., Tight junctions in inflammatory bowel diseases and

- inflammatory bowel disease associated colorectal cancer. *World J. Gastroenterol.* 2016. **22**: 3117–3126.
- 36 Ventura, M. T., Polimeno, L., Amoroso, A. C., Gatti, F., Annoscia, E., Marinaro, M., Di Leo, E. et al., Intestinal permeability in patients with adverse reactions to food. *Dig. Liver Dis.* 2006. **38**: 732–736.
- 37 Elliott, D. E., Setiawan, T., Metwali, A., Blum, A., Urban, J. F. and Weinstock, J. V., *Heligmosomoides polygyrus* inhibits established colitis in IL-10-deficient mice. *Eur. J. Immunol.* 2004. **34**: 2690–2698.
- 38 Smith, P., Mangan, N. E., Walsh, C. M., Fallon, R. E., McKenzie, A. N. J., van Rooijen, N. and Fallon, P. G., Infection with a helminth parasite prevents experimental colitis via a macrophage-mediated mechanism. *J. Immunol.* 2007. **178**: 4557–4566.
- 39 Bhardwaj, E. K., Else, K. J., Rogan, M. T. and Warhurst, G., Increased susceptibility to *Trichuris muris* infection and exacerbation of colitis in *Mdr1a*^{-/-} mice. *World J. Gastroenterol.* 2014. **20**: 1797–1806.
- 40 Osterfeld, H., Ahrens, R., Strait, R., Finkelman, F. D., Renauld, J. C. and Hogan, S. P., Differential roles for the IL-9/IL-9 receptor alpha-chain pathway in systemic and oral antigen-induced anaphylaxis. *J. Allergy Clin. Immunol.* 2010. **125**: 469–476.e2.
- 41 Wakelin, D., Acquired immunity to *Trichuris muris* in the albino laboratory mouse. *Parasitology.* 1967. **57**: 515–524.
- 42 DeSantis, T. Z., Hugenholtz, P., Larsen, N., Rojas, M., Brodie, E. L., Keller, K., Huber, T. et al., Greengenes, a chimera-checked 16S rRNA gene database and workbench compatible with ARB. *Appl. Environ. Microbiol.* 2006. **72**: 5069–5072.
- 43 Oksanen, J. B. F., Kindt, R., Legendre, P., and O'Hara, R. B., *Vegan*: community ecology package. R package version 1.17–10. 2011.
- 44 McMurdie, P. J. and Holmes, S., *Phyloseq*: an R package for reproducible interactive analysis and graphics of microbiome census data. *PLoS One* 2013. **8**: e61217.

Abbreviations: BrdU: 5-bromo-2'-deoxyuridine · E/S: excretory/secretory · FBS: fetal bovine serum · IBD: inflammatory bowel disease · IL: interleukin · MCP2: mast cell protease · DPBS: phosphate-buffered saline

Full correspondence: Dr. Marcus Svensson-Frej, Immunology Section, Department of Experimental Medical Sciences, Medical Faculty, Lund University, BMC D14, SE-221 84 Lund, Sweden Fax: +46 46 2220412 e-mail: marcus.svensson_frej@med.lu.se

Received: 22/9/2016

Revised: 8/11/2016

Accepted: 24/11/2016

Accepted article online: 28/11/2016

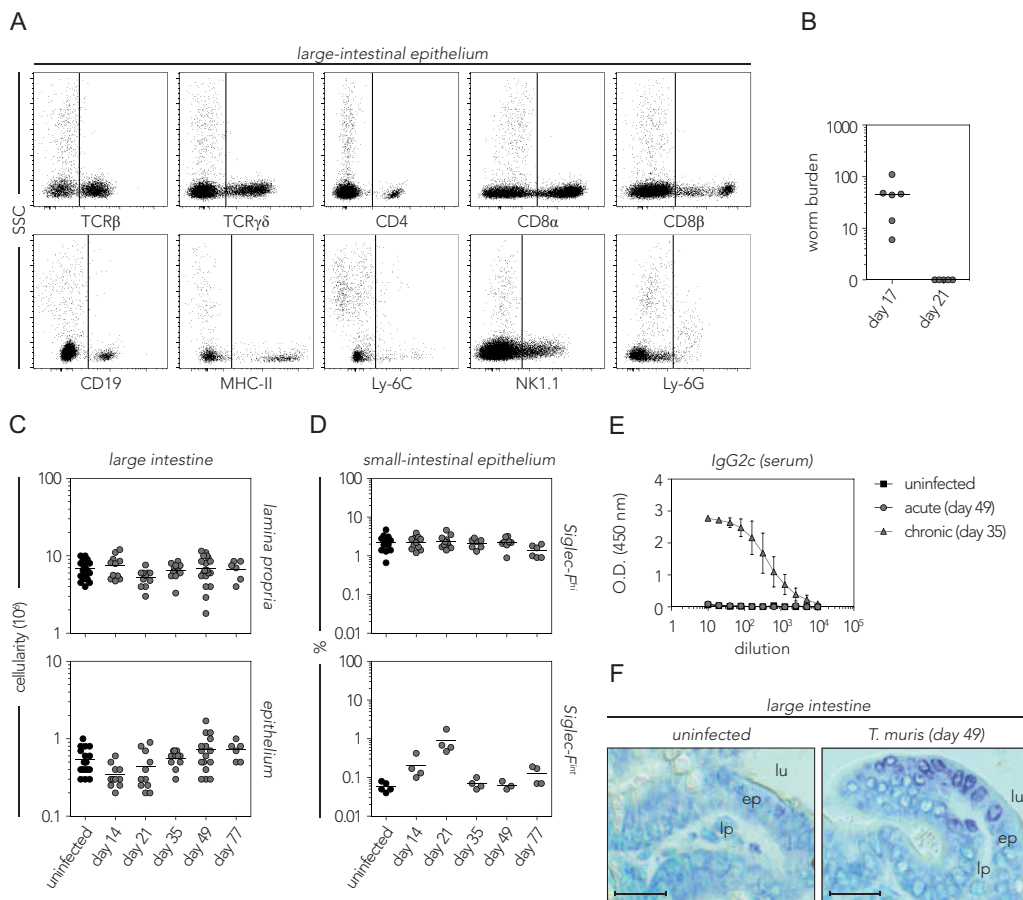


Figure S1.

C57BL/6 mice were infected with a high dose of *T. muris* and monitored over time for granulocyte accumulation in the small and large intestine.

(A) Representative flow-cytometry plots of total viable hematopoietic cells in the large-intestinal epithelium of *T. muris*-infected mice at day 14 after infection.

(B) Worm burden of *T. muris*-infected mice. Lines depict the mean worm burden, with symbols representing individual mice ($n = 5-6$).

(C) Kinetics depicting total hematopoietic cell number (cellularity) in the large-intestinal lamina propria (top graph) and epithelium (bottom graph) after *T. muris* infection. Lines depict the mean frequency of cells, with symbols representing individual mice ($n = 6-19$, from 3-7 individual experiments).

(D) Kinetics depicting frequency of Siglec-F^{hi} (top graph) and Siglec-F^{int} (bottom graph) cells in the small-intestinal epithelium after *T. muris* infection. Lines depict the mean frequency of cells, with symbols representing individual mice ($n = 3-11$, from 1-2 individual experiments).

(E) E/S antigen-specific IgG2c (measured by ELISA) in the serum of uninfected, as well as *T. muris*-infected mice at day 49 post acute or day 35 post chronic infection ($n = 3-5$ per group).

(F) Toluidine blue-stained histology sections of paraffin-embedded tissue (cecal-colonic junction) from uninfected (left) and *T. muris*-infected (right) mice at day 49 after infection. Mast cell granules appear purple. Abbreviations: ep = epithelium, lp = lamina propria, lu = lumen. Scale bars = 50 μm

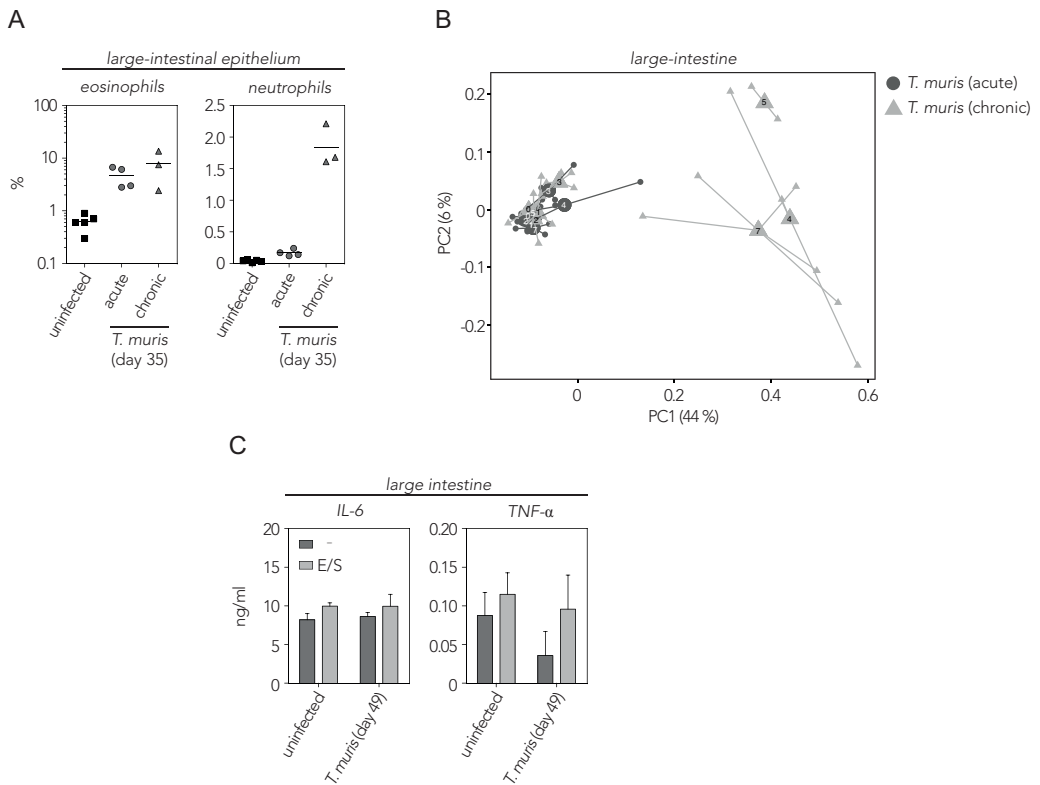


Figure S2.

C57BL/6 mice were infected with either a high (acute) or low (chronic) dose of *T. muris* eggs and monitored over time in the large intestine.

(A) Graphs depicting the frequency of eosinophils (left) and neutrophils (right) in the large-intestinal epithelium of uninfected and *T. muris*-infected mice at day 35 after infection. Lines depict the mean frequency of cells, with symbols representing individual mice (n = 3-5).

(B) Principal Component Analysis (PCoA) plot depicting fecal microbiota from mice sampled at various time points (denoted in weeks) after acute (dark gray circles) or chronic (light gray triangles) *T. muris* infection.

(C) Bar graphs depicting the concentration of IL-6 (left) and TNF- α (right) in the supernatant of *ex vivo*-cultured cells from the large-intestinal lamina propria from uninfected and *T. muris*-infected mice at day 49 after infection. Dark gray = unstimulated, light gray = E/S-stimulated.

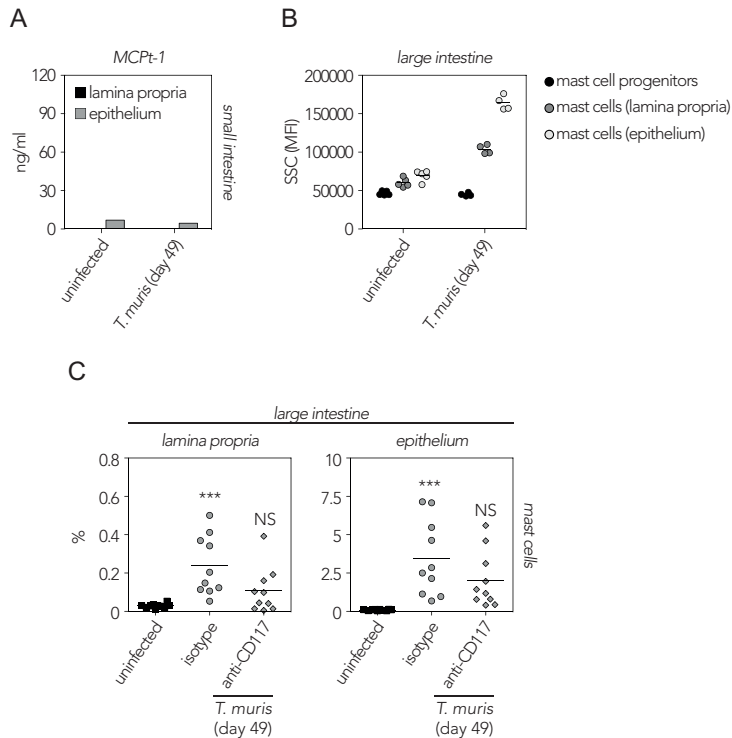


Figure S4.

C57BL/6 mice were infected with a high dose of *T. muris* and monitored over time for mast cell accumulation in the large intestine and MCPt-1 in the small intestine.

(A) Graph depicting the concentration of MCPt-1 in the supernatant of *ex vivo*-cultured small-intestinal lamina propria (black) and epithelial (gray) cells of uninfected and *T. muris*-infected mice at day 49 after infection. Values represent pooled cell suspensions from 4-5 mice.

(B) Graph depicting the SSC mean fluorescence intensity (MFI) of mast cells and mast cell progenitors in the large intestine of uninfected and *T. muris*-infected mice at day 49 after infection.

(C) Graph depicting the frequency of mast cells in the large-intestinal lamina propria (left) and epithelium (right) of mice treated with depleting anti-CD117 antibody, according to Figure 4D. Data are pooled from two individual experiments and analyzed with one-way ANOVA and Tukey's post-test for multiple comparison. *** ($p < 0.001$), NS (not significant).

Paper 2

RESEARCH ARTICLE

Chronic *Trichuris muris* Infection Decreases Diversity of the Intestinal Microbiota and Concomitantly Increases the Abundance of Lactobacilli

Jacob Bak Holm¹*, Daniel Sorobetea²*, Pia Kiilerich¹, Yulixias Ramayo-Caldas³, Jordi Estellé³, Tao Ma¹, Lise Madsen^{1,4}, Karsten Kristiansen^{1,4}*, Marcus Svensson-Frej^{2,4}*

1 Laboratory of Genomics and Molecular Biomedicine, Department of Biology, University of Copenhagen, Copenhagen, Denmark, **2** Immunology Section, Department of Experimental Medical Sciences, Medical Faculty, Lund University, Lund, Sweden, **3** INRA, UMR1313 Génétique Animale et Biologie Intégrative (GABI), Jouy-en-Josas, France, **4** National Institute of Nutrition and Seafood Research, Bergen, Norway



* These authors contributed equally to this work.

‡ These authors are joint senior authors on this work.

* marcus.svensson_frej@med.lu.se (MSF); kk@bio.ku.dk (KK)

OPEN ACCESS

Citation: Holm JB, Sorobetea D, Kiilerich P, Ramayo-Caldas Y, Estellé J, Ma T, et al. (2015) Chronic *Trichuris muris* Infection Decreases Diversity of the Intestinal Microbiota and Concomitantly Increases the Abundance of Lactobacilli. PLoS ONE 10(5): e0125495. doi:10.1371/journal.pone.0125495

Academic Editor: Irving Coy Allen, Virginia Tech University, UNITED STATES

Received: January 26, 2015

Accepted: March 13, 2015

Published: May 5, 2015

Copyright: © 2015 Holm et al. This is an open access article distributed under the terms of the [Creative Commons Attribution License](https://creativecommons.org/licenses/by/4.0/), which permits unrestricted use, distribution, and reproduction in any medium, provided the original author and source are credited.

Data Availability Statement: All sequence data is available from the European Nucleotide Archive (ENA) with study accession number: PRJEB6560. Immunological raw data is available from Dryad Digital Repository (doi:10.5061/dryad.md0vg).

Funding: This work was supported by grants from the Novo Nordisk Foundation (www.novonordiskfonden.dk), The Carlsberg Foundation (www.carlsbergfondet.dk), and the Swedish Medical Research Council (www.vr.se). Yulixias Ramayo-Caldas was funded by the European Union, in the framework of the Marie-Curie FP7 COFUND People

Abstract

The intestinal microbiota is vital for shaping the local intestinal environment as well as host immunity and metabolism. At the same time, epidemiological and experimental evidence suggest an important role for parasitic worm infections in maintaining the inflammatory and regulatory balance of the immune system. In line with this, the prevalence of persistent worm infections is inversely correlated with the incidence of immune-associated diseases, prompting the use of controlled parasite infections for therapeutic purposes. Despite this, the impact of parasite infection on the intestinal microbiota, as well as potential downstream effects on the immune system, remain largely unknown. We have assessed the influence of chronic infection with the large-intestinal nematode *Trichuris muris*, a close relative of the human pathogen *Trichuris trichiura*, on the composition of the murine intestinal microbiota by 16S ribosomal-RNA gene-based sequencing. Our results demonstrate that persistent *T. muris* infection dramatically affects the large-intestinal microbiota, most notably with a drop in the diversity of bacterial communities, as well as a marked increase in the relative abundance of the *Lactobacillus* genus. In parallel, chronic *T. muris* infection resulted in a significant shift in the balance between regulatory and inflammatory T cells in the intestinal adaptive immune system, in favour of inflammatory cells. Together, these data demonstrate that chronic parasite infection strongly influences the intestinal microbiota and the adaptive immune system. Our results illustrate the complex interactions between these factors in the intestinal tract, and contribute to furthering the understanding of this interplay, which is of crucial importance considering that 500 million people globally are suffering from these infections and their potential use for therapeutic purposes.

Programme, through the award of an AgreenSkills' fellowship (under grant agreement n° 267196; www.agreenskills.eu). The funding sources had no role in study design, data collection and analysis, decision to publish, or preparation of the manuscript.

Competing Interests: The authors have declared that no competing interests exist.

Introduction

The gastrointestinal tract harbours a myriad of microorganisms, collectively termed the microbiota, which have evolved complex interdependent relationships with the host[1, 2]. The microbiota is critical to the health of the host by metabolising nutrients[3, 4], maturing the immune system[5–7] and competing out pathogens[8, 9], as evidenced by studies utilising mice raised under germ free conditions devoid of commensal organisms. Thus, resident bacteria shape the host immune system and small disturbances in the balance between different microbial communities can have adverse effects on its integrity. Likewise, activation of the immune system, for example during infection, may lead to alterations in the composition of the microbiota[10, 11], and thereby affect the balance of the intestinal microenvironment. An imbalance in this host-microbial relationship is thought to contribute to multiple inflammatory and autoimmune diseases[6, 12].

Parasitic worms are among the most prevalent pathogens that afflict humans, and they share a long evolutionary history with us. Hence, worm infections are rarely lethal but can nonetheless cause a wide variety of health issues such as abdominal pain, anaemia, stunted growth and impaired cognitive development[13, 14]. On the other hand, parasites may incur benefits to the host by educating the immune system early in life and providing signals that serve to dampen inflammation and strengthen the regulatory immune response[15]. Signs of this may be seen in developed countries, where the absence of worm infections has been correlated with an increased incidence of various immune-associated diseases including allergies, inflammatory bowel disease (IBD), multiple sclerosis, rheumatoid arthritis (RA) and type 1 diabetes (T1D)[16–18]. Encouraged by results from various laboratory models[19–24], much emphasis has been placed on the potential therapeutic value of parasitic infections in treating human diseases[25–28]. Indeed, therapeutic infection with the porcine nematode *Trichuris suis* is currently in clinical trial for treatment of IBD[29]. Interestingly, diseases that have been associated with the absence of parasitic worms, including IBD, RA and T1D, have also been correlated with alterations in the intestinal microbiota[30]. It is therefore plausible that the lack of parasitic worm infections, via modulation of the intestinal microbiota, might confer protection against these disorders.

Trichuris muris is the murine-specific counterpart to the human pathogen *Trichuris trichiura* that infects approximately 500 million people globally[31]. Its life cycle follows a strict faecal-oral route. Thus, following infection of the large intestine, *T. muris* worms remain in the caecal and colonic epithelium throughout their lifespan. During the first three weeks after hatching, the larvae reside embedded in syncytial tunnels formed through adjacent intestinal epithelial cells, but from the L2-L3 moulting stage, worms start protruding out into the intestinal lumen, reaching adulthood five weeks after infection. In line with other intestinal parasites, protective immunity to *T. muris* infection is dependent on induction of a T helper cell type 2 (Th2) response[32]. However, at sufficiently low doses, *T. muris* establishes a chronic infection by invoking a Th1 response characterised by the production of the cytokine interferon- γ (IFN- γ)[33].

Given that *T. muris* larvae occupy the same niche as the majority of the intestinal microbiota it is plausible that these organisms influence each other, which may subsequently affect the intestinal microenvironment of the host. Interestingly, oral administration of *Lactobacillus casei* can increase the susceptibility to *T. muris* infections[34] and intestinal luminal bacteria are important for enabling the *T. muris* larvae to hatch during the initial infection[35], further illustrating the complex inter-species relationships that characterise the intestinal microenvironment. However, data on the influence of *Trichuris* parasites on intestinal bacterial communities is limited. Studies in pigs infected with *T. suis* have demonstrated changes in bacterial

diversity and metabolic networks after infection[36, 37], whereas studies in humans infected with *T. trichiura* have yielded conflicting data[38, 39], emphasising the need for further research.

We set out to study the effect of chronic *T. muris* infection on the gut microbiota and immune response. Here, we provide evidence that persistent *T. muris* infection resulted in dramatic alterations in microbial communities, in both the caecum and colon, which became apparent approximately three weeks after infection and became increasingly established with time. Overall, these changes resulted in a less diverse microbiota, and were characterised by a marked increase in the relative abundance of the bacterial family *Lactobacillaceae*. In addition, chronic *T. muris* infection affected the balance between inflammatory and regulatory immune cells in the intestinal mucosa, although this seemed to occur prior to the increase in *Lactobacillaceae*. These findings highlight the importance of understanding the intricate interactions of the microbiota, particularly with regard to parasitic worm infections, and their contribution to health and disease.

Materials and Methods

Mice

Mice were obtained from Harlan Laboratories (An Venray, Netherlands). Experiments were conducted with age-matched, male C57BL/6 mice that were eight weeks old at the start of the experimentation. Mice were sacrificed by cervical dislocation.

Ethics Statement

All experiments were conducted in strict accordance with animal welfare laws, as determined by Swedish authorities (Swedish Board of Agriculture, Act 1988:534). The protocol was approved by Malmö/Lund Ethical Board for Animal Research, Lund/Malmö, Sweden (permit no. M467-12), and all efforts were made to minimize suffering of the mice. Mice were monitored daily for signs of stress or disease, such as condition of fur and general movement. None of the mice developed diarrhoea or other intestinal-related issues.

Trichuris muris

T. muris (strain E) was maintained, and worm-derived excretory/secretory (E/S) antigens were generated and purified as previously described[40]. To obtain a chronic *T. muris* infection, mice were infected with a low dose of approximately twenty infective eggs in sterile-filtered (0.2 μm) tap water by oral gavage. To assess the worm burden of infected mice, large intestines were excised and frozen at -20°C . During the analysis, intestines were cut longitudinally, and scraped free of worms, which were subsequently counted under a reverse phase-contrast microscope.

Experimental Outline

Mice were co-housed for at least two weeks prior to experimentation to ensure normalisation of their microbiota, and were subsequently placed in individual cages during experiments to avoid cross-contamination. Experiments were conducted according to the scheme in [S1 Fig 10](#) mice were infected at day 0 with a low dose *T. muris* eggs and 20 mice were left uninfected. 10 of the uninfected were sacrificed at day 0 while the remaining 10 were sampled over a 35 days period alongside with the 10 infected mice. Fresh faeces were sampled regularly throughout the experiment, after each larval moulting stage: L2 (day 13), L3 (day 20) and L4 (day 27). The faecal samples were immediately frozen on dry ice upon collection. At the end point (day 35),

luminal contents were collected from both the caecum and colon. We sampled the luminal colon content distally, to make them correspond to the fresh faeces samples. For simplicity, luminal colon content sampled upon termination and fresh faeces sampled throughout the infection are collectively referred to as "faecal samples". Finally, to ensure that mice had been properly infected, a separate group of five mice was infected and sacrificed at day 35 for assessment of their worm burden.

Cell Isolation

Mesenteric lymph nodes (MLN) were stripped of surrounding adipose tissue and mashed in Dulbecco's phosphate-buffered saline (DPBS; Life Technologies), followed by filtration through 70 μm cell strainers (Fisher Scientific). The large intestines were stripped of attached adipose tissue, opened longitudinally and washed thoroughly in DPBS to remove the faeces. To isolate cells from the large-intestinal lamina propria (LI LP) the intestines were cut into approximately one cm pieces, and incubated thrice in epithelial dissociation buffer consisting of Hank's balanced salt solution (HBSS; Life Technologies) supplemented with 15 mM 4-(2-hydroxyethyl)-1-piperazineethanesulfonic acid (HEPES; Life Technologies), 2% foetal bovine serum (FBS; Sigma-Aldrich), 5 mM ethylenediaminetetraacetic acid (EDTA; Merck-Millipore), 100 U/ml penicillin + 100 $\mu\text{g}/\text{ml}$ streptomycin (Life Technologies), 50 $\mu\text{g}/\text{ml}$ gentamicin (Life Technologies) and 1.25 $\mu\text{g}/\text{ml}$ Fungizone (Life Technologies) for 15 minutes at 37°C, on continuous shaking. For the first round of treatment, 1 mM DL-dithiothreitol (DTT; Sigma-Aldrich) was added to aid the removal of mucous. After a brief wash, the remaining tissue pieces were subsequently enzymatically digested in R10 buffer consisting of RPMI 1640 (Life Technologies) supplemented with 10 mM HEPES, 10% FBS, 2 mM L-glutamine (Life Technologies), 1 mM sodium pyruvate (Life Technologies), 100 U/ml penicillin + 100 $\mu\text{g}/\text{ml}$ streptomycin, 50 $\mu\text{g}/\text{ml}$ gentamicin and 1.25 $\mu\text{g}/\text{ml}$ Fungizone, along with 0.3 Wünsch-units/ml liberase TM (Roche), 30 $\mu\text{g}/\text{ml}$ DNase I (Roche) and 5 mM CaCl_2 for 45 minutes at 37°C with magnetic stirring. The resulting cell suspension was filtered through 100 μm cell strainers (Fisher Scientific), and subjected to a density gradient centrifugation using Percoll (GE Healthcare) according to manufacturer's instructions. Briefly, cells were suspended in 40% Percoll and centrifuged over a 70% Percoll layer for 20 minutes, 600 g without brake at room temperature. Cells were collected from the 40/70 interphase and washed with R10 buffer. Cell numbers were assessed with a KX-21N automated hematology analyzer (Sysmex).

Ex vivo Cell Stimulations and Cytokine Analyses

For cytokine secretion analyses, cells were suspended in R10 buffer, seeded at 2.5×10^6 cells/ml in TC MicroWell 96U Nunclon plates (Thermo Fisher Scientific), and incubated with 50 $\mu\text{g}/\text{ml}$ E/S antigens for 48 hours at 37°C, 5% CO_2 . Cell-free supernatants were collected and frozen at -20°C for subsequent analyses. Cytokine secretion was measured with BD cytometric bead array (BD Biosciences) according to manufacturer's instructions with the following modification: the amount of capture beads and detection reagents as well as sample volumes was scaled down five-fold. Samples were acquired on a BD LSR II flow cytometer (BD Biosciences) and data analysed with FACS Array v3.0 (SoftFlow Inc.).

For intracellular cytokine analyses, cells were suspended in R10 buffer, seeded at 5×10^6 cells/ml in 5 ml polystyrene round-bottom tubes (BD Falcon), and incubated with 250 ng/ml phorbol 12-myristate 13-acetate (PMA; Sigma-Aldrich), 500 ng/ml ionomycin (Sigma-Aldrich) and 10 $\mu\text{g}/\text{ml}$ brefeldin A (Sigma-Aldrich), or brefeldin A alone as a negative control, for 3 hours at 37°C, 5% CO_2 . Cells were then washed with R10 buffer followed by staining for flow cytometry analysis.

Flow Cytometry

Cells were fluorescently labelled for 30–60 minutes on ice with the following antibodies and reagents: BV510-conjugated rat anti-mouse CD45 (clone 30-F11; BioLegend), BV605-conjugated Armenian hamster anti-mouse TCR β (H57-597; BD Biosciences), PE-conjugated rat anti-mouse IL-10 (JES5-16E3; eBioscience), PE-CF594-conjugated rat anti-mouse CD4 (RM4-5; BD Biosciences), PerCP-Cy5.5-conjugated mouse anti-human/mouse T-bet (4B10; eBioscience), PE-Cy7-conjugated rat anti-mouse IFN- γ (XMG1.2; BioLegend), APC-conjugated rat anti-mouse/rat FoxP3 (FJK-16; eBioscience), AF700-conjugated rat anti-mouse CD19 (6D5; BioLegend), AF700-conjugated rat anti-human/mouse B220 (RA3-6B2; eBioscience), AF700-conjugated mouse anti-mouse NK1.1 (PK136; BioLegend), AF700-conjugated rat anti-mouse Ter-119 (TER-119; BioLegend), biotin-conjugated rat anti-mouse CD8 α (53-6.7; BioLegend), APC-eF780-conjugated streptavidin (eBioscience), along with Violet Live/Dead (Life Technologies) according to manufacturer's instructions to label dead cells. Cells were stained intracellularly with FoxP3/Transcription factor staining buffer set (eBioscience) according to manufacturer's instructions. Cells were analysed on a BD LSR II flow cytometer, and data analysed with FlowJo software v9.7 (Tree Star Inc.). Dead cells and aggregates were excluded from all analyses.

Amplicon Sequencing

Bacterial DNA from caecal and faecal samples were extracted using a NucleoSpin soil kit (Macherey-Nagel) according to manufacturer's instructions. DNA yield and integrity were assessed using a Nanodrop and agarose gel electrophoresis, respectively. The PCR-based library formation was performed using 10 ng bacterial DNA, 0.2 μ M of each barcoded forward and reverse primer, 0.2 mM dNTPs and 0.5 units Phusion high fidelity DNA polymerase (Thermo Scientific) in a total volume of 25 μ l. To target the 16S rRNA gene's variable region 4 (V4) a forward primer 515F (5' AATGATACGGCGACCACCGAGATCTACAC NNNNNNNN TATGGTAATTGTGTGCCAGCMGCCGCGGTAA 3'; "N" indicates the nucleotides of the barcode sequence) and a reverse primer 806R (5' CAAGCAGAAGACGGCATACGAGAT NNNNNNNNNNNN AGTCAGTCAG CC GGACTACHVGGGTWTCTAAT 3') were used, both with Illumina adaptor sequences in the 5' end [41, 42]. Cycling condition was as follows: 98°C for 30 seconds followed by 35 cycles of 98°C for 5 s, 56°C for 20 s and 70°C for 20 s. PCR products were purified and normalised to 1–2 ng/ μ l using the SequelPrep Normalisation Plate kit (Life Technologies Europe). Subsequently, samples were pooled (2 μ l of each sample) and quantified using a KAPA Library Quantification Kit (KAPA Biosystems) on a Stratagene Mx3000 (Agilent Technologies Denmark). 6.65 pM library and 0.35 pM PhiX Control v3 (Illumina) was sequenced using an Illumina MiSeq V2 PE500 cartridge (500 cycles) on an Illumina MiSeq.

Bioinformatics

Generated sequences were analysed using qiime_pipe (https://github.com/maasha/qiime_pipe) using QIIME v1.7.0 with default settings, which performs quality-based sequence trimming, primer removal and assembly of paired-end sequences followed by the execution of a QIIME workflow including chimera checking [41]. De novo OTU-picking was performed using UCLUST [43] with 97% sequence similarity. Representative sequences were assigned taxonomy against the Greengenes database v11_2 [44] using the RDP-classifier [45] with an 80% confidence threshold. Subsequent analyses were performed in R v3.1.1 using the metagenome-Seq [46], PhyloSeq [47], Vegan [48] and GGplot2 [49] packages. Data was filtered for low-abundance OTUs by removal of OTUs present in fewer than 3 of the 140 samples and with a

relative abundance across all samples $\leq 0.005\%$. A single day 35 faecal sample from one of the infected mice and a single day 0 caecal sample from one of the uninfected mice were left out due to our cut off of at least 10,000 sequences per sample after filtering. Analyses in R were performed with an average of $25,060 \pm 6,480$ (SD) sequences per sample before, and with $20,912 \pm 5,091$ (SD) sequences per sample after filtering. Alpha and gamma diversity were estimated using unfiltered data. Beta diversity was performed using filtered data and calculated for time point/treatment using Vegan. Read counts were normalised with metagenomeSeq[46] that uses a cumulative-sum scaling in which raw counts are divided by the cumulative sum of counts up to a particular quantile. Statistical analyses for Table 1 and S2 Table comparing uninfected with infected were performed on data filtered based on effective sample sizes. Taxa were not included if they had fewer than X effective number of positive samples, where X is the median of estimated effective samples per feature calculated using metagenomeSeq. Phylogenetic analyses were conducted using 16S rRNA gene sequences from the given family downloaded from The Ribosomal Database Project (RDP)[50]. The representative sequences, from the OTUs classified to be members of the given family were combined with the RDP sequences. Sequence-alignment using MUSCLE[51] and phylogenetic tree building using the Maximum Likelihood method based on the Tamura-Nei model[52] were performed using MEGA v6.06 [50]. All sequence data is available from the European Nucleotide Archive (ENA) with study accession number: PRJEB6560. Immunological raw data is available from Dryad Digital Repository (doi:10.5061/dryad.md0vg).

Results

Chronic *T. muris* Infection Induces Major Changes in the Gut Microbiota

To examine whether chronic *T. muris* infection affects the composition of the intestinal microbiota, we infected male C57BL/6 mice with a low dose of *T. muris* eggs by oral gavage, and collected faecal samples at various time points after infection, coinciding with the different larval developmental stages (S1 Fig). Five weeks after infection, the experiment was terminated and the caecum and colon contents were collected. To confirm the chronic nature of the infection, we assessed the intestinal worm burden of a parallel group of mice infected at the same time. As expected, none of the mice had cleared the infection after five weeks, harbouring 20 ± 3 worms (mean \pm SD; $n = 5$) and were thus, by definition, chronically infected.

Next, we investigated the composition of the intestinal microbiota utilising 16S rRNA gene-based sequencing and found that chronic *T. muris*-infection induced clear changes in microbial communities of the large intestine (Fig 1). While minor alterations were seen at early time points after infection, the first substantial microbial changes appeared from day 20 (Fig 1 and S2 Fig and S1 Table for statistical summary). The changes became more pronounced with time (Fig 1 and S2 Fig and S3 Fig) and were very distinct at day 35 after infection, compared to the uninfected mice (Fig 1 and S2 Fig and S1 Table for statistical summary). The infection had similar effects on the faecal and caecal microbiota (S4 Fig). Importantly, we detected only very minor changes over time in the microbial composition of the uninfected mice (S5 Fig), demonstrating that differences observed in the infected mice reflected infection-dependent changes. Thus, chronic infection with *T. muris* is associated with pronounced changes in the microbiota.

Table 1. Bacterial taxa that differed significantly within faecal samples after *T. muris* infection.

Time after infection	Phylum	Class	Order	Family	Genus	Prevalence		Counts		Abundance (%)		Adj. P-value
						Uninfected	Infected	Uninfected	Infected	Uninfected	Infected	
13 days	Actinobacteria	Actinobacteria	Bifidobacteriales	Bifidobacteriaceae	Bifidobacterium†	8/10	10/10	1674	2663	0.66	0.88	0.56 4.6E-02
						10/10	10/10	3334	11895	1.65	0.24	4.49 0.83 4.1E-02
	Firmicutes	Bacilli†	Lactobacillales†	Lactobacillaceae†	Lactobacillus†	10/10	10/10	3525	11764	1.64	0.24	4.48 0.83 3.9E-02
						10/10	10/10	3316	11676	1.64	0.24	4.44 0.83 4.0E-02
20 days	Proteobacteria	Deltaiproteobacteria†	Desulfuromonadales†	Desulfuromonadaceae†	Desulfuromonas†	10/10	10/10	3303	11638	0.83	0.24	4.43 0.83 3.1E-02
						10/10	10/10	1820	1020	0.89	0.12	0.40 0.06 3.4E-02
						10/10	10/10	1820	1020	0.89	0.12	0.40 0.06 4.4E-02
						10/10	10/10	1803	1008	0.88	0.11	0.40 0.06 4.0E-02
27 days	Firmicutes	Erysipelotrichi†	Bacilli†	Lactobacillales†	Lactobacillus†	10/10	10/10	2840	28576	1.32	0.16	11.41 3.12 4.0E-03
						10/10	10/10	2793	28565	1.30	0.15	11.40 3.12 6.8E-03
						10/10	10/10	2790	28543	1.30	0.15	11.39 3.12 2.0E-04
						10/10	10/10	2790	28433	1.30	0.15	11.35 3.11 7.0E-04
35 days	Firmicutes	Erysipelotrichi†	Bacilli†	Lactobacillales†	Lactobacillus†	10/10	10/10	2885	1416	1.39	0.20	0.63 0.19 4.0E-02
						10/10	9/9	1801	23269	0.94	0.25	14.84 3.41 6.6E-05
						10/10	9/9	1795	23237	0.93	0.25	14.84 3.41 3.9E-04
						10/10	9/9	1785	23123	0.93	0.24	14.74 3.38 6.1E-04
Erysipelotrichi†	Coccidiales	Bacteroidales	Bacteroidales	Lactobacillaceae†	Lactobacillus†	10/10	10/10	1782	28865	0.93	0.24	14.65 3.36 2.1E-05
						10/10	9/9	1924	5944	5.62	1.38	2.92 1.73 6.6E-05
						10/10	9/9	1824	5944	5.62	1.38	2.92 1.73 3.6E-04
						10/10	9/9	1824	5944	5.62	1.38	2.92 1.73 8.4E-05
Erysipelotrichales†	Coccidiales	Bacteroidales	Bacteroidales	Erysipelotrichaceae†	Alibaculum†	10/10	9/9	1804	5892	5.56	1.38	2.90 1.72 2.8E-03
						10/10	9/9	163	16	0.08	0.03	0.01 0.00 1.5E-02
						10/10	9/9	1611	528	0.85	0.16	0.25 0.08 1.5E-02
						10/10	7/9	55	131	0.03	0.01	0.06 0.03 2.5E-02
Proteobacteria	Bacteroidales	Bacteroidales	Bacteroidales	Alcaligenaceae	Parsuella†	10/10	9/9	1440	9032	0.71	0.16	4.30 1.75 1.6E-02
						8/10	7/9	24	54	0.01	0.00	0.03 0.01 3.7E-03
						10/10	7/9	22	32	0.01	0.00	0.02 0.00 2.9E-02
						10/10	7/9	3437	1319	1.74	0.27	0.69 0.38 8.8E-03

List of significantly (adj. p-value <0.05) increased or decreased abundance of bacteria at multiple taxonomic ranks when comparing infected with uninfected samples at the given time points. Data are illustrated with the prevalence for each given bacteria, absolute counts, and relative abundance. Significantly increased or decreased bacterial groups are depicted in bold letters with up- or down arrows, respectively. Statistics were performed using metagenomeSeq[46].

doi:10.1371/journal.pone.0125495.t001

Fig 1. Time-dependent changes of the microbiota diversity due to chronic *T. muris* infection. Non-metric Multi-Dimensional Scaling (NMDS) plot using Bray-Curtis dissimilarity indices from (A) faecal microbiota from 10 infected mice sampled at various time points from day 0 to day 35, and (B) caecal microbiota from uninfected mice at day 0 and uninfected/infected mice at day 35. Ellipses are labelled according to the corresponding day of analysis. Relative abundance at family level was fitted as vectors based on 9999 permutations and scaled by their correlation coefficient.

doi:10.1371/journal.pone.0125495.g001

Chronic *T. muris* Infection Decreases Alpha and Gamma, but Increases Beta Diversity of the Microbiota

In order to examine whether chronic *T. muris* infection influenced the diversity of the intestinal microbiota we determined alpha (within sample) and beta (between samples) diversity for each sample and group, respectively. Alpha diversity analysis was performed on unfiltered data using Shannon index (Fig 2A). The alpha diversity of the faecal samples from the infected mice was significantly decreased after 27 days of infection, and even further decreased after 35 days, while no decrease was observed in the uninfected mice. Similarly, a significant decrease in the alpha diversity in caecal samples was evident after 35 days of infection (Fig 2A). By contrast, beta diversity between the faecal samples from the infected mice was increased after 27 and 35 days, and similarly, increased beta diversity was observed in caecal samples after 35 days

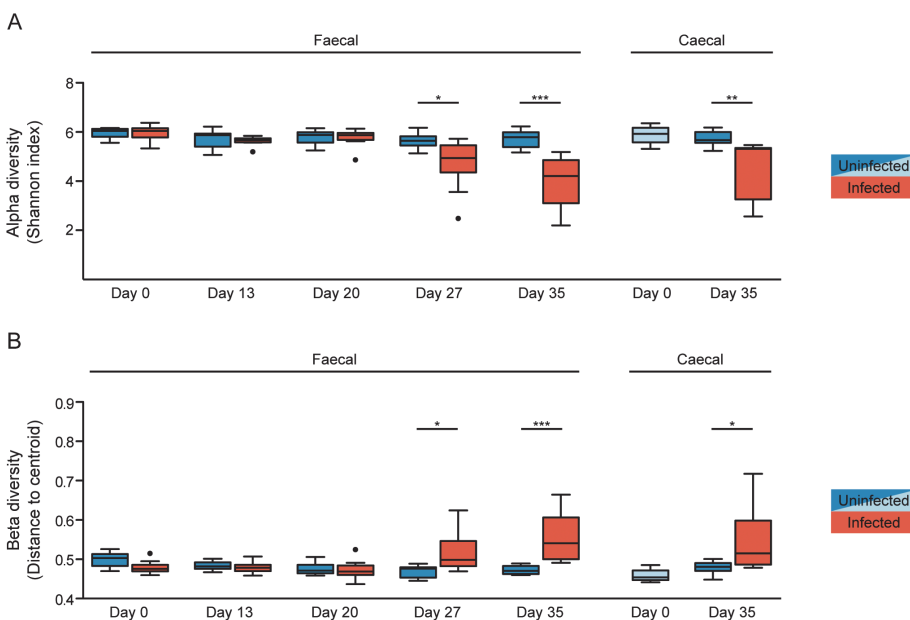


Fig 2. Chronic *T. muris* infection results in decreased alpha but increased beta diversity of the microbiota. (A) Median alpha diversity based on Shannon index of unfiltered microbiota data for faecal and caecal samples. The upper and lower whiskers correspond to the 25th and 75th percentiles. (B) Median beta diversity based on Sørensen index for faecal and caecal samples. The whiskers correspond to the 25th and 75th percentiles. Statistical analyses were performed with one-way ANOVA, followed by Tukey's post-test for multiple comparisons using Prism (GraphPad software). The light blue colour for uninfected caecal samples indicates the ten mice sacrificed at day 0, and therefore not repeated sampling as for the faecal samples. The following definitions were used to denote statistical significance: * ($p < 0.05$), ** ($p < 0.01$), *** ($p < 0.001$), while $p > 0.05$ was considered not significant (NS).

doi:10.1371/journal.pone.0125495.g002

(Fig 2B). We therefore investigated whether there was an overall gain or loss of diversity by examining the combined microbiota from all infected mice (gamma diversity) compared to all the uninfected mice. Thus, all untrimmed data were pooled according to treatment and the gamma diversity (between groups) of the infected and uninfected pools was compared using the Shannon index. In accordance with the alpha diversity, we found a decline in gamma diversity at day 27 and 35 after infection in the faecal samples and at day 35 for the caecal samples (S6 Fig). Together, these data demonstrate that chronic *T. muris* infection causes an overall decrease in microbial diversity of the large intestine.

T. muris Infection Alters the Composition of the Faecal and Caecal Microbiota

Next, we examined the alterations in intestinal microbial composition following *T. muris* infection by taking taxonomical classifications of operational taxonomic units (OTU) into account. At the phylum level, *T. muris* infection led to increased abundance of *Firmicutes* (day 27 and 35) and *Proteobacteria* (day 35) while decreasing *Bacteroidetes* (day 27 and 35) in the faecal samples ($p < 0.05$, repeated-measures ANOVA, S7 Fig). *Firmicutes*, *Proteobacteria* and *Bacteroidetes* accounted for more than 90% of the microbiota at all time points. The *T. muris* infection increased the relative abundance of *Firmicutes* in faecal samples from $37 \pm 3\%$ to $43 \pm 6\%$ between day 0 and 35. Likewise, the caecal samples from the infected mice contained $58 \pm 6\%$ *Firmicutes* at day 35 compared to $30 \pm 2\%$ and $36 \pm 2\%$ in the uninfected mice sacrificed at day 0 and 35, respectively. *Proteobacteria* and *Bacteroidetes* are traditionally lipopolysaccharide-containing gram-negative bacteria whereas *Firmicutes* are, with minor exceptions, gram-positive bacteria, thus, the microbiota was characterised by an increased proportion of gram-positive bacteria after infection due to the increase in *Firmicutes*.

To further investigate the changes in the microbiota composition following the *T. muris* infection, we analysed the microbiota composition in a taxa summary plot on family level (Fig 3), statistical analysis on multiple taxonomic ranks (Table 1), heat-mapping at genus level, including hierarchical cluster analysis (Fig 4), and phylogenetic tree analysis to identify candidates at species level (S8 Fig). Hierarchical cluster analysis of Bray-Curtis dissimilarity indices identified day 0 and day 13 to be the most similar, with day 20 as the closest relative, while day 27 and 35 were distinctly clustered on two separated branches (Fig 4), indicating that major changes in the microbiota occurred from day 20 after the infection with *T. muris*.

Using metagenomeSeq [46] we identified bacteria that were significantly altered due to infection at any given time point. We focused on the most common effects of the infection, which we defined as affected taxa detected in at least as many or more samples compared to the median of the estimated effective sample size, as calculated by MetagenomeSeq. With an increase at day 13 after infection, *Bifidobacterium* was identified as the only significantly affected genus before the major changes to the microbiota occurring at day 20 and onward (Table 1). The most notable change observed was an increase in the relative abundance of the bacterial family *Lactobacillaceae* that remained relatively unaltered until day 20, after which it gradually increased in abundance from $<5\%$ between day 0 and 20, to 11% and 15% after days 27 and 35, respectively (Table 1 and Fig 3). While the increase in *Lactobacillaceae* occurred in 8 out of 9 mice, other changes were less general (S9 Fig), further illustrating the variability between individual mice as reflected by the increase in beta diversity described earlier. Interestingly, some genera were affected only at certain time points after infection and then remained stable (Fig 4 and Table 1). Among these we detected an increase in the relative abundance of *Alistipes* and *Odoribacter* from the *Bacteroidales* family at day 20, as well as a decrease in *Allobaculum* and *Barnesiella* and a sharp increase in *Parasutterella* at day 35 (Fig 4 and Table 1). The abundance

of *Lactobacillus*, *Allobaculum* and *Barnesiella* were also found to be significantly affected in the caecal samples by the infection with the addition of a >10-fold increased abundance of *Mucispirillum* and a decrease of the low-abundant *Sporobacter* selectively in the caecal samples (S2 Table).

By phylogenetic tree analysis, comparing the representative sequences for the OTUs classified within each family and 16S rRNA gene sequences downloaded from the Ribosomal Database Project[50], we identified candidate species for the *Lactobacillaceae* family affected by *T. muris* infection. A single OTU (L#1 in S8 Fig) accounted for more than 80% of the relative abundance in faecal samples 35 days after infection, the sequence of which was identical to that of *L. apodemi*, *L. murinus* and *L. animalis* (S8 Fig). The second most abundant OTU was identical to *L. gasserii* and *L. taiwanensis*. The same OTUs and similar relative abundance within families were found for caecal samples (data not shown).

A Skewed Intestinal Regulatory/Inflammatory T Cell Balance is Induced upon Chronic *T. muris* Infection

Finally, we wanted to investigate whether the profound changes observed in the microbiota composition correlated with infection-driven responses in the intestinal immune

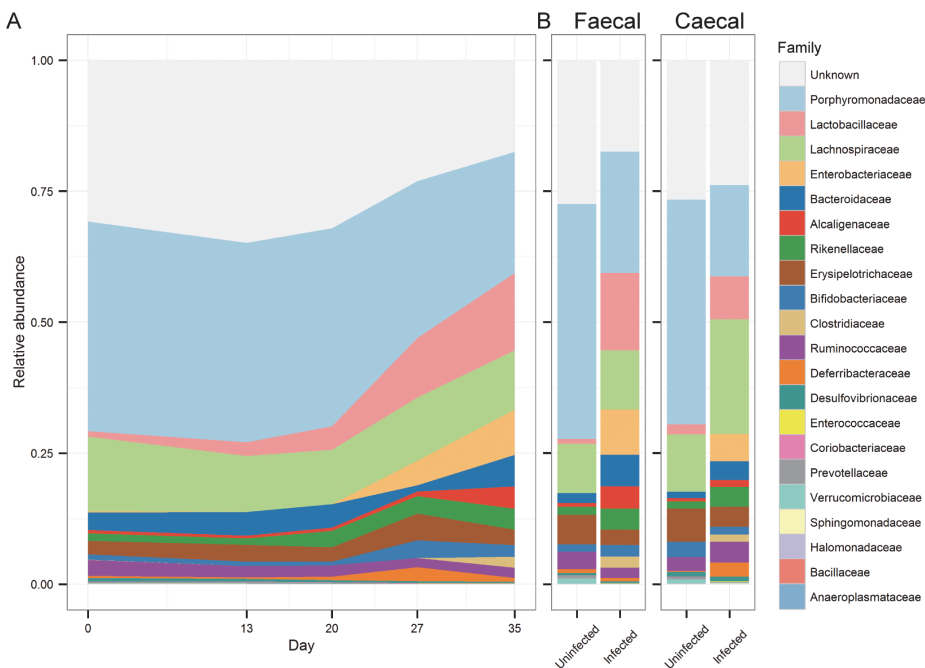


Fig 3. Chronic *T. muris* infection affects the composition of the microbiota. Taxa summary plots at family level showing (A) changes in microbiota composition of faecal samples from the infected mice from day 0 to day 35, and (B) the microbiota composition of uninfected and infected mice at day 35 for faecal and caecal samples. "Unknown" refers to OTUs that we were unable to classify. Data represent mean relative abundance.

doi:10.1371/journal.pone.0125495.g003

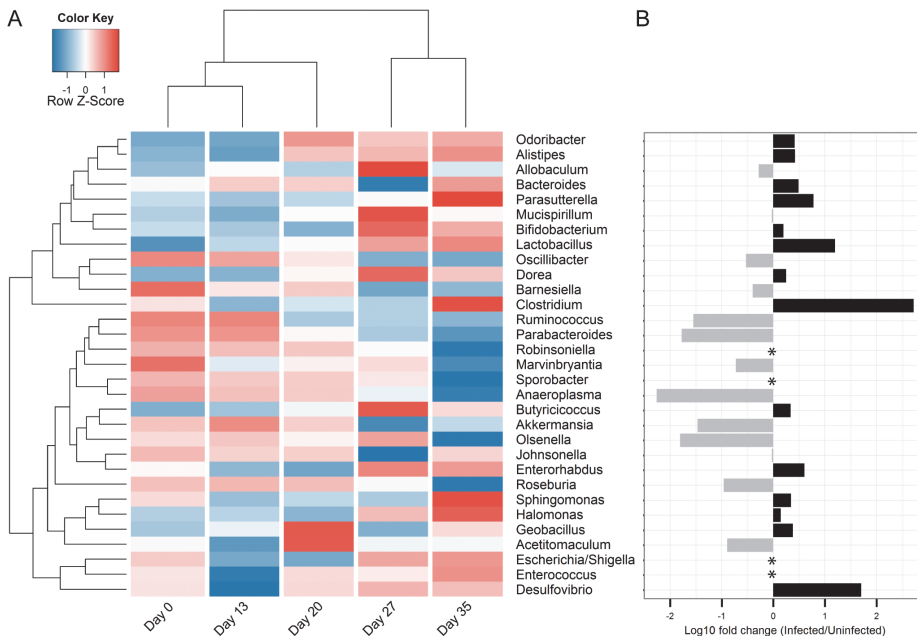


Fig 4. Chronic *T. muris* infection alters the relative abundance of multiple genera. (A) Heat-map illustrating changes over time in mean relative abundance at genus level for faecal samples from infected mice. Data are \log_{10} transformed and colour-scaled in the horizontal direction. Blue indicates low values and red indicates high values. Dendrograms are based on hierarchical cluster analysis with Bray-Curtis dissimilarity indices. (B) \log_{10} fold change between infected and uninfected faecal samples from day 35. (*) Indicates that the genus was undetected in either infected or uninfected samples. Detected only in uninfected: *Robinsoniella* (0.003%), *Sporobacter* (0.06%). Detected only in infected: *Escherichia/Shigella* (0.06%), *Enterococcus* (0.04%).

doi:10.1371/journal.pone.0125495.g004

compartment, which could indicate a potential causal link between these processes. $CD4^+$ T cells are crucial effector cells during acute *T. muris* infections. At low doses of infection both $CD4^+$ and $CD8^+$ T cells polarise into IFN- γ -secreting effector cells, resulting in the host being unable to expel the worms[53]. In order to confirm that the low infection dose resulted in induction of a Th1 response we therefore tracked and profiled the accumulation of adaptive immune cells in the large-intestinal lamina propria (LI LP) and draining mesenteric lymph nodes (MLN) following chronic *T. muris* infection. Initial experimentation indicated that there were substantial changes to the intestinal immune system at day 35 after infection, leading us to conduct an additional experiment, with analysis at key time points concurrent with the kinetics of the observed alterations in the microbiota. Moreover given the established capacity of certain bacterial species[54–56], as well as some parasites[57, 58], to promote induction of regulatory T cells (Treg), we also assessed the generation of these cells during chronic *T. muris* infection.

As expected, mice chronically infected with *T. muris* developed intestinal inflammation with an accumulation of haematopoietic cells, both in the LI LP (Fig 5A) and MLN (S10A Fig). This was apparent at day 20 and persisted throughout the course of infection. Similarly, the proportion of $CD4^+$ T cells in the LI LP was also increased at day 20 and remained stable with

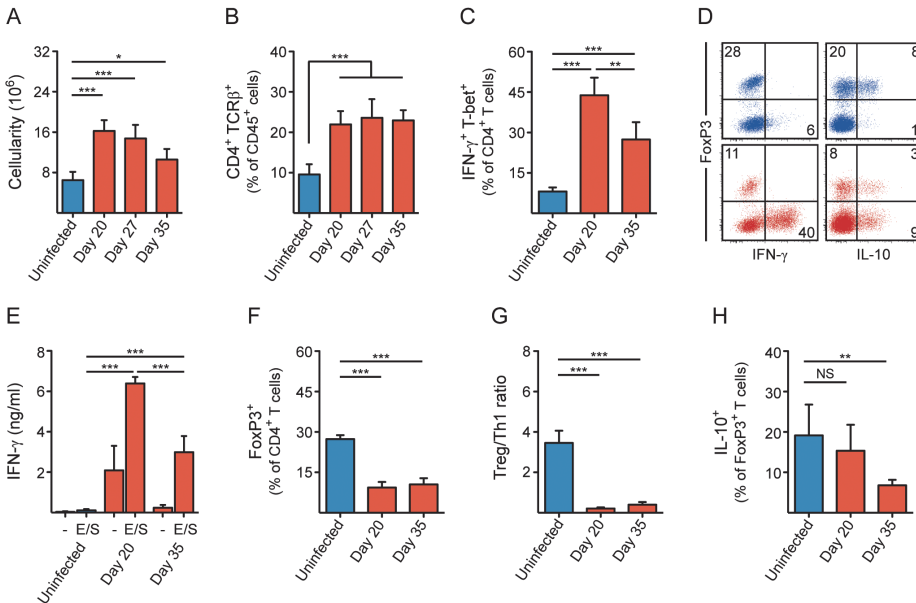


Fig 5. Chronic *T. muris* infection alters the regulatory/inflammatory T cell balance in the large intestine. (A) Haematopoietic cell numbers (cellularity) in the LI LP of *T. muris*-infected and uninfected mice. (B-C) Proportion of (B) CD4⁺ TCRβ⁺ cells, and (C) IFN-γ⁺ T-bet⁺ CD4⁺ T cells in the LI LP of *T. muris*-infected and uninfected mice. (D) Representative flow cytometry plots of FoxP3, IFN-γ and IL-10-expressing CD4⁺ T cells in the LI LP. Numbers indicate frequencies of CD4⁺ T cells. Blue = uninfected, red = *T. muris*-infected (day 20). (E) *T. muris*-derived E/S antigen-specific secretion of IFN-γ by cells isolated from the LI LP of *T. muris*-infected and uninfected mice after *ex vivo* stimulation for 48 h. (F) Proportion of FoxP3⁺ CD4⁺ T cells in the LI LP of *T. muris*-infected and uninfected mice. (G) Ratio between FoxP3⁺ and IFN-γ⁺ T-bet⁺ CD4⁺ T cells in the LI LP of *T. muris*-infected and uninfected mice. (H) Proportion of IL-10⁺ FoxP3⁺ CD4⁺ T cells in the LI LP of *T. muris*-infected and uninfected mice. Bar graphs are displayed as mean (n = 6) with standard deviation. Statistical analyses were performed with one-way ANOVA, followed by Tukey's post-test for multiple comparisons using Prism (GraphPad software). The following definitions were used to denote statistical significance: * (p<0.05), ** (p<0.01), *** (p<0.001), while p>0.05 was considered not significant (NS).

doi:10.1371/journal.pone.0125495.g005

time (Fig 5B), with a similar trend for CD8⁺ T cells (S10B Fig). In order to investigate potential driving forces from the microbiota on the nature of the adaptive immune response after infection, we focused our analysis on time points either prior to (at day 20) or after (at day 35) the major alterations observed in microbial communities, most notably the *Lactobacillaceae*. Consistent with our expectations, a large fraction of the total CD4⁺ T cells in the LI LP expressed classical markers of inflammatory Th1 cells; the cytokine IFN-γ (Fig 5C and 5D) and the transcriptional regulator T-bet (S10C Fig) after infection. The Th1 response was established early after infection (at latest day 20) but interestingly abated as *T. muris* reached adulthood (Fig 5C). CD8⁺ T cells, although fewer in numbers relative to CD4⁺ T cells, were also positive for IFN-γ and T-bet to a similar extent (S10D Fig). Consistent with the T cell response, single-cell suspensions of both LI LP (Fig 5E) and MLN (S10E Fig) from infected mice showed a dramatic IFN-γ secretion upon stimulation with *T. muris*-derived excretory/secretory (E/S) antigens. Moreover, we detected a slight induction of FoxP3⁺ Tregs in the MLN as the infection progressed (S10F Fig). However, contrary to what has been reported in other parasite models, we did not detect an increased proportion of FoxP3⁺ CD4⁺ T cells in the LI LP at this infection

dose, but rather a substantial decrease (Figs 5D and 5F), a change that was apparent already at day 20 and remained as the infection progressed (Fig 5F). Strikingly, the ratio between regulatory and inflammatory CD4⁺ T cells was reduced almost 16-fold in the LI LP as a consequence of infection (Fig 5G). Treg cells were not only fewer in proportion, but also seemed less prone to produce interleukin-10 (IL-10) at day 35 (Fig 5H and S10C Fig), a cytokine known to be involved in tolerogenic and anti-inflammatory responses. In fact, most of the T cell-derived IL-10 during infection was produced by FoxP3⁺ IFN- γ ⁺ cells (Fig 5D and S10G Fig), and was reflected by IL-10 secretion from E/S-stimulated LI LP cells (S10H Fig). Taken together, these results demonstrate that low dose infection with *T. muris* led to chronic inflammation of the large intestine, with a decreased ratio between regulatory and inflammatory CD4⁺ T cells, which was clearly manifested after 20 days of infection and remained as the infection progressed.

Discussion

We have performed a comprehensive study analysing the influence of chronic *T. muris* infection on the murine gut microbiota using 16S rRNA gene-based sequencing. By infecting mice with *T. muris*, we have been able to longitudinally study the effect of chronic nematode infection in a highly controlled manner, with sampling at multiple time points. We found that persistent worm infection led to a decrease in bacterial diversity of the large-intestinal microbiota as compared to uninfected mice, with an associated increase in the relative abundance of *Lactobacillaceae*. In parallel, we detected an overall change in the intestinal regulatory/inflammatory T cell balance following chronic *T. muris* infection.

Two recent publications describe the effect of *T. trichiura* infection on the intestinal microbiota of infected humans [38, 39]. Compared with the effects of *T. muris* infection reported here, the effect of *T. trichiura* infection in humans appeared less drastic. Cooper *et al.* found no decrease in the alpha diversity in *T. trichiura*-infected children compared to an uninfected control group, and similarly no apparent difference was detected following curative treatment [38]. In contrast, Lee *et al.* detected a minor increase in alpha diversity of the intestinal microbiota in infected individuals, which included combinations of *T. trichiura*, *Ascaris lumbricoides* and hookworm co-infections [39]. However apart from likely species-related differences, human field studies are often less controlled compared to laboratory-based studies in mice (e.g. variation in infection dose, duration and timing of infection), and many additional environmental factors will undoubtedly influence the results, e.g. lifestyle, gender, age, hygiene and/or previous pathogen exposure.

We found that chronic *T. muris* infection had a strong effect on the alpha, beta and gamma diversity of both the faecal and caecal microbiota. The decreased alpha diversity suggests that the microbiota became less diverse within each individual mouse, whereas the concurrent increase in beta diversity illustrates that each individual mouse responded differently to infection, resulting in a larger diversity between the mice. Nevertheless, overall we found the gamma diversity to be decreased, indicating that the total number of different species of bacteria existing in an infected population of mice is reduced compared to an uninfected population. Besides parasite infection, a reduced microbial diversity has been observed in patients suffering from IBD [59], indicating that this phenomenon may be a by-product of the inflammatory process itself rather than being a specific outcome of the parasite infection. On the other hand, *Toxoplasma gondii* infection was recently found to induce antigen- as well as commensal-specific T cell responses [60]; it is therefore conceivable that *T. muris* infection *per se* also results in bacteria-specific responses, which may be driving at least some of the observed changes.

It remains to be established what drives the pronounced and significant changes in the composition of the intestinal microbiota, especially those occurring from day 20 after infection. Several possibilities can be envisaged, which may involve direct as well as indirect mechanisms via the immune system. The time point for the major changes observed in microbial composition coincides with the larvae progressing from the L2 to the L3 developmental stage, a transition that is associated with the worms increasing in size and starting to protrude from the syncytial tunnels into the intestinal lumen. Thus, the physical presence of larvae in the intestinal lumen may be associated with a larger influence on the intestinal environment that may alter the intestinal microbiota. Coincidentally, the parasite may influence its microenvironment by secreting effector molecules that affect the microbiota directly or indirectly via stimulation of host immune cells. A large fraction of the E/S components secreted by the parasite during infection is made up of serine proteases that have a documented capacity to degrade the major intestinal mucin, *muc2*[61]. Given that many of the intestinal microbes actively attach to the mucous layer it is plausible that the worms, by affecting the integrity of the mucous layer in order to promote their own survival in the intestine, may indirectly also affect the capacity of mucous-adhering bacteria to remain in their intestinal niche[62]. In fact, consistent with such a mechanism, a recent study showed that immune-driven alterations to goblet cell-mediated mucous production led to reduced bacterial attachment to the mucous during *T. trichiura* infection in macaques[63]. Finally, there are indications that the parasite itself may be driving the changes to the microbiota independent of the adaptive immune response. Along these lines, Rausch *et al.* found that mice infected with the hookworm *Heligmosomoides polygyrus* responded with a Th2 response and had altered intestinal microbiota composition[10]. However following infection of IL-4R α ^{-/-} mice, which are compromised in their capacity to generate a Th2 response, they found similar changes in the gut microbiota composition, indicating that the hookworm was able to alter the microbiota independently of the IL-4-regulated adaptive Th2 response[10].

The most notable change of the microbiota following the *T. muris* infection was an increased abundance of the gram-positive, facultative anaerobic family *Lactobacillaceae*, suggesting a positive correlation between these bacteria and the nematode infection. This is in agreement with Walk *et al.*, who found the abundance of the *Lactobacillus* genus to be increased following infection with *H. polygyrus*, and speculated that the increase in lactobacilli could be an immune-modulating effect of *H. polygyrus* infection as part of a mutualistic relationship with the resident bacteria[11]. Moreover, Reynolds *et al.* identified the species *L. taiwanensis* to be increased by *H. polygyrus* infection, and showed that administration of *L. taiwanensis* to BALB/c mice facilitated subsequent infection with the nematode[64]. Furthermore, Dea-Ayuela *et al.* found that treating mice orally with either viable or dead *L. casei* enhanced the susceptibility of B10Br mice to *T. muris* infection[34], and that viable *L. casei* abrogated the IFN- γ response in MLN after infection. We found a similarly decreased IFN- γ response in both the LI LP and MLN between day 20 to 35, concurrent with an increase in relative abundance of lactobacilli, indicating a possible negative correlation between the IFN- γ response and the presence of lactobacilli. Taken together, this may indicate that the increase in lactobacilli during infection is a process that favours the survival of *T. muris*, and vice versa, lending credence to the mutualism hypothesis.

Despite prior studies having demonstrated that the microbiota can influence the development and function of the host's immune system, we detected little correlation between the kinetics of microbial changes and the development of the adaptive immune response. Treg cells play a critical role in controlling immune responses toward both pathogens and the gut microbiota[65], as well as preventing autoimmunity[66]. Furthermore, some parasitic infections are known to induce Treg cells that dampen effector responses[57, 58], in part serving as the

rationale for therapeutic worm infection as treatment for human diseases. Our data suggests that this does not seem to be the case for chronic *T. muris* infection. Rather, the infection drastically reversed the regulatory/inflammatory balance of the intestinal immune system, with the ratio of regulatory to inflammatory T cells going from $\sim 4:1$ in uninfected mice to $\sim 1:4$ following infection. These findings are surprising also given the documented ability of several *Lactobacillus* species to promote the induction or expansion of Treg cells in various tissues, under different conditions, including parasite infection [64, 67–69]. The change in the balance between regulatory/inflammatory cells was established at an early time point after infection, prior to the observed increase in *Lactobacillaceae*, and remained relatively stable over time, leading us to conclude that other mechanisms control the differentiation and development of the adaptive immune response. We cannot however rule out that the altered microbiota may influence on the immune response at later stages of the infection.

The Treg cells in our experiments appeared less prone to produce IL-10 as the infection progressed. Nonetheless, we did observe an early burst in IL-10 production by FoxP3⁺ IFN- γ ⁺ cells, possibly as a compensatory mechanism. However, this also abated with time, as did production of IFN- γ ⁺ and the inflammatory response in general. It is therefore possible that *T. muris* causes immune exhaustion at later stages of chronic infection. Together, this implies a strategy adopted by the immune system to prevent pathology rather than a direct mechanism by the worm to prevent expulsion, as expulsion cannot take place at these low doses without immune intervention, such as blockade of IFN- γ . It is important to note however that these findings only apply to low dose infections. High dose infections are cleared within 2–3 weeks in most mouse strains [70], and it is possible that Treg cell induction occurs by a different kinetic and plays a different role under these conditions.

In summary, our data demonstrate that chronic infection with the nematode *T. muris* results in an altered intestinal microbiota as well as a perturbed immune regulatory/inflammatory balance. Our results are largely consistent and complementary to those of Houlden *et al.* published simultaneously to this paper [71], highlighting the reliability of our findings. These studies are of fundamental importance and considerable relevance, especially given the high incidence of worm infections worldwide and current efforts to use parasitic nematodes to ameliorate disorders associated with perturbations in the immune system.

Supporting Information

S1 Fig. Experimental outline of chronic *T. muris* infection. Thirty mice were divided into three groups, each consisting of ten individuals. The first group of ten mice was sacrificed at day 0, and caecal and faecal samples were collected as reference. Of the remaining two groups of ten mice, one was infected (“Infected”) with approximately twenty infective *T. muris* eggs, while the other was left uninfected (“Uninfected”). Fresh faeces were sampled regularly from mice of both groups and the mice were monitored over time until day 35 after infection, when the mice were sacrificed. Caecum and colon contents were collected and analysed for microbiota composition. * These caecal samples are from ten mice sacrificed at day 0 and do therefore not represent repeated sampling as for the faecal samples. (EPS)

S2 Fig. Early grouping visualised when comparing infected with uninfected faecal samples. NMDS plots using Bray-Curtis dissimilarity indices of faecal microbiota samples from 10 chronically infected and 10 uninfected mice sampled from day 0 to day 35. Ellipses are coloured according to treatment (infected/uninfected). Relative abundance at family level are fitted as vectors-based 9999 permutations and scaled by their correlation coefficient. (EPS)

S3 Fig. Early grouping visualised when comparing faecal samples at different time points after infection. NMDS plots using Bray-Curtis dissimilarity indices of faecal microbiota samples from 10 chronically infected mice sampled from day 0 to day 35. Ellipses are labelled according to the corresponding day of analysis. Relative abundance at family level are fitted as vectors-based 9999 permutations and scaled by their correlation coefficient. (EPS)

S4 Fig. Microbiota samples at day 35 after infection illustrate similar effects of chronic *T. muris* on both the faecal and caecal microbiota. NMDS plot using Bray-Curtis dissimilarity indices of colonic and caecal microbiota samples from day 35. Mouse ID numbers are indicated with numbers inside the data points. Faecal and caecal samples are indicated with triangle and circle, respectively. Dotted line separates infected from uninfected samples. (EPS)

S5 Fig. No grouping was apparent as effect of time in the uninfected faecal samples. NMDS plot using Bray-Curtis dissimilarity indices of faecal microbiota samples from 10 uninfected mice sampled from day 0 to day 35. (EPS)

S6 Fig. Chronic *T. muris* infection results in decreased gamma diversity of the microbiota. Gamma diversity (measurement of overall diversity of pooled data) based on Shannon index of untrimmed microbiota data for faecal and caecal samples. Data were pooled group- and time point-wise. The light blue colour for caecal samples from uninfected mice indicates the ten mice sacrificed at day 0, and therefore not repeatedly sampled as for the faecal samples. No statistics were applied as the samples were pooled and thereby only provide one single value per time point and treatment. (EPS)

S7 Fig. The microbiota composition is highly affected by chronic *T. muris* infection at the phylum level. Taxa summary plots at phylum level showing (A) changes in microbiota composition of faecal samples from the infected mice from day 0 to day 35 and (B) the different microbiota composition between uninfected and infected mice at day 35 for faecal and caecal samples. "Unknown" refers to OTUs that we were unable to classify. Data represents mean relative abundance. (EPS)

S8 Fig. Phylogenetic analysis of *Lactobacillaceae* by Maximum Likelihood-method illustrates species candidates affected by chronic *T. muris* infection. The bar-plot illustrates the relative abundance of the OTUs classified within the *Lactobacillaceae* family in day 35 faecal samples from infected mice. Phylogenetic analyses were conducted using the representative sequences from the given OTUs (shown in red) and classified 16S rRNA gene sequences from the *Lactobacillaceae* family downloaded from The Ribosomal Database Project (RDP)[50]. The branch labels contain the RDP sequence identifier number, species name and information on the strain from which the sequence was obtained. The tree with the highest log likelihood (-2535,1977) is shown. The tree is drawn to scale, with branch lengths measured in the number of substitutions per site. (EPS)

S9 Fig. Distinct responses to chronic *T. muris* infection in the faecal microbiota at the family level. Taxa summary plots at family level showing changes in microbiota composition at day 35 of faecal samples from each individual (A) uninfected and (B) infected mouse. "Unknown"

refers to OTUs that we were unable to classify.
(EPS)

S10 Fig. Effects of chronic *T. muris* infection on inflammatory and regulatory T cell populations in the LI LP and MLN. (A) Haematopoietic cell numbers (cellularity) in the MLN of *T. muris*-infected and uninfected mice. (B) Proportion of CD8 α^+ TCR β^+ cells in the LI LP of *T. muris*-infected and uninfected mice. (C) Histograms of T-bet (left) and IL-10 (right) expression by IFN- γ^+ and FoxP3 $^+$ CD4 $^+$ T cells, respectively, in the LI LP of *T. muris*-infected and uninfected mice. Blue = uninfected, red = *T. muris*-infected (day 35), grey = staining control. (D) Proportion of IFN- γ^+ T-bet $^+$ CD8 α^+ T cells, in the LI LP of *T. muris*-infected and uninfected mice. (E) *T. muris*-derived E/S antigen-specific secretion of IFN- γ by cells isolated from the MLN of *T. muris*-infected and uninfected mice after *ex vivo* stimulation for 48 h. (F-G) Proportion of (F) FoxP3 $^+$ CD4 $^+$ T cells, and (G) IL-10 $^+$ IFN- γ^+ FoxP3 $^+$ CD4 $^+$ T cells in the MLN and LI LP, respectively of *T. muris*-infected and uninfected mice. (H) E/S antigen-specific secretion of IL-10 by cells isolated from the LI LP of *T. muris*-infected and uninfected mice after *ex vivo* stimulation for 48 h. Bar graphs are displayed as mean (n = 6) with standard deviation. Statistical analyses were performed with one-way ANOVA, followed by Tukey's post-test for multiple comparisons, using Prism (GraphPad software). The following definitions were used to denote statistical significance: * (p<0.05), ** (p<0.01), *** (p<0.001), while p>0.05 was considered not significant (NS).
(EPS)

S1 Table. Adonis test of significance illustrates a significant effect of chronic *T. muris* on the microbiota. Adonis test of significance performed using Bray-Curtis distance matrix. The following definitions were used to denote statistical significance: * (p \leq 0.05), ** (p \leq 0.01), *** (p \leq 0.001), while p>0.05 was considered not significant.
(DOCX)

S2 Table. Bacterial taxa that differed significantly within caecal samples after *T. muris* infection. List of significantly (adj. p-value <0.05) increased or decreased abundance of bacteria at multiple taxonomic ranks when comparing infected with uninfected samples at the given timepoints. Statistics were performed using metagenomeSeq[46]. Data are given with the prevalence for the given bacteria, absolute counts, and relative abundance.
(EPS)

S3 Table. The Representative Sequences for the OTUs classified in the *Lactobacillaceae* family and used for the Phylogenetic analysis to identify species candidates affected by chronic *T. muris* infection. The 9 OTUs named L#1 to L#9 were classified in the *Lactobacillaceae* family according to Greengenes database v11_2 [44] using the RDP-classifier [45] with an 80% confidence threshold.
(DOCX)

Acknowledgments

The technical assistance of Marianne Knudsen (University of Copenhagen) is greatly acknowledged.

Author Contributions

Conceived and designed the experiments: JBH DS PK KK MSF. Performed the experiments: JBH DS. Analyzed the data: JBH DS. Contributed reagents/materials/analysis tools: PK YRC JE TM. Wrote the paper: JBH DS PK YRC JE LM KK MSF.

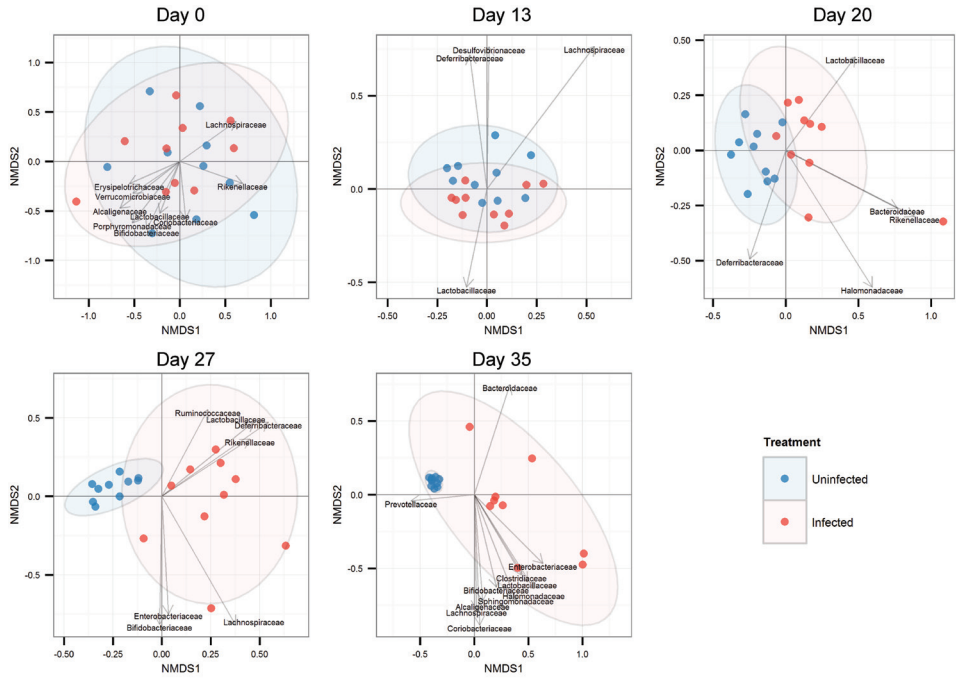
References

- Sommer F, Backhed F. The gut microbiota—masters of host development and physiology. *Nature reviews Microbiology*. 2013; 11(4):227–38. doi: [10.1038/nrmicro2974](https://doi.org/10.1038/nrmicro2974) PMID: [23435359](https://pubmed.ncbi.nlm.nih.gov/23435359/)
- Tremaroli V, Backhed F. Functional interactions between the gut microbiota and host metabolism. *Nature*. 2012; 489(7415):242–9 doi: [10.1038/nature11552](https://doi.org/10.1038/nature11552) PMID: [22972297](https://pubmed.ncbi.nlm.nih.gov/22972297/)
- Backhed F, Ding H, Wang T, Hooper LV, Koh GY, Nagy A, et al. The gut microbiota as an environmental factor that regulates fat storage. *Proceedings of the National Academy of Sciences of the United States of America*. 2004; 101(44):15718–23. PMID: [15505215](https://pubmed.ncbi.nlm.nih.gov/15505215/)
- Russell WR, Hoyles L, Flint HJ, Dumas ME. Colonic bacterial metabolites and human health. *Current opinion in microbiology*. 2013; 16(3):246–54. doi: [10.1016/j.mib.2013.07.002](https://doi.org/10.1016/j.mib.2013.07.002) PMID: [23880135](https://pubmed.ncbi.nlm.nih.gov/23880135/)
- Mazmanian SK, Liu CH, Tzianabos AO, Kasper DL. An immunomodulatory molecule of symbiotic bacteria directs maturation of the host immune system. *Cell*. 2005; 122(1):107–18. PMID: [16009137](https://pubmed.ncbi.nlm.nih.gov/16009137/)
- Hooper LV, Littman DR, Macpherson AJ. Interactions between the microbiota and the immune system. *Science*. 2012; 336(6086):1268–73. doi: [10.1126/science.1223490](https://doi.org/10.1126/science.1223490) PMID: [22674334](https://pubmed.ncbi.nlm.nih.gov/22674334/)
- Ivanov II, Atarashi K, Manel N, Brodie EL, Shima T, Karaoz U, et al. Induction of intestinal Th17 cells by segmented filamentous bacteria. *Cell*. 2009; 139(3):485–98. doi: [10.1016/j.cell.2009.09.033](https://doi.org/10.1016/j.cell.2009.09.033) PMID: [19836068](https://pubmed.ncbi.nlm.nih.gov/19836068/)
- Reeves AE, Koenigsnecht MJ, Bergin IL, Young VB. Suppression of *Clostridium difficile* in the gastrointestinal tracts of germfree mice inoculated with a murine isolate from the family Lachnospiraceae. *Infection and immunity*. 2012; 80(11):3786–94. doi: [10.1128/IAI.00647-12](https://doi.org/10.1128/IAI.00647-12) PMID: [22890996](https://pubmed.ncbi.nlm.nih.gov/22890996/)
- Kamada N, Kim YG, Sham HP, Vallance BA, Puente JL, Martens EC, et al. Regulated virulence controls the ability of a pathogen to compete with the gut microbiota. *Science*. 2012; 336(6086):1325–9. doi: [10.1126/science.1222195](https://doi.org/10.1126/science.1222195) PMID: [22582016](https://pubmed.ncbi.nlm.nih.gov/22582016/)
- Rausch S, Held J, Fischer A, Heimesaat MM, Kuhl AA, Bereswill S, et al. Small intestinal nematode infection of mice is associated with increased enterobacterial loads alongside the intestinal tract. *PLoS one*. 2013; 8(9):e74026. doi: [10.1371/journal.pone.0074026](https://doi.org/10.1371/journal.pone.0074026) PMID: [24040152](https://pubmed.ncbi.nlm.nih.gov/24040152/)
- Walk ST, Blum AM, Ewing SA, Weinstock JV, Young VB. Alteration of the murine gut microbiota during infection with the parasitic helminth *Heligmosomoides polygyrus*. *Inflammatory bowel diseases*. 2010; 16(11):1841–9. doi: [10.1002/ibd.21299](https://doi.org/10.1002/ibd.21299) PMID: [20848461](https://pubmed.ncbi.nlm.nih.gov/20848461/)
- Frank DN, St Amand AL, Feldman RA, Boedeker EC, Harpaz N, Pace NR. Molecular-phylogenetic characterization of microbial community imbalances in human inflammatory bowel diseases. *Proceedings of the National Academy of Sciences of the United States of America*. 2007; 104(34):13780–5. PMID: [17699621](https://pubmed.ncbi.nlm.nih.gov/17699621/)
- Callender JE, Grantham-McGregor S, Walker S, Cooper ES. *Trichuris* infection and mental development in children. *Lancet*. 1992; 339(8786):181. PMID: [1370339](https://pubmed.ncbi.nlm.nih.gov/1370339/)
- Nokes C, Grantham-McGregor SM, Sawyer AW, Cooper ES, Bundy DA. Parasitic helminth infection and cognitive function in school children. *Proceedings Biological sciences / The Royal Society*. 1992; 247(1319):77–81. PMID: [1349184](https://pubmed.ncbi.nlm.nih.gov/1349184/)
- Hewitson JP, Grainger JR, Maizels RM. Helminth immunoregulation: the role of parasite secreted proteins in modulating host immunity. *Molecular and biochemical parasitology*. 2009; 167(1):1–11. doi: [10.1016/j.molbiopara.2009.04.008](https://doi.org/10.1016/j.molbiopara.2009.04.008) PMID: [19406170](https://pubmed.ncbi.nlm.nih.gov/19406170/)
- Molodecky NA, Soon IS, Rabi DM, Ghali WA, Ferris M, Chernoff G, et al. Increasing incidence and prevalence of the inflammatory bowel diseases with time, based on systematic review. *Gastroenterology*. 2012; 142(1):46–54 e42; quiz e30. doi: [10.1053/j.gastro.2011.10.001](https://doi.org/10.1053/j.gastro.2011.10.001) PMID: [22001864](https://pubmed.ncbi.nlm.nih.gov/22001864/)
- Kondrashova A, Seiskari T, Ilonen J, Knip M, Hyoty H. The 'Hygiene hypothesis' and the sharp gradient in the incidence of autoimmune and allergic diseases between Russian Karelia and Finland. *APMIS: acta pathologica, microbiologica, et immunologica Scandinavica*. 2013; 121(6):478–93. doi: [10.1111/apm.12023](https://doi.org/10.1111/apm.12023) PMID: [23127244](https://pubmed.ncbi.nlm.nih.gov/23127244/)
- Kramer A, Bekeschus S, Broker BM, Schleibinger H, Razavi B, Assadian O. Maintaining health by balancing microbial exposure and prevention of infection: the hygiene hypothesis versus the hypothesis of early immune challenge. *The Journal of hospital infection*. 2013; 83 Suppl 1:S29–34. doi: [10.1016/S0195-6701\(13\)60007-9](https://doi.org/10.1016/S0195-6701(13)60007-9) PMID: [23453173](https://pubmed.ncbi.nlm.nih.gov/23453173/)
- Saunders KA, Raine T, Cooke A, Lawrence CE. Inhibition of autoimmune type 1 diabetes by gastrointestinal helminth infection. *Infection and immunity*. 2007; 75(1):397–407. PMID: [17043101](https://pubmed.ncbi.nlm.nih.gov/17043101/)
- Cooke A, Tonks P, Jones FM, O'Shea H, Hutchings P, Fulford AJ, et al. Infection with *Schistosoma mansoni* prevents insulin dependent diabetes mellitus in non-obese diabetic mice. *Parasite immunology*. 1999; 21(4):169–76. PMID: [10320614](https://pubmed.ncbi.nlm.nih.gov/10320614/)

21. McSorley HJ, O'Gorman MT, Blair N, Sutherland TE, Filbey KJ, Maizels RM. Suppression of type 2 immunity and allergic airway inflammation by secreted products of the helminth *Heligmosomoides polygyrus*. *European journal of immunology*. 2012; 42(10):2667–82. doi: [10.1002/eji.201142161](https://doi.org/10.1002/eji.201142161) PMID: [22706967](https://pubmed.ncbi.nlm.nih.gov/22706967/)
22. Ferreira I, Smyth D, Gaze S, Aziz A, Giacomin P, Ruysers N, et al. Hookworm excretory/secretory products induce interleukin-4 (IL-4)+ IL-10+ CD4+ T cell responses and suppress pathology in a mouse model of colitis. *Infection and immunity*. 2013; 81(6):2104–11. doi: [10.1128/IAI.00563-12](https://doi.org/10.1128/IAI.00563-12) PMID: [23545299](https://pubmed.ncbi.nlm.nih.gov/23545299/)
23. Elliott DE, Setiawan T, Metwali A, Blum A, Urban JF Jr., Weinstock JV. *Heligmosomoides polygyrus* inhibits established colitis in IL-10-deficient mice. *European journal of immunology*. 2004; 34(10):2690–8. PMID: [15368285](https://pubmed.ncbi.nlm.nih.gov/15368285/)
24. Smith P, Mangan NE, Walsh CM, Fallon RE, McKenzie AN, van Rooijen N, et al. Infection with a helminth parasite prevents experimental colitis via a macrophage-mediated mechanism. *J Immunol*. 2007; 178(7):4557–66. PMID: [17372014](https://pubmed.ncbi.nlm.nih.gov/17372014/)
25. Bager P, Arned J, Ronborg S, Wohlfahrt J, Poulsen LK, Westergaard T, et al. *Trichuris suis* ova therapy for allergic rhinitis: a randomized, double-blind, placebo-controlled clinical trial. *The Journal of allergy and clinical immunology*. 2010; 125(1):123–30 e1-3. doi: [10.1016/j.jaci.2009.08.006](https://doi.org/10.1016/j.jaci.2009.08.006) PMID: [19800680](https://pubmed.ncbi.nlm.nih.gov/19800680/)
26. Broadhurst MJ, Leung JM, Kashyap V, McCune JM, Mahadevan U, McKerron JH, et al. IL-22+ CD4+ T cells are associated with therapeutic *trichuris trichiura* infection in an ulcerative colitis patient. *Science translational medicine*. 2010; 2(60):60ra88. doi: [10.1126/scitranslmed.3001007](https://doi.org/10.1126/scitranslmed.3001007) PMID: [21123811](https://pubmed.ncbi.nlm.nih.gov/21123811/)
27. Fleming JO, Isaak A, Lee JE, Luzzio CC, Carrithers MD, Cook TD, et al. Probiotic helminth administration in relapsing-remitting multiple sclerosis: a phase 1 study. *Mult Scler*. 2011; 17(6):743–54. doi: [10.1177/1352458511398054](https://doi.org/10.1177/1352458511398054) PMID: [21372112](https://pubmed.ncbi.nlm.nih.gov/21372112/)
28. Summers RW, Elliott DE, Urban JF Jr., Thompson R, Weinstock JV. *Trichuris suis* therapy in Crohn's disease. *Gut*. 2005; 54(1):87–90. PMID: [15591509](https://pubmed.ncbi.nlm.nih.gov/15591509/)
29. Weinstock JV, Elliott DE. Translatability of helminth therapy in inflammatory bowel diseases. *International journal for parasitology*. 2013; 43(3–4):245–51. doi: [10.1016/j.ijpara.2013.06.010](https://doi.org/10.1016/j.ijpara.2013.06.010) PMID: [23911309](https://pubmed.ncbi.nlm.nih.gov/23911309/)
30. Cenit MC, Matzaraki V, Tigchelaar EF, Zhernakova A. Rapidly expanding knowledge on the role of the gut microbiome in health and disease. *Biochimica et biophysica acta*. 2014.
31. Pullan RL, Smith JL, Jasarasaria R, Brooker SJ. Global numbers of infection and disease burden of soil transmitted helminth infections in 2010. *Parasites & vectors*. 2014; 7:37.
32. Else KJ, Hultner L, Grecnis RK. Cellular immune responses to the murine nematode parasite *Trichuris muris*. II. Differential induction of TH-cell subsets in resistant versus susceptible mice. *Immunology*. 1992; 75(2):232–7. PMID: [1532377](https://pubmed.ncbi.nlm.nih.gov/1532377/)
33. Else KJ, Finkelman FD, Maliszewski CR, Grecnis RK. Cytokine-mediated regulation of chronic intestinal helminth infection. *The Journal of experimental medicine*. 1994; 179(1):347–51. PMID: [8270879](https://pubmed.ncbi.nlm.nih.gov/8270879/)
34. Dea-Ayuela MA, Rama-Iniguez S, Bolas-Fernandez F. Enhanced susceptibility to *Trichuris muris* infection of B10Br mice treated with the probiotic *Lactobacillus casei*. *International immunopharmacology*. 2008; 8(1):28–35. PMID: [18068097](https://pubmed.ncbi.nlm.nih.gov/18068097/)
35. Hayes KS, Bancroft AJ, Goldrick M, Portsmouth C, Roberts IS, Grecnis RK. Exploitation of the intestinal microflora by the parasitic nematode *Trichuris muris*. *Science*. 2010; 328(5984):1391–4. doi: [10.1126/science.1187703](https://doi.org/10.1126/science.1187703) PMID: [20538949](https://pubmed.ncbi.nlm.nih.gov/20538949/)
36. Li RW, Wu S, Li W, Navarro K, Couch RD, Hill D, et al. Alterations in the porcine colon microbiota induced by the gastrointestinal nematode *Trichuris suis*. *Infection and immunity*. 2012; 80(6):2150–7. doi: [10.1128/IAI.00141-12](https://doi.org/10.1128/IAI.00141-12) PMID: [22493085](https://pubmed.ncbi.nlm.nih.gov/22493085/)
37. Wu S, Li RW, Li W, Beshah E, Dawson HD, Urban JF Jr. Worm burden-dependent disruption of the porcine colon microbiota by *Trichuris suis* infection. *PLoS one*. 2012; 7(4):e35470. doi: [10.1371/journal.pone.0035470](https://doi.org/10.1371/journal.pone.0035470) PMID: [22532855](https://pubmed.ncbi.nlm.nih.gov/22532855/)
38. Cooper P, Walker AW, Reyes J, Chico M, Salter SJ, Vaca M, et al. Patent human infections with the whipworm, *Trichuris trichiura*, are not associated with alterations in the faecal microbiota. *PLoS one*. 2013; 8(10):e76573. doi: [10.1371/journal.pone.0076573](https://doi.org/10.1371/journal.pone.0076573) PMID: [24124574](https://pubmed.ncbi.nlm.nih.gov/24124574/)
39. Lee SC, Tang MS, Lim YA, Choy SH, Kurtz ZD, Cox LM, et al. Helminth colonization is associated with increased diversity of the gut microbiota. *PLoS neglected tropical diseases*. 2014; 8(5):e2880. doi: [10.1371/journal.pntd.0002880](https://doi.org/10.1371/journal.pntd.0002880) PMID: [24851867](https://pubmed.ncbi.nlm.nih.gov/24851867/)
40. Wakelin D. Acquired immunity to *Trichuris muris* in the albino laboratory mouse. *Parasitology*. 1967; 87(3):515–24. PMID: [6048569](https://pubmed.ncbi.nlm.nih.gov/6048569/)

41. Caporaso JG, Kuczynski J, Stombaugh J, Bittinger K, Bushman FD, Costello EK, et al. QIIME allows analysis of high-throughput community sequencing data. *Nature methods*. 2010; 7(5):335–6. doi: [10.1038/nmeth.f.303](https://doi.org/10.1038/nmeth.f.303) PMID: [20383131](https://pubmed.ncbi.nlm.nih.gov/20383131/)
42. Kozich JJ, Westcott SL, Baxter NT, Highlander SK, Schloss PD. Development of a dual-index sequencing strategy and curation pipeline for analyzing amplicon sequence data on the MiSeq Illumina sequencing platform. *Applied and environmental microbiology*. 2013; 79(17):5112–20. doi: [10.1128/AEM.01043-13](https://doi.org/10.1128/AEM.01043-13) PMID: [23793624](https://pubmed.ncbi.nlm.nih.gov/23793624/)
43. Edgar RC. Search and clustering orders of magnitude faster than BLAST. *Bioinformatics*. 2010; 26(19):2460–1. doi: [10.1093/bioinformatics/btq461](https://doi.org/10.1093/bioinformatics/btq461) PMID: [20709691](https://pubmed.ncbi.nlm.nih.gov/20709691/)
44. DeSantis TZ, Hugenholtz P, Larsen N, Rojas M, Brodie EL, Keller K, et al. Greengenes, a chimera-checked 16S rRNA gene database and workbench compatible with ARB. *Applied and environmental microbiology*. 2006; 72(7):5069–72. PMID: [16820507](https://pubmed.ncbi.nlm.nih.gov/16820507/)
45. Wang Q, Garrity GM, Tiedje JM, Cole JR. Naive Bayesian classifier for rapid assignment of rRNA sequences into the new bacterial taxonomy. *Applied and environmental microbiology*. 2007; 73(16):5261–7. PMID: [17586664](https://pubmed.ncbi.nlm.nih.gov/17586664/)
46. Paulson JN, Stine OC, Bravo HC, Pop M. Differential abundance analysis for microbial marker-gene surveys. *Nature methods*. 2013; 10(12):1200–2. doi: [10.1038/nmeth.2658](https://doi.org/10.1038/nmeth.2658) PMID: [24076764](https://pubmed.ncbi.nlm.nih.gov/24076764/)
47. McMurdie PJ, Holmes S. phyloseq: an R package for reproducible interactive analysis and graphics of microbiome census data. *PLoS one*. 2013; 8(4):e61217. doi: [10.1371/journal.pone.0061217](https://doi.org/10.1371/journal.pone.0061217) PMID: [23630581](https://pubmed.ncbi.nlm.nih.gov/23630581/)
48. Oksanen J BF, Kindt R, Legendre P, O'Hara RB. *Vegan: Community Ecology Package*. R package version 1.17–10. 2011.
49. Wickham H. *Ggplot2: elegant graphics for data analysis*. New York: Springer; 2009. viii, 212 p. p.
50. Cole JR, Wang Q, Fish JA, Chai B, McGarrell DM, Sun Y, et al. Ribosomal Database Project: data and tools for high throughput rRNA analysis. *Nucleic acids research*. 2014; 42(Database issue):D633–42. doi: [10.1093/nar/gkt1244](https://doi.org/10.1093/nar/gkt1244) PMID: [24288368](https://pubmed.ncbi.nlm.nih.gov/24288368/)
51. Edgar RC. MUSCLE: multiple sequence alignment with high accuracy and high throughput. *Nucleic acids research*. 2004; 32(5):1792–7. PMID: [15034147](https://pubmed.ncbi.nlm.nih.gov/15034147/)
52. Tamura K, Nei M. Estimation of the number of nucleotide substitutions in the control region of mitochondrial DNA in humans and chimpanzees. *Molecular biology and evolution*. 1993; 10(3):512–26. PMID: [8336541](https://pubmed.ncbi.nlm.nih.gov/8336541/)
53. Humphreys NE, Worthington JJ, Little MC, Rice EJ, Grensis RK. The role of CD8+ cells in the establishment and maintenance of a *Trichuris muris* infection. *Parasite immunology*. 2004; 26(4):187–96. PMID: [15367296](https://pubmed.ncbi.nlm.nih.gov/15367296/)
54. Atarashi K, Tanoue T, Shima T, Imaoka A, Kuwahara T, Momose Y, et al. Induction of colonic regulatory T cells by indigenous Clostridium species. *Science*. 2011; 331(6015):337–41. doi: [10.1126/science.1198469](https://doi.org/10.1126/science.1198469) PMID: [21205640](https://pubmed.ncbi.nlm.nih.gov/21205640/)
55. Atarashi K, Tanoue T, Oshima K, Suda W, Nagano Y, Nishikawa H, et al. Treg induction by a rationally selected mixture of Clostridia strains from the human microbiota. *Nature*. 2013; 500(7461):232–6. doi: [10.1038/nature12331](https://doi.org/10.1038/nature12331) PMID: [23842501](https://pubmed.ncbi.nlm.nih.gov/23842501/)
56. Geuking MB, Cahenzli J, Lawson MA, Ng DC, Slack E, Hapfelmeier S, et al. Intestinal bacterial colonization induces mutualistic regulatory T cell responses. *Immunity*. 2011; 34(5):794–806. doi: [10.1016/j.immuni.2011.03.021](https://doi.org/10.1016/j.immuni.2011.03.021) PMID: [21596591](https://pubmed.ncbi.nlm.nih.gov/21596591/)
57. Grainger JR, Smith KA, Hewitson JP, McSorley HJ, Harcus Y, Filbey KJ, et al. Helminth secretions induce de novo T cell Foxp3 expression and regulatory function through the TGF-beta pathway. *The Journal of experimental medicine*. 2010; 207(11):2331–41. doi: [10.1084/jem.20101074](https://doi.org/10.1084/jem.20101074) PMID: [20876311](https://pubmed.ncbi.nlm.nih.gov/20876311/)
58. McSorley HJ, Harcus YM, Murray J, Taylor MD, Maizels RM. Expansion of Foxp3+ regulatory T cells in mice infected with the filarial parasite *Brugia malayi*. *J Immunol*. 2008; 181(9):6456–66. PMID: [18941236](https://pubmed.ncbi.nlm.nih.gov/18941236/)
59. Kostic AD, Xavier RJ, Gevers D. The microbiome in inflammatory bowel disease: current status and the future ahead. *Gastroenterology*. 2014; 146(6):1489–99. doi: [10.1053/j.gastro.2014.02.009](https://doi.org/10.1053/j.gastro.2014.02.009) PMID: [24560869](https://pubmed.ncbi.nlm.nih.gov/24560869/)
60. Hand TW, Dos Santos LM, Bouladoux N, Molloy MJ, Pagan AJ, Pepper M, et al. Acute gastrointestinal infection induces long-lived microbiota-specific T cell responses. *Science*. 2012; 337(6101):1553–6. PMID: [22923434](https://pubmed.ncbi.nlm.nih.gov/22923434/)
61. Hasnain SZ, McGuckin MA, Grensis RK, Thornton DJ. Serine protease(s) secreted by the nematode *Trichuris muris* degrade the mucus barrier. *PLoS neglected tropical diseases*. 2012; 6(10):e1856. doi: [10.1371/journal.pntd.0001856](https://doi.org/10.1371/journal.pntd.0001856) PMID: [23071854](https://pubmed.ncbi.nlm.nih.gov/23071854/)

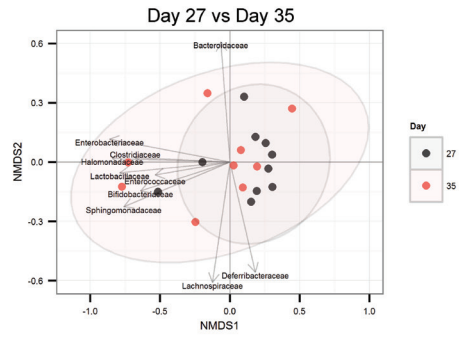
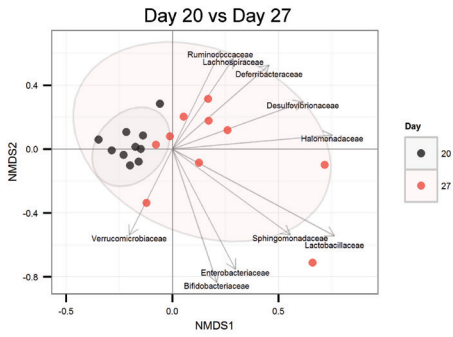
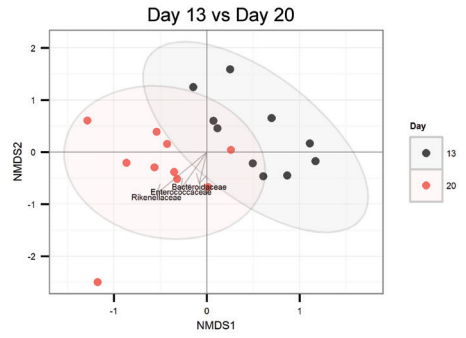
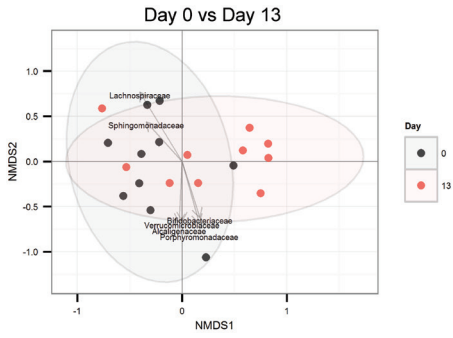
62. Van den Abbeele P, Van de Wiele T, Verstraete W, Possemiers S. The host selects mucosal and luminal associations of coevolved gut microorganisms: a novel concept. *FEMS microbiology reviews*. 2011; 35(4):681–704. doi: [10.1111/j.1574-6976.2011.00270.x](https://doi.org/10.1111/j.1574-6976.2011.00270.x) PMID: [21361997](https://pubmed.ncbi.nlm.nih.gov/21361997/)
63. Broadhurst MJ, Ardeshtir A, Kanwar B, Mirpuri J, Gundra UM, Leung JM, et al. Therapeutic helminth infection of macaques with idiopathic chronic diarrhea alters the inflammatory signature and mucosal microbiota of the colon. *PLoS pathogens*. 2012; 8(11):e1003000. doi: [10.1371/journal.ppat.1003000](https://doi.org/10.1371/journal.ppat.1003000) PMID: [23166490](https://pubmed.ncbi.nlm.nih.gov/23166490/)
64. Reynolds L, Smith K, Filbey K, Harcus Y, Hewitson J, Redpath S, et al. Commensal-pathogen interactions in the intestinal tract: Lactobacilli promote infection with, and are promoted by, helminth parasites. *Gut microbes*. 2014; 5(4). doi: [10.4161/gmic.32130](https://doi.org/10.4161/gmic.32130) PMID: [25244596](https://pubmed.ncbi.nlm.nih.gov/25244596/)
65. Bollrath J, Powrie FM. Controlling the frontier: regulatory T-cells and intestinal homeostasis. *Seminars in immunology*. 2013; 25(5):352–7. doi: [10.1016/j.smim.2013.09.002](https://doi.org/10.1016/j.smim.2013.09.002) PMID: [24184013](https://pubmed.ncbi.nlm.nih.gov/24184013/)
66. Rubtsov YP, Rasmussen JP, Chi EY, Fontenot J, Castelli L, Ye X, et al. Regulatory T cell-derived interleukin-10 limits inflammation at environmental interfaces. *Immunity*. 2008; 28(4):546–58. doi: [10.1016/j.immuni.2008.02.017](https://doi.org/10.1016/j.immuni.2008.02.017) PMID: [18387831](https://pubmed.ncbi.nlm.nih.gov/18387831/)
67. Karimi K, Inman MD, Bienenstock J, Forsythe P. Lactobacillus reuteri-induced regulatory T cells protect against an allergic airway response in mice. *American journal of respiratory and critical care medicine*. 2009; 179(3):186–93. doi: [10.1164/rccm.200806-951OC](https://doi.org/10.1164/rccm.200806-951OC) PMID: [19029003](https://pubmed.ncbi.nlm.nih.gov/19029003/)
68. Kim HJ, Kim YJ, Kang MJ, Seo JH, Kim HY, Jeong SK, et al. A novel mouse model of atopic dermatitis with epicutaneous allergen sensitization and the effect of Lactobacillus rhamnosus. *Experimental dermatology*. 2012; 21(9):672–5. doi: [10.1111/j.1600-0625.2012.01539.x](https://doi.org/10.1111/j.1600-0625.2012.01539.x) PMID: [22742655](https://pubmed.ncbi.nlm.nih.gov/22742655/)
69. Jang SO, Kim HJ, Kim YJ, Kang MJ, Kwon JW, Seo JH, et al. Asthma Prevention by Lactobacillus Rhamnosus in a Mouse Model is Associated With CD4(+)CD25(+)Foxp3(+) T Cells. *Allergy, asthma & immunology research*. 2012; 4(3):150–6.
70. Cliffe LJ, Grenicis RK. The *Trichuris muris* system: a paradigm of resistance and susceptibility to intestinal nematode infection. *Advances in parasitology*. 2004; 57:255–307. PMID: [15504540](https://pubmed.ncbi.nlm.nih.gov/15504540/)
71. Houlden A, Hayes KS, Bancroft AJ, Worthington JJ, Wang P, Grenicis RK, et al. Chronic *Trichuris muris* infection in C57BL/6 mice causes significant changes in host microbiota and metabolome: effects reversed by pathogen clearance. *PLoS ONE*.



S2 Fig.

S2 Table

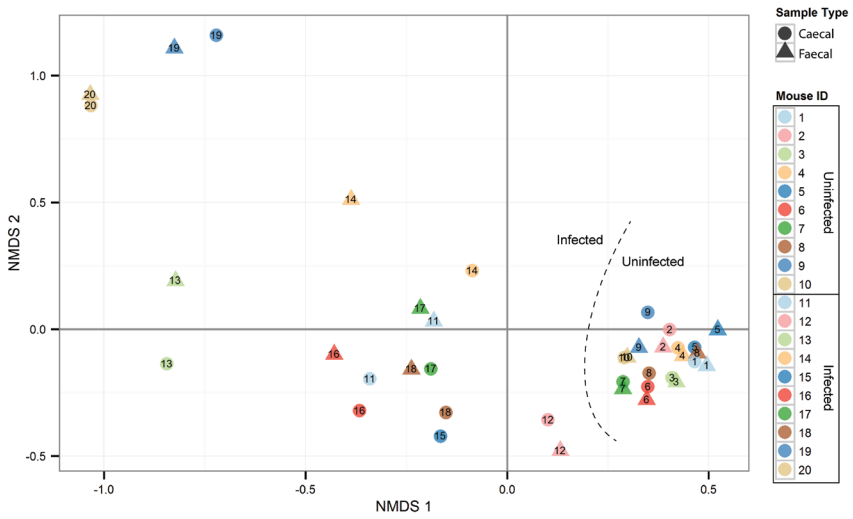
Days after infection	Phylum	Class	Order	Family	Genus	Prevalence		Counts		Abundance (%)		adj. P-value		
						Uninfected	Infected	Uninfected	Infected	Uninfected	Infected		SEM	SEM
35 days	Firmicutes	Bacilli ↑	Lactobacillales ↑	Lactobacillaceae	Lactobacillus ↑	10/10	10/10	3825	17986	1.94	0.33	8.38	2.88	1.7E-02
						10/10	10/10	3825	17933	1.93	0.33	8.35	2.88	1.4E-02
						10/10	10/10	3768	17522	1.92	0.33	8.14	2.83	7.5E-03
						10/10	10/10	12346	6528	6.36	1.79	3.80	3.45	3.8E-03
						10/10	10/10	12346	6528	6.36	1.79	3.80	3.45	8.7E-03
						10/10	10/10	12346	6528	6.36	1.79	3.80	3.45	2.9E-02
						10/10	10/10	12226	6509	6.29	1.78	3.80	3.45	2.3E-03
						10/10	6/10	100	10	0.05	0.01	0.01	0.00	3.7E-04
						10/10	9/10	2756	1151	1.48	0.23	0.58	0.40	1.5E-03
						10/10	8/10	465	5548	0.24	0.05	2.68	0.96	2.2E-02
						10/10	10/10	291	109	0.15	0.02	0.05	0.01	1.4E-02
						10/10	10/10	291	109	0.15	0.02	0.05	0.01	2.2E-02



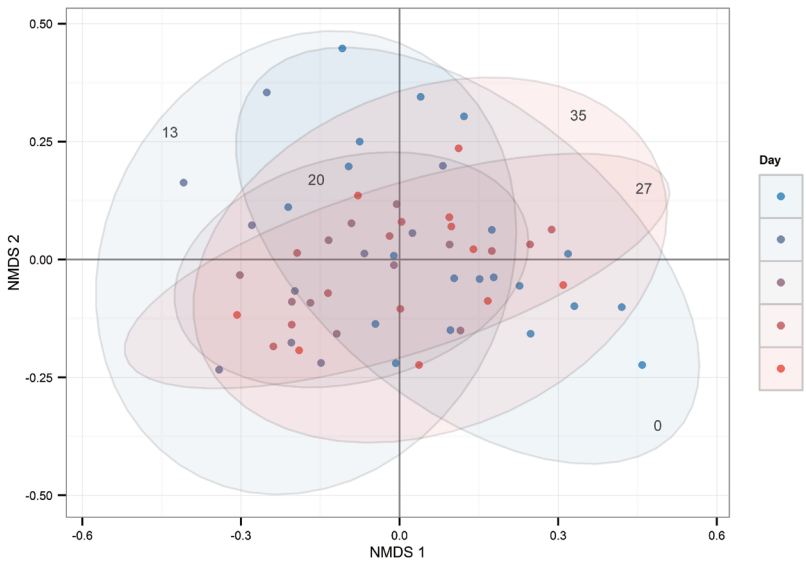
S3 Fig.

S3 Table

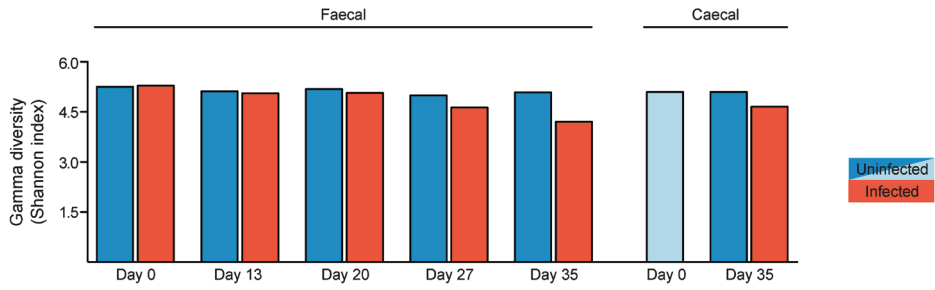
ID	Sequence
L#1	tacGTAGGTGGCAAGCGTTATCCGGATTTATTGGCCGTAAAGGGAAACGCAGCGCGTCTTTAAAGTCTGATGTGAAAGCCTTCCGCTTAACCCGGAGTAGTGCAATGGAACTGGAGACTTGAGTGCAGAAAGAGAGAGTGAACCTCCATGTGTAGCCGGTGAATGCGTAGATATATGGAAAGAACACCAGTGGCGAAAGCGGCTCTCTGGTCTGTAAC TGACGCTGAGGTTTCGAAAGCGTGGGTAGCAACcagg
L#2	tacGTAGGTGGCAAGCGTTATCCGGATTTATTGGCCGTAAAGGGAAACGCAGCGCGTCTTTAAAGTCTGATGTGAAAGCCTTCCGCTCAACCCGGAGAAATGCATCAGAAACTGTTGAACTTGAGTGCAGAAAGAGAGAGTGAACCTCCATGTGTAGCCGGTGAATGCGTAGATATATGGAAAGAACACCAGTGGCGAAAGCGGCTCTCTGGTCTGTAAC TGACGCTGAGGTTTCGAAAGCGTGGGTAGCAACcagg
L#3	tacGTAGGTGGCAAGCGTTATCCGGATTTATTGGCCGTAAAGGGAAACGCAGCGCGTCTTTAAAGTCTGATGTGAAAGCCTTCCGCTTAACCCGGAGTAGTGCAATGGAACTGGAGACTTGAGTGCAGAAAGAGAGAGTGAACCTCCATGTGTAGCCGGTGAATGCGTAGATATATAGGAGGAACACCAGTGGCGAAAGCGGCTCTCTGGTCTGCAACTGACGCTGAGGCTCGAAAGCATGGGTAGCGAAcagg
L#4	tacGGAGGATCGGAGCGTTATCCGGATTTATTGGCCGTAAAGGGAAACGCAGCGCGTCTTTAAAGTCTGATGTGAAAGCCTTCCGCTTAACCCGGAGTAGTGCAATGGAACTGGAGACTTGAGTGCAGAAAGAGAGAGTGAACCTCCATGTGTAGCCGGTGAATGCGTAGATATATGGAAAGAACACCAGTGGCGAAAGCGGCTCTCTGGTCTGCAACTGACGCTGAGGCTCGAAAGCATGGGTAGCGAAcagg
L#5	tacggggatgagcggttccggatttattggcgtaagggcagcggcggttgcTTAGGCTGATGTGAAAGCCTTCCGGCTTAACCCGAAGAGTGCATCGAAACCGGCAACTTGAGTGCAGAAAGAGAGAGTGAACCTCCATGTGTAGCCGGTGAATGCGTAGATATATGGAAAGAACACCAGTGGCGAAAGCGGCTCTCTGGTCTGCAACTGACGCTGAGGCTCGAAAGCATGGGTATCGAAcagg
L#6	tacGTAGGTGGCAAGCGTTATCCGGATTTATTGGCCGTAAAGCGAGCGCGCGGTTGCTTAGGCTGATGTGAAAGCCTTCCGGCTTAACCCGGAAAGTGCATCGGAAACCGGCGACTTGAGTGCAGAAAGAGAGAGTGAACCTCCATGTGTAGCCGGTGAATGCGTAGATATATGGAAAGAACACCAGTGGCGAAAGCGGCTGTCTGGTCTGCAACTGACGCTGAGGCTCGAAAGCATGGGTAGCGAAcagg
L#7	tacGTAGGTGGCAAGCGTTGTCGGGATTTATTGGCCGTAAAGCGAGTGCAGCGGTTCAATAAGTCTGATGTGAAAGCCTTCCGCTTAACCCGGAGTAGTGCAATGGAACTGGAGACTTGAGTGCAGAAAGAGAGAGTGAACCTCCATGTGTAGCCGGTGAATGCGTAGATATATGGAAAGAACACCAGTGGCGAAAGCGGCTCTCTGGTCTGCAACTGACGCTGAGGCTCGAAAGCATGGGtagcagaagg
L#8	tacGTAGGTGGCAAGCGTTGTCGGGATTTATTGGCCGTAAAGCGAGTGCAGCGGTTCAATAAGTCTGATGTGAAAGCCTTCCGCTCAACCCGGAGAAATGCATCAGAAACTGTTGAACTTGAGTGCAGAAAGAGAGAGTGAACCTCCATGTGTAGCCGGTGAATGCGTAGATATATGGAAAGAACACCAGTGGCGAAAGCGGCTCTCTGGTCTGCAACTGACGCTGAGGCTCGAAAGCATGGGtagcagaagg
L#9	tacGTAGGTGGCAAGCGTTGTCGGGATTTATTGGCCGTAAAGCGAGCGCGGCGGAAAGATAAGTCTGATGTGAAAGCCCTCCGCTTAACCCGAGGAATTCATCGAAACTGTGTTTCTTGAGTGCAGAAAGAGAGAGTGAACCTCCATGTGTAGCCGGTGAATGCGTAGATATATGAAAGAACACCAGTGGCGAAAGCGGCTCTCTGGTCTGTAAC TGACGCTGAGGCTCGAAAGCATGGGTAGCGAAcagg



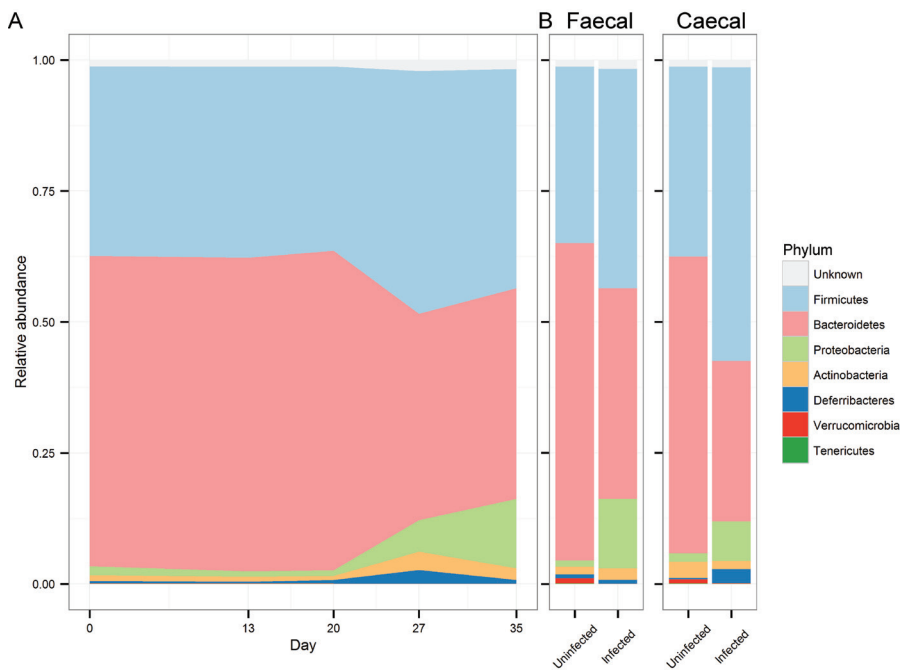
S4 Fig.



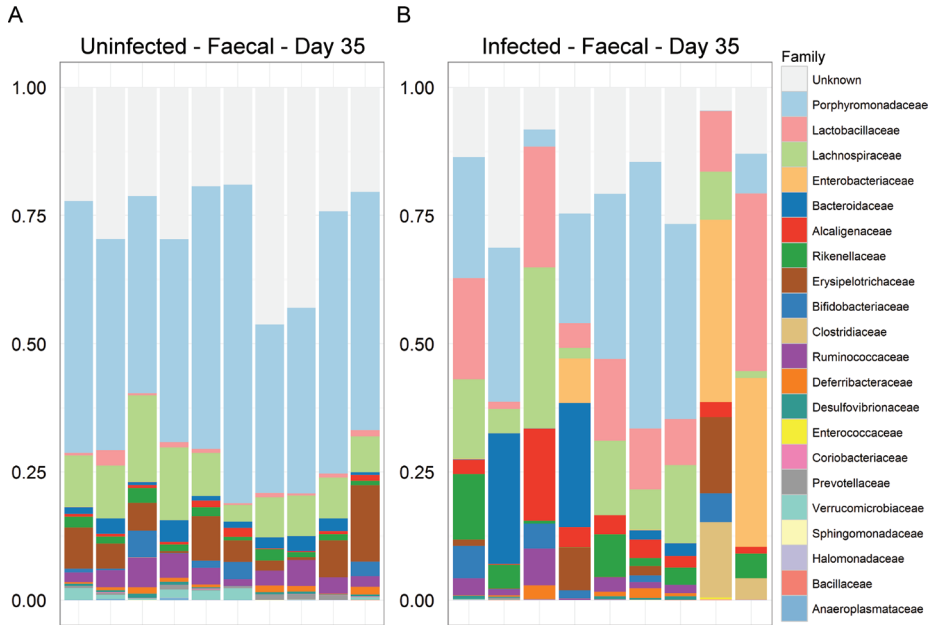
S5 Fig.



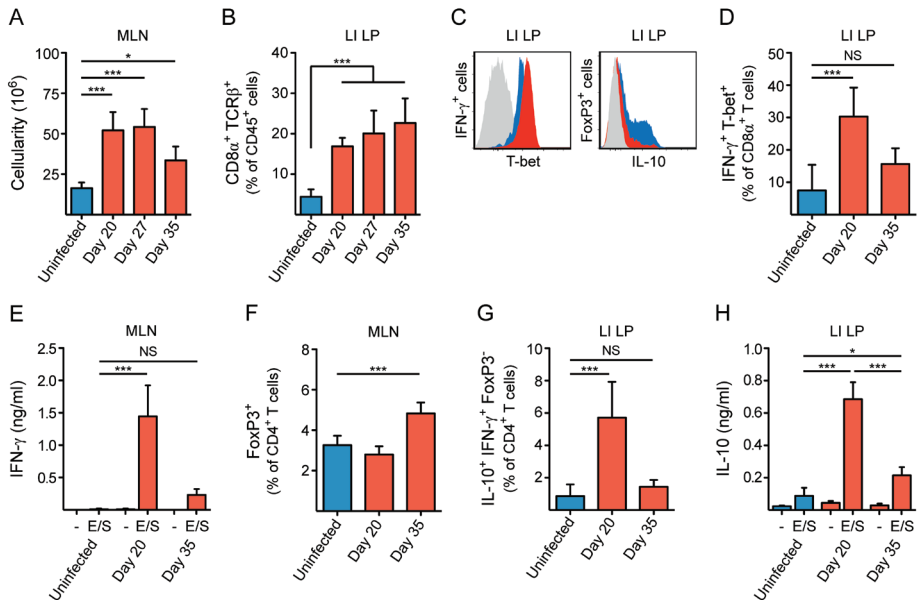
S6 Fig.



S7 Fig.



S9 Fig.



S10 Fig.

Paper 3

Secreted antigens from the parasite *Trichuris muris* facilitate inflammasome activation by modulating Toll-like receptor signaling

Authors

Daniel Sorobetea, Dóra Hancz, Henrietta Henningsson, Christine Valfridsson, Marcus Svensson-Frej and Jenny J Persson

Affiliation

Section for Immunology, Department of Experimental Medical Sciences, Faculty of Medicine, Lund University, Lund, Sweden

Keywords

Nlrp3 inflammasome, E/S antigens, *T. muris*, macrophage, caspase-8

Corresponding author

Jenny J. Persson

Immunology Section

BMC D14

SE-221 84 Lund

Sweden

Telephone: +46 46 222 04 27

E-mail: jenny_j.persson@med.lu.se

Abbreviations

IL = Interleukin

TLR = Toll-like receptor

MyD88 = Myeloid differentiation primary response gene 88

TRIF = TIR-domain-containing adapter-inducing interferon- β

Nlrp = NACHT, LRR and PYD domains-containing protein

Nlrc = NLR family CARD domain-containing protein

Naip = Baculoviral IAP repeat-containing protein

ATP = Adenosine triphosphate

E/S = Excretory/Secretory antigens

Caspase = Cystein-aspartic protease

TNF = Tumor necrosis factor

LPS = Lipopolysaccharide

Rip = Receptor-interacting protein

Abstract

Inflammasome activation is a key feature of innate immunity with important consequences on health and disease. Pathogens, including helminthic parasites, have evolved strategies to manipulate host immunity, often at the innate level. However, the impact of intestinal helminths on inflammasome function is largely unexplored. In this study, we demonstrate that secreted antigens from the large-intestinal nematode *Trichuris muris* reprogram murine innate immune cells, allowing subsequent Nlrp3 inflammasome activation and release of IL-1 β downstream of Toll-like receptor ligation. This activation proceeded with slower kinetics than canonical Nlrp3 activation, did not induce pyroptosis and relied on caspase-8 activity. Our findings thus suggest that these secreted antigens may have significant impact on the inflammatory potential in tissues after helminth infection, conceivably with important consequences for both host and parasite.

Introduction

Upon pathogen encounter the host must be able to rapidly initiate an acute inflammatory response. Much of this vital task falls onto cells of the innate immune system such as neutrophils, dendritic cells and macrophages. An integral component of this process is the formation of large cytosolic protein complexes known as inflammasomes, which are important for the activation of the highly potent inflammatory cytokines IL-1 β and IL-18, as well as propagating inflammation through a process of cell death called pyroptosis [1]. Several inflammasomes have been identified to date, characterized by the pattern-recognition receptors that govern their activation, with the Nlrp3 inflammasome being the most extensively studied. In contrast to other inflammasomes, which can be activated by a relatively limited spectrum of antigens, the Nlrp3 inflammasome is activated by a wide variety of molecules of both endogenous and microbial origin [2]. In macrophages, the unifying feature of these stimuli is the requirement for a two-step activation mechanism, wherein the first signal consists of priming by a ligand capable of triggering the transcription factor NF- κ B, such as LPS, which ultimately leads to expression of the inactive pro-form of IL-1 β , in addition to components of the inflammasome itself in conjunction with essential post-translational modifications. Signal two, the inflammasome activating trigger, can be provided by pathogen-derived as well as endogenous molecules that are usually not found in the extracellular space, such as ATP, indicative of cell and tissue damage [2]. Inflammasomes have been intensely studied in the context of bacterial infections, but little is known with regards to whether multicellular parasites and their secreted products are capable of inducing inflammasome activation, and its downstream consequences.

Trichuris muris is a mouse-specific large-intestinal nematode, closely related to the human pathogen *Trichuris trichiura*, which is estimated to infect approximately 500 million people [3]. *T. muris* infection is mediated by ingestion of eggs, and once hatched in the cecum, larvae penetrate the mucus barrier and burrow into the epithelial layer, forming tunnels through epithelial cells. *Trichuris* worms are thought to achieve this feat at least in part by producing a complex mixture of molecules termed excretory/secretory (E/S) antigens, which aid in degrading mucins [4] and extracellular matrix proteins [5], as well as weakening epithelial membrane integrity [6,7]. Immunity is presumed to result from recognition of E/S antigens by innate antigen-presenting cells and the subsequent priming of appropriate adaptive responses, although the mechanisms are poorly understood. Mice lacking the pattern-recognition receptor TLR4 or its adaptor protein MyD88 will clear an otherwise chronic infection [8], suggesting that signaling via TLR4 in the host might be critical for the worms to maintain their niche. More recently it was shown that expression of the intracellular receptor NOD2 in epithelial cells is required for efficient worm expulsion and thus host resistance [9], highlighting the importance also of intracellular recognition pathways in mediating protective immune responses against this pathogen. The position of inflammasomes in

such processes remains enigmatic, and little is known about the mechanisms and consequences of inflammasome activation during *T. muris* infection. In addition, the role of IL-1 β and IL-18 in these infections is complex. While IL-1 β -deficient mice are unable to expel *T. muris* due to an impaired capability of generating type 2 immunity [10], IL-18-deficient mice cannot induce type 1 immunity and are therefore resistant [11], suggesting a context-dependent role for these often inflammasome-dependent cytokines.

We set out to study the molecular pathways involved in the recognition of *T. muris*-derived antigens and found that E/S antigens modulated macrophages in a TLR4-dependent manner to respond to subsequent TLR-stimulation with Nlrp3-inflammasome activation, which normally does not occur. This TLR-induced inflammasome assembly was slower than conventional activation, devoid of pyroptosis and dependent on caspase-8 activity. Our findings indicate that parasite-derived antigens can alter downstream responses to microbial triggers with potentially important consequences on health and disease.

Results

T. muris-derived E/S antigens prime for canonical inflammasome activation

Macrophages make up a major portion of the antigen-presenting cells in the intestinal tract and are known to activate the inflammasome upon certain stimuli. While studies in other infection models have demonstrated that some extracellular intestinal parasites can activate the canonical Nlrp3 inflammasome in macrophages and dendritic cells via release of parasite-derived antigens [12-14], it remains to be established whether antigens released by *T. muris* could have similar effects. To address this question, we utilized the well-established in vitro system of bone marrow-derived macrophages.

Stimulation of bone marrow-derived macrophages with E/S antigens resulted in a distinct pattern of cytokine secretion, characterized by secretion of TNF and IL-6 but not IL-10, thus partially resembling LPS-induced activation (Figure 1A). While *T. muris* is a known inducer of both type 1 and type 2 immunity *in vivo*, E/S-stimulated macrophages did not secrete any detectable IFN- γ , IL-4, IL-5, IL-9 or IL-13 (data not shown). As expected, neither E/S nor LPS stimulation alone was sufficient to drive IL- β secretion (Figure 1A). Like LPS, E/S antigens were able to prime macrophages for caspase-1-dependent inflammasome activation, as judged by the release of IL-1 β upon subsequent ATP stimulation (Figure 1B). Release of lactate dehydrogenase (LDH) into the culture medium indicated that there was substantial cell death accompanied with ATP stimulation of both E/S and LPS-primed cells (Figure 1C). Interestingly, IL-1 β release after E/S and ATP stimulation was abolished in TLR4 and Myd88-deficient mice (Figure 1D), and moderately reduced in cells lacking the adapter protein TRIF (Figure 1E).

E/S antigens released by *T. muris* contain multiple proteins. Notably, while LPS was resistant to heat inactivation, E/S-mediated priming was blocked by overnight treatment at 50°C (Figure 1F). This indicates that the priming effect of E/S is mediated by a heat-labile component, most likely a protein. Importantly, these data also exclude the possibility that a potential endotoxin contamination in the E/S antigen preparation is responsible for the priming effect observed with E/S. Taken together, these results demonstrate that E/S, similar to LPS, can mediate priming for inflammasome activation and suggest that this priming proceed via a TLR4- and MyD88-dependent, and potentially partially TRIF-dependent pathway.

E/S antigens license macrophages for LPS-mediated inflammasome activation

Epithelial cells and innate immune cells in the intestinal mucosa are continuously exposed to microbial antigens from the microbiota. We therefore assessed whether E/S-stimulation would alter the downstream response of macrophages to microbial triggers, such as LPS. Indeed, while LPS by itself normally does not activate the inflammasome in murine macrophages, E/S-stimulated macrophages exposed to LPS induced robust dose-dependent IL- β secretion (Figure 2A). The E/S-mediated

activation did not result in any detectable IL-18 secretion (data not shown). By contrast, no other combination of E/S or LPS-mediated priming and/or activation led to any substantial IL-1 β secretion (Figure 2B). As observed for E/S-mediated priming for inflammasome activation (Figure 1F), this effect was also abrogated by heat inactivation of the E/S (Figure 2C).

While ATP-induced inflammasome activation was associated with massive cell death in E/S-stimulated cells (Figure 1C), LPS-induced inflammasome activation did not affect cell viability (data not shown). LPS-induced inflammasome activation after E/S-mediated licensing was ablated in caspase-1/11-, Asc- and Nlrp3-deficient macrophages, while no reduction was observed in cells devoid of Nlr4 and Naip5, implicating the Nlrp3 inflammasome (Figure 2D). One of the major components of *T. muris* E/S is a 43 kDa protein with a known capacity to affect membrane integrity, potentially by formation of membrane pores [6]. Because cytosolic LPS has been shown to induce the activation of a caspase-11-dependent non-canonical inflammasome [15-17], and the macrophages used herein to establish caspase-dependency in inflammasome activation lack both caspase-1 and caspase-11 (Figure 2D), we examined whether E/S-licensed inflammasome activation by LPS was dependent on caspase-11. However, since E/S-stimulated caspase-11-deficient macrophages were equally capable of secreting IL-1 β upon LPS-induced inflammasome activation (Figure 2E), we conclude that the observed inflammasome activation is dependent on caspase-1 but not caspase-11.

Finally, potassium efflux and production of mitochondrial reactive-oxygen species (mROS) along with other mitochondrial components have been linked to activation of Nlrp3 and may in part explain how such a vast array of different stimuli can converge onto Nlrp3 activation [18-23]. We therefore examined the role for these pathways in E/S-licensed inflammasome activation by LPS and found that similar to canonical Nlrp3 activation, LPS-induced Nlrp3 activation in E/S-stimulated cells was dependent on both potassium efflux and mROS activity (Figure 2F), as determined by the addition of high extracellular concentrations of potassium chloride and the mROS blocker MitoTEMPO, respectively. Thus, our data suggest that E/S antigens can modulate bone marrow-derived macrophages to respond to subsequent LPS stimulation with inflammasome-dependent IL-1 β release. Notably, although this inflammasome activation is induced by an unconventional stimulus, it involves many features of canonical Nlrp3 inflammasome activation.

TLR-dependence of unconventional inflammasome activation

Because both E/S and LPS signal through TLR4, the potential dependency on this receptor in the E/S priming versus the LPS activating steps can not be separated by analysis of TLR4-deficient cells only. Thus we next addressed whether signals via other TLRs could elicit a similar Nlrp3 activation. This was indeed the case as the synthetic TLR7/8 ligand R848 and the TLR1/2 ligand Pam3CSK4 also induced

inflammasome activation in E/S-treated cells, in a similar manner to LPS (Figure 3A). By contrast, poly(I:C), which signals through TLR3, did not induce inflammasome activation in E/S-stimulated cells (Figure 3A), despite a robust type I-interferon response (Figure 3B). To confirm that the inflammasome activation observed in E/S-treated cells stimulated with different TLR ligands was indeed dependent on each respective TLR, we stimulated TLR2-, TLR4- and TLR7-deficient macrophages with E/S, followed by either Pam3CSK4, LPS or R848 to address the contribution of the different receptors. As E/S antigens primarily signal through TLR4 (Figure 1D) and E/S-induced licensing thus can be predicted to not occur in absence of this receptor, all other ligands were unable to induce IL-1 β release in TLR4-deficient cells (Figure 3C). Importantly, neither of the TLR ligands were able to induce substantial inflammasome activation in their respective receptor-deficient cells, demonstrating that cognate TLR signaling through several TLRs can drive the activation step in E/S stimulated cells (Figure 3C). TLR signaling is mainly propagated through the adaptor protein Myd88, but can occur also via TRIF in the case of TLR3 and endosomal TLR4. We therefore assessed whether TLR-induced inflammasome activation depended on these pathways and found that Myd88-deficient cells were incapable of activating any TLR-induced inflammasome (Figure 3D), probably due to deficiency in both the priming (Figure 1D) and activating steps. However, TRIF-deficient cells did not secrete IL-1 β upon LPS-induced activation (Figure 3E), despite being only partially required for ATP-induced inflammasome activation upon E/S priming (Figure 1E), suggesting a prominent role for TRIF-mediated signaling in the LPS-induced inflammasome activating step. TRIF-deficient macrophages also displayed strongly reduced (but not absent) IL-1 β secretion upon Pam3CSK4 and R848-induced inflammasome activation, possibly due to the partial contribution of TRIF in the priming phase (Figure 1D) although a role for TRIF also in the inflammasome activation step downstream of TLR2 and TLR7 can not be excluded. In conclusion, E/S antigens can modify the signaling networks in macrophages thus allowing inflammasome activation upon subsequent ligation of several MyD88 dependent TLRs.

TLR-mediated inflammasome activation in E/S-licensed cells is caspase-8-dependent

Since TLRs are receptors driving transcriptional responses, it was plausible that transcription (and translation) were required for TLR-induced inflammasome assembly. We first examined the kinetics with which IL-1 β was being released upon TLR-induced inflammasome activation. As compared to ATP-induced activation, which is substantial already after 30 minutes (Figure 1B), TLR-induced activation only resulted in detectable IL-1 β after four hours of LPS stimulation (Figure 4A), consistent with the possibility of new transcription and translation being induced upon TLR ligation. However, whereas addition of the translation inhibitor cycloheximide during E/S stimulation efficiently prevented successive TLR-induced inflammasome activation, addition during the activation step failed to inhibit IL-1 β

release (Figure 4B), suggesting that TLR-induced activation of the inflammasome after E/S stimulation is independent of translational responses.

Inflammasome activation proceeding with slow kinetics has been described under certain settings [24], especially in the context of caspase-8-mediated activation [25]. We therefore assessed whether caspase-8 was involved in the TLR-mediated inflammasome activation and found that chemical inhibition of caspase-8 activity prevented IL-1 β release (Figure 4C). Furthermore, Rip3 kinase and caspase-8 double-deficient mice (caspase-8 single-deficient mice are embryonically lethal) had substantially reduced IL-1 β release (Figure 4D), implicating caspase-8 in E/S-mediated inflammasome-activation. Importantly, Rip3 kinase deficient macrophages responded to E/S and LPS stimulation similarly to wild-type cells (Figure 4D). Furthermore, as Rip1 kinase activity has been linked to caspase-8-mediated inflammasome assembly [26], we also assessed a potential contribution of Rip1 kinases. Indeed, Rip1 kinase inhibition reduced the amount of IL-1 β released following E/S-stimulation and LPS-activation (Figure 4E), implicating Rip1 kinases in the pathway of TLR-mediated inflammasome activation.

In summary, TLR-induced inflammasome activation subsequent to E/S stimulation of macrophages is independent of transcriptional and translational responses but dependent on caspase-8 and Rip1 kinase activity.

Discussion

In this study, we have demonstrated that *T. muris*-derived E/S antigens modulate the signaling networks in murine macrophages, thus allowing Nlrp3 inflammasome activation upon successive TLR ligation. The E/S-licensed TLR-induced inflammasome activation has properties similar to classical Nlrp3 inflammasome activation, such as dependency on the presence of caspase-1, Asc and Nlrp3, an important role for potassium efflux and mROS production, as well as the requirement for two consecutive signals prior to activation. However, it also differs from classical inflammasome activation in key respects: first of all, it did not result in IL-18 secretion or pyroptosis. Furthermore, it proceeded with slower kinetics and was dependent on caspase-8 activity and, to a certain extent, Rip1-kinase activity. These features of inflammasome activation have been described before (albeit in separate studies) in some cell types in response to certain activating stimuli [24,25,27-29]. More importantly, this study is also the first to show that E/S (and potentially other TLR4 ligands) can reprogram bone marrow-derived macrophages to allow for inflammasome activation in response to common TLR ligands signaling through MyD88. With regard to inflammasome biology, TLR ligands have hitherto been considered to provide only the first priming step in murine cells, but our data suggest that they can facilitate inflammasome activation when applied as the second activating signal in specific settings. A similar phenotype has been observed in human monocytes, where LPS was shown to mediate inflammasome activation in a single step [29]. Since the reprogramming ability of E/S relies on TLR4 engagement, we hypothesize that other TLR4 ligands, including damage-associated molecules, could have similar properties, in effect decreasing the threshold for inflammasome activation and IL-1 β secretion in response to invading pathogens following tissue damage and the release of numerous damage-associated molecules.

While most *Trichuris* research has focused on the murine system, one study evaluated the effect of the related porcine-specific whipworm and found that *Trichuris suis*-derived E/S antigens (in conjunction with LPS) dampened LPS-induced IL-1 β release from human macrophages in a TLR4-dependent manner, and was associated with down-regulation of inflammasome-related genes, including the P2X7 receptor [30]. As mentioned above, human monocytes can activate the Nlrp3 inflammasome in only one step [29], and so the discrepancies between these data and ours are most likely due to experimental setup and species used. Furthermore, our data relied on antigens derived from the natural murine-specific parasite and so are not affected by inter-species disparities.

The potential contribution of E/S-mediated inflammasome activation *in vivo* is currently unclear. While other studies have concentrated on the products of inflammasome activation (IL-1 β and IL-18), neither have addressed whether the inflammasome activation is E/S-driven, nor what cell types are involved. The context of antigen dose has also been ignored. High-dose *T. muris* infections

naturally increase the availability of E/S antigens, and cause more tissue damage as compared to low-dose infections, and so may be associated with different patterns of inflammasome activation. Furthermore, colonic macrophages are in a tolerized state due to the presence of the microbiota and downstream IL-10 signaling [31,32]. The Nlrp3 inflammasome, in particular, is actively suppressed at the mRNA level via ubiquitination resulting in the macrophages being less responsive to Nlrp3 stimuli, including LPS [33]. Nonetheless, our data would suggest that E/S stimulation could alter the subsequent response to LPS and allow an unconventional form of Nlrp3 inflammasome activation, thus possibly breaking the tolerance. Whether Nlrp3-deficient mice are susceptible to *T. muris* infection remains to be established. However, this question is somewhat complicated by the finding that Nlrp3 acts as an intrinsic modulator of Th2 cells [34], likely compromising adaptive immunity as well as innate inflammasome activation.

In conclusion, while TLR signaling is traditionally regarded as driving transcriptional responses, and thus prime murine macrophages for inflammasome activation, we have shown that TLR-Myd88 signaling can also induce inflammasome activation upon E/S stimulation, profoundly altering our basic understanding of the flexibility of the signaling networks in innate immune cells.

Materials and methods

Mice

C57BL/6 mice were purchased from ENVIGO (An Venray, Netherlands). Caspase-1/11^{-/-} [35], caspase-11^{-/-} [15], Nlrp3^{-/-} [36], Asc^{-/-} [37], Nlr4^{-/-} [37], Naip5^{-/-} [38] on C57BL/6 background were kindly provided by Professor Russell E Vance (University of California, Berkeley, California, U.S.A.), Bengt Johansson-Lindbom (Lund University) and Genentech Inc., and were bred and maintained in the BMC barrier facility at Lund University. Egil Lien (University of Massachusetts Medical School, Massachusetts, U.S.A.) kindly provided bones from Rip3^{-/-} [39] and Rip3/caspase-8^{-/-} [40] mice. TLR2^{-/-} mice were obtained from the MTG facility (Karolinska Institute, Stockholm, Sweden). TRIF^{-/-}, TRIF^{+/+} control mice (on mixed background), TLR7^{-/-} and Myd88^{-/-} were bred in the MIG facility at Lund University. Experiments were conducted in strict accordance with animal welfare laws, as determined by Swedish authorities (Swedish Board of Agriculture, Act 1988:534). The protocol was approved by Malmö/Lund Ethical Board for Animal Research, Lund/Malmö, Sweden (permit: M14-16), and all efforts were made to minimize animal suffering.

Bone marrow-derived macrophages

Femurs were excised in a sterile fashion and bone marrow was flushed out with a syringe containing culture medium consisting of RPMI 1640 (Thermo Fisher Scientific) supplemented with 10% fetal bovine serum (Thermo Fisher Scientific), 10% L929 cell-conditioned medium, 2 mM L-glutamine (Thermo Fisher Scientific) and 100 U/ml penicillin + 100 µg/ml streptomycin (Thermo Fisher Scientific). Bone fragments and larger debris were removed by centrifugation at 50 x g for one minute. Next, cells were pelleted by centrifugation at 200 x g for 10 minutes, suspended in 30 ml culture medium, plated in 15 cm Petri dishes (three plates/femur) and subsequently incubated for seven days at 37°C, 5% CO₂, with an additional 10 ml culture medium being added after four days. On the seventh day, the culture medium was removed and 10 ml cold PBS was added to loosen the cells. Cells were detached with a cell scraper and centrifuged for 7 min at 200 x g. Cells were enumerated in Bürker chambers by Trypan blue exclusion and suspended in freezing buffer consisting of 95% fetal bovine serum and 5% dimethyl sulfoxide, frozen in aliquots of 5 x 10⁶ cells per cryovial at -80°C overnight then transferred to -150°C.

In vitro assays and cytokine analyses

Macrophages were thawed, briefly washed, suspended in culture medium, seeded at 10⁶ cells/ml (75 x 10³ cells per well) in uncoated Microtest 96F plates (Sarstedt) and left to adhere. Cells were primed with 25 µg/ml E/S antigens for four hours and given fresh medium for subsequent stimulations with either LPS (1 µg/ml; Sigma-Aldrich), R848 (1 µg/ml; Roche), Pam3CKS4 (1 µg/ml; Invivogen), poly(I:C) (5 µg/ml; Invivogen) or ATP (5 µM; Sigma-Aldrich) with the following reagents and inhibitors: cycloheximide (20 µg/ml; Sigma-Aldrich), Z-IETD-FMK (12.5 µM; BD Biosciences), necrostatin-1 (75 µM; Sigma-Aldrich), mitoTEMPO (5 mM Thermo-Fisher Scientific)

or KCl (50 mM; Sigma-Aldrich). Cell-free supernatants were frozen at -20°C . IL-1 β , IL-6 and TNF were measured with cytometric bead array (BD Biosciences) according to manufacturer's instructions with the following modification: the amount of capture beads, detection reagent and sample sizes were scaled down five-fold. Samples were acquired on a BD Accuri C6 flow cytometer (BD Biosciences) and data analyzed with FCAP Array v3.0 (SoftFlow Inc.). Type I interferons were measured using the VeriKine ELISA kit (PBL Assay Science) according to manufacturer's instructions.

Cytotoxicity assays

Cell death was assessed by indirect measurement of lactate dehydrogenase release into the culture medium using CytoTox 96 assay (Promega) according to manufacturer's instructions. Untreated cells were used to determine background levels and lysed cells were used as a reference for maximal cytotoxicity.

Trichuris muris

T. muris (strain E) was maintained [41] as previously described. To generate E/S antigens, mice of a susceptible strain were infected with approximately 150 *T. muris* eggs, and killed 6 weeks later. Large intestines were excised, opened longitudinally, and rinsed thrice with sterile Dulbecco's phosphate-buffered saline (DPBS; Thermo-Fisher Scientific) supplemented with 500 U/mL penicillin + 500 $\mu\text{g}/\text{mL}$ streptomycin. Adult worms were pulled out with forceps, placed in sterile RPMI 1640 supplemented with antibiotics as described above and incubated at 37°C for 20 minutes, followed by a 24-hour incubation in fresh medium. The medium was collected the following day and centrifuged at $500 \times g$ for 10 minutes to pellet the eggs. E/S antigens were concentrated in a series of centrifugation steps (10–30 minutes) in centriprep-centrifugal columns with 10 000 NMWL (Merck-Millipore) at $2000 \times g$, and dialyzed to DPBS in a series of centrifugation steps in Amicon Ultracel-3K Centrifugal Filters with 3000 NMWL (Merck-Millipore) at $14\,000 \times g$. The resulting protein concentration was measured at 280 nm on a SPECTROstar Nano plate reader (BMG Labtech). The antigens were frozen at -80°C .

Statistics

Statistical analyses were performed with Prism v5.0 (GraphPad software). Data were analyzed using unpaired t-test (two groups), one-way ANOVA followed by Dunnett's post-test (three or more groups with one categorical variable) or two-way ANOVA followed by Bonferroni's post-test (three or more groups with two categorical variables) and are displayed as mean of three biological replicates plus standard deviation. † (below assay detection limit), *** ($p < 0.001$), ** ($p < 0.01$), * ($p < 0.05$).

Acknowledgements

We would like to acknowledge Lisbeth Hansen for aiding us with the type I interferon ELISA, and Bengt Johansson Lindbom for supplying us with poly(I:C).

References

1. Martinon F, Mayor A, Tschopp J. The inflammasomes: guardians of the body. *Annu. Rev. Immunol.* 2009; 27:229–265. DOI: 10.1146/annurev.immunol.021908.132715.
2. Elliott EI, Sutterwala FS. Initiation and perpetuation of NLRP3 inflammasome activation and assembly. *Immunol. Rev.* 2015; 265:35–52. DOI: 10.1111/imr.12286.
3. Pullan RL, Smith JL, Jasrasaria R, Brooker SJ. Global numbers of infection and disease burden of soil transmitted helminth infections in 2010. *Parasit. Vectors.* 2014; 7:37. DOI: 10.1186/1756-3305-7-37.
4. Hasnain SZ, McGuckin MA, Grecnis RK, Thornton DJ. Serine Protease(s) Secreted by the Nematode *Trichuris muris* Degrade the Mucus Barrier. *PLoS Negl. Trop. Dis.* 2012; 6:e1856. DOI: 10.1371/journal.pntd.0001856.
5. Drake L, Bianco A, Bundy D, Ashall F. Characterization of peptidases of adult *Trichuris muris*. *Parasitology.* 1994; 109:623–630. DOI: 10.1017/S0031182000076502.
6. Drake L, Korchev Y, Bashford L, Djamgoz M, Wakelin D, Ashall F, Bundy D. The major secreted product of the whipworm *Trichuris*, is a pore-forming protein. *Proc. R. Soc. London B.* 1994; 257:255–261. DOI: 10.1086/303379.
7. Hiemstra IH, Klaver EJ, Vrijland K, Kringel H, Andreasen A, Bouma G, Kraal G, et al. Excreted/secreted *Trichuris suis* products reduce barrier function and suppress inflammatory cytokine production of intestinal epithelial cells. *Mol. Immunol.* 2014; 60:1–7. DOI: 10.1016/j.molimm.2014.03.003.
8. Helmbly H, Grecnis RK. Essential role for TLR4 and MyD88 in the development of chronic intestinal nematode infection. *Eur. J. Immunol.* 2003; 33:2974–2979. DOI: 10.1002/eji.200324264.
9. Bowcutt R, Bramhall M, Logunova L, Wilson J, Booth C, Carding SR, Grecnis R, et al. A role for the pattern recognition receptor Nod2 in promoting recruitment of CD103(+) dendritic cells to the colon in response to *Trichuris muris* infection. *Mucosal Immunol.* 2014; 7:1–12. DOI: 10.1038/mi.2013.125.
10. Helmbly H, Grecnis RK. Interleukin-1 plays a major role in the development of Th2-mediated immunity. *Eur. J. Immunol.* 2004; 34:3674–3681. DOI: 10.1002/eji.200425452.
11. Helmbly H, Takeda K, Akira S, Grecnis RK. Interleukin (IL)-18 promotes the development of chronic gastrointestinal helminth infection by downregulating IL-13. *J. Exp. Med.* 2001; 194:355–64. DOI: 10.1084/jem.194.3.355.
12. Ritter M, Gross O, Kays S, Ruland J, Nimmerjahn F, Saijo S, Tschopp J, et al. *Schistosoma mansoni* triggers Dectin-2, which activates the Nlrp3 inflammasome and alters adaptive immune responses. *Proc. Natl. Acad. Sci. U. S. A.* 2010; 107:20459–64. DOI: 10.1073/pnas.1010337107.
13. Zaiss MM, Maslowski KM, Mosconi I, Guenat N, Marsland BJ, Harris NL. IL-1 β Suppresses Innate IL-25 and IL-33 Production and Maintains Helminth Chronicity. *PLoS Pathog.* 2013; 9. DOI: 10.1371/journal.ppat.1003531.
14. Ferguson BJ, Newland SA, Gibbs SE, Touloumou P, Fernandes dos Santos P,

- Patel MN, Hall SW, et al. The *Schistosoma mansoni* T2 ribonuclease omega-1 modulates inflammasome-dependent IL-1 β secretion in macrophages. *Int. J. Parasitol.* 2015; 45:809–813. DOI: 10.1016/j.ijpara.2015.08.005.
15. Kayagaki N, Warming S, Lamkanfi M, Walle L Vande, Louie S, Dong J, Newton K, et al. Non-canonical inflammasome activation targets caspase-11. *Nature.* 2011; 479:117–121. DOI: 10.1038/nature10558.
 16. Hagar JA, Powell DA, Aachoui Y, Ernst RK, Miao EA. Cytoplasmic LPS Activates Caspase-11: Implications in TLR4-Independent Endotoxic Shock. *Science.* 2013; 341:1250–1253. DOI: 10.1126/science.1240988.
 17. Shi J, Zhao Y, Wang Y, Gao W, Ding J, Li P, Hu L, et al. Inflammatory caspases are innate immune receptors for intracellular LPS. *Nature.* 2014; 514:187–192. DOI: 10.1038/nature13683.
 18. Pétrilli V, Papin S, Dostert C, Mayor A, Martinon F, Tschopp J. Activation of the NALP3 inflammasome is triggered by low intracellular potassium concentration. *Cell Death Differentiation.* 2007; 14:1583–1589. DOI: 10.1038/sj.cdd.4402195.
 19. Zhou R, Yazdi A, Menu P, Tschopp J. A role for mitochondria in NLRP3 inflammasome activation. *Nature.* 2011; 469:221–225. DOI: 10.1038/nature09663.
 20. Nakahira K, Haspel JA, Rathinam VAK, Lee S-J, Dolinay T, Lam HC, Englert JA, et al. Autophagy proteins regulate innate immune responses by inhibiting the release of mitochondrial DNA mediated by the NALP3 inflammasome. *Nat. Immunol.* 2011; 12:222–30. DOI: 10.1038/ni.1980.
 21. Shimada K, Crother TR, Karlin J, Dagvadorj J, Chiba N, Chen S, Ramanujan VK, et al. Oxidized Mitochondrial DNA Activates the NLRP3 Inflammasome during Apoptosis. *Immunity.* 2012; 36:401–414. DOI: 10.1016/j.immuni.2012.01.009.
 22. Katsnelson MA, Rucker LG, Russo HM, Dubyak GR. K⁺ Efflux Agonists Induce NLRP3 Inflammasome Activation Independently of Ca²⁺ Signaling. *J. Immunol.* 2015; 194:3937–3952. DOI: 10.4049/jimmunol.1402658.
 23. Zhong Z, Umemura A, Diaz-meco MT, Moscat J, Karin M, Zhong Z, Umemura A, et al. NF- κ B Restricts Inflammasome Activation via Elimination of Damaged Mitochondria Article NF- κ B Restricts Inflammasome Activation via Elimination of Damaged Mitochondria. *Cell.* 2016; 164:896–910. DOI: 10.1016/j.cell.2015.12.057.
 24. Duong BH, Onizawa M, Malynn BA, Ma A, Duong BH, Onizawa M, Oses-prieto JA, et al. A20 Restricts Ubiquitination of Pro-Interleukin-1 β Protein Complexes and Suppresses NLRP3 Inflammasome Activity Article A20 Restricts Ubiquitination of Pro-Interleukin-1 β Protein Complexes and Suppresses NLRP3 Inflammasome Activity. *Immunity.* 2015; 42:55–67. DOI: 10.1016/j.immuni.2014.12.031.
 25. Antonopoulos C, Russo HM, El Sanadi C, Martin BN, Li X, Kaiser WJ, Mocarski ES, et al. Caspase-8 as an effector and regulator of NLRP3 inflammasome signaling. *J. Biol. Chem.* 2015; 290:20167–20184. DOI: 10.1074/jbc.M115.652321.
 26. Wang X, Jiang W, Yan Y, Gong T, Han J, Tian Z, Zhou R. RNA viruses promote activation of the NLRP3 inflammasome through a RIP1-RIP3-DRP1 signaling pathway. *Nat. Immunol.* 2014; 15:1126–1133. DOI: 10.1038/ni.3015.

27. Weng D, Marty-Roix R, Ganesan S, Proulx MK, Vladimer GI, Kaiser WJ, Mocarski ES, et al. Caspase-8 and RIP kinases regulate bacteria-induced innate immune responses and cell death. *Proc. Natl. Acad. Sci.* 2014; 111:7391–7396. DOI: 10.1073/pnas.1403477111.
28. Kang S, Fernandes-Alnemri T, Rogers C, Mayes L, Wang Y, Dillon C, Roback L, et al. Caspase-8 scaffolding function and MLKL regulate NLRP3 inflammasome activation downstream of TLR3. *Nat. Commun.* 2015; 6:7515. DOI: 10.1038/ncomms8515.
29. Gaidt MM, Ebert TS, Chauhan D, Schmidt T, Schmid-Burgk JL, Rapino F, Robertson AAB, et al. Human Monocytes Engage an Alternative Inflammasome Pathway. *Immunity.* 2016; 44:833–846. DOI: 10.1016/j.immuni.2016.01.012.
30. Ottow MK, Klaver EJ, van der Pouw Kraan TCTM, Heijnen PD, Laan LC, Kringel H, Vogel DYS, et al. The helminth *Trichuris suis* suppresses TLR4-induced inflammatory responses in human macrophages. *Genes Immun.* 2014; 15:477–86. DOI: 10.1038/gene.2014.38.
31. Shouval DS, Biswas A, Goettel JA, McCann K, Conaway E, Redhu NS, Mascanfroni ID, et al. Interleukin-10 receptor signaling in innate immune cells regulates mucosal immune tolerance and anti-inflammatory macrophage function. *Immunity.* 2014; 40:706–719. DOI: 10.1016/j.immuni.2014.03.011.
32. Zigmond E, Bernshtein B, Friedlander G, Walker CR, Yona S, Kim KW, Brenner O, et al. Macrophage-restricted interleukin-10 receptor deficiency, but not IL-10 deficiency, causes severe spontaneous colitis. *Immunity.* 2014; 40:720–733. DOI: 10.1016/j.immuni.2014.03.012.
33. Filardy AA, He J, Bennink J, Yewdell J, Kelsall BL. Posttranscriptional control of NLRP3 inflammasome activation in colonic macrophages. *Mucosal Immunol.* 2016; 9:850–8. DOI: 10.1038/mi.2015.109.
34. Bruchard M, Rebé C, Derangère V, Togbé D, Ryffel B, Boidot R, Humblin E, et al. The receptor NLRP3 is a transcriptional regulator of TH2 differentiation. *Nat. Immunol.* 2015; 16:859–870. DOI: 10.1038/ni.3202.
35. Li P, Allen H, Banerjee S, Franklin S, Herzog L, Johnston C, McDowell J, et al. Mice deficient in IL-1 β -converting enzyme are defective in production of mature IL-1 β and resistant to endotoxic shock. *Cell.* 1995; 80:401–411. DOI: 10.1016/0092-8674(95)90490-5.
36. Mariathasan S, Weiss DS, Newton K, McBride J, O'Rourke K, Roose-Girma M, Lee WP, et al. Cryopyrin activates the inflammasome in response to toxins and ATP. *Nature.* 2006; 440:228–232. DOI: 10.1038/nature04515.
37. Mariathasan S, Newton K, Monack DM, Vucic D, French DM, Lee WP, Roose-Girma M, et al. Differential activation of the inflammasome by caspase-1 adaptors ASC and Ipaf. *Nature.* 2004; 430:213–218. DOI: 10.1038/nature02664.
38. Lightfield KL, Persson J, Brubaker SW, Witte CE, von Moltke J, Dunipace EA, Henry T, et al. Critical function for Naip5 in inflammasome activation by a conserved carboxy-terminal domain of flagellin. *Nat. Immunol.* 2008; 9:1171–

1178. DOI: ni.1646 [pii]\r10.1038/ni.1646.

39. Newton K, Sun X, Dixit VM. Kinase RIP3 is dispensable for normal NF-kappa Bs, signaling by the B-cell and T-cell receptors, tumor necrosis factor receptor 1, and Toll-like receptors 2 and 4. *Mol. Cell. Biol.* 2004; 24:1464–1469. DOI: 10.1128/MCB.24.4.1464.
40. Kaiser WJ, Upton JW, Long AB, Livingston-Rosanoff D, Daley-Bauer LP, Hakem R, Caspary T, et al. RIP3 mediates the embryonic lethality of caspase-8-deficient mice. *Nature.* 2011; 471:368–372. DOI: 10.1038/nature09857.
41. Wakelin, D., Acquired immunity to *Trichuris muris* in the albino laboratory mouse. *Parasitology.* 1967; 57: 515–524.

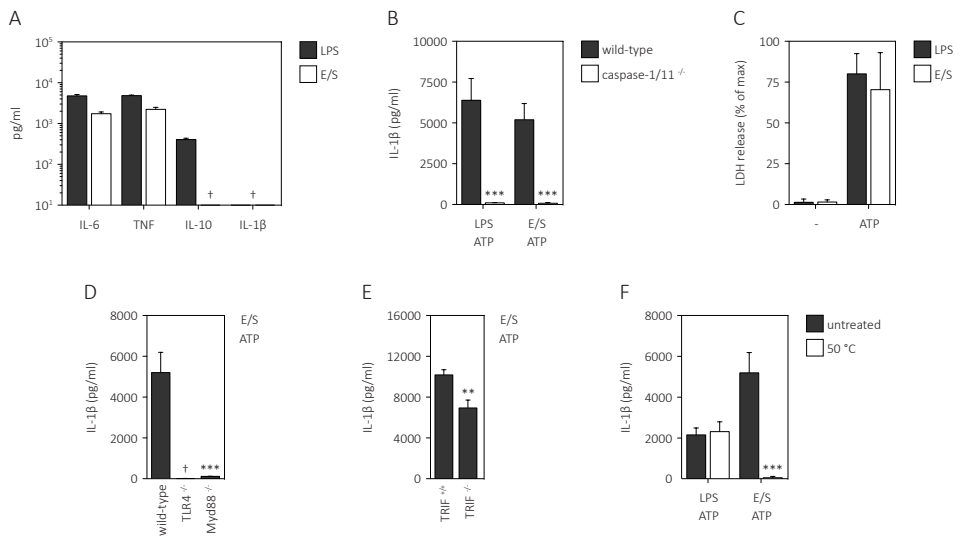


Figure 1. *T. muris*-derived E/S antigens mediate ATP-induced inflammasome activation

(A) Cytokine secretion by wild-type bone marrow-derived macrophages upon stimulation with either LPS (1 μ g/ml) or *T. muris*-derived E/S antigens (25 μ g/ml). (B) IL-1 β secretion by wild-type and caspase-1/11-deficient macrophages upon ATP-induced inflammasome activation after LPS or E/S stimulation. (C) Assessment of cell death by measurement of lactate dehydrogenase (LDH) release upon ATP-induced inflammasome activation after LPS or E/S stimulation. (D-E) IL-1 β secretion by wild-type and gene-deficient macrophages upon ATP-induced inflammasome activation after E/S stimulation. (F) IL-1 β secretion by wild-type macrophages upon ATP-induced inflammasome activation after stimulation with heat-treated (50°C for 8-12 hours) and untreated LPS or E/S. Graphs are representative of at least three independent experiments. Statistical analyses were performed as described in the materials and methods.

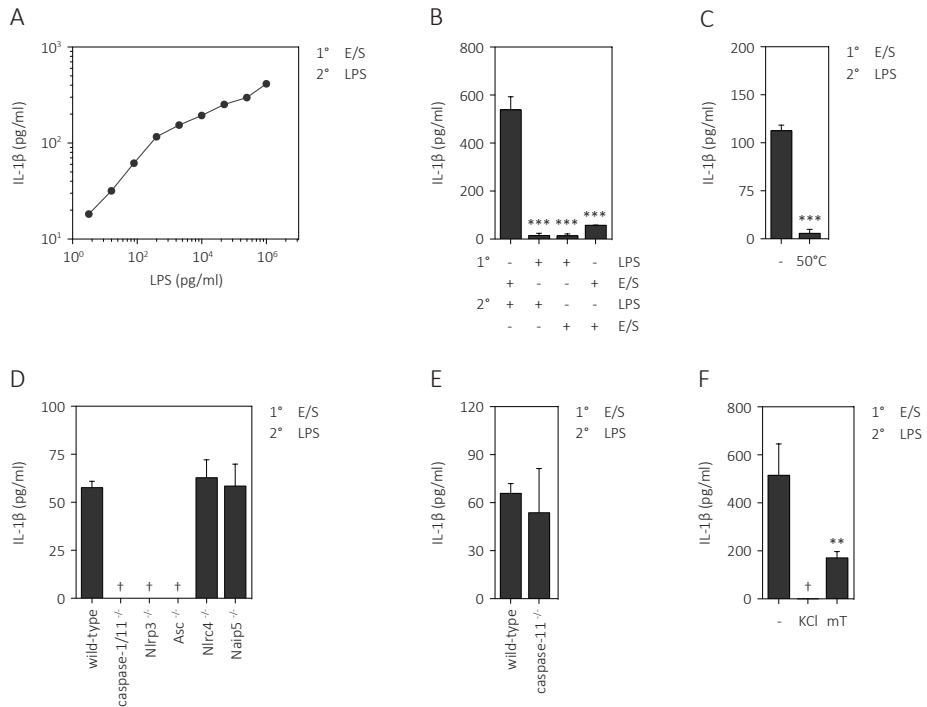


Figure 2. E/S antigens mediate LPS-induced Nlrp3 inflammasome activation (A) IL-1 β secretion by wild-type bone marrow-derived macrophages upon stimulation with 1° E/S, and 2° increasing concentrations of LPS. (B) IL-1 β secretion by wild-type macrophages upon stimulation with different combinations of LPS and E/S. (C) IL-1 β secretion by wild-type macrophages upon LPS-induced inflammasome activation after stimulation with heat-treated (50°C for 8-12 hours) or untreated E/S. (D-E) IL-1 β secretion by wild-type and various inflammasome-deficient macrophages upon LPS-induced inflammasome activation after E/S stimulation. (F) IL-1 β secretion by wild-type macrophages upon LPS-induced inflammasome activation in the presence of mitoTEMPO (mT; 5 mM) or extracellular KCl (50 mM) in step 2 to assess the role of mROS and potassium efflux, respectively. Graphs are representative of three to five independent experiments.

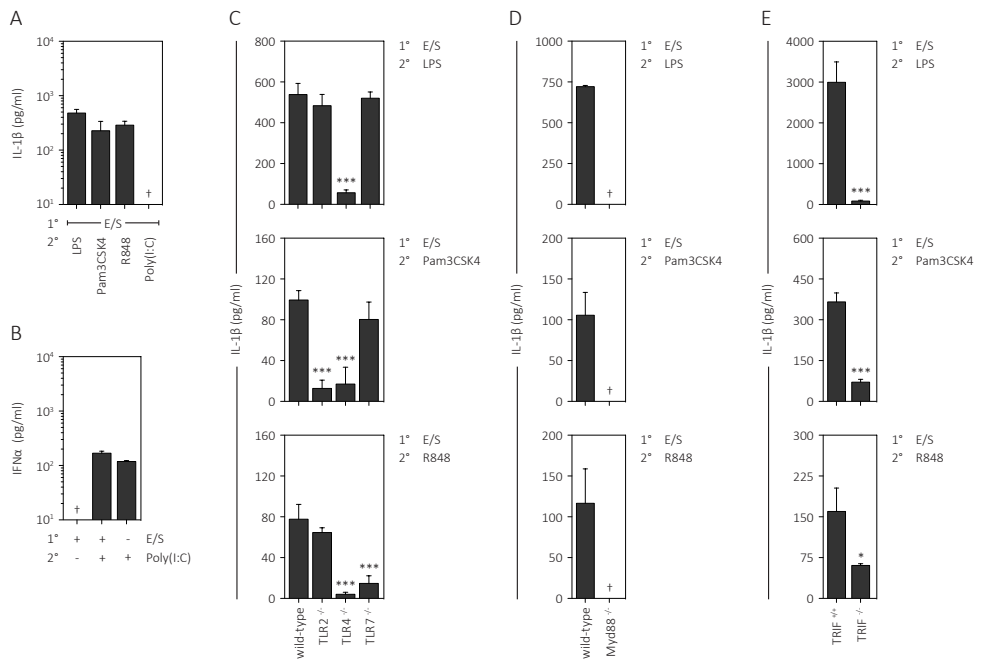


Figure 3. E/S-mediated inflammasome activation is TLR dependent (A-E) Cytokine secretion by wild-type and gene-deficient bone marrow-derived macrophages stimulated in two consecutive steps with 1^o E/S, and 2^o various synthetic or pathogen-derived TLR-ligands. Graphs are representative of two to four independent experiments.

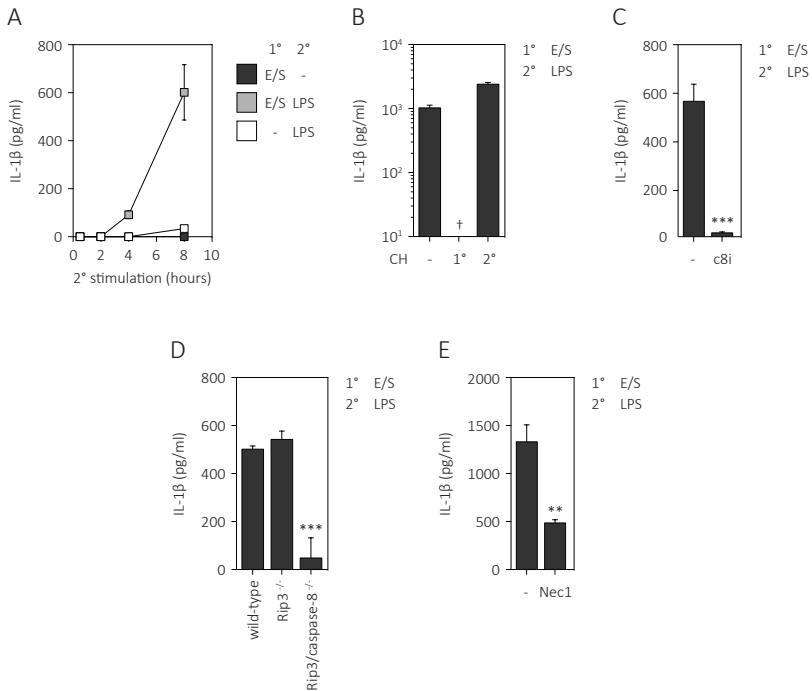


Figure 4. LPS-induced inflammasome activation is slow and caspase-8 dependent IL-1 β secretion by wild-type and gene-deficient bone marrow-derived macrophages upon stimulation with 1°) E/S and 2°) LPS, in the presence of specific inhibitors. (A) Kinetic of LPS-induced inflammasome activation. (B) Addition of the translation inhibitor cycloheximide (CH; 20 μ g/ml) during step 1 or 2. (C) Addition of the caspase-8-specific inhibitor Z-IETD-FMK (c8i; 12.5 μ M) during step 2. (D) Comparison between wild-type, RIP3-deficient and RIP3/caspase-8 double-deficient cells. (E) Addition of Rip1-kinase inhibitor necrostatin-1 (Nec1; 75 μ M) during step 2. Graphs are representative of (A) one and (B-E) three to five independent experiments.

Paper 4

Eosinophils are key regulators of perivascular adipose tissue and vascular functionality

Authors

Sarah B. Withers¹, Ruth Forman², Selene Meza-Perez^{3,5}, Daniel Sorobetea³, Kasia Sitnik⁴, Thomas Hopwood², Catherine B. Lawrence², William W. Agace^{3,4}, Kathryn J. Else², Anthony M. Heagerty¹, Marcus Svensson-Frej³ and Sheena M. Cruickshank²

Affiliations

1. Institute of Cardiovascular Sciences, University of Manchester, Manchester, United Kingdom.
2. Faculty of Biology, Medicine and Health, University of Manchester, Manchester, United Kingdom.
3. Section for Immunology, Lund University, BMC D14, SE-22184 Lund, Sweden.
4. Section for Immunology and Vaccinology, Danish Technical University, Veterinary Institute, Bülowsvej 27, DK-1870, Copenhagen, Denmark.
5. University of Alabama at Birmingham, Birmingham, Alabama

Corresponding author

Sheena Cruickshank
A.V. Hill Building, University of Manchester
Oxford Road, Manchester, M13 9PL
United Kingdom
Telephone: +44 161 275 1582
E-mail: sheena.cruickshank@manchester.ac.uk

Abstract

Obesity impairs the relaxant capacity of adipose tissue surrounding the vasculature (PVAT) and has been implicated in resultant obesity-related hypertension and impaired glucose intolerance. Resident immune cells are thought to regulate adipocyte activity. We investigated the role of eosinophils in mediating normal PVAT function. Healthy PVAT elicits an anti-contractile effect, which was lost in mice deficient in eosinophils, mimicking the obese phenotype, and was restored upon eosinophil reconstitution. *Ex vivo* studies demonstrated that the loss of PVAT function was due to reduced bioavailability of adiponectin and adipocyte-derived nitric oxide, which was restored after eosinophil reconstitution. Mechanistic studies demonstrated that adiponectin and nitric oxide are released after activation of adipocyte-expressed β_3 adrenoceptors by catecholamines, and identified eosinophils a novel source of these mediators. We conclude that adipose tissue eosinophils play a key role in the regulation of normal PVAT anti-contractile function.

Introduction

Most of the peripheral circulation is invested by a layer of perivascular adipose tissue (PVAT) [1], which comprises adipocytes, stromal cells and immune cells. In health, PVAT confers an anti-contractile effect on the vasculature through a balance of adipocyte-derived pro- and anti-contractile factors (including adiponectin [2]) and immune cell populations [3], as well as contributing to the regulation of physiological processes, including glucose homeostasis and lipid metabolism. In response to sustained caloric excess, there is adipocyte enlargement, hypoxia and subsequent PVAT inflammation leading to increased arterial tone [4], which has profound effects on peripheral resistance [5] and nutritive flow [6], thereby linking obesity-associated hypertension [7] and type 2 diabetes with vascular dysfunction [8].

The involvement of immune cells in metabolic events in adipose tissue has come to the forefront of obesity research (reviewed in [9]). The contribution of eosinophils to the regulation of physiological events in these tissues, under steady state and in the inflammatory setting, is undefined; increased knowledge in this area is an unmet need with important implications for the treatment of obesity-associated disorders. Historically, eosinophils have been viewed as end-stage effector cells associated with Th2 inflammatory disorders such as parasitic infections and allergies, where they become activated and release cytotoxic granule proteins [10]. However, recent reports demonstrate that eosinophils are steady state constituents of the cellular pool in several organs, including the gastrointestinal tract [11] and adipose tissue, and play a role in metabolic homeostasis [12]. Despite this, little attention has been paid to the direct role that eosinophils may play in adipose tissue function. We employed mouse models of eosinophil-deficiency and reconstitution, complemented by *in vitro* studies, to address the significance of eosinophils on PVAT function and vascular reactivity. For the first time, we have identified a central role for eosinophils in the maintenance of healthy PVAT functionality. Mechanistically, we define the release of nitric oxide as well as adiponectin, as central in regulation of PVAT anti-contractile function, and importantly identify the eosinophil as a key cell type controlling the release of these mediators via catecholamine mediated-activation of adipocyte-expressed β_3 adrenoceptors.

Results

Healthy PVAT exerts an anti-contractile effect that is lost in obesity

Initially, we compared the vascular reactivity in healthy twelve-week old C57BL/6 mice fed standard chow to mice on a high fat diet (HFD). In mice on standard chow, contractile responses of small mesenteric arteries (approximately 200 μm internal diameter) to cumulative doses of norepinephrine (NE) showed that vascular constriction was reduced in the presence of PVAT, compared with vessels from the same mouse in the absence of PVAT ($P=0.001$; Fig. 1a). In contrast, in age-matched obese C57BL/6 mice fed a HFD, the anti-contractile capacity of PVAT was completely abolished, with no difference in contractility to NE whether PVAT was intact or removed (Fig. 1a).

Histological analyses of PVAT demonstrated significant adipocyte hypertrophy in HFD mice compared with standard chow fed control mice ($P<0.0001$; Fig. 1b,c). Furthermore, immunohistochemical and flow cytometric analyses of enzymatically digested mesenteric adipose tissue demonstrated a significant reduction in the number of eosinophils present in HFD mice compared with chow fed age-matched controls ($P=0.0113$; Fig. 1d, and data not shown), consistent with previous reports [12]. Thus, impaired vascular function in HFD mice is associated with a dramatic reduction in the number of adipose tissue eosinophils.

Eosinophils contribute directly to the regulation of vascular tone

Anti-contractile PVAT function is lost in eosinophil-deficient $\Delta\text{dblGATA-1}$ mice

To further investigate the role of eosinophils in vascular function we analyzed eosinophil-deficient $\Delta\text{dblGATA-1}$ mice [13]. Flow cytometric analysis confirmed that eosinophils reside constitutively within mesenteric adipose tissue of wildtype (WT) mice (mean: 4.5% of all CD45^+ cells, $\pm\text{SD}$: 2.9%; $n=11$), but are absent in $\Delta\text{dblGATA-1}$ mice (Fig. 2a). As changes in perivascular adipose tissue has been shown to alter vascular function [14] we examined the contractile and dilator response of small mesenteric arteries of $\Delta\text{dblGATA-1}$ mice and their WT littermate controls by wire myography. In contrast with WT mice, in which there was a significant anti-contractile effect of PVAT (WT mice, PVAT vs. no PVAT: $P<0.0001$, $n=15$) (Fig. 2b), there was no PVAT-mediated anti-contractile effect to cumulative doses of NE in $\Delta\text{dblGATA-1}$ mice ($\Delta\text{dblGATA-1}$ mice, PVAT vs. no PVAT: $P=\text{NS}$, $n=15$) (Fig. 2b). We additionally analyzed vessels with and without PVAT from IL-5 Tg mice that have excessive numbers of eosinophils and showed that IL-5 Tg arteries with or without PVAT responded in the same manner as WT arteries (Fig S1a,b). Additionally, we observed that $\Delta\text{dblGATA-1}$ mice had increased peripheral mean arterial blood pressure by an occlusion tail-cuff system (CODA) ($P<0.046$; Fig. S1c) and elevated fasting blood glucose ($P=0.0106$; Fig. S1d) compared with their littermate controls. Overall our data suggest that eosinophils are required for the PVAT-mediated regulation of vascular function.

Eosinophil reconstitution restores normal PVAT function

To confirm that changes in PVAT function in Δ dblGATA-1 mice were attributable to eosinophil-deficiency we performed eosinophil reconstitution (AdBac) by intravenous injection of purified eosinophils. Flow cytometric analysis confirmed that donor eosinophils localized to the adipose tissue of the mesenteric bed (Fig. 2a), as well as perigonadal adipose tissue and the small and large intestine (data not shown). Thirty days after eosinophil reconstitution functional evaluation of mesenteric vessels with and without PVAT to NE-stimulation further demonstrated that reconstitution of eosinophils completely restored the loss of PVAT-associated anti-contractile capacity ($P=0.0023$; Fig. 2c) to levels comparable with WT controls (data not shown). The restoration of the anti-contractile capacity of PVAT following eosinophil reconstitution was independent of effects on smooth muscle, because neither AdBac nor Δ dblGATA-1 vessels devoid of PVAT had any significant differences in response to NE stimulation (Fig. 2c), demonstrating that the effect of eosinophils is mediated via PVAT. Moreover, a restoration of both peripheral MAP and blood glucose to WT levels was observed in Δ dblGATA-1 following reconstitution with eosinophils (MAP: WT vs. Δ dblGATA-1, $P=0.025$; WT vs. AdBac: $P=NS$) (Fig. S1e; data not shown).

Eosinophils do not influence SMA⁺ pericytes or other immune populations

Further analysis of Δ dblGATA-1 mice showed no differences in the proportion of splenic or blood dendritic cells, neutrophils and monocytes compared with WT animals (Fig. S2b and c). In addition, we examined hemoglobin (HGB) and hematocrit (HCT) levels and red blood cell (RBC) counts in Δ dblGATA-1 and age- and sex-matched littermate control mice, as these parameters were reported to be affected in eosinophil-deficient mice [13]. While the levels of RBCs (RBC (WT vs Δ dblGATA-1): 9.7 ± 0.2 vs. 8.8 ± 0.2 / 10^9 cells/mL; $P=0.0338$) were reduced in Δ dblGATA-1 mice, consistent with previous reports [13], we detected no significant difference in the hemoglobin (HGB: 140.6 ± 3.6 vs. 130.0 ± 3.3 g/L) or hematocrit (HCT: 0.51 ± 0.01 vs. 0.48 ± 0.01 L/L) levels.

Pericytes, including smooth muscle actin (SMA)⁺ contractile pericytes, are localized in the perivascular area, and are thought to be involved in vascular maintenance and function, including regulation of vascular constriction [15,16]. We therefore determined the frequency of pericytes in enzymatically digested mesenteric adipose tissue from WT and Δ dblGATA-1 mice. We detected no difference in the frequency of total or SMA⁺ contractile pericytes in Δ dblGATA-1 compared with WT mice (Fig. 2d and Fig. S2a). Similarly, we observed no difference in the total weight of the mesenteric adipose tissue between WT and Δ dblGATA-1 mice (Fig. 2e). Eosinophils have also been shown to affect macrophage functionality in adipose tissue [12], and adipose tissue macrophages have in turn been shown to influence PVAT function [14]. To ascertain whether the altered vascular function in Δ dblGATA-1 mice could be attributed indirectly to a loss of eosinophil-mediated modulation

of macrophage activation, we performed flow cytometry analysis of enzymatically digested mesenteric adipose tissue from Δ dblGATA-1 and WT mice. Macrophages were defined as live CD45⁺ F4/80⁺ CD11b⁺ CD64⁺ MHC-II⁺ Ly6G⁻ cells, and were further examined for expression of markers associated with alternatively activated macrophages (AAM), RELM α /FIZZ-1 and CD206 [17,18] (Fig. S2d). We detected no difference in the frequency and number of total CD45⁺ CD64⁺ CD11b⁺ MHC-II⁺ Ly6G⁻ macrophages in the mesenteric adipose tissue between WT and Δ dblGATA-1 mice (Fig. 2f) and, similarly, found no difference in the number of macrophages expressing RELM α and CD206, two markers associated with alternatively activated macrophages [17,18] (defined as CD45⁺ F4/80⁺ CD64⁺ CD11b⁺ MHC-II⁺ Ly6G⁻ RELM α ⁺ CD206⁺ cells) (Fig. 2g). Analysis of adipose tissue by qPCR also revealed no differences in levels of the AAM markers arginase-1, fizz-1 and ym-1 between Δ dblGATA-1 and WT mice (Fig. S2e-g). Taken together, these data suggest that alterations in pericyte or macrophage composition, or adipose tissue hypertrophy, do not explain the impaired vascular reactivity in Δ dblGATA-1 mice, indicating that eosinophils may be directly involved in the regulation of PVAT function rather than acting via other cell populations.

Eosinophils influence vascular reactivity via PVAT-mediated release of soluble mediators

To determine whether eosinophils directly influence PVAT function to modulate downstream vascular reactivity, purified eosinophils were added to pre-constricted (1×10^{-5} M NE) mesenteric arteries \pm PVAT from Δ dblGATA-1 mice. The addition of purified eosinophils (100 to 30,000 cells) was associated with a significantly greater dose dependent relaxation in vessels with PVAT compared with vessels without PVAT ($P < 0.0001$) (Fig. 3a). Relaxation occurred within 30 seconds of addition of eosinophils to the organ bath, demonstrating a rapid effect of eosinophils at both the vascular and perivascular level *in vitro* (Fig. 3b). In contrast, addition of 10,000 purified macrophages had no PVAT-dependent relaxant effect (data not shown).

To establish whether eosinophils promoted the release of a soluble anti-contractile factor(s) from PVAT, organ bath solution transfer experiments were performed. Total organ bath solution from pre-constricted (1×10^{-5} M NE) small mesenteric arteries was transferred from donor arteries (with PVAT) to recipient arteries (without PVAT). These experiments demonstrated that healthy WT PVAT secretes a soluble relaxing factor (Fig. 3c) 19. However, relaxation was impaired when solution from Δ dblGATA-1 donor arteries was transferred to WT recipient arteries (Δ dblGATA-1 to WT, $P = 0.049$; Fig. 3c). Furthermore, transfer studies between WT donor arteries and Δ dblGATA-1 recipient arteries demonstrated reduced relaxation compared with WT control solution transfer (data not shown). Importantly, *in vivo* reconstitution with eosinophils restored normal PVAT function. Thus, vessel relaxation was restored to the same levels as WT to WT transfer in both donor and recipient AdBac transfers with WT vessels (Fig. 3c and data not shown). These data implicate a role

for eosinophils in mediating the secretion of a soluble relaxant factor(s) by PVAT.

To determine whether the relaxant effect of eosinophils was due to the release of eosinophil-derived soluble factors or via direct eosinophil interaction with PVAT, relaxation of C57BL/6 mesenteric arteries + PVAT was compared following application of 10,000 NE-stimulated eosinophils or the filtered supernatant from 10,000 NE-stimulated eosinophils. The filtered eosinophil supernatant was capable of inducing relaxation of mesenteric vessels to the same extent as the addition of eosinophils (Fig. 3d). Furthermore, to ensure that our results were not due to an effect of NE-dilution when eosinophils are added to NE-precontracted arteries, eosinophils were added in a buffer containing 1×10^{-5} M NE. However, as eosinophils express adrenergic receptors 20 and could potentially respond to NE; we examined the effect of NE-treatment on eosinophils. Supernatant from 10,000 eosinophils stimulated with 1×10^{-5} M NE or supernatant from unstimulated eosinophils supplemented with 1×10^{-5} M NE was added to Δ dblGATA-1 arteries with PVAT. The NE-supplemented supernatant from unstimulated eosinophils induced a significantly reduced relaxation of the mesenteric vessels in comparison with NE-stimulated eosinophils ($P=0.0068$; Fig. 3d), suggesting that eosinophil stimulation with NE is important in mediating eosinophil-induced vascular relaxation. Collectively, these data implicate a soluble factor released from NE-stimulated eosinophils, rather than cell to cell contact, in mediating eosinophil-induced PVAT function.

Eosinophils act via adrenergic stimulation of nitric oxide and adiponectin release

Our previous data have shown that adiponectin [4,19] and nitric oxide [21] are important in mediating normal PVAT relaxing function. Furthermore, IL-4 is a previously recognised eosinophil-derived effector molecule. Therefore, we tested the functional role of these putative mediators on the vascular reactivity of vessels in response to the addition of 10,000 eosinophils. To this end, mesenteric vessels + PVAT isolated from Δ dblGATA-1 mice and/or purified eosinophils were incubated with the NO-signalling inhibitor L-NMMA (1×10^{-5} M) [21], adiponectin blocking peptide (ABP; a soluble fragment of the Type-1 adiponectin receptor; 5 μ g/mL) 4 or anti-IL-4 antibody (0.4 μ g/mL) for 30 minutes before pre-constriction of the vessels with 10^{-5} M NE and addition of 10,000 stimulated eosinophils (1×10^{-5} M NE). Incubation of vessel + PVAT alone with ABP and L-NMMA, but not anti-IL-4, reduced eosinophil-induced relaxation (ABP vs control, $P<0.01$; L-NMMA vs control, $P<0.05$; Fig. 4a), whereas incubation of eosinophils alone with the inhibitors had no effect on relaxation (data not shown). There was also a significant reduction in relaxation observed following incubation of both vessels and eosinophils with L-NMMA and ABP, but not anti-IL-4, compared with the addition of stimulated eosinophils alone (L-NMMA vs. control: $P<0.01$; ABP vs. control: $P<0.001$; Fig. 4b). In contrast, incubation of eosinophils, vessel or eosinophils and vessels with the inhibitors in the absence of PVAT failed to alter relaxation of the arteries to NE-stimulated eosinophils (data not shown). Similarly, addition of D-NMMA, IgG or a

control peptide (the negative controls for L-NMMA, anti-IL-4 and ABP, respectively) to vessels + PVAT had no effect on PVAT function (data not shown).

To examine if eosinophils could act as source of NO or adiponectin, we performed eosinophil reconstitution experiments using bone marrow-derived eosinophils from WT, iNOS^{-/-} or adiponectin^{-/-} mice. PVAT vessels from reconstituted mice showed a loss of anti-contractile function following reconstitution with adiponectin^{-/-} eosinophils, but not iNOS^{-/-} or WT eosinophils (adipo^{-/-} vs WT: P=0.0085; Fig. 4c and d). Collectively, these data suggest that adiponectin and NO signalling are critical components of the regulation of vascular activity, and further, that eosinophils may act as a source of adiponectin, as well as inducing the release of downstream adiponectin from PVAT, resulting in relaxation of vessels via NO-dependent mechanisms.

Given the rapid effect on PVAT function following addition of eosinophils (Fig. 3b), we hypothesized that eosinophils may directly exert their effect via adrenoreceptors. To explore this idea, we incubated mesenteric vessels + PVAT with eosinophils in the presence or absence of antagonists of β 1- β 3, α 1 or β 3 adrenoreceptors. After addition of antagonists against β 1- β 3 or α 1 adrenoreceptors, there was no inhibition of relaxation in the presence of exogenous PVAT or exogenous PVAT with eosinophils (Fig. 5a). In contrast, a specific β 3 adrenoreceptor antagonist (SR-592,30A) [22] significantly reduced relaxation in the presence of exogenous PVAT or exogenous PVAT with eosinophils (β 3 adrenoreceptor antagonist vs. time control, P<0.001 and β 3 adrenoreceptor antagonist vs. vessel control, P<0.05; Fig. 5a). Moreover, the direct addition of the β 3 adrenoreceptor agonist (CL-316,243) [23] to Δ dblGATA-1 arteries with PVAT resulted in a significant relaxation of these vessels in comparison to control Δ dblGATA-1 arteries with PVAT (P<0.001; Fig 5b), suggesting that this elicits the same response as the addition of eosinophils. The only known agonists of β 3 adrenoreceptors are catecholamines, the production of which is critically dependent on the enzyme tyrosine hydroxylase [24]. As our data demonstrated that eosinophils secrete a soluble factor that mediates a relaxant effect on PVAT, we hypothesised that eosinophils may be a source of catecholamines. Immunocytochemical staining revealed high expression of tyrosine hydroxylase in eosinophil granules (Fig. 5c). To examine the functional significance of this, 10,000 eosinophils were incubated with or without a tyrosine hydroxylase inhibitor (AMPT). Addition of eosinophils pre-incubated with AMPT to mesenteric vessels + PVAT isolated from Δ dblGATA-1 mice resulted in a significantly decreased relaxation compared to untreated eosinophils (P=0.0472; Fig 5d). Finally, we demonstrated that eosinophils are able to constitutively produce epinephrine, NE and dopamine, and with a trend towards increased NE and dopamine secretion following activation of eosinophils with IL-5 and eotaxin (Fig 5d). Together these data demonstrate that PVAT functionality depends on tyrosine hydroxylase-dependent eosinophil production of catecholamines that signal via PVAT-located β 3 adrenoreceptors.

Discussion

The anti-contractile function of perivascular adipose tissue (PVAT) is lost in obesity, a disorder with an underlying immunological component [9,25] that has been linked with increased peripheral vascular resistance and elevated peripheral blood pressure [5,7]. While a role of eosinophils in regulation of these events have not previously been recognized, our data identify mechanisms by which obesity-induced alterations to the eosinophil population may perturb the influence from PVAT on small arteries and the physiological consequences thereof [4,6]. Thus, for the first time, we demonstrate that eosinophils play a central role in the release of vasorelaxing factors from healthy PVAT, via the release of eosinophil-derived catecholamines, to mediate adipocyte-localised β_3 adrenoceptor activation and downstream adiponectin- and nitric oxide-signalling. Loss of PVAT function was also associated with increased arterial tone, with a potential role of eosinophils in the regulation of these processes being further supported by our observations that hypertensive eosinophil-deficient mice recovered upon eosinophil reconstitution. Furthermore, the loss of a vasodilatory paracrine effect from adipose tissue has been suggested to limit downstream microcirculatory nutritive flow [6], thereby contributing to insulin resistance and metabolic dysregulation. It is clear from these studies that eosinophils play a vital role in sustaining normal PVAT function in health to maintain adipose tissue homeostasis, which have important downstream physiological consequences.

Previous work to understand the mechanisms responsible for the anti-contractile effect of PVAT have focused attention on the macrophage [14], whilst other leukocyte populations have largely been ignored. Eosinophils have previously been shown to be indirectly involved in regulation of events in adipose tissue by controlling adipose tissue macrophage functionality [12], which in turn can influence PVAT function in inflammation [14]. For example in obesity, factors such as tissue hypoxia and aldosterone signaling are thought to alter macrophage activation, which subsequently impacts on PVAT anti-contractile function, manifesting in hypertension [14]. Macrophages have also been shown to play a role in being of fat and thermoregulation [26]. A recent report implicated eosinophils in regulation of the polarization of white adipose tissue macrophages to an AAM phenotype. Thus, Wu et al [12] detected a decrease in a subpopulation of YFP⁺ macrophages expressing high levels of CD11b and F4/80 in the perigonadal adipose tissue of Δ dblGATA-1 BALB/c mice crossed with mice expressing YFP under the arginase-1 promoter. In apparent contrast to these results, we detected no change in the frequency of total or AAM in the mesenteric adipose tissue of Δ dblGATA-1 compared with WT mice. Although the reason for this discrepancy is not entirely clear, we speculate that differences in the source of adipose tissue or analysis may underlie the difference. Thus, while Wu et al examined a population of GFP-positive cells among a population of F4/80^{hi} CD11b^{hi} perigonadal adipose tissue macrophages in arginase-reporter mice [12], we analyzed expression of RELM α and

CD206 on total CD11b⁺ CD64⁺ mesenteric adipose tissue macrophages. Consistent with our flow cytometry analysis, qPCR analysis of mesenteric adipose tissue from WT or Δ dblGATA-1 mice revealed no differences in the expression of arginase-1, fizz-1 or ym-1. Finally, we also addressed a potential role of IL-4 in PVAT function, as IL-4 secretion from eosinophils has been proposed to be a key mechanism by which eosinophils sustain AAM and regulate glucose homeostasis [12]. However, neutralization of IL-4 had no impact on vessel reactivity in our system. Although we cannot exclude the possibility that macrophages may indirectly contribute to PVAT function, the current study demonstrate that eosinophils contribute to regulation of vascular function directly, by release of catecholamines that act rapidly via PVAT to promote vessel relaxation. This appears to be a unique function of eosinophils, and cannot be mediated by other immune cells, including macrophages. Taken together we conclude that eosinophils exert an effect on healthy PVAT function directly, and independently of other immune cell populations.

Adipocytes and eosinophils are known to secrete a number of adipokines and cytokines, which influence downstream biological responses [10,12,27]. The balance of pro- and anti-inflammatory adipokines is important in mediating the anti-contractile capacity, energy homeostasis and inflammatory status of PVAT. Ours and others' previous data in humans and rodent species (rats and mice) have shown that adiponectin [4,19] and nitric oxide signaling [21,28] are important in mediating normal PVAT function. Thus, adiponectin-deficient mice demonstrate a loss of PVAT function in response to adrenergic stimulation [19] and have been shown to be hypertensive [29]. Furthermore, healthy PVAT-induced vascular relaxation is attenuated by inhibition of NO, and NO signaling is dysregulated in a rat model of the metabolic syndrome associated with enhanced vasoconstriction to norepinephrine [28]. Indeed in line with this, we confirmed that adiponectin and NO signaling were essential for the anti-contractile function of PVAT also in mice, and that eosinophils were necessary for promoting the adiponectin- and NO-dependent anti-contractile function of PVAT. Furthermore, to examine if eosinophils could act as a direct source of NO or adiponectin, we performed in vivo reconstitution experiments using eosinophils generated from WT, iNOS^{-/-} or adiponectin^{-/-} mice. Interestingly, our experiments revealed that eosinophil-derived adiponectin, but not NO, contributed to the anti-contractile capacity of PVAT. Thus, our data suggest that eosinophils may act as a source of adiponectin as well as inducing the release of downstream adiponectin from PVAT, resulting in relaxation of vessels via NO-dependent mechanisms.

The eosinophil cytoplasm contains numerous preformed granules containing a variety of effector molecules; therefore we hypothesized that eosinophils may act on PVAT via secreted factors. In support of this hypothesis, addition of filtered eosinophil supernatant to vessels + PVAT mimicked the relaxant effect of eosinophil addition. Moreover, as the eosinophil-dependent effect was so rapid, we focused

our studies on adrenoreceptor-mediated activation of PVAT rather than genomic manifestations of eosinophil-deficiency. Addition of a panel of adrenoreceptor inhibitors in our experimental model demonstrated that the vessel-relaxing interaction of eosinophils with PVAT occurred via the β_3 adrenoreceptor, supporting a previous study that identified a role for β_3 adrenoreceptors in mediating the adipocyte-derived hyperpolarizing factor (ADRF)-induced hyperpolarization of smooth muscle [23]. Catecholamines are the only known activators of the β_3 adrenoreceptor, and depend on the enzyme tyrosine hydroxylase for their production [24]. Immunocytochemical analysis of purified eosinophils demonstrated that eosinophils indeed express this enzyme, which was necessary for the eosinophil-mediated effect on vascular reactivity. Furthermore, we showed that eosinophils constitutively secrete catecholamines. To our knowledge, this is the first time that eosinophils have been reported to express tyrosine hydroxylase and secrete catecholamines.

In conclusion, our data demonstrate for the first time a direct role for eosinophils in regulation of adipose tissue functionality, further emphasizing the surprising contribution of eosinophils to physiological processes beyond immune function. We have demonstrated that eosinophils play a crucial role in mediating normal PVAT function, the dysfunction of which is associated with conditions such as hypertension and type 2 diabetes. Thus, eosinophil-deficiency within adipose tissue led to physiological consequences on vascular reactivity, independent of other immune cell populations. The effects on PVAT and vascular function are mediated via regulation of NO-signaling and release of adiponectin, following secretion of catecholamines that promote β_3 adrenoreceptor-dependent PVAT anti-contractile function (Fig. 7). Taken together, our data identifies eosinophils as novel targets for the development of therapies for obesity and related cardiovascular complications.

Materials and Methods

Δ dblGATA-1, IL-5 Tg and littermate control mouse details, standard experimental procedures, and more detailed descriptions of protocols and analyses are presented in the Supplemental Experimental Procedures-section.

Eosinophil purification and transfer

Eosinophils were purified from IL-5 Tg mice by negative selection using MACS columns or by cell sorting, and were approximately 95% pure irrespective of purification method (data not shown), as assessed by flow cytometry of CD11b⁺ SiglecF⁺ SSC^{high} cells. For adoptive transfers, eosinophils were resuspended in sterile phosphate buffered saline (PBS), and 100-150 million cells injected intravenously, and recipient mice analysed 30 days after transfer. Bone marrow-derived eosinophils were grown as described previously [30]. After 12-14 days in culture the cells were >90% pure as determined by flow cytometry analysis; cells were resuspended in sterile PBS, and 1-3 million cells injected intravenously per mouse, and recipient mice analysed five days after transfer.

Adipose tissue digest

For isolation of the adipose stromal vascular fraction (SVF), white mesenteric adipose tissue was finely minced and incubated in medium containing 1mg/mL type I collagenase and 30 μ g/mL DNase I at 37°C for 45 min with magnetic stirring at 350rpm. The resulting cell suspension was spun to separate floating adipocytes from the SVF pellet, and passed through 40 μ m filters to generate a single-cell suspension. Leukocytes were further enriched by density centrifugation using Percoll, followed by phenotypic and quantitative analysis by flow cytometry.

Pharmacological assessment of vascular reactivity by wire myography

The mesenteric bed was removed and placed in ice-cold physiological salt solution (PSS); first-order arteries were identified and dissected clean of PVAT or left with surrounding PVAT intact as indicated. Vessels were mounted on a wire myograph, equilibrated, normalised and viability assessed as previously described [4,21,31]. Vascular contractility was assessed in vessels to increasing concentrations of norepinephrine (NE).

Solution transfer experiments were performed between wildtype (WT), IL-5 Tg, Δ dblGATA-1 and eosinophil-reconstituted Δ dblGATA-1 (AdBac) mice. Arteries were precontracted with NE and a stable constriction established; next, total myograph bath solution (6mLs) taken from donor arteries with PVAT were used to replace the solution from a recipient artery devoid of PVAT.

In order to investigate the direct effect of eosinophils on vascular contractility, the exogenous addition of (1×10^2 to 1×10^6) eosinophils to precontracted mesenteric arteries (1×10^{-5} M NE) from Δ dblGATA-1 mice was assessed in the presence and

absence of PVAT. To establish whether eosinophils interacted directly or indirectly, the supernatant from NE-stimulated eosinophils was added to precontracted vessels.

Adiponectin blocking peptide, L-NMMA, anti-IL-4, propranolol and SR-592,30A or appropriate controls were incubated for 30 minutes at 37°C with either eosinophils only, arteries±PVAT, or both eosinophils and arteries (± PVAT). Both eosinophils and vessels were treated with NA (1×10^{-5} M) before addition of eosinophils to the vessels. The response to eosinophil addition was measured as a percentage relaxation.

Ethical approval

Procedures were performed in accordance with the United Kingdom Animals (Scientific Procedures) Act of 1986, and conformed to the Directive 2010/63/EY of the European Parliament. Ethical permission was obtained from the Local Ethical Committee at Lund University, Sweden, and the University of Manchester Animal Welfare and Ethical Review Board and performed under a Home Office approved grant.

References

1. Verlohren, S. et al. Visceral periadventitial adipose tissue regulates arterial tone of mesenteric arteries. *Hypertension* 44, 271-276, doi:10.1161/01.HYP.0000140058.28994.ec (2004).
2. Gu, P. & Xu, A. Interplay between adipose tissue and blood vessels in obesity and vascular dysfunction. *Reviews in endocrine & metabolic disorders* 14, 49-58, doi:10.1007/s11154-012-9230-8 (2013).
3. Apostolopoulos, V. et al. The complex immunological and inflammatory network of adipose tissue in obesity. *Molecular nutrition & food research* 60, 43-57, doi:10.1002/mnfr.201500272 (2016).
4. Greenstein, A. S. et al. Local inflammation and hypoxia abolish the protective anticontractile properties of perivascular fat in obese patients. *Circulation* 119, 1661-1670, doi:10.1161/CIRCULATIONAHA.108.821181 (2009).
5. Gollasch, M. & Dubrovskaja, G. Paracrine role for periadventitial adipose tissue in the regulation of arterial tone. *Trends in pharmacological sciences* 25, 647-653, doi:10.1016/j.tips.2004.10.005 (2004).
6. Yudkin, J. S., Eringa, E. & Stehouwer, C. D. "Vasocrine" signalling from perivascular fat: a mechanism linking insulin resistance to vascular disease. *Lancet* 365, 1817-1820, doi:10.1016/S0140-6736(05)66585-3 (2005).
7. Gao, Y. J. Dual modulation of vascular function by perivascular adipose tissue and its potential correlation with adiposity/lipoatrophy-related vascular dysfunction. *Current pharmaceutical design* 13, 2185-2192 (2007).
8. Wang, Z. V. & Scherer, P. E. Adiponectin, cardiovascular function, and hypertension. *Hypertension* 51, 8-14, doi:10.1161/HYPERTENSIONAHA.107.099424 (2008).
9. Han, J. M. & Levings, M. K. Immune regulation in obesity-associated adipose inflammation. *Journal of immunology* 191, 527-532, doi:10.4049/jimmunol.1301035 (2013).
10. Furuta, G. T., Atkins, F. D., Lee, N. A. & Lee, J. J. Changing roles of eosinophils in health and disease. *Annals of allergy, asthma & immunology : official publication of the American College of Allergy, Asthma, & Immunology* 113, 3-8, doi:10.1016/j.anai.2014.04.002 (2014).
11. Carlens, J. et al. Common gamma-chain-dependent signals confer selective survival of eosinophils in the murine small intestine. *Journal of immunology* 183, 5600-5607, doi:10.4049/jimmunol.0801581 (2009).
12. Wu, D. et al. Eosinophils Sustain Adipose Alternatively Activated Macrophages Associated with Glucose Homeostasis. *Science* 332, 243-247, doi:10.1126/science.1201475 (2011).
13. Yu, C. et al. Targeted deletion of a high-affinity GATA-binding site in the GATA-1 promoter leads to selective loss of the eosinophil lineage in vivo. *The Journal of experimental medicine* 195, 1387-1395 (2002).
14. Withers, S. B. et al. Macrophage activation is responsible for loss of anticontractile function in inflamed perivascular fat. *Arteriosclerosis, thrombosis, and vascular biology* 31, 908-913, doi:10.1161/ATVBAHA.110.221705 (2011).

15. Malhotra, D. et al. Transcriptional profiling of stroma from inflamed and resting lymph nodes defines immunological hallmarks. *Nature immunology* 13, 499-510, doi:10.1038/ni.2262 (2012).
16. Hamilton, N. B., Attwell, D. & Hall, C. N. Pericyte-mediated regulation of capillary diameter: a component of neurovascular coupling in health and disease. *Frontiers in neuroenergetics* 2, doi:10.3389/fnene.2010.00005 (2010).
17. Jenkins, S. J. et al. Local macrophage proliferation, rather than recruitment from the blood, is a signature of TH2 inflammation. *Science* 332, 1284-1288, doi:10.1126/science.1204351 (2011).
18. Gordon, S. & Martinez, F. O. Alternative activation of macrophages: mechanism and functions. *Immunity* 32, 593-604, doi:10.1016/j.immuni.2010.05.007 (2010).
19. Lynch, F. M. et al. Perivascular adipose tissue-derived adiponectin activates BK(Ca) channels to induce anticontractile responses. *American journal of physiology. Heart and circulatory physiology* 304, H786-795, doi:10.1152/ajpheart.00697.2012 (2013).
20. Johnson, M. Effects of beta2-agonists on resident and infiltrating inflammatory cells. *The Journal of allergy and clinical immunology* 110, S282-290 (2002).
21. Withers, S. B., Simpson, L., Fattah, S., Werner, M. E. & Heagerty, A. M. cGMP-dependent protein kinase (PKG) mediates the anticontractile capacity of perivascular adipose tissue. *Cardiovascular research* 101, 130-137, doi:10.1093/cvr/cvt229 (2014).
22. Nisoli, E., Tonello, C., Landi, M. & Carruba, M. O. Functional studies of the first selective beta 3-adrenergic receptor antagonist SR 59230A in rat brown adipocytes. *Molecular pharmacology* 49, 7-14 (1996).
23. Weston, A. H. et al. Stimulated release of a hyperpolarizing factor (ADHF) from mesenteric artery perivascular adipose tissue: involvement of myocyte BKCa channels and adiponectin. *British journal of pharmacology* 169, 1500-1509, doi:10.1111/bph.12157 (2013).
24. Daubner, S. C., Le, T. & Wang, S. Tyrosine hydroxylase and regulation of dopamine synthesis. *Archives of biochemistry and biophysics* 508, 1-12, doi:10.1016/j.abb.2010.12.017 (2011).
25. Brestoff, J. R. et al. Group 2 innate lymphoid cells promote beiging of white adipose tissue and limit obesity. *Nature* 519, 242-246, doi:10.1038/nature14115 (2015).
26. Qiu, Y. et al. Eosinophils and type 2 cytokine signaling in macrophages orchestrate development of functional beige fat. *Cell* 157, 1292-1308, doi:10.1016/j.cell.2014.03.066 (2014).
27. Makki, K., Froguel, P. & Wolowczuk, I. Adipose tissue in obesity-related inflammation and insulin resistance: cells, cytokines, and chemokines. *ISRN inflammation* 2013, 139239, doi:10.1155/2013/139239 (2013).
28. Marchesi, C., Ebrahimian, T., Angulo, O., Paradis, P. & Schiffrin, E. L. Endothelial nitric oxide synthase uncoupling and perivascular adipose oxidative stress and inflammation contribute to vascular dysfunction in a rodent model of metabolic

- syndrome. *Hypertension* 54, 1384-1392 (2009).
29. Ohashi, K. et al. Adiponectin replenishment ameliorates obesity-related hypertension. *Hypertension* 47, 1108-1116 (2006).
 30. Dyer, K. D. et al. Functionally competent eosinophils differentiated ex vivo in high purity from normal mouse bone marrow. *Journal of immunology* 181, 4004-4009 (2008).
 31. Mulvany, M. J. & Halpern, W. Contractile properties of small arterial resistance vessels in spontaneously hypertensive and normotensive rats. *Circulation research* 41, 19-26 (1977).

Acknowledgements

We would like to acknowledge the technical assistance of Larisa Logunova. We thank our funders; The Wellcome Trust 092323 (SC, KJE, MSF and WA), The Royal Physiographic Society (Lund, Sweden) (MSF), Lars Hierta's Minne (MSF), Alfred Österlund's Foundation (MSF), Sigurds and Elsa Goije's Minne (MSF) and Åke Wiberg's Foundation (MSF).

Author Contribution

S.W., R.F., M.S.F. and S.C. designed and performed experiments, analysed data and wrote the manuscript. D.S., S.M.P., T.H. and K.S. performed experiments and provided input for interpretation.

C.B.L., W.A., A.H., K.J.E., M.S.F., and S.C. conceptualised the research, directed the study and edited the manuscript.

Additional Information

Competing financial interests: The authors declare no competing financial interests.

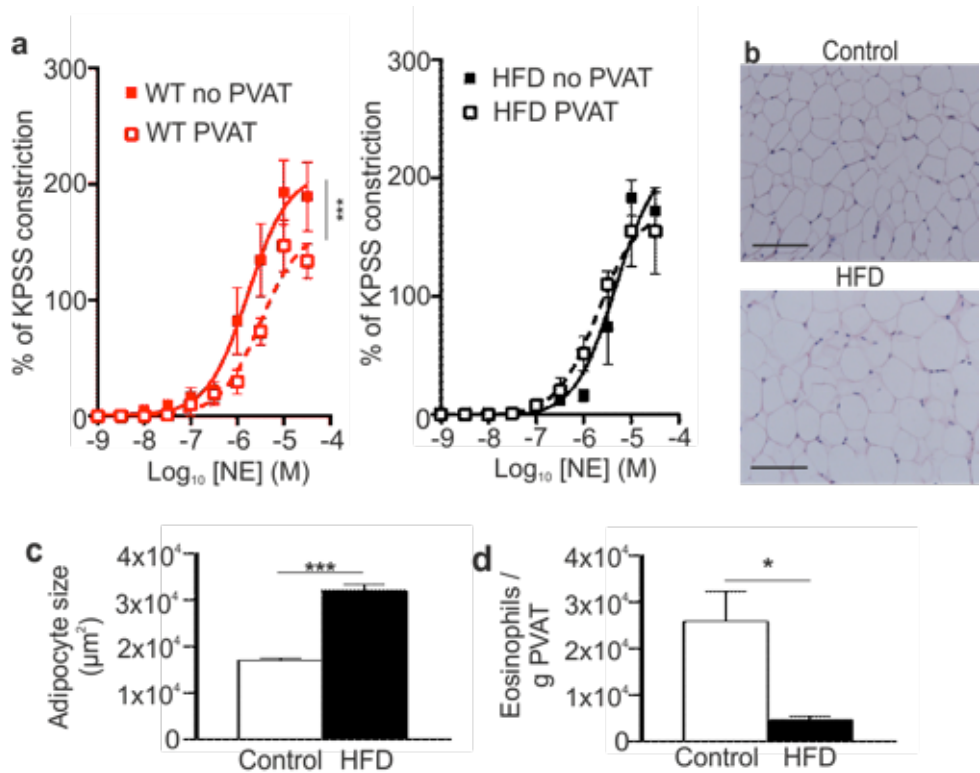


Figure 1. Obese mice have impaired vascular reactivity and increased blood pressure. (a) The anti-contractile effect of PVAT observed in WT mice is lost in HFD mice (mean \pm SEM from one experiment; n=8 (WT) and 5 (HFD); P=NS, two-way ANOVA) (no PVAT (closed symbols) and PVAT (open symbols)). (b) Representative H&E staining of mesenteric adipose tissue from control and HFD mice, and (c) analysis of adipocyte size (HFD: n=5, and WT: n=8; ***P<0.0001, Student's t-test). Scale bar shows 100 μm . (d) Mesenteric adipose tissue of HFD and control mice was analyzed for number of eosinophils (mean \pm SEM; HFD: n=5, and WT: n=8; *P=0.0113, Student's t-test).

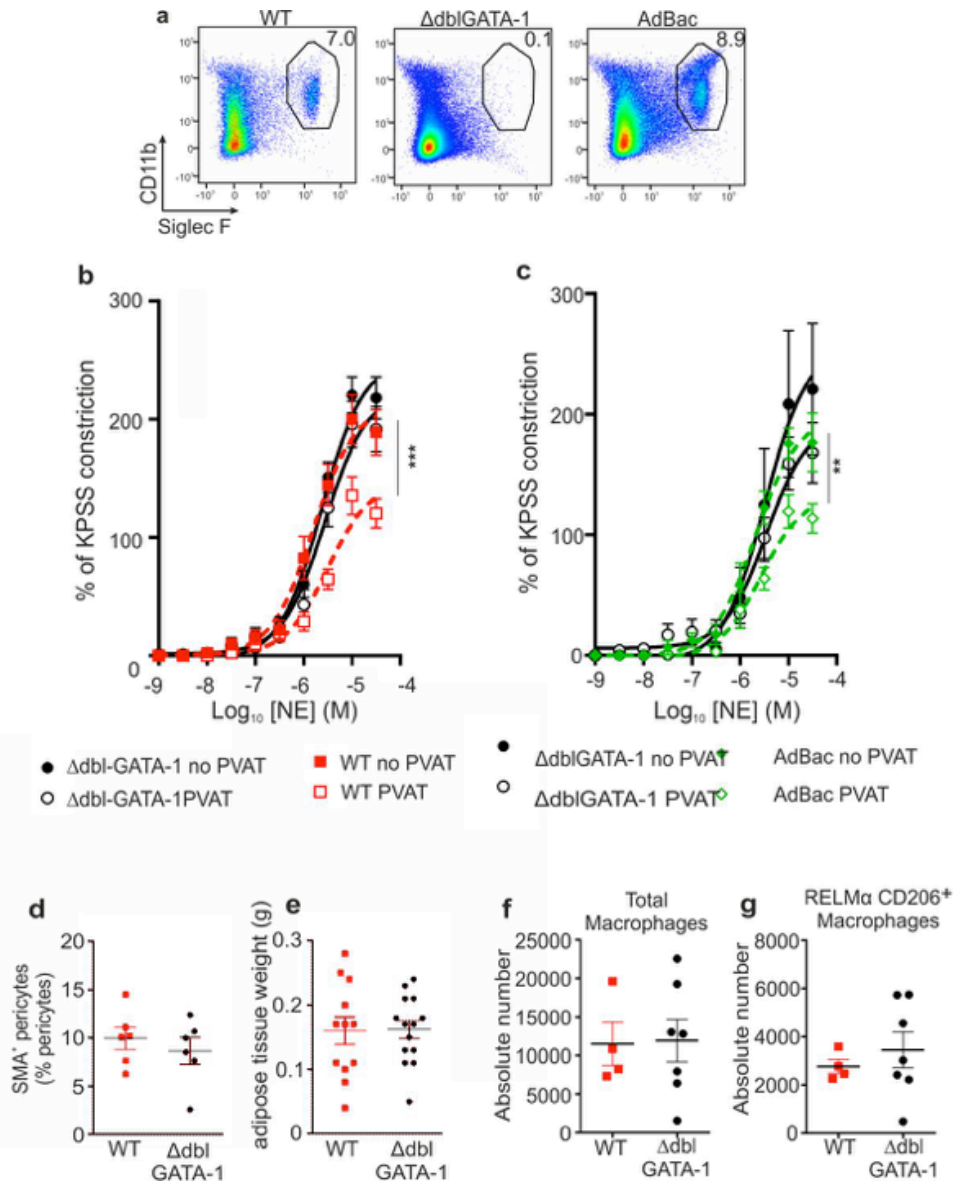


Figure 2. Eosinophil-deficient mice have impaired vascular reactivity which is restored by in vivo reconstitution with eosinophils but no effect on other immune cell populations. (a) Flow cytometric analysis of mesenteric adipose tissue eosinophils from WT, Δ dblGATA-1 and eosinophil-reconstituted (AdBac) mice (n=11, 6 and 5, respectively). (b) Eosinophil-deficient mice have impaired vascular reactivity. NE-induced constriction of arteries from WT and Δ dblGATA-1 mice (n=15, data pooled from 3 experiments; ***P<0.0001, two-way ANOVA) (Δ dblGATA-1 no PVAT (-●-), Δ dblGATA-1 PVAT (-○-), WT no PVAT (-■-) and WT PVAT (-□-)). (c) The PVAT-mediated anti-contractile response of eosinophil-deficient Δ dblGATA-1 mice (no PVAT (-●-) and Δ dblGATA-1 PVAT (-○-)) is restored by in vivo reconstitution with eosinophils (AdBac no PVAT (●) and AdBac PVAT (◇)). (d) SMA⁺ pericytes (% pericytes) in mesenteric adipose tissue. (e) Adipose tissue weight (g) in mesenteric adipose tissue. (f) Total Macrophages absolute number in mesenteric adipose tissue. (g) RELM α CD206⁺ Macrophages absolute number in mesenteric adipose tissue.

PVAT (-o-) to NE-induced constriction is restored upon eosinophil-reconstitution (AdBac PVAT (-∅-) vs. AdBac no PVAT (-●-) mean±SEM; n=10; P=0.0023, two-way ANOVA) (d) Flow cytometry quantification of SMA⁺ contractile pericytes (mean±SEM frequency pooled from 4 individual experiments; n=6, P=NS, student's t-test) showed no significant differences between WT (black) and ΔdblGATA-1 mice (red) in mesenteric adipose tissue, and (e) mesenteric adipose weight is similar in ΔdblGATA-1 and WT littermate control mice WT: n=12 (black) and ΔdblGATA-1 (red) mice: n=14 from 3 individual experiments; P=NS, student's t-test). Flow cytometry analysis of digested mesenteric adipose tissue to identify (f) total and (g) RELMα⁺ CD206⁺ macrophages in mesenteric adipose tissue of WT (-■-) and ΔdblGATA-1 (-●-) mice. Graphs display the absolute numbers of total macrophages and RELMα⁺ CD206⁺ macrophages in the mesenteric adipose tissue (WT: n=4 and ΔdblGATA-1: n=7, P=NS, Student's t-test).

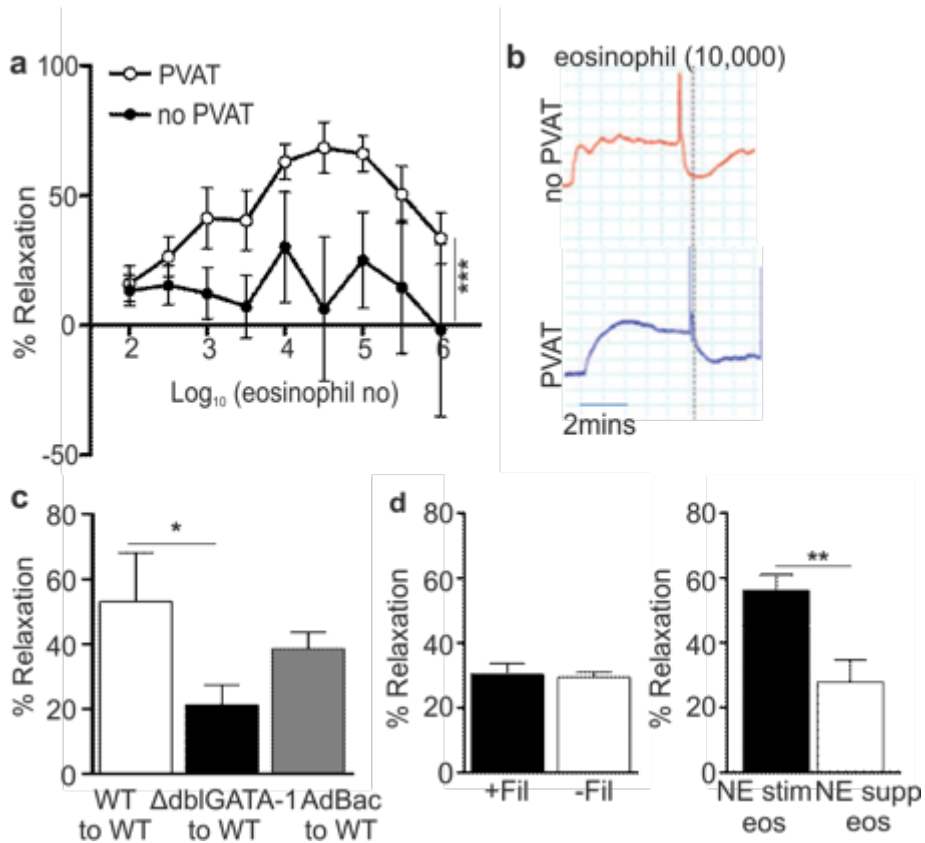


Figure 3. Exogenous application of purified eosinophils induces vessel relaxation. (a) Exogenous application of eosinophils induced dose-dependent relaxation of Δ dblGATA-1 arteries in the presence (○) but not absence (●) of PVAT ($n=8$, pooled from 8 individual experiments; $***P<0.0001$, two-way ANOVA). (b) Trace representative of a pre-constricted Δ dblGATA-1 artery \pm PVAT responding to 10,000 eosinophils. Note the rapid drop in constriction following addition of eosinophils (dotted line). (c) Solution transfer experiments to assess generation of a transferable factor that mediates relaxation ($n=10$, pooled from 2 experiments; $*P=0.049$, Student's t-test). (d) Vessel relaxation in response to application of (left) NE-stimulated eosinophils (-Fil) or filtered supernatant from NE-stimulated eosinophils (+Fil) to WT mesenteric arteries, or (right) addition of NE-stimulated or NE-supplemented eosinophil supernatant ($n=6$; $**P=0.0068$, student's t-test).

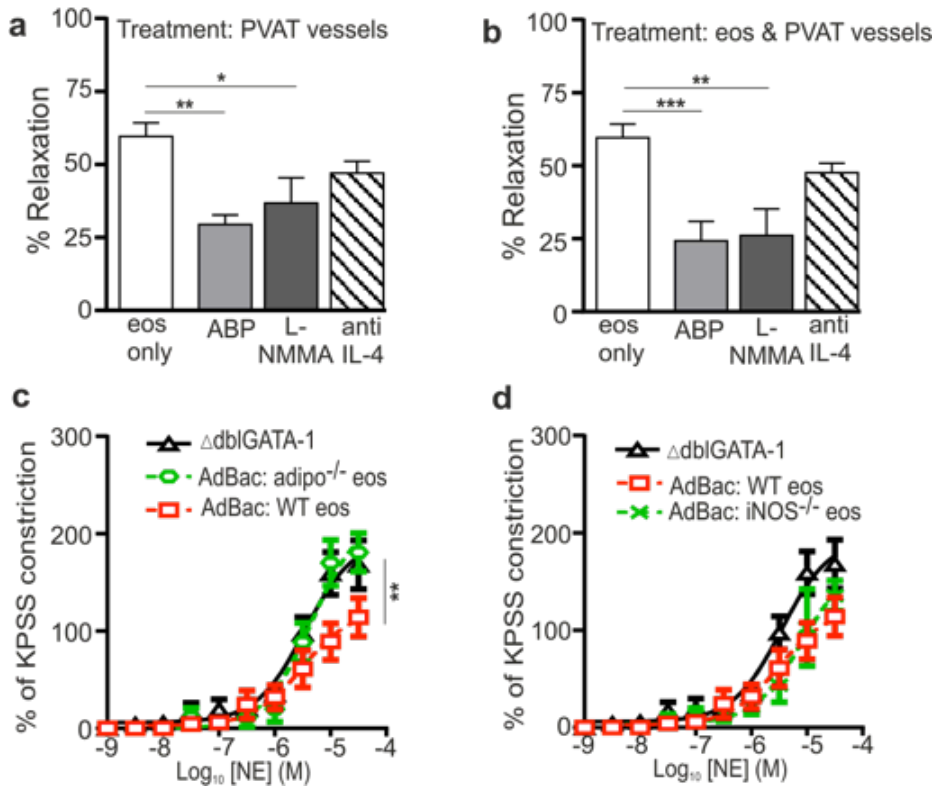
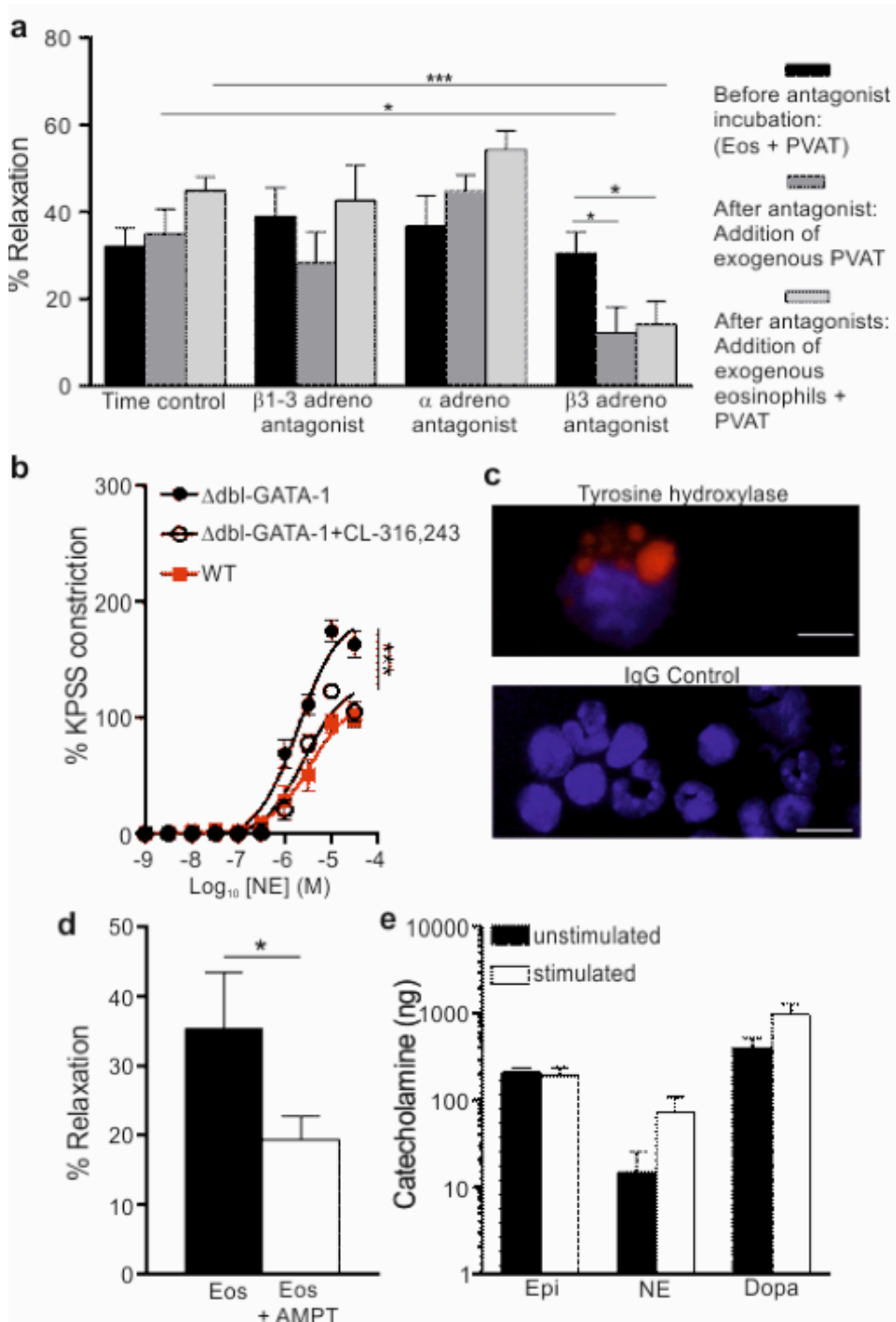


Figure 4. Eosinophils induce adiponectin- and NO-dependent PVAT-induced vessel relaxation (a, b) Vessel relaxation in response to exogenous application of 10,000 NE-stimulated eosinophils (eos) to precontracted Δ dblGATA-1 mesenteric arteries+PVAT following incubation of (a) PVAT (L-NMMA, anti-IL-4: n=9, ABP: n=8; *P<0.05 and **P<0.01, one-way ANOVA with post hoc Dunnett's), or (b) PVAT and eosinophils (L-NMMA, ABP, anti-IL-4: n=9; **P<0.01, ***P<0.001, one-way ANOVA with post hoc Dunnett's). (c, d) The PVAT anti-contractile effect of NE constricted arteries from Δ dblGATA-1 mice reconstituted with (c) adiponectin^{-/-} (circles), (c, d) WT (squares), or (d) iNOS^{-/-} (crosses) eosinophils (*adipo*^{-/-} vs WT: n=4, **P=0.0085, two-way ANOVA; iNOS^{-/-} vs WT: n=5; P=NS, two-way ANOVA)



β_3 , α_1 or β_3 adrenoreceptors and the anti-contractile response of NE-constricted arteries assessed (β_3 adrenoreceptor antagonist vs. time control: *** $P < 0.001$, one-way ANOVA; β_3 adrenoreceptor antagonist vs. vessel control, $n=6$; * $P < 0.05$, one-way ANOVA). (b) The β_3 adrenoreceptor agonist (CL-316,243) was added to $\Delta dbfGATA-1$ arteries with PVAT and contractile responses compared with WT ($P < 0.001$, $n=5$, one-way ANOVA with post hoc Dunnett's). (c) Immunocytochemical analysis for tyrosine hydroxylase in purified and cytopun eosinophils and IgG control staining. (d) Eosinophils were incubated with or without a tyrosine hydroxylase inhibitor (AMPT) and the vascular reactivity of the vessels in response to addition of 10,000 eosinophils tested (* $p=0.0472$, $n=5$, t-test). (e) Levels of epinephrine, norepinephrine and dopamine were measured from unstimulated and stimulated eosinophils ($n=4$).

Supplemental Experimental Procedures

Study Design

The hypothesis of this work was that eosinophils, a major cell component of mesenteric adipose tissue, would have an effect on PVAT function. Thus, initial experiments aimed at defining such a role, with further work designed to unravelling the mechanisms and testing whether the effect of eosinophils was direct or indirect. Animal numbers in each experiment were based on the minimum required per group to show statistical significance. From our previous experience this is typically 5-8 per group. Outcome parameters were in the form of numerical data and most studies were based on a 'fixed effects' model that compares either one, or several, treatment(s) to control. Data were normally distributed, and no data have been excluded. Mice were selected based on genotype, sex and age, and all mice were matched with littermate controls; only males of the ages 8-14 weeks were used in the study. Mice were randomly assigned to treatment groups from different cages and litters: the records were all kept on an excel spreadsheet that contained no information about cage location or cage number, and mice were randomly selected from this list and allocated to the appropriate treatment group. Blood pressure and glucose readings were recorded in a blinded manner, by allocating a number to each mouse. After all readings were completed, mice were unblinded and their genotype identified.

Endpoints *in vivo* were defined based on ability to detect eosinophils. Initial experiments used long-term (30 days) reconstitution of mice with eosinophils, but subsequent experiments revealed the data obtained 5d post-reconstitution was comparable to that from d30 post-reconstitution and therefore used a shorter time frame. Similarly, the original number of cells for the reconstitution was based on published methods, but subsequent optimisation experiments revealed that identical results were achieved using a lower cell numbers. There were no anticipated adverse effects and none were observed. Most experiments were performed at least twice on at least 4-6 mice per group, as stated on the corresponding figures. Units were mice for *in vivo* experiments and for *ex vivo* analysis.

Animals

Δ dblGATA-1 mice were a kind gift from Professor Avery August, Pennsylvania State University, USA. Δ dblGATA-1 mice were bred with C57BL/6 mice and F1 hybrid offspring mated with their siblings to produce the F2 generation, this F2 generation was then maintained by intercrossing heterozygous females and hemizygous males. All experimental Δ dblGATA-1 and WT animals used are littermate F2 mice. IL-5 transgenic (IL-5Tg) mice were from Professor James Lee (Mayo Clinic, USA) and were maintained by crossing heterozygous mice with C57BL/6 mice. Where indicated, obese C57BL/6 DIO mice (HFD) (The Jackson Laboratory, USA) were maintained from weaning on a high-fat diet (composition: protein: 20%, carbohydrate: 20%, fat: 60%; Research Diets, Inc., D12492) [1] and used at 12 weeks of age. Bones from

iNOS^{-/-} mice (generous gift from Dr Caroline Chadwick, University of Birmingham) and adiponectin^{-/-} mice (generous gift from Dr Yu Wang, Hong Kong University) were used to generate bone marrow-derived eosinophils [2]. Mice were culled by CO₂ followed by cervical dislocation. Animal numbers were based on the minimum required per group to show statistical significance; from our previous experience this is typically 4-8 mice per group. Outcome parameters were in the form of numerical data and most studies were based on a 'fixed effects' model that compares either one, or several, treatment(s) to control. Mice were selected based on genotype, sex and age, and all mice were matched with littermate controls.

Physiological parameters

Systemic Arterial Blood pressure

Systolic and diastolic blood pressure was measured non-invasively, by determining the tail blood volume with a volume pressure recording sensor and an occlusion tail-cuff (CODA System, Kent Scientific, Torrington, CT) [3,4]. Mice were subject to equilibration readings before measurement of actual blood pressure from 8-10 readings per mouse. Measurements that did not satisfy the volume occlusion specifications or were deemed too short were excluded from analysis. Blood pressure was measured at the same time of the day for each experimental group and recorded in a blinded manner, by allocating a number to each mouse. After all readings were completed, mice were unblinded and their group belongings identified.

Blood glucose

Mice were fasted overnight for 16 hours and blood glucose was measured from tail-vein samples using a hand-held glucose monitor (Accu-Check Aviva, Roche, UK)

Cell isolation

Eosinophil purification

Eosinophils were purified from IL-5 Tg mice by negative selection using MACS columns or by cell sorting, and were approximately 90-96% or >95% pure for in vivo and in vitro experiments irrespective of purification method, respectively, as assessed by flow cytometry of CD11b⁺ SiglecF⁺ SSC^{high} cells. For adoptive transfers, eosinophils were resuspended in sterile PBS, and 100-150 million cells injected intravenously. Bone marrow-derived eosinophils were grown as described previously [2]. After 12-14 days in culture the cells were >90% pure as determined by flow cytometry analysis; cells were resuspended in sterile PBS, and 1-3 million cells injected intravenously per mouse, with analysis five days after transfer.

Catecholamine ELISA

Splenic eosinophils were isolated from IL-5Tg mice and purified as described above. Eosinophils were purified using MACS columns and stimulated with eotaxin (200ng/ml; R&D systems), IL-5 (400U/ml; R&D systems) and cytochalasin B (50µg/ml, Sigma-

Aldrich) for 2 hours. Catecholamine levels were determined using the Alpco Tri-CAT ELISA according to manufacturer instructions.

Characterisation of adipose tissue cell populations

Adipose tissue digest

For isolation of the adipose stromal vascular fraction (SVF), white mesenteric adipose tissue was finely minced and incubated in medium (DMEM (Life technologies), 25mM HEPES (Life technologies), 4% (w/v) BSA (Sigma-Aldrich)) containing 1mg/mL type I collagenase (Life technologies) and 30 μ g/mL DNase I (Roche diagnostics) at 37°C for 45 min with magnetic stirring at 350rpm. The resulting cell suspension was spun at 1000 \times g for 10 min to separate floating adipocytes from the SVF pellet and the isolated SVF resuspended in MACS buffer (PBS (Life technologies), 2% FCS (Sigma-Aldrich), 2mM EDTA (Sigma-Aldrich), 0.05% NaN₃ (Sigma-Aldrich)) and passed through 40 μ m filters to generate a single-cell suspension. Leukocytes were enriched by density centrifugation using 40 and 70% Percoll (GE Healthcare) at 600 \times g for 20 min at room temperature. The layer over the 70% Percoll was harvested, washed, and resuspended in MACS buffer.

Flow cytometry analysis

Single cell suspensions were incubated with 5 μ g/mL anti-CD16/CD32 antibody (clone 2.4G2; BD Biosciences) in MACS buffer for 20 min on ice to block Fc receptors, followed by staining with indicated antibodies for 20 min on ice, and data acquisition on a LSRII flow cytometer (BD Biosciences). The following monoclonal antibodies and reagents were used: anti-Siglec-F (E50-2440; BD Biosciences), anti-CD11c (N418; eBiosciences), anti-F4/80 (BM8; eBiosciences), anti-CD11b (M1/70; BioLegend), anti-CD45 (104; BioLegend), anti-MHC-II (M5/114.15.2; BioLegend), anti-CD63 (NVG-2; BioLegend), anti-CD206 (C068C2; BioLegend), anti-CD64 (X54-5/7.1; BioLegend), anti-SMA (1A4; Abcam), and-CD31 (390; eBiosciences), anti-PDGFRb (APB5; eBiosciences), and anti-gp38 (8.1.1; BioLegend). LIVE/DEAD Fixable Violet Dead reagent (Life Technologies) was used to distinguish dead cells. For intracellular staining for RELM α , cells were surface-labelled as described above, followed by fixation/permeabilization using the foxp3 staining buffer set (eBioscience). Cells were labelled with polyclonal rabbit-anti-mouse RELM α (Peprotech), followed by incubation with Zenon anti-rabbit secondary reagent (Life technologies).

Pharmacological assessment of vascular reactivity by wire myography

The mesenteric bed was removed and placed in ice-cold PSS (119mM NaCl, 4.7mM KCl, 25mM NaHCO₃, 1.17mM KH₂PO₄, 1.17mM MgSO₄, 0.026mM EDTA, 1.6mM CaCl₂ and 5.5mM glucose; Sigma-Aldrich); first-order arteries were identified (diameter: 200 μ m, length: 0.5-1mm) and one part was dissected clean of PVAT, whereas the other part was left with surrounding PVAT intact. Vessels were mounted on two 40 μ m tungsten wires in a wire myograph (Danish MyoTech, Aarhus, Denmark).

Vessels were incubated in PSS at 37°C and bubbled with 95% air/5% CO₂ to saturate the vessel bath whilst maintaining pH ≈7.4, as previously described [5, 6]. Following equilibration for 30 min [7], vessel wall tension and diameter were normalised using a standardised procedure according to the Laplace equation and stabilised for a further 30 min 7. Constriction of arteries with high-potassium PSS (60 mM) (KPSS) was used to assess arterial viability and addition of 1×10⁻⁵ M acetylcholine (ACh) (Sigma-Aldrich) determined endothelial integrity of the arteries; arteries exhibiting a relaxation of >25% were deemed to have impaired endothelium and excluded from the study. Vascular contractility was assessed in vessels with and without PVAT to increasing concentrations of NE (1×10⁻⁹ to 3×10⁻⁵M) (Sigma-Aldrich). Constriction with KPSS was performed after each NE concentration response curve, acting as an internal time control and reference of contractility for each response curve [5, 8, 9].

Solution transfer experiments

Solution transfer experiments were employed to study the role of eosinophils in the release of relaxing factors from PVAT or in mediating the downstream vascular response. Experiments were performed between WT, IL-5 Tg, ΔdblGATA-1 and AdBac mice. Arteries with and without PVAT were precontracted with NE (1×10⁻⁵M) and stable constriction established for 3 min 10. Total myograph bath solution (6mLs) was taken from donor arteries with PVAT and used to replace the solution from a recipient artery devoid of PVAT (Supplementary Fig. 3). Change in tension was calculated as percentage relaxation of the constricted artery and compared with relaxation following solution transfer between WT-donor to WT-recipient transfer.

Investigating the direct effect of eosinophils on vascular reactivity

In order to investigate the direct effect of eosinophils on vascular contractility, the exogenous addition of (1×10² to 1×10⁶) eosinophils to precontracted mesenteric arteries (1×10⁻⁵M NE) from ΔdblGATA-1 mice was assessed in the presence and absence of PVAT. Eosinophils were purified from IL-5Tg spleens and assessed for purity by flow cytometry analysis as described. The response to eosinophil addition was measured as a percentage relaxation from the maximum constriction to baseline. In all experiments, eosinophils were added in a buffer containing 1×10⁻⁵M NE to avoid effects of NE-dilution on recipient arteries.

To establish whether eosinophils interacted directly or indirectly (via release of an eosinophil-derived factor), NE-stimulated eosinophils were centrifuged at 400g for 5 min and resulting supernatant passed through a 0.2μm filter before addition to NE-precontracted WT or ΔdblGATA-1 vessels. Changes in vessel tension were compared with time controls, whereby bath solution was replaced by PSS+NE (1×10⁻⁵M).

Addition of 10,000 purified eosinophils (described above) was used to delineate the mechanism involved in mediating eosinophil-derived relaxation of precontracted

mesenteric arteries from Δ dblGATA-1 mice. Adiponectin blocking peptide (5 μ g/mL) (Enzo Life Sciences) [5, 8, 11], L-NMMA (1 $\times 10^{-5}$ M) 6 (Sigma-Aldrich), and anti-IL-4 (0.4 μ g/mL) (Peprotech) were used to inhibit adiponectin, nitric oxide (NO) and IL-4 respectively. IgG isotype control (0.4 μ g/mL) (Peprotech) was used as a control for IL-4; D-NMMA (1 $\times 10^{-5}$ M, Sigma-Aldrich) as a control for L-NMMA and a control peptide was used for adiponectin (5 μ g/mL, Enzo Life Sciences). Intrinsic time controls were included for each inhibitor. To address the role of adrenoreceptors, we used propranolol (1 μ M), phentolamine (0.1 μ M, both Sigma-Aldrich), SR-592,30A (0.3 μ M, R&D Systems) CL-316, 243 (10 μ M, R&D Systems) and AMPT (3mM, Sigma-Aldrich). All inhibitors were incubated for 30 min at 37°C with either eosinophils only, arteries \pm PVAT, or both eosinophils and arteries (\pm PVAT). Both eosinophils and vessels were treated with NE (1 $\times 10^{-5}$ M) before addition of eosinophils to the vessels. The response to eosinophil addition was measured as a percentage relaxation.

Histological characterization of PVAT

Mesenteric adipose tissue was removed and fixed with adapted neutral buffered formalin (4% v/v formaldehyde (BDH), 0.154M NaCl (Sigma-Aldrich), 2% v/v glacial acetic acid (BDH), 1.37 μ M hexadecyl trimethyl-ammonium bromide (Sigma-Aldrich) for 24 hrs. Fixed tissues were dehydrated, cleared in xylol and infiltrated with paraffin in a dehydration automat (Citadel 2000, Shandon) using a standard protocol. Specimens were embedded in paraffin (Histocentre2, Shandon), sectioned on a microtome (5 μ m sections). Prior to staining slides were deparaffinised with citrocLEAR and rehydrated through alcohol (100% to 70%) to water. Haematoxylin & eosin (H&E) staining was performed by staining in Harris haematoxylin (Sigma-Aldrich), differentiation in acidified alcohol (1% HCl (Sigma-Aldrich) in 70% ethanol) and counterstaining with Eosin Y (Sigma-Aldrich) prior to dehydration and mounting using Depex mountant (BDH Laboratory Supplies).

Immunocytochemistry for Tyrosine Hydroxylase

Cytospins of splenic eosinophils were isolated from IL-5 Tg mice, purified by immunoisolation (>95% pure), and fixed in 4% paraformaldehyde. Immunocytochemical analysis was performed following permeabilisation (0.1% Triton-X in PBS, 10 minutes) using the rabbit polyclonal primary antibody to tyrosine hydroxylase (0.02mg/mL, 1h, room temperature) (AbCam), followed by a Texas Red-conjugated goat anti-rabbit IgG (H+L) secondary antibody (0.005mg/mL, 1h, room temperature) (Life Technologies), and mounted using DAPI-containing mounting medium (Vectorlabs). IgG controls were performed alongside. Images were captured using the Leica DM5000B microscope with DFC 3000G camera and Leica application suite-X software.

Statistics

Differences in response to NE were expressed as a percentage of constriction to KPSS [5, 6, 10, 12]; functional differences between groups were examined for

statistical significance using two-way ANOVA when appropriate, with the Bonferroni post-hoc test or one-way ANOVA with post hoc Dunnett's test when appropriate. All other statistical analysis was performed by student's t-test, unless stated. P-values below 0.05 were considered significant (* $P < 0.05$, ** $P < 0.01$, *** $P < 0.001$). Data are expressed as mean \pm SEM unless otherwise stated. GraphPad Prism, version 6.00 for Windows was used for data analysis.

Supplemental References

1. Wang CY, Liao JK. A mouse model of diet-induced obesity and insulin resistance. *Methods Mol Biol.* 2012;821:421-433
2. Dyer KD, Moser JM, Czapiga M, Siegel SJ, Percopo CM, Rosenberg HF. Functionally competent eosinophils differentiated ex vivo in high purity from normal mouse bone marrow. *J Immunol.* 2008;181:4004-4009
3. Feng M, Whitesall S, Zhang Y, Beibel M, D'Alecy L, DiPetrillo K. Validation of volume-pressure recording tail-cuff blood pressure measurements. *Am J Hypertens.* 2008;21:1288-1291
4. Zhao X, Ho D, Gao S, Hong C, Vatner DE, Vatner SF. Arterial pressure monitoring in mice. *Curr Protoc Mouse Biol.* 2011;1:105-122
5. Greenstein AS, Khavandi K, Withers SB, Sonoyama K, Clancy O, Jeziorska M, Laing I, Yates AP, Pemberton PW, Malik RA, Heagerty AM. Local inflammation and hypoxia abolish the protective anticontractile properties of perivascular fat in obese patients. *Circulation.* 2009;119:1661-1670
6. Withers SB, Simpson L, Fattah S, Werner ME, Heagerty AM. Cgmp-dependent protein kinase (pkg) mediates the anticontractile capacity of perivascular adipose tissue. *Cardiovasc Res.* 2014;101:130-137
7. Mulvany MJ, Halpern W. Contractile properties of small arterial resistance vessels in spontaneously hypertensive and normotensive rats. *Circ Res.* 1977;41:19-26
8. Dubrovskaja G, Verlohren S, Luft FC, Gollasch M. Mechanisms of adrf release from rat aortic adventitial adipose tissue. *American journal of physiology. Heart and circulatory physiology.* 2004;286:H1107-1113
9. Gao YJ, Lu C, Su LY, Sharma AM, Lee RM. Modulation of vascular function by perivascular adipose tissue: The role of endothelium and hydrogen peroxide. *Br J Pharmacol.* 2007;151:323-331
10. Lynch FM, Withers SB, Yao Z, Werner ME, Edwards G, Weston AH, Heagerty AM. Perivascular adipose tissue-derived adiponectin activates bk(ca) channels to induce anticontractile responses. *American journal of physiology. Heart and circulatory physiology.* 2013;304:H786-795
11. Oriowo MA. Perivascular adipose tissue, vascular reactivity and hypertension. *Med Princ Pract.* 2015;24 Suppl 1:29-37
12. Withers SB, Agabiti-Rosei C, Livingstone DM, Little MC, Aslam R, Malik RA, Heagerty AM. Macrophage activation is responsible for loss of anticontractile function in inflamed perivascular fat. *Arterioscler Thromb Vasc Biol.* 2011;31:908-913

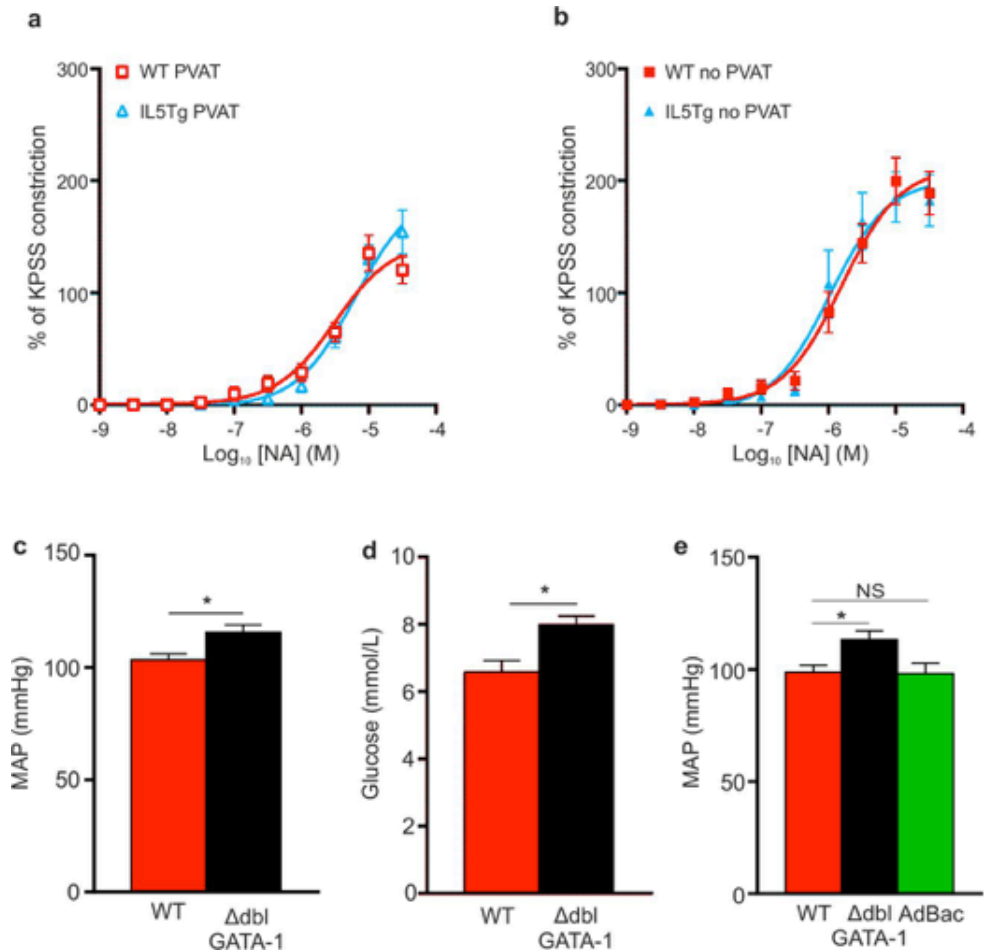


Figure 2 – figure supplement 1. Vascular reactivity of IL-5Tg mesenteric arteries and blood pressure and glucose tolerance in eosinophil deficient mice (a, b) NA-induced constriction of mesenteric arteries from IL-5Tg and WT mice (a) with or (b) without PVAT (IL-5Tg: n=11; WT: n=15; two-way ANOVA) (c) Peripheral MAP analysis of WT and Δ dblGATA-1 mice (WT: n=10, Δ dblGATA-1: n=5; *P=0.046, Mann Whitney test). (d) Blood glucose analysis of WT and Δ dblGATA-1 mice (mean \pm SEM; WT: n=6, Δ dblGATA-1: n=5; *P=0.0106, Student's t-test). (e) Peripheral MAP analysis of WT, Δ dblGATA-1 and AdBac mice (WT: n=5, Δ dblGATA-1: n=10 and AdBac mice: n=5; *P=0.025, one-way ANOVA).

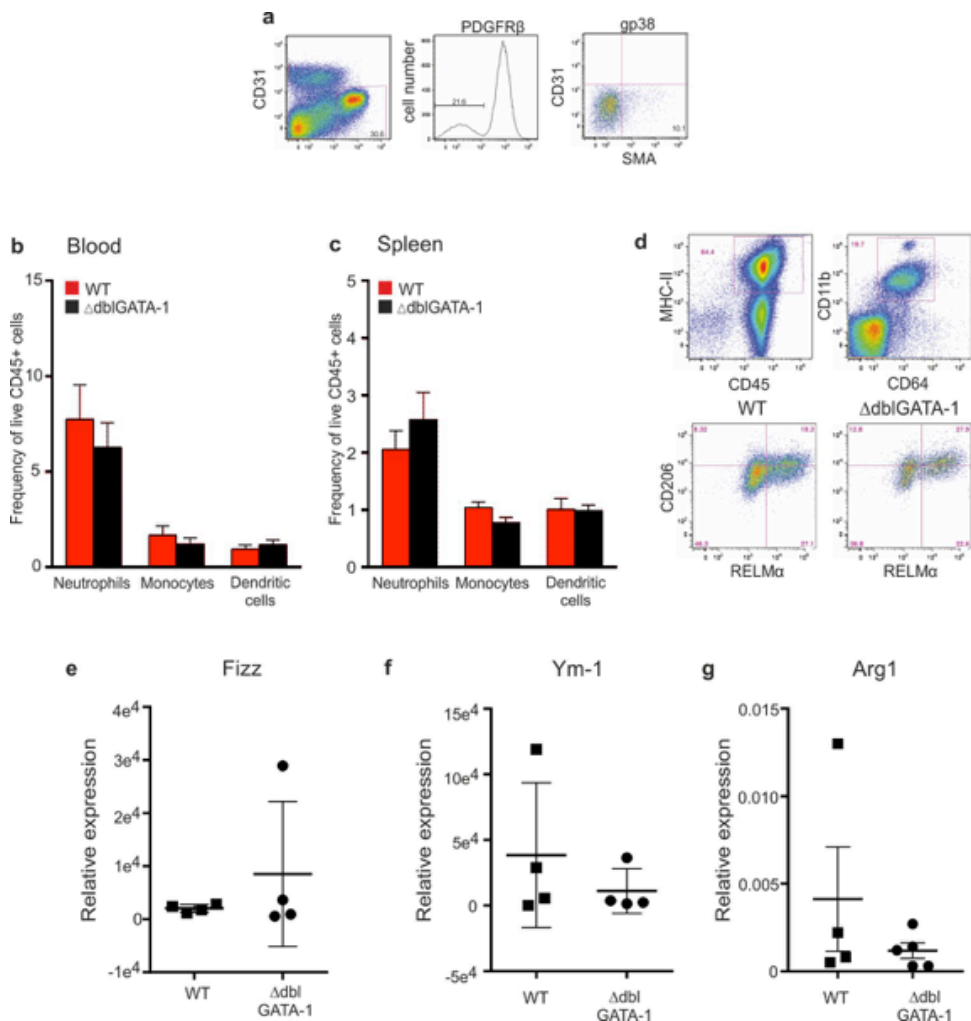


Figure 2 – figure supplement 2. Eosinophil mediated effects on PVAT are independent of pericytes and macrophages. (a) Flow cytometry gating of SMA⁺ pericytes (defined as live CD45⁻ CD31⁻ PDGFR β ⁺ gp38⁻ SMA⁺ cells). Plots are pre-gated on live CD45⁻ cells. (b) Flow cytometry analysis of the blood and (c) spleen of Δ dblGATA-1 and WT mice showed no significant differences in the proportions of dendritic cells, neutrophils and monocytes between strains (mean \pm SEM; n=4 and 7 for WT and Δ dblGATA-1, respectively). (d) Gating strategy for flow cytometry analysis of digested mesenteric adipose tissue to identify total and RELM α ⁺ CD206⁺ macrophages in mesenteric adipose tissue of WT and Δ dblGATA-1 mice. (e) Fizz-1 (f) Ym-1 (WT: n=4, Δ dblGATA-1: n=4; P=NS, Student's t-test; one of two independent experiments), and (g) Arg-1 in mesenteric adipose tissue (WT: n=4, Δ dblGATA-1: n=5; P=NS).

